ISSN 0392-6672

International Journal of Speleology

Official Journal of the Union Internationale de Spéléologie

Volume 48 (1) - January 2019

International Journal of Speleology

Scholarcommons.usf.edu/ijs/

Volume 48 (1), January 2019

Original papers

Comments/Replies

International Journal of Speleology	48 (1)	1-9	Tampa, FL (USA)	January 2019

Available online at scholarcommons.usf.edu/ijs

International Journal of Speleology

Official Journal of Union Internationale de Spéléologie

Sulfur ($^{34}S/^{32}S$) isotope composition of gypsum and implications for deep cave formation on the Nullarbor Plain, Australia

Matej Lipar[1*], Mateja Ferk[1], Sonja Lojen[2,3], and Milo Barham[4]

[1]Anton Melik Geographical Institute, Research Centre of the Slovenian Academy of Sciences and Arts, Gosposka ulica 13, SI – 1000 Ljubljana, Slovenia
[2]Department of Environmental Sciences, Jožef Stefan Institute, Jamova cesta 39, SI – 1000 Ljubljana, Slovenia
[3]Faculty of Environmental Sciences, University of Nova Gorica, Glavni trg 8, SI – 5271 Vipava, Slovenia
[4]Centre for Exploration and Targeting, School of Earth and Planetary Sciences, Curtin University, GPO Box U1987, Perth, WA 6845, Australia

Abstract: Large deep caves with little relation to surface topography are distinctive karst features on the Nullarbor Plain of Australia. The presence of gypsum deposits and chemoautotrophic bacteria within the caves have been suggested as evidence for cave formation and (or) enlargement via sulfuric acid speleogenesis. To test this hypothesis, the stable sulfur isotope compositions ($\delta^{34}S$) of both cave gypsum and surface gypsum were measured. Analyses yielded relatively high, positive $\delta^{34}S$ values from both cave gypsum and surface gypsum, arguing against gypsum genesis via microbial chemoautotrophy, and more broadly, sulfuric acid speleogenesis. Instead, the gypsum is interpreted as forming via evaporation of seawater during the Quaternary.

Keywords: gypsum, sulfuric acid speleogenesis, karst, cave, Australia

Received 28 March 2018; Revised 17 July 2018; Accepted 17 July 2018

Citation: Lipar M., Ferk M., Lojen S. and Barham M., 2019. Sulfur ($^{34}S/^{32}S$) isotope composition of gypsum and implications for deep cave formation on the Nullarbor Plain, Australia. International Journal of Speleology, 48 (1), 1-9. Tampa, FL (USA) ISSN 0392-6672
https://doi.org/10.5038/1827-806X.48.1.2196

INTRODUCTION

In contrast to the typical genesis of carbonate-hosted caves that form by epigene karst system processes with carbonic acid dissolution, a less well studied sub-population of caves can form through the activity of sulfuric acid by a process commonly termed "*sulfuric acid speleogenesis*" (SAS). SAS is thought to originate most commonly from oxidation of sulfide associated with deeper basin fluids (Palmer & Hill, 2012) or from activities of chemoautotrophic sulfur-oxidizing bacteria (Engel et al., 2004). The basic principle of SAS is that sulfide reacts with oxygenated meteoric waters to form sulfate in an acidic solution, creating large cavities at and around the water table (Ford & Williams, 2007). Acidic groundwater enriched in sulfide is capable of dissolving host carbonate units and taking calcium ions into solution. Sulfide becomes oxidized in oxygenated groundwater to sulfate and a hydrogen ion, with the free sulfate and calcium ions reacting and ultimately replacing carbonate minerals with gypsum ($CaSO_4 \cdot 2H_2O$) (Thode, 1970, 1991; Zerkle et al., 2016 and references therein).

Speleogenesis linked to sulfuric acid has been invoked for caves in a variety of settings such as the caves in the Guadalupe Mountains of New Mexico, USA (Jagnow et al., 2000), the Frasassi caves of Ancona, Italy (Galdenzi & Maruoka, 2003), the caves in Bahia Province, Brazil (Auler & Smart, 2003), the caves of the Cerna Valley, Romania (Onac et al., 2011), and Baume Galinière Cave, France (Audra et al., 2015). The presence and source of sulfur is a key diagnostic feature for confirming/refuting SAS, with analyzable sulfur most frequently hosted in cave gypsum.

Gypsum is a common mineral in caves (White, 1976; Hill & Forti, 1997; Onac, 2012) and has been reported from Australian caves such as Jenolan and Wombeyan Caves in eastern Australia and Exit Cave and Mole Creek Caves in Tasmania (Mingaye, 1899; Pogson et al., 2011). Gypsum from the caves on the Nullarbor Plain has been previously described by Caldwell et al. (1982), Goede et al. (1990) and James (1991), and new caves with abundant gypsum are still being discovered (Jackson, 2018). Gypsum may precipitate from supersaturated drip water or during water evaporation, with sulfur variously derived from meteogenic sources (from sea spray or precipitation), decomposition of organic matter in soil or in caves (e.g., guano), biotic or abiotic oxidative recycling of sulfide from the aquifer, or pyrite in nearby strata

*matej.lipar@gmail.com

(Swezey et al., 2002, 2017; Onac, 2012; Onac et al., 2011; Pogson et al., 2011, White, 2015).

The presence of cave gypsum may be an indicator of SAS processes (Jagnow et al., 2000), or may be an indicator of sulfur derived from sulfide minerals in nearby strata without necessarily invoking SAS processes (e.g., Onac et al., 2011). Stable isotope compositions ($\delta^{34}S$) may be used to constrain the origin of sulfate in caves, because large isotope fractionation occurs in the sulfur biogeochemical cycle. In particular, microbially mediated reactions, such as bacterial sulfate reduction and sulfide oxidation result in significantly lighter $\delta^{34}S$ values of the reaction products (Thode, 1970, 1991; Zerkle et al., 2016).

Limited knowledge of deep cave formation on the Nullarbor Plain (Webb & James, 2006), presence of chemoautotrophic aquatic microbial communities (James & Rogers, 1994; Holmes et al., 2001), little or no relation to surface karst geomorphology, and the occurrence of gypsum could link deep caves on the Nullarbor Plain to SAS. Except for a brief notice by Jennings (1983) of similarities between caves of the Nullarbor Plain and caves in the Guadalupe Mountains of New Mexico, SAS on the Nullarbor Plain has not yet been considered or tested. James (1991), however, postulated that the major source of sulfate in Nullarbor caves was aerosols derived from seawater and transported by rain.

The aim of this paper is to provide additional constraints on the origin of gypsum in the Nullarbor caves. In addition, this paper discusses the hypothesis of SAS using the sulfur isotope composition of gypsum.

STUDY AREA – THE NULLARBOR PLAIN

The Nullarbor Plain in central-southern Australia (Fig. 1) represents the largest contiguous karst area globally (~200,000 km^2) and the surface expression of the Cenozoic Eucla Basin. The carbonate-dominated Eucla Basin overlies Mesozoic siliciclastic strata that form the Madura Shelf, which extends offshore as part of the rift-related Bight Basin. In turn, the Bight Basin partially overlies the southerly extension of the Neoproterozoic to early Paleozoic Officer Basin in the north and east, as well as enigmatic isolated Neoproterozoic to Paleozoic strata in the west (Barham et al., 2018). Pre-Cenozoic strata underlying the Eucla Basin are sandstone and mudstone that are interpreted as recording a gradual transition from high-energy fluvio-lacustrine to open marine shelf conditions through the Cretaceous (Fig. 2; Lowry, 1970). The Madura Shelf Mesozoic strata consist of a basal unit of spatially discontinuous beds of unconsolidated, poorly sorted sand and gravel with rarer beds of clay that are mapped collectively as the Loongana Formation. This basal unit is overlain by beds of finer, commonly charcoal-bearing sandstone and siltstone that are mapped collectively as the Madura Formation. The Madura Formation is overlain by an disconformity, above which lie grey siltstone that is mapped as the Toondi Formation. In turn, the Toondi Formation is capped by a disconformity, above which lie beds of glauconitic and fossiliferous siltstone that are mapped collectively as the Nurina Formation (Fig. 2; Cockbain & Hocking, 1989). Minor pyrite is present throughout parts of the Madura, Toondi and Nurina Formations. The combined strata of the Bight and Eucla basins beneath the central Nullarbor Plain has been estimated to reach a maximum thickness of ~800 m, but is more typically ~400 m thick (Scheib et al., 2016; Barham et al., 2018). Basement underlying the entire sedimentary succession comprises Meso- to Palaeo-proterozoic crust (Kirkland et al., 2017).

The Cenozoic strata are predominantly carbonates with basal and marginal clastics. The basal Cenozoic unit is a poorly consolidated, fossiliferous quartz sand that is interpreted to be of marine origin and is mapped as the Eocene Hampton Sandstone. This sandstone is overlain by carbonate strata that are mapped as the Eucla Group, and are subdivided into the following three units (from base to top):

(i) A 150 to 300 m thick white to grey bryozoan-rich limestone (wackestone to packstone) that is mapped as the Middle to Upper Eocene Wilson Bluff Limestone. This unit is interpreted as having accumulated on a temperate marine shelf (Playford et al., 1975; James & Bone, 1991; Benbow et al., 1995).

(ii) A 5 to 100 m thick unit of yellow skeletal- and bryozoan-rich limestone (packstone to grainstone) that is mapped as the Upper Oligocene to Lower Miocene Abrakurrie Limestone. This unit is interpreted as having accumulated in cool to temperate marine conditions (Playford et al., 1975; James & Bone, 1991; Benbow et al., 1995; Miller et al., 2012).

(iii) A 20 to 35 m thick unit of bioclastic and micritic limestone (packstone to rudstone) that is mapped as the Middle Miocene Nullarbor Limestone. This unit is interpreted as having accumulated in subtropical to warm temperate marine environments (Lowry, 1970; Playford et al., 1975; James & Bone, 1991; Benbow et al., 1995; Webb & James, 2006; Miller et al., 2012; O'Connell et al., 2012). The basalt part of the Nullarbor Limestone in the center of the basin is mapped as the Mullamullang Member, and in the northern part the Nullarbor Limestone grades laterally into the quartz and carbonate sandstone with minor claystone and conglomerate mapped as the Colville Sandstone (Lowry, 1968a).

A unit of sandy clay with a few thin beds of dolomite and oolitic and shelly limestone is mapped as the Princess Royal Spongolite on the western margin of the Nullarbor Plain and is correlated with the terrigenous (a supply of non-carbonate material in the form of a delta at the edge of the Eucla Basin) upper part of the Wilson Bluff Limestone in the Kitchener area (Jones, 1990). A number of other marginal carbonate units have been described around and west of the Kitchener area (Fig 1), but these details are outside the scope of this paper.

Unconsolidated sand, clay and calcrete represent the youngest surface sediment. Limited to the southern low-lying Roe and Isrealite Plains (Fig. 1), the late Pliocene poorly cemented molluscan calcarenite is mapped as the Roe Calcarenite (James

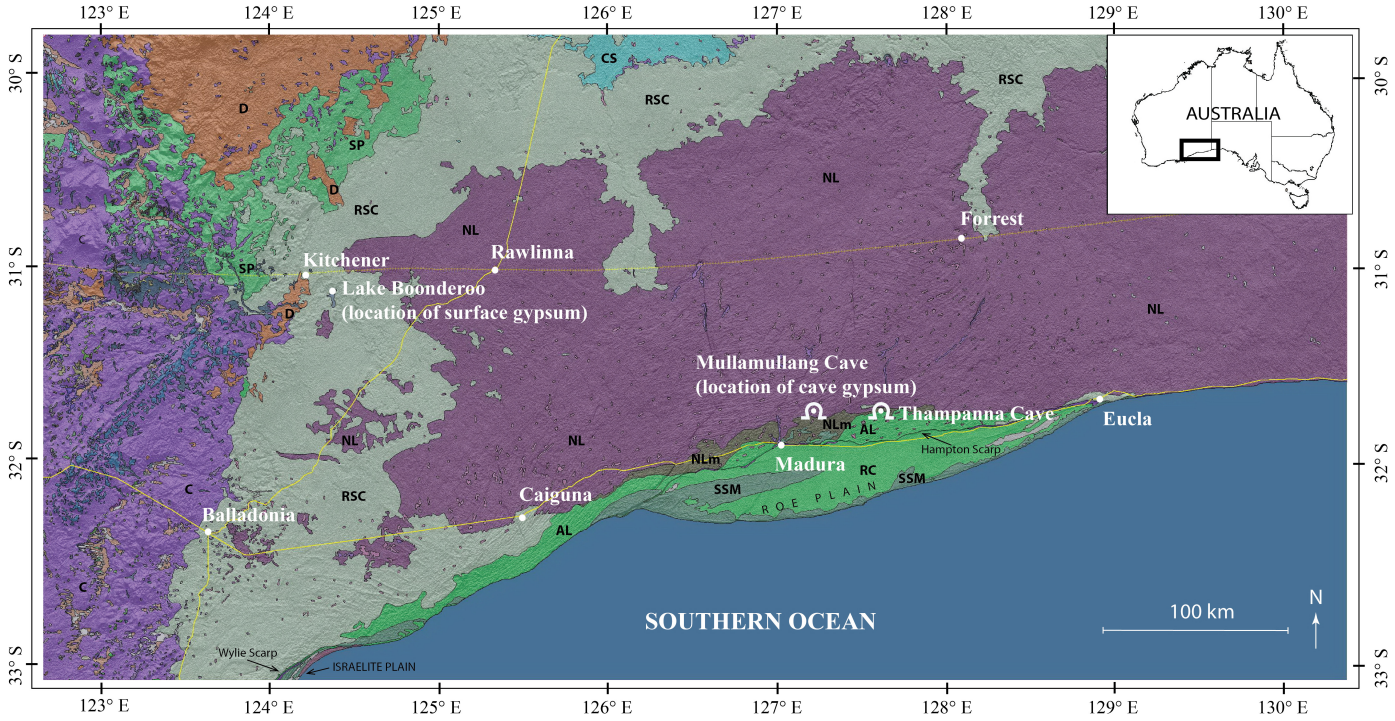

Fig. 1. Locality map of Nullarbor Plain in Australia. DEM downloaded from Shuttle Radar Topography Mission website (NASA, 2002), geology based on Surface Geology of Australia, 1:1 000 000 scale, 2012 edition (Geoscience Australia, 2012). AL = Oligocene-Miocene Abrakurrie Limestone; C = colluvium and residual deposits; CS = Miocene Colville Sandstone; D = dunes; NL = Miocene Nullarbor Limestone; NLm = Mullamullang Member of the Nullarbor Limestone; SP = sand plain; RC = Pliocene-Pleistocene Roe Calcarenite; RSC = residual sediments and calcrete; SSM = Holocene Semaphore Sand Member of the Saint Kilda Formation.

et al., 2006), while Holocene aeolian and beach quartz-carbonate sand is mapped as the Sempahore Sand member of the Saint Kilda Formation (Stewart et al., 2008).

The Nullarbor Plain became emergent as a result of falling sea-levels and regional uplift during the Middle Miocene, approximately 15 Ma ago (Lowry, 1970; Sandiford, 2007). Since this time, the carbonate strata have been exposed to chemical weathering, denudation, and meteoric diagenesis (Miller et al., 2012).

The surface relief of the Nullarbor Plain is generally subdued with isolated local disruptions from small-scale fault scarps with a maximum of a few tens of meters vertical offset (Clark et al., 2012), vestiges of ancient river drainage (Hou et al., 2008), and areas of ridge and corridor topography (Jennings, 1983). Karst features on the Nullarbor Plain include closed depressions of various sizes such as dayas (Goudie, 2010), dongas (Gillieson & Spate, 1992), blowholes (Lowry, 1968b), and collapse dolines (Grozdicki, 1985; Gillieson & Spate, 1992) that can lead to underground cave passages and chambers.

The Nullarbor caves are typically categorized as “shallow” or “deep” (Jennings, 1963; Lowry & Jennings, 1974), extending <30 m and 50-150 m below the surface, respectively (Webb & James, 2006). Shallow cave passages range in length from 0.25 to 20 m (Miller et al., 2012) and are characterized by low passages above collapsed chambers with abundant deposits of dark brown calcite, as well as halite and gypsum (Webb & James, 2006). These shallow caves are associated with pocket valleys in the Hampton and Wylie Scarps (Fig. 1; Lipar & Ferk, 2015), and their genesis is associated with mixing corrosion during the Pliocene sea-level highstand (Burnett et al., 2013).

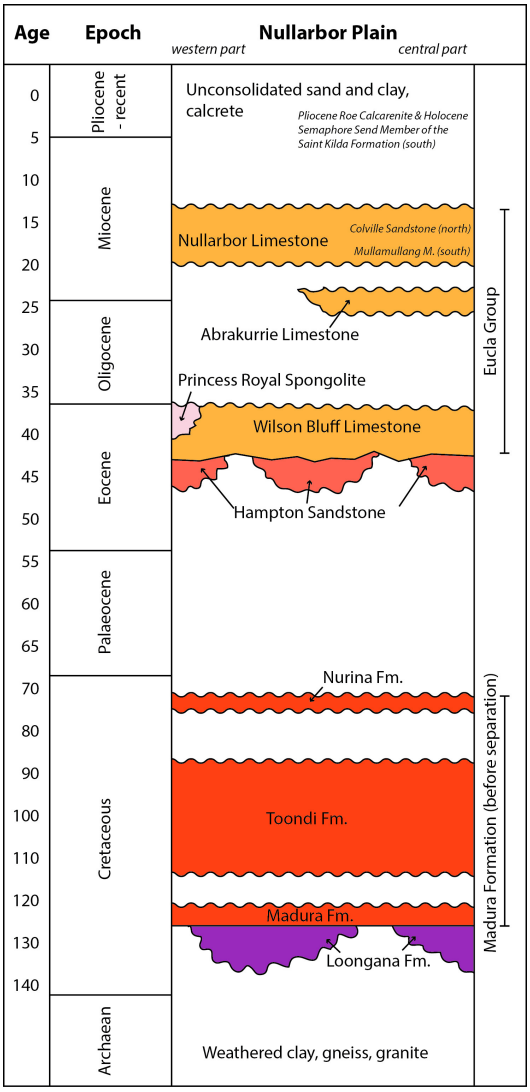

Fig. 2. A generalized stratigraphic column of the western and central Nullarbor Plain (after Jones, 1990; Benbow et al., 1995; Hou et al., 2008).

Deep caves, formed primarily in Wilson Bluff Limestone, extend upwards through collapses and are several kilometers long (the longest - Old Homestead Cave - has >30 km of explored passages) with passages tens of meters wide and high (Webb & James, 2006). Abrakurrie Cave, as an example, has the largest chamber in Australia at approximately 150,000 m^3 (Webb & James, 2006). Besides the significant size of their passages and chambers, the deep caves are characterized by extensive collapses, the absence of calcite deposits, and continuation below the water table. The exact genesis of the deep caves is complex, and the following several processes, which may have occurred simultaneously, have been implicated: (1) crystal weathering (e.g., salt, gypsum; Lowry, 1968a; Gillieson & Spate, 1992); (2) mixing corrosion (James, 1992); (3) biospeleogenesis (James et al., 2012); and (4) dissolution during wetter climate intervals, such as the warm-wet of the Oligocene (Webb & James, 2006) or late Miocene (Miller et al., 2012).

METHODS

Cave gypsum (Fig. 3) was collected in Mullamullang Cave, the deepest (135 m) and second longest cave (>13 km) on the Nullarbor Plain (Fig. 1; James et al., 2012). Naturally broken fragments of gypsum were found and collected ~2.5 km inside from the cave entrance (north-east direction) near the underground White Lake.

Dry lake beds and other topographic depressions were located using satellite and TanDEM-X data, and later investigated in the field to search for gypsum. The nearest surface gypsum was found and collected in the dry lake bed of Boonderoo near Kitchener (Fig. 1).

Back-scattered electron imaging was performed on a Hitachi TM3030 scanning electron microscope (SEM) to investigate compositional heterogeneity in the samples. Energy dispersive x-ray spectrometry (EDS) using an Oxford Swift ED3000 connected to a Hitachi TM3030 at Curtin University (Perth, Australia) was employed to obtain semiquantitative data on the elemental compositions of sampled crusts. Imaging and analyses were carried out on uncoated rough samples attached to a carbon adhesive tab on a 25 mm aluminum stub, with an accelerating voltage of 15 kV, a working distance of 10 mm, and at low vacuum. EDS spectra were obtained on areas varying between 10x10 µm and 200x200 µm with 60 s acquisition time. Beam alignment and calibration of the EDS detectors were undertaken prior to the analytical session following standard procedures.

Sulfur isotope analyses were performed at the Jožef Stefan Institute (Ljubljana, Slovenia). Gypsum crystals and gypsum in carbonate crusts were manually crushed and pulverized in an agate mortar. The carbonate crusts containing gypsum were dissolved in 3 M HCl and filtered through a 0.2 µm membrane filter (Sartorius). Sulfate was precipitated

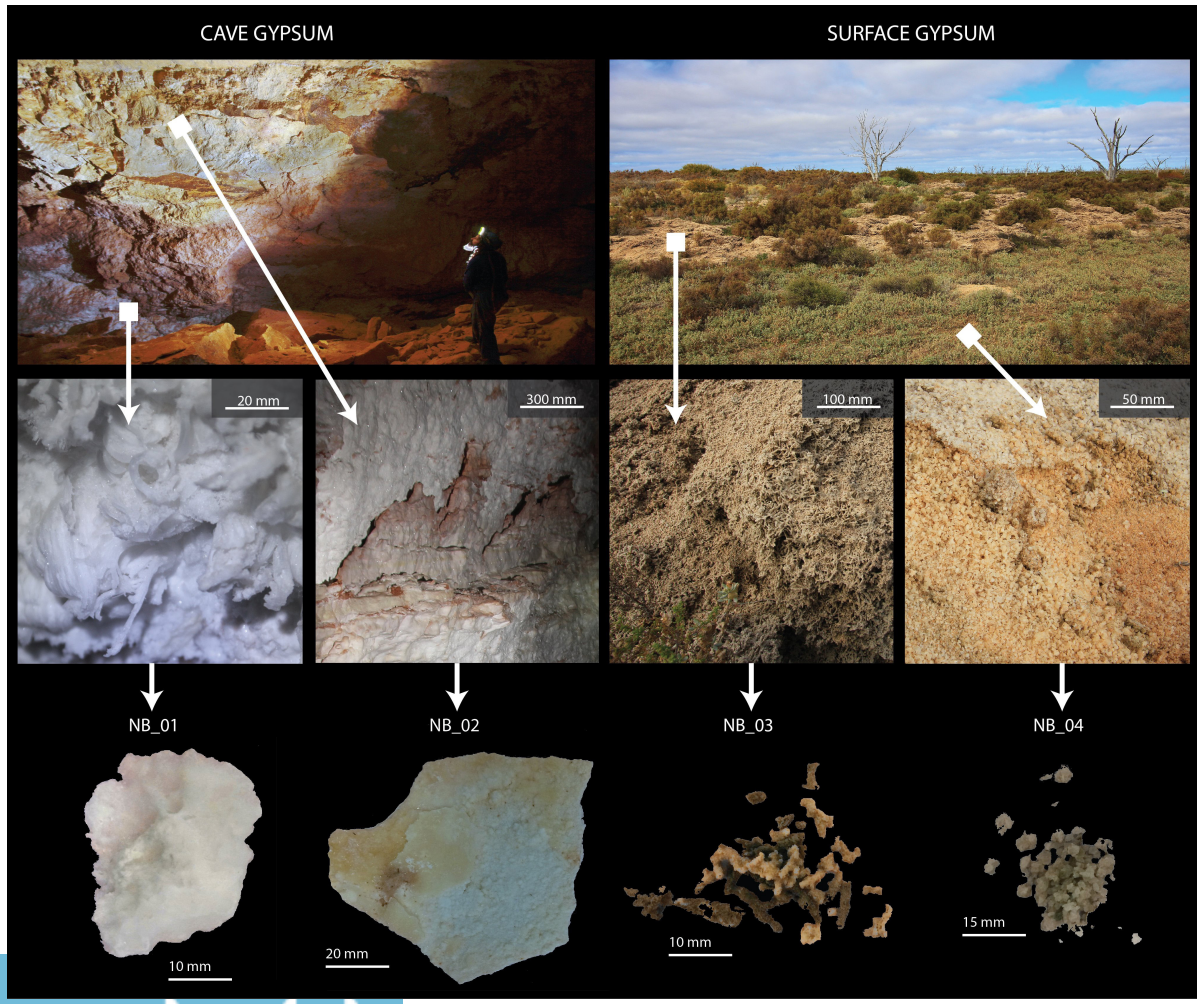

Fig. 3. Photographs of analyzed samples and their localities.

as $BaSO_4$ after addition of 10% $BaCl_2$. The precipitate was repeatedly washed with MiliQ water, filtered, and oven dried. For the isotope analysis, samples of 0.3 mg of gypsum and 0.4 mg $BaSO_4$ were mixed with tungsten oxide and packed into tin capsules. An IsoPrime 100 isotope ratio mass spectrometer with elemental analyzer (PyroCube) was used for the analysis. Results are reported as relative delta (δ) values (i.e., the difference of the isotope $^{34}S/^{32}S$ ratio of the sample and the standard expressed in per mil). Measured values are given relative to the Vienna-Canyon Diablo Troilite (VCDT). The IAEA SO-5, IAEA SO-6, and NBS 127 reference materials with $\delta^{34}S_{VCDT}$ values of 0.5‰, -34.1‰, and 20.3‰, respectively, were used for calibration. All samples and reference materials were analyzed in triplicate, with standard deviation equal to or less than 0.25‰.

RESULTS

The $\delta^{34}S$ values of gypsum samples are high (from +17.1‰ to +21.6‰, Table 1) with a 4.5‰ variation recorded in cave gypsum. The two crystals of surface gypsum returned less variable results (Table 1).

Compositional contrast imaging using backscattered electrons (BSE) indicates relatively simple mineralogies of the crystalline material sampled, with gypsum identified as the major calcium sulfate phase on the basis of elevated proportions of oxygen to calcium and sulfur (~6:1:1; $CaSO_4 \cdot 2H_2O$) (Fig. 4). Sample NB_1 comprises the most pure gypsum identified among the samples, featuring well-defined crystals with a platy cleavage and a Ca:S:O atomic ratio of 1:1:5.7. Sample NB_2 was dominated by low-Mg calcium carbonate with at least two distinct phases of growth and only a minor gypsum component internally. Rounded detrital carbonate and siliciclastic grains (quartz and plagioclase being the most significant on the basis of Si and Al peaks in spectra) are clearly visible in sample NB_4. Minor spectral peaks for Si and Al (in particular) in sample NB_3 are also interpreted to represent EDS activation volumes including minor detrital phases contributing <1% to the overall sample composition.

Table 1. Sulfur isotope values of analyzed samples.

Sample Number	Description	$\delta^{34}S_{VCDT}$ (‰)
NB_01	Gypsum flower – Mullamullang Cave	+17.1
NB_02	Gypsum containing crust – Mullamullang Cave	+21.6
NB_03	Gypsum sponge-work – dry lake (surface)	+18.4
NB_04	Gypsum crystals – dry lake (surface)	+18.0

DISCUSSION

All four samples of gypsum are characterized by $\delta^{34}S$ values that range from +17.1‰ to +21.6‰ (Table 1; Fig. 5). This range of sulfur isotope values resembles the ranges of marine sulfate (Thode, 1970, 1991; Claypool et al., 1980).

Sulfur isotope data alone cannot distinguish between a seawater source and (or) a bedrock source of sulfur in the analyzed gypsum. However, several possible sources of sulfur may be eliminated from consideration. Gypsum derived from microbiological or hydrothermal processes in sulfuric acid caves yield significantly lighter $\delta^{34}S$ values than either group of gypsum samples from the Nullarbor Plain. Hydrocarbon-related sulfide may have a large range of positive $\delta^{34}S$ values (Hoşgörmez et al., 2014; Zhu et al., 2017), but is nevertheless usually several ‰ lighter than the evaporites (Krouse et al., 1988); considering the geology of the area, such an origin is unlikely.

A comparison with sulfur isotope data from gypsum in other caves throughout the world is useful. For example, sulfur isotope values range from -16‰ to -23‰ in Kraushöhle Cave, Austria (Puchelt & Blum, 1989); from -8‰ to -24‰ in the Frasassi cave system, Italy (Galdenzi & Maruoka, 2003); from -8‰ to -10‰ in Corkscrew Cave, Arizona, USA (Onac et al., 2007); from -8‰ to +1‰ in Cave Provalata, Macedonia (Temovski et al., 2013, 2018); from -15‰ to -24‰ in Kinderlinsk Cave, Russia (Chervyatsova et al., 2016); and from -18‰ to -1‰ in several caves in Virginia and West Virginia, USA (Swezey et al., 2002,

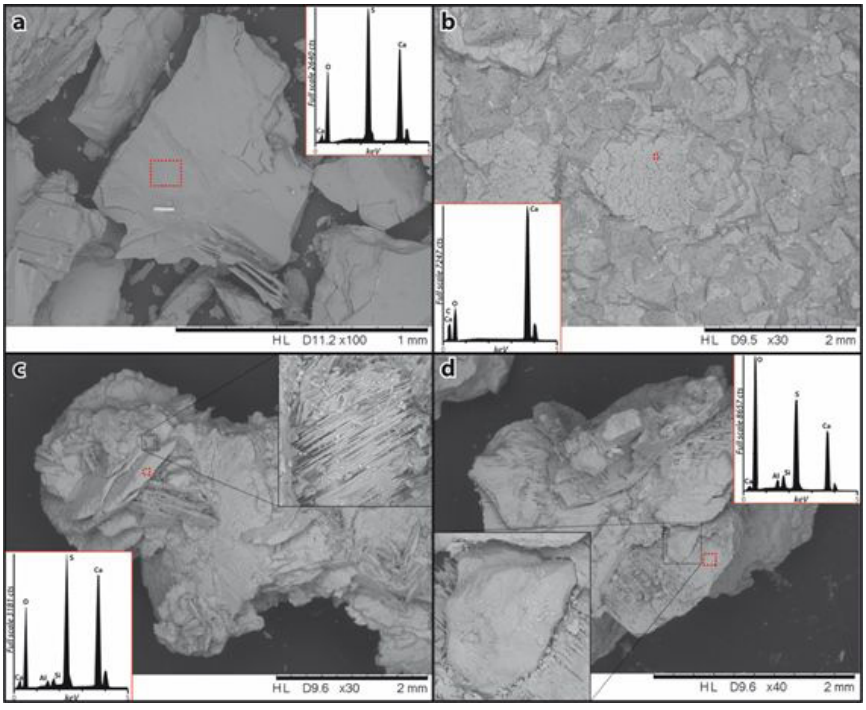

Fig. 4. Back-scattered electron images and associated energy dispersive x-ray spectra (EDS) of samples analyzed herein. Red boxes indicate area analyzed via EDS, with black dashed lines and boxes corresponding to relevant enlarged insets. a) sample NB_1 gypsum crystal fragment; b) surface of carbonate sample NB_2; c) gypsum sample NB_3 with inset platy morphology highlighted; d) gypsum sample NB_4 with inset detrital grain.

White, 2015). However, a relatively wider range of $\delta^{34}S$ values (from -28‰ to +19‰) were reported by Onac et al. (2011) from the caves in the Cerna Valley of southwestern Romania.

For example, the sulfur isotope compositions of gypsum from the Nullarbor Plain are similar to reported values from surface gypsum in southern Western Australia and South Australia, where the highest $\delta^{34}S$ values (~+21‰) occur near coastlines and decrease to $\delta^{34}S$ values of ~+14‰ further inland (Chivas et al., 1991). This systematic variation of isotope values suggests a seawater source for the sulfur, with aerosols being a viable ionic supply mechanism in the hydrochemistry of modern continental arid-zone systems up to a thousand kilometers from the coast (Warren, 2016). The results are therefore in agreement with James (1991), who postulated that the major source of sulfate in Nullarbor caves was aerosols derived from seawater.

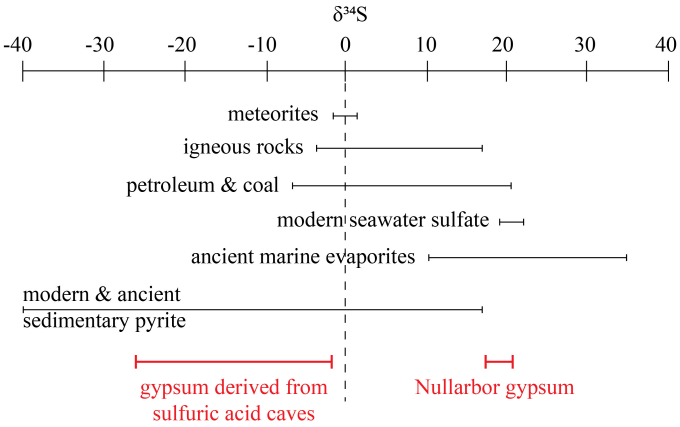

Fig. 5. Variable $\delta^{34}S$ values from different sources. Modified from Seal (2006) with added SAS gypsum values from Puchelt & Blum (1989), Galdenzi & Maruoka (2003), Onac et al. (2011), Temovski et al. (2013), and Chervyatsova et al. (2016).

A bedrock source of sulfur is also possible for the gypsum samples analyzed for this study. Average $\delta^{34}S$ values of marine evaporitic and structurally substituted sulfate in carbonates from 30 to 55 Ma ago (Eocene through Early Oligocene) range from +18.7‰ to +22.0‰, and the $\delta^{34}S$ values from 10 to 20 Ma ago (Miocene) range from +20.4‰ to +22.2‰ (Kampschulte & Strauss, 2004; similar values are also reported by Claypool et al., 1980). These time intervals are approximately equivalent to the time of accumulation of the Wilson Bluff Limestone (Eocene) and the Nullarbor Limestone (Miocene), respectively. However, there is no evidence for evaporitic units or aquatic restriction in any of the underlying successions encountered in drillcore beneath the Nullarbor Plain.

Hill & Forti (1997) regarded oxidation of pyrite as a common source of sulfate minerals in caves. No pyrite inclusions in the Eucla Group carbonates are known to the authors, although pyrite was reported in the Princess Royal Spongolite (Jones, 1990). Furthermore, pyrite is present in the siltstone of the Madura, Toondi and Nurina Formations (Lowry, 1970). The $\delta^{34}S$ values from this pyrite have not been published, and therefore this pyrite cannot be excluded as the source of sulfur in the cave gypsum. It is noteworthy, however, that $\delta^{34}S$ values of pyrite in siliciclastic rocks are most commonly much lighter than the values obtained from the Nullarbor Plain (Ohmoto & Goldhaber, 1997; Hofman et al., 2009). Furthermore, finer claystone units within the Madura, Toondi and Nurina Formations are unlikely to facilitate large-scale fluid migration, with onshore drilling encountering difficult swelling clays, and offshore lithological equivalents being recognized as seals that inhibit fluid migration (Totterdell et al., 2000). A lack of cementation in the Hampton Sandstone between the Cretaceous Madura Shelf strata and Cenozoic Eucla Group carbonates further argues against significant fluid mobilization at depth.

The only published age from gypsum of the Nullarbor Plain is a ~185 ka U/Th date obtained by Goede et al. (1990) from Thampanna Cave (Fig. 1). This relatively recent age (Late Quaternary) from the gypsum contrasts with much older (Pliocene) ages of calcite deposition (Woodhead et al., 2006; Blyth et al., 2010), and is consistent with the occurrence of substantial speleothems of gypsum superimposed on carbonate speleothems (Goede et al., 1990). Consequently, these ages suggest that the gypsum, found in the caves of the Nullarbor Plain today, may post-date the cave formation and consequently may not be a recorder of speleogenesis. Gypsum also is notably fragile and soluble, which means that an absence of deposits proven contemporaneous with cave genesis cannot exclude the possibility of SAS.

Although further research is needed to confirm/refute the unlikely correlation of cave sulfate minerals with pyrite in underlying Madura Formation, the similar $\delta^{34}S$ values for cave and surface gypsum, and young age of gypsum in Thampanna Cave, strongly suggest that sulfate minerals in the Nullarbor caves are evaporites derived ultimately from seawater. The gypsum analyzed during this study most probably formed by evaporation of seawater, with evaporation during increased aridity driving the increased salinity and mineral saturation of saline groundwater already influenced by marine aerosols. Strongly positive $\delta^{34}S$ values do not indicate sulfuric acid speleogenesis of deep caves on the Nullarbor Plain, nor activity of chemoautotrophic sulfur-oxidizing bacteria.

CONCLUSIONS

Possible sulfuric acid speleogenesis of the deep caves on the Nullarbor Plain of Australia is suggested by several features such as little or no relation to surface karst topography, a presence of chemoautotrophic bacteria, and gypsum deposits. Stable sulfur isotope compositions of cave and surface gypsum on the Nullarbor Plain were analyzed in an attempt to test cave origin via sulfuric acid speleogenesis. The analysis of both cave gypsum and surface gypsum yielded sulfur isotope values ranging from +17.1‰ to +21.6‰. Such heavy $\delta^{34}S$ values for the gypsum, and the similarity of values from both cave gypsum and surface gypsum, suggest that sulfuric acid speleogenesis was not a process involved in the cave formation. Instead, gypsum in caves of the Nullarbor Plain is considered to be an evaporite deposit of

Quaternary age derived from saline groundwaters influenced by seawater.

ACKNOWLEDGEMENT

The field work was financially supported by Anton Melik Geographical Institute, Research Centre of the Slovenian Academy of Sciences and Arts, Ministry of Education, Science and Sport, Slovenian Research Agency, research programme P6-0101 and OP20.01261, and Australian Speleological Federation Karst Conservation Fund. TanDEM-X data was approved and received through a science proposal DEM_GEOL2288. Many thanks to Ann-Marie Meredith for help and support in the field.

The isotope analyses (J. Stefan Institute) were financially supported by the Slovenian Research Agency, research programme P1-0143, and the Horizon 2020 research and innovation programme under grant agreement No. 692241 (MASSTWIN – Spreading excellence and widening participation in support of mass spectrometry and related techniques in health, the environment and food analysis). Authors thank reviewer Christopher Swezey and an anonymous reviewer for thoughtful comments and suggestions, which substantially improved the manuscript.

REFERENCES

Audra P., Gázquez F., Rull F., Bigot J.-Y. & Camus H., 2015 – *Hypogene Sulfuric Acid Speleogenesis and rare sulfate minerals in Baume Galinière Cave (Alpes-de-Haute-Provence, France). Record of uplift, correlative cover retreat and valley dissection.* Geomorphology, **247**: 25-34. https://doi.org/10.1016/j.geomorph.2015.03.031

Auler A.S., Smart P.L., 2003 – *The influence of bedrock-derived acidity in the development of surface and underground karst: evidence from the Precambrian carbonates of semi-arid northeastern Brazil.* Earth Surface Processes and Landforms, **28 (2)**: 157-168. https://doi.org/10.1002/esp.443

Barham M., Reynolds S., Kirkland C.L., O'Leary M.J., Evans N.J., Allen H., Haines P.W., Hocking R.M. & McDonald B.J., 2018 – *Sediment routing and basin evolution in Proterozoic to Mesozoic east Gondwana: a case study from southern Australia.* Gondwana Research, **58**: 122-140. https://doi.org/10.1016/j.gr.2018.03.006

Benbow M.C., Lindsay J.M. & Alley N.F., 1995 – *Eucla Basin and palaeodrainage.* In: Drexel J.F. & Preiss W.V. (Eds.), *The geology of South Australia. Vol. 2, The Phanerozoic.* South Australia Geological Survey. Bulletin, **54**, p. 178-186.

Blyth A.J., Watson J.S., Woodhead J. & Hellstrom J., 2010 – *Organic compounds preserved in a 2.9 million year old stalagmite from the Nullarbor Plain, Australia.* Chemical Geology, **279**: 101-105. https://doi.org/10.1016/j.chemgeo.2010.10.006

Burnett S., Webb J.A. & White S., 2013 – *Shallow caves and blowholes on the Nullarbor Plain, Australia – Flank margin caves on a low gradient limestone platform.* Geomorphology, **201**: 246-253. https://doi.org/10.1016/j.geomorph.2013.06.024

Caldwell J.R., Davey A.G., Jennings J.N. & Spate A.P., 1982 – *Colour in some Nullarbor Plain speleothems.* Helictite, **20**: 3-10.

Chervyatsova O.Y., Potapov S.S. & Sadykov S.A., 2016 – *Sulfur isotopic composition of sulfur deposits in Ural karst caves.* Izvestiya Ural'skogo Gosudarstvennogo Gornogo Universiteta (News of the Ural State Mining University), **2**: 37-41.

Chivas A.R., Andrews A.S., Lyons W.B., Bird M.I. & Donnelly T.H., 1991 – *Isotopic constraints on the origin of salts in Australian playas. 1. Sulphur.* Palaeogeography, Palaeoclimatology, Palaeoecology, **84 (1-4)**: 309-332. https://doi.org/10.1016/0031-0182(91)90051-R

Claypool G.E., Holser W.T., Kaplan I.R., Sakai H. & Zak I., 1980 – *The age curves of sulfur and oxygen isotopes in marine sulfate and their mutual interpretation.* Chemical Geology, **28**: 199-260. https://doi.org/10.1016/0009-2541(80)90047-9

Clark D., McPherson A. & Van Dissen R., 2012 – *Long-term behaviour of Australian stable continental region (SCR) faults.* Tectonophysics, **566-567**: 1-30. https://doi.org/10.1016/j.tecto.2012.07.004

Cockbain A.E. & Hocking R.M., 1989 – *Revised stratigraphic nomenclature in Western Australian Phanerozoic basins.* Record 1989/15, Geological Survey of Western Australia, Perth, Western Australia, 11 p.

Engel A.S., Stern L.A. & Bennett P.C., 2004 – *Microbial contributions to cave formation: New insights into sulfuric acid speleogenesis.* Geology, **32**: 369-372. https://doi.org/10.1130/G20288.1

Ford D. & Williams P., 2007 – *Karst hydrogeology and geomorphology.* John Wiley and Sons, Chichester, 562 p. https://doi.org/10.1002/9781118684986

Galdenzi S. & Maruoka T., 2003 – *Gypsum deposits in the Frasassi Caves, central Italy.* Journal of Cave and Karst Studies, **65**: 111-125.

Geoscience Australia, 2012 – *Surface geology of Australia. 1:1 000 000 scale, 2012 edition.* Bioregional Assessment Source Dataset.

Gillieson D.S. & Spate A., 1992 – *The Nullarbor karst.* In: Gillieson D.S. (Ed.), *Geology, climate, hydrology and karst formation: Field symposium in Australia.* Guidebook Special Publication 4, Australian Defense Force Academy, Canberra, p. 65-99.

Goede A., Harmon R.S., Atkinson T.C. & Rowe P.J., 1990 – *Pleistocene climatic change in southern Australia and its effect on speleothem deposition in some Nullarbor caves.* Journal of Quaternary Science, **5**: 29-38. https://doi.org/10.1002/jqs.3390050104

Goudie A.S., 2010 – *Dayas: distribution and morphology of dryland solutional depressions developed in limestones.* Zeitschrift für Geomorphologie, **54 (2)**: 145-159. https://doi.org/10.1127/0372-8854/2010/0054-0010

Grodzicki J., 1985 – *Genesis of the Nullarbor Plain caves in southern Australia.* Zeitschrift für Geomorphologie, **29**: 37-49.

Hill C.A. & Forti P., 1997 – *Cave minerals of the world* (2nd Ed.). National Speleological Society, Huntsville, 463 p.

Hofman A., Bekker A., Rouxel O., Rumble D. & Master S., 2009 – *Multiple sulphur and iron isotope composition of detrital pyrite in Archaean sedimentary rocks: A new tool for provenance analysis.* Earth and Planetary Science Letters, **286**: 436-445. https://doi.org/10.1016/j.epsl.2009.07.008

Holmes A.J., Tujula N.A., Holley M., Contos A., James J.M., Rogers P. & Gillings M.R., 2001 – *Phylogenetic structure of unusual aquatic microbial formations in Nullarbor caves, Australia.* Environmental Microbiology, **3**: 256-264. https://doi.org/10.1046/j.1462-2920.2001.00187.x

Hoşgörmez H., Yalçın M.N., Soylu C. & Bahtiyar İ., 2014 – *Origin of the hydrocarbon gases carbon dioxide and*

hydrogen sulfide in Dodan Field (SE-Turkey). Marine and Petroleum Geology **57**: 433-444. https://doi.org/10.1016/j.marpetgeo.2014.05.012

Hou B., Frakes L.A., Sandiford M., Worrall L., Keeling J. & Alley N.F., 2008 – *Cenozoic Eucla Basin and associated palaeovalleys, southern Australia – climatic and tectonic influences on landscape evolution, sedimentation and heavy mineral accumulation.* Sedimentary Geology, **203 (1-2)**: 112-130. https://doi.org/10.1016/j.sedgeo.2007.11.005

Jackson A., 2018 – *Bunda Cliffs, Nullarbor Plain 2017.* Caves Australia, **204**: 11-14.

Jagnow D.H., Hill C.A., Davis D.G., DuChene H.R., Cunningham K.I., Northup D.E. & Queen J.M., 2000 – *History of sulfuric acid theory of speleogenesis in the Guadalupe Mountains, New Mexico.* Journal of Cave and Karst Studies, **62**: 54-59.

James J.M., 1991 – *The sulfate speleothems of Thampanna Cave, Nullarbor Plain, Australia.* Helictite, **29**: 19-23.

James J.M., 1992 – *Corrosion par mélange des eaux dans les grottes de la plaine de Nullarbor, Australie.* In: Salomon J.-N. & Maire R. (Eds.), *Karst et évolutions climatiques.* Presses Universitaires, Bordeaux, p. 333-348.

James J.M. & Rogers P., 1994 – *The "mysterious" calcite precipitating organism of the Nullarbor caves, Australia.* In: Sasowsky I.D. & Palmer M.V. (Eds.), *Breakthroughs in Karst Geomicrobiology and Redoy Geochemistry.* Conference Abstracts and Field Guide. Karst Waters Institute, p. 34-35.

James J.M., Contos A.K. & Barnes C.M., 2012 – *Nullarbor caves, Australia.* In: Culver D.C. & White W.B. (Eds.), *Encyclopedia of caves* (2nd Ed.). Academic Press, New York, p. 568-576. https://doi.org/10.1016/B978-0-12-383832-2.00084-0

James N.P. & Bone Y., 1991 – *Origin of a cool-water Oligo-Miocene deep-self limestone, Eucla Platform, southern Australia.* Sedimentology, **60**: 323-341. https://doi.org/10.1111/j.1365-3091.1991.tb01263.x

James N.P., Bone Y., Carter R.M. & Murray-Wallace C.V., 2006 – *Origin of the Late Neogene Roe Plains and their calcarenite veneer: implications for sedimentology and tectonics in the Great Australian Bight.* Australian Journal of Earth Sciences, **53**: 407-419. https://doi.org/10.1080/08120090500499289

Jennings J.N., 1963 – *Some geomorphological problems of the Nullarbor Plain.* Transactions of the Royal Society of South Australia, **87**: 41-62.

Jennings J.N., 1983 – *The disregarded karst of the arid and semiarid domain.* Karstologia, **1**: 61-73. https://doi.org/10.3406/karst.1983.2041

Jones B.G., 1990 – *Cretaceous and Tertiary sedimentation on the western margin of the Eucla Basin.* Australian Journal of Earth Sciences, **37**: 317-329. https://doi.org/10.1080/08120099008727930

Kampschulte A. & Strauss H., 2004 – *The sulfur isotopic evolution of Phanerozoic seawater based on the analysis of structurally substituted sulfate in carbonates.* Chemical Geology, **20**: 255-286. https://doi.org/10.1016/j.chemgeo.2003.11.013

Kirkland C.L., Smithies R.H., Spaggiari C.V., Wingate M.T.D., Quentin de Gromard R., Clark C., Gardiner N.J. & Belousova E.A., 2017 – *Proterozoic crustal evolution of the Eucla basement, Australia: Implications for destruction of oceanic crust during emergence of Nuna.* Lithos, **278-281**: 427-444. https://doi.org/10.1016/j.lithos.2017.01.029

Krouse H.R., Viau C.A., Eliuk L.S., Ueda A. & Halas S., 1988 – *Chemical and isotopic evidence of thermochemical sulfate reduction by light hydrocarbon gases in deep carbonate reservoirs.* Nature, **333**: 415-419. https://doi.org/10.1038/333415a0

Lipar M. & Ferk M., 2015 – *Karst pocket valleys and their implications on Pliocene–Quaternary hydrology and climate: Examples from the Nullarbor Plain, southern Australia.* Earth-Science Reviews, **150**: 1-13. https://doi.org/10.1016/j.earscirev.2015.07.002

Lowry D.C., 1968a – *Tertiary stratigraphic units in the Eucla Basin in Western Australia.* Department of Mines. Annual Report 1967, p. 36-40.

Lowry D.C., 1968b – *The origin of blow-holes and the development of domes by exsudation in caves of the Nullarbor Plain. Geological Survey of Western Australia Annual Report: 1967.* Geological Survey of Western Australia, Perth, p. 40-44.

Lowry D.C., 1970 – *Geology of the western Australian part of the Eucla Basin.* Perth, Geological Survey of Western Australia, 199 p.

Lowry D.C. & Jennings J.N., 1974 – *The Nullarbor karst, Australia.* Zeitschrift für Geomorphologie, **18**: 35-81.

Miller C.R., James N.P. & Bone Y., 2012 – *Prolonged carbonate diagenesis under an evolving late Cenozoic climate; Nullarbor Plain, southern Australia.* Sedimentary Geology, **261-262**: 33-49. https://doi.org/10.1016/j.sedgeo.2012.03.002

Mingaye J.H., 1899 – *On the occurrence of phosphate deposits in Jenolan Caves, New South Wales.* Records of the Geological Survey of New South Wales, **6**: 111-116.

NASA – *Shuttle Radar Topography Mission.* http://www.jpl.nasa.gov/srtm/. U.S. National Aeronautics and Space Administration [accessed: 2013].

O'Connell L.G., James N.P. & Bone Y., 2012 – *The Miocene Nullarbor Limestone, southern Australia; deposition on a vast subtropical epeiric platform.* Sedimentary Geology, **253-254**: 1-16. https://doi.org/10.1016/j.sedgeo.2011.12.002

Ohmoto H. & Goldhaber M.B., 1997 – *Sulfur and carbon isotopes.* In: Barnes H.L. (Ed.), *Geochemistry of hydrothermal ore deposits* (3rd Ed.). Wiley, New York, p. 517-611.

Onac B.P., 2012 – *Minerals.* In: Culver D.C. & White W.B. (Eds.), *Encyclopedia of caves* (2nd Ed.). Academic Press, New York, p. 499-508. https://doi.org/10.1016/B978-0-12-383832-2.00072-4

Onac B.P., Hess J.W. & White W.B., 2007 – *The relationship between the mineral composition of speleothems and mineralization of breccia pipes: evidence from Corkscrew Cave, Arizona, USA.* The Canadian Mineralogist, **45 (5)**: 1177-1188. https://doi.org/10.2113/gscanmin.45.5.1177

Onac B.P., Wynn J.G. & Sumrall J.B., 2011 – *Tracing the sources of cave sulfates: a unique case from Cerna Valley, Romania.* Chemical Geology, **288**: 105-114. https://doi.org/10.1016/j.chemgeo.2011.07.006

Palmer A.N. & Hill C.A., 2012 – *Sulfuric acid caves.* In: Culver D.C. & White W.B. (Eds.), *Encyclopedia of caves* (2nd Ed.). Elsevier Academic Press, New York, p. 810-819. https://doi.org/10.1016/B978-0-12-383832-2.00117-1

Playford P.E., Cope R.N., Cockbain A.E., Low G.H. & Lowry D.C., 1975 – *Phanerozoic.* In: Geology of Western Australia. Western Australia Geological Survey, Perth, p. 223-433.

Pogson R.E., Osborne R.A.L., Colchester D.M. & Cendón D.I., 2011 – *Sulfate and phosphate speleothems at Jenolan Caves, New South Wales, Australia.* Acta Carsologica, **40**: 239-254. https://doi.org/10.3986/ac.v40i2.9

Puchelt H. & Blum N., 1989 – *Geochemische Aspekte der Bildung des Gipsvorkommens der Kraushöhle/*

Steiermark. Oberrheinische geologische Abhandlungen, **35**: 87-99.

Sandiford M., 2007 – *The tilting continent: A new constraint on the dynamic topographic field from Australia*. Earth and Planetary Science Letters, **261:** 152-163. https://doi.org/10.1016/j.epsl.2007.06.023

Scheib A., Morris P., Murdie R. & Delle Piane C., 2016 – *A passive seismic approach to estimating the thickness of sedimentary cover on the Nullarbor Plain, Western Australia*. Australian Journal of Earth Sciences, **63**: 583-598. https://doi.org/10.1080/08120099.2016.1233455

Seal R.R., 2006 – *Sulfur Isotope Geochemistry of Sulfide Minerals*. Reviews in Mineralogy & Geochemistry, **61**: 633-677. https://doi.org/10.2138/rmg.2006.61.12

Stewart A.J., Sweet I.P., Needham R.S., Raymond O.L., Whitaker A.J., Liu S.F., Phillips D., Retter A.J., Connolly D.P. & Stewart G., 2008 – *Surface geology of Australia 1:1,000,000 scale, Western Australia (Digital Dataset)*. Canberra, The Commonwealth of Australia, Geoscience Australia.

Swezey C.S., Piatak N.M., Seal R.R. & Wandless G.A., 2002 – *Sulfur and oxygen isotopic composition of gypsum in caves of Virginia and West Virginia*. Geological Society of America, Abstracts with Programs, **34**: 231.

Swezey C.S., Haynes J.T., Lucas P.C. & Lambert R.A., 2017 – *Geologic controls on cave development in Burnsville Cove, Bath and Highland Counties, Virginia*. In: Bailey C.M. & Jaye S. (Eds.), *From the Blue Ridge to the Beach: Geological field excursions across Virginia*. Geological Society of America Field Guide, **47**: 89-123. https://doi.org/10.1130/2017.0047(04)

Temovski M., Audra P., Mihevc A., Spangenberg J.E., Polyak V., McIntosh W. & Bigot J.Y., 2013 – *Hypogenic origin of Provalata Cave, Republic of Macedonia: a distinct case of successive thermal carbonic and sulfuric acid speleogenesis*. International Journal of Speleology, **42**: 235-246. https://doi.org/10.5038/1827-806X.42.3.7

Temovski M., Futó I., Túri M. & Palcsu L., 2018 – *Sulfur and oxygen isotopes in the gypsum deposits of the Provalata sulfuric acid cave (Macedonia)*. Geomorphology, **315**: 80-90. https://doi.org/10.1016/j.geomorph.2018.05.010

Thode H.G., 1970 – *Sulfur isotope geochemistry and fractionation between coexisting sulfide minerals*. Mineralogical Society of America Special Paper, **3**: 133-144.

Thode H.G., 1991 – *Sulphur isotopes in nature and the environment: an overview*. In: Krouse H.R. & Grinenko V.A. (Eds.), *Stable isotopes in the assessment of natural and anthropogenic sulphur in the environment*. John Wiley & Sons, Chichester, p. 1-26.

Totterdell J.M., Blevin J.E., Struckmeyer H.I.M., Bradshaw B.E., Colwell J.B. & Kennard J.M., 2000 – *A new sequence framework for the Great Australian Bight: starting with a clean slate*. The Australian Petroleum Production & Exploration Association Journal, **40**: 95-117. https://doi.org/10.1071/AJ99007

Warren J.K., 2016 – *Depositional chemistry and hydrology*. In: Warren K.K. (Ed.), *Evaporites, a geological compendium* (2nd Ed.). Springer, p. 85-205. https://doi.org/10.1007/978-3-319-13512-0_2

Webb J.A. & James, J.M., 2006 – *Karst evolution of the Nullarbor Plain, Australia*. In: Harmon R.S. & Wicks C. (Eds.), *Perspectives on karst geomorphology, hydrology, and geochemistry – A tribute volume to Derek C. Ford and William B. White*. Geological Society of America Special Paper 404, p. 65-78. https://doi.org/10.1130/2006.2404(07)

White W.B., 1976 – *Cave minerals and speleothems*. In: Ford T.D. & Cullingford C.H.D. (Eds.), *The science of speleology*. Academic Press, London, p. 267-327.

White W.B., 2015 – *Minerals and speleothems in Burnsville Cove caves*. In: White W.B. (Ed.), *The caves of Burnsville Cove, Virginia*. Springer International Publishing, Cham, p. 421-441. https://doi.org/10.1007/978-3-319-14391-0_23

Woodhead J., Hellstrom J., Maas R., Drysdale R., Zanchetta G., Devine P. & Taylor E., 2006 – *U–Pb geochronology of speleothems by MC-ICPMS*. Quaternary Geochronology, **1**: 208-221. https://doi.org/10.1016/j.quageo.2006.08.002

Zerkle A.L., Jones D.S., Farquhar J. & Macalady J.L., 2016 – *Sulfur isotope values in the sulfidic Frasassi cave system, central Italy: A case study of a chemolithotrophic S-based ecosystem*. Geochimica et Cosmochimica Acta, **173**: 373-386. https://doi.org/10.1016/j.gca.2015.10.028

Zhu G., Liu X., Yang H., Su J., Zhu Y., Wang Y. & Sun C., 2017 – *Genesis and distribution of hydrogen sulfide in deep heavy oil of the Halahatang area in the Tarim Basin, China*. Journal of Natural Gas Geoscience, **2**: 57-71. https://doi.org/10.1016/j.jnggs.2017.03.004

International Journal of Speleology	48 (1)	11-20	Tampa, FL (USA)	January 2019

Available online at scholarcommons.usf.edu/ijs

International Journal of Speleology

Official Journal of Union Internationale de Spéléologie

A review of fractals in karst

Eulogio Pardo-Igúzquiza[1*], Peter A. Dowd[2], Juan J. Durán[1], and Pedro Robledo-Ardila[3]

[1]Instituto Geológico y Minero de España (IGME), Ríos Rosas 23, 28001 Madrid, Spain
[2]Computer and Mathematical Sciences, The University of Adelaide, Adelaide SA 5005, Australia
[3]Unidad del IGME en las Islas Baleares. C/Felicià Fuster 7, 07006. Palma de Mallorca, Spain

Abstract: Many features of a karst massif can either be modelled using fractal geometry or have a fractal distribution. For the exokarst, typical examples include the geometry of the landscape and the spatial location and size-distribution of karst depressions. Typical examples for the endokarst are the geometry of the three-dimensional network of karst conduits and the length-distribution of caves. In addition, the hydrogeological parameters of the karst massif, such as hydraulic conductivity, and karst spring hydrographs may also exhibit fractal behaviour. In this work we review the karst features that exhibit fractal behaviour, we review the literature in which they are described, and we propose hypotheses and conjectures about the origin of such behaviour. From the review and analysis, we conclude that fractal behaviour is exhibited at all scales in karst systems.

Keywords: scale-invariance, self-similarity, landscape, sinkholes, caves, conduit networks

Received 27 June 2018; Revised 11 October 2018; Accepted 11 October 2018

Citation: Pardo-Igúzquiza E., Dowd P.A., Durán J.J. and Robledo-Ardila P., 2019. A review of fractals in karst. International Journal of Speleology, 48 (1), 11-20. Tampa, FL (USA) ISSN 0392-6672 https://doi.org/10.5038/1827-806X.48.1.2218

INTRODUCTION

Scale-invariance and self-similarity (Mandelbrot, 1967; Stoyan & Stoyan, 1994; Ben-Avraham & Havlin, 2000) are important concepts in geology (Korvin, 1992; Turcotte, 1997) in general, and in geomorphology (Dodds & Rothman, 2000) in particular. A third concept of universality (Sapoval, 2001) is becoming more evident and relevant as, increasingly, spatial structures of very different physical origin are being shown to exhibit similar spatial patterns, which is reflected in the exponents that characterize their scaling laws. The geometry of river networks (Tarboton et al., 1988; Nikora & Sapozhnikov, 1993; Rodríguez-Iturbe & Rinaldo, 2001) and the statistical structure of topography (Xu et al., 1993; Klinkenberg & Goodchild, 1992) are typical examples of fractals in geomorphology (Dodds & Rothman, 2000). These concepts are increasingly evident in so many areas of Earth Sciences that the hypothesis is shifting towards whether nature itself is fractal (Mandelbrot, 1983; Avnir et al., 1998).

Loosely speaking, a geometrical object or a set is said to be fractal if it exhibits at least one self-similar property in an exact way (deterministic fractals) or through a probabilistic distribution (random or statistical fractals), (Hutchinson, 1981; Falconer, 1990; Schroeder, 1991).

For our presentation and subsequent discussion, we follow the distinction of geometric fractals and probabilistic fractals as described in Crovelli & Barton (1995) and in Ghanbarian & Hunt (2017): fractal geometries of random sets and properties (random variables) of random sets for which the probability density function follows a power law (fractal-like behaviour). The former has a fractal dimension that describes its irregularity or how a random set in a topological space of integer dimension i fills the fractal space of non-integer dimension greater than i. The latter does not have a fractal dimension but has an exponent that characterizes the power law; the characteristic analysed (for example, size) can be considered a random variable for which the probability density function is a power law and there is no need to relate it to an irregular geometry. In any case, the essential assumption of the fractal model is self-similarity which makes it possible to describe fractals by parameters that are either dimensions (fractal geometry of a set) or exponents (fractal property of a set).

Geometrical fractals are geometric shapes or patterns that have a fractional dimension (i.e., the fractal dimension of the geometry of a given set of interest). The fractal dimension can be estimated by different methods. For example, the fractal dimension of a one-dimensional geometry (e.g., a contour), that

*e.pardo@igme.es

characterizes its irregularity, can be determined by calculating its length using measures of different size. If the line is fractal, the relationship between the length of the line and the length of the measure would be expected to follow a power law of the form (Stoyan & Stoyan, 1994):

$$l(r) = cr^{1-D} \qquad (1)$$

where c is a constant. A perfect straight line, i.e. without irregularities, will still follow the power law in equation (1), but with $D = 0$ that is, its dimension is integer not fractal.

Taking logarithms of both sides of the equation (1) gives:

$$\ln l(\mathrm{r}) = \ln c - (1 - \mathrm{D}) \ln r \qquad (2)$$

which is the equation of a straight line with a slope equal to one minus the fractal dimension. Similar power laws are used in other methods to estimate the fractal dimension of sets in the plane and in three dimensions.

Probabilistic fractals (i.e., random variables with fractal behaviour) have a probability density function that follows a power law distribution, which requires that the number of objects, N, with a size greater than r, follows a power law distribution:

$$N(R > r) = Ar^{-K} \qquad (3)$$

where R is a measurable property, A is a constant and K is the exponent characterising the power law.

Thus, power law behaviour can be assessed by studying the probability distribution fitted to a given set of data. This distribution could, for example, take the form of Zipf's law (Laverty, 1987; Schroeder, 1991) or the Korcak-law (Mandelbrot, 1975; Imre and Novotny, 2016). The power-law distribution is a scale-free distribution and represents the spatial distribution of phenomena that do not have a characteristic size but one that varies across several orders of magnitude. Taking logarithms of both sides of equation (3) gives:

$$\ln N = \ln A - K \ln r \qquad (4)$$

which is the equation of a straight line with a slope equal to the Korcak exponent. Thus, probabilistic fractals are characterized by the exponent of a power law. In some cases, this exponent is related to a fractal dimension (Jang & Jang, 2012).

It should be noted that size, shape, abundance, spatial location and distribution of karst geoforms can have a fractal behaviour. In addition, the same geoform can be assessed from several points of view. For example, we can calculate the fractal dimension of the irregularities of the contour of a single sinkhole (or doline). For a family of sinkholes in a given karst terrain, which have been mapped by appropriate means, there are various aspects that could be assessed for fractal behaviour; for example, their size-distribution and the spatial location of their centroids. For geometrical fractals, the fractal dimension (the exponent in the power law in equation 1) describes, in simple terms, how the fractal object fills the available Euclidean space. The contour (one-dimensional object) of a sinkhole on a plane (two-dimensional Euclidean space) will be a number between 1 and 2. The larger the number, the more irregular is the contour. For probabilistic fractals, the interpretation of the fractal dimension is related to the frequency of the size of the objects. The frequency of an occurrence of a given size is inversely proportional to some power of its size. In karst terrains, fractality (i.e. karst features that can be modelled using fractal geometry or karst characteristics that have a fractal distribution) can be found in the exokarst, the endokarst and the karst hydrogeology, which we review in separate sections.

FRACTALS IN THE EXOKARST

Sinkholes (or dolines) are considered the most typical landform in karst landscapes (Ford & Williams 2007). As areas of preferential recharge, they have important implications for karst hydrogeology. They trap sediments that can provide information about past climate conditions, they may indicate geological tectonic activity and they can host important ecosystems.

Reams (1992) found that sinkhole perimeters of large sinkholes appear to be fractals with fractal dimensions ranging from 1.20 to 1.56; i.e., the contours of sinkholes have irregularities that can be quantitatively assessed by their fractal dimension. The same author also concludes that large sinkhole size-number distributions are fractal. Nevertheless, it should be noted that White & White (1987) were the first to test sinkhole populations for their fractal character and their results were negative.

The results of a fractal analysis of sinkholes depend on how the experimental data are obtained. Thus, if data are obtained from maps which are not on a sufficiently small scale, only large sinkholes can be mapped, and the level of detail in the contours will not be sufficient for the analysis, as they will be much smoother than reality. This may explain why the size-distribution of dolines has long been assumed to be log-normal (Telbisz et al., 2009).

The situation has changed with modern digital elevation models (DEM) of topography that allow, subject to the DEM resolution, the detection and delineation of karst depressions in an automatic, exhaustive and efficient manner (Pardo-Igúzquiza et al., 2013; Pardo-Igúzquiza et al., 2014a). Fig. 1 shows the high-quality resolution of mapped sinkholes in the Sierra de las Nieves karst massif in Southern Spain using a DEM with a resolution of 5 m, i.e., each cell of the DEM represents the altitude of a pixel of 5 m by 5m in terrain units. The authors of this work have verified the procedure in the field and even one-cell karst depressions proved to be real dolines in the field. It should be noted that the success of this method also depends on high-quality altimetric precision of the DEM. Thus, the mapped depressions are reliable, and the contours of the sinkholes in Figure 1 do not have the irregularities that would have been introduced if the DEM was noisy and of poor quality. The DEM was obtained as a free download from the web-site of the Instituto Geográfico Nacional of Spain. The DEM for the whole country (an area of

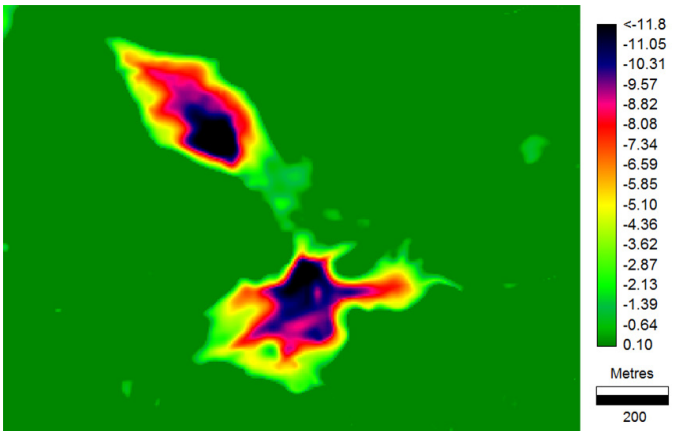

Fig. 1. High resolution karst depressions (dolines and uvalas) mapped by an automatic procedure (Pardo-Igúzquiza et al., 2013) and using a digital elevation model with a resolution of 5 m (size length of the square pixel or cell). The map legend is the depth of each karst depression (in metres) from its rim. The high quality of the mapped contours of the depressions and of the mapped depth is evident.

half a million of square kilometres) has a resolution of 5m and for many parts of the country the resolution increases to 1 m. All mapped karst depressions are shown in Figure 2. The power-law size-distribution of the population of sinkholes is shown in Figure 3.

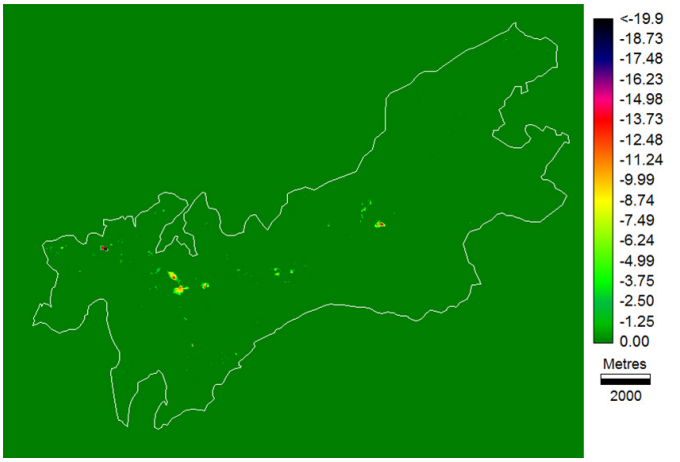

Fig. 2. Karst depressions (dolines and uvalas) in the Sierra de las Nieves karst massif in Southern Spain. The statistics of these sinkholes are given in Pardo-Igúzquiza et al. (2016b).

The same procedure can be used to map karst hills as described in Pardo-Igúzquiza et al. (2016b). The fractal dimension of these doline fields can be used as a geomorphometric parameter to compare different karst massifs.

Other aspects of sinkholes can be assessed when each sinkhole is replaced by its centroid, giving a spatial distribution of points in the plane. Figure 4A shows the point field obtained with the 3,100 sinkholes of the karst massif of Sierra Gorda (López-Chicano, 1995) in Southern Spain and Figure 4B shows the 2,457 sinkholes of the karst massif of Cotiella (Belmonte-Ribas, 2004) in Northern Spain. The fractal dimension of a point field can be assessed by the pair correlation function (Bour et al., 2002):

$$C(r) = \frac{2N_p(r)}{\left[N(N-1)\right]} \qquad (5)$$

where $C(r)$ is the pair correlation function; $N_p(r)$is the number of pairs separated by a distance less than r and N is the total number of points.

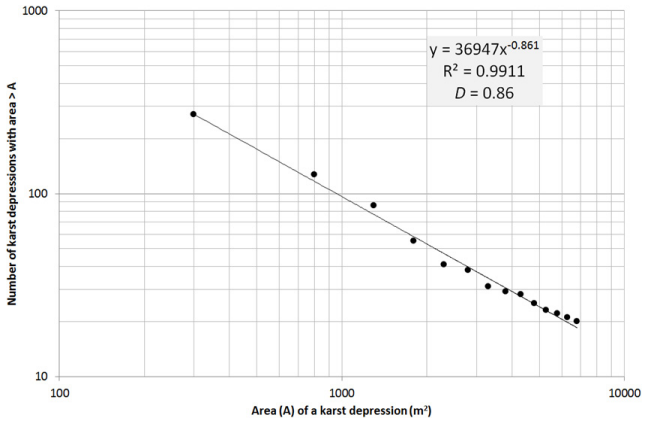

Fig. 3. Graph showing a power law fitted to the number of sinkholes (shown in Fig. 2) with an area larger than a value given by the X axis. The straight line in a log–log plot indicates fractal behaviour. The fractal exponent of the power law is equal to 0.86.

If the point field has a fractal behaviour, the correlation function will scale with distance following a power-law:

$$C(r) \propto r^{D_M} \qquad (6)$$

where D_M is the so-called mass fractal dimension.

A third point field is shown in Fig. 4C, in which each point represents a galaxy. Fig. 4C is a full cylinder section of the 2MASS Redshift Survey database (Huchra et al., 2012). The thickness of the cylinder is 1,000 km s^{-1}, and its radius is 15,000 km s^{-1}. The mass fractal dimension has been calculated for the three point-fields in Figure 4 and the results are shown in Figure 5. The mass fractal dimensions for the Sierra Gorda karst massif, Cotiella karst massif and celestial galaxies map are, respectively, 1.67, 1.46, and 1.25. The Cotiella and galaxies graphs in Figure 5 are similar for short distances. These figures confirm the intuitive similarity of the spatial patterns in Figure 4 and they reflect the universality of the fractal law: very different physical processes give rise to similar spatial patterns. Pardo-Igúzquiza et al. (2016c) and Yizhaq et al. (2017) have recently demonstrated the fractal character of sinkholes.

Other important aspects of the exokarst are the karst landscape (or karst topography) and karren (Ford & Willians, 2007). Karren has also been shown to be a scale-free karst surface dissolution feature. Maire et al. (2004) found that different types of karren have a fractal character, although they do not provide the fractal exponents of the karren scaling.

We now review the fractal character of karst landscapes. Fractal analysis of surface roughness has been widely used for both the natural landscape (Borrough, 1981; Klinkenberg & Goodchild, 1992; Xu et al., 1993, Liucci & Melelli, 2017) and artificial surfaces (Persson, 2014). This type of analysis has improved with the availability of digital elevation models that allow global and local fractal dimensions of landscape to be calculated.

The global fractal dimension quantifies in a single number the complexity and irregularities of the landscape, while the local fractal dimension provides a spatial map of the landscape fractal dimension that quantifies the variations in landscape roughness across the study area. The resulting fractal dimensions

have been used as geomorphometric parameters and as textural indices (Taud & Parrot, 2005). There are no widely available studies of the fractal analysis of karst landscapes and the most recent account is provided by Pardo-Igúzquiza & Dowd (2018). In the latter reference the variogram is used to estimate the local fractal dimension of a karst massif and the authors conclude that the complexity of the karst landscape, as revealed by local fractal analysis, is related to the abundance of karst depressions and karst hills on a range of scales accessible from the available digital elevation model.

This complexity can be assessed for different zones of the study area by calculating the histogram of the local fractal dimension of specified areas. Remarkably, they also found that most local fractal dimensions in karst terrains are less than 2.3, as was theoretically proposed by Persson (2014) for natural and engineered surfaces.

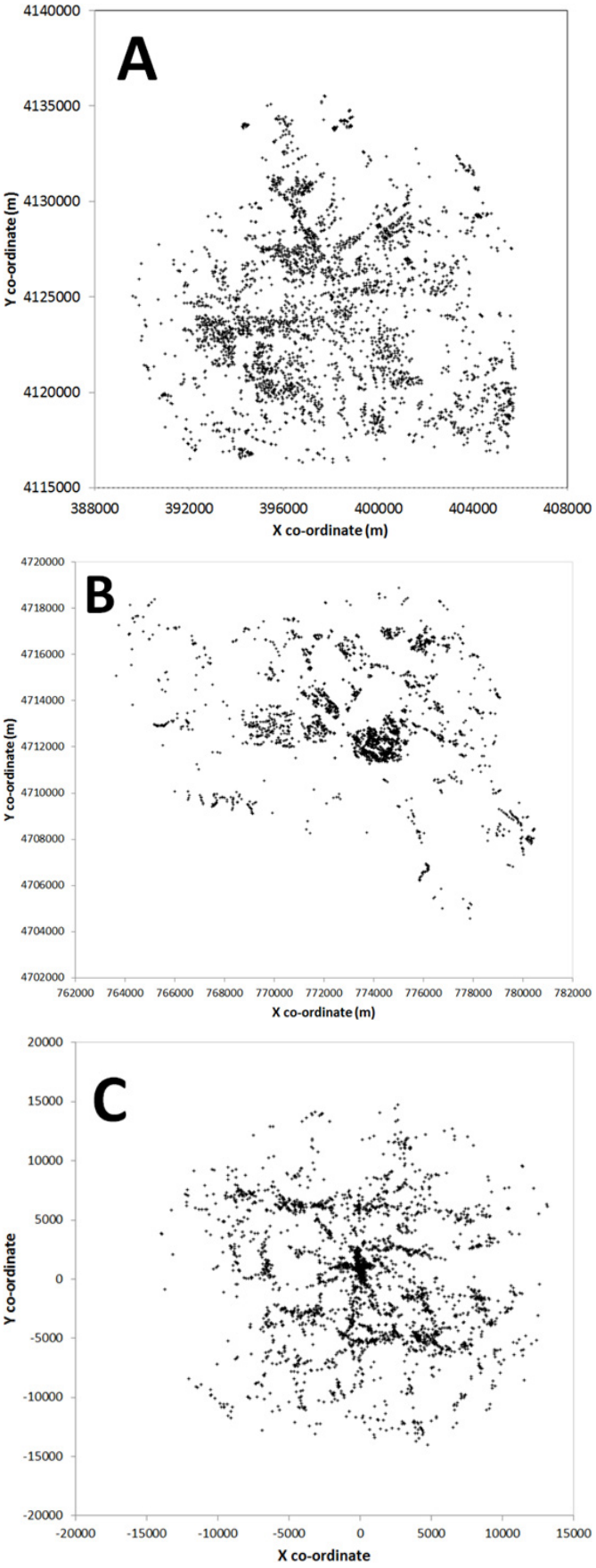

Fig. 4. A) Sierra Gorda karst massif point field in which each point is the location of a doline; B) Cotiella karst massif point field in which each point is the location of a doline; C) Top-down view of a cylindrical portion of the universe where each point represents a Galaxy.

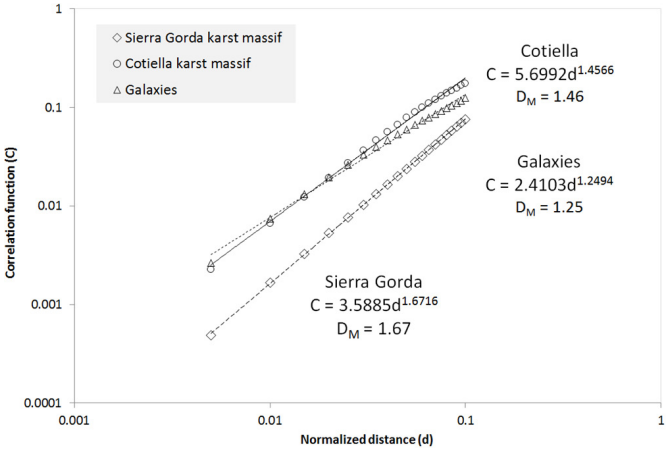

Fig. 5. Pair correlation functions for the point fields in Fig. 4. The distance has been normalized by the maximum distance between points in each set. The mass fractal dimension DM is 1.67, 1.46 and 1.25 for the Sierra Gorda karst, Cotiella karst and galaxies, respectively.

FRACTALS IN THE ENDOKARST

Several decades ago Curl (1960, 1966) showed that the length-distribution of caves is fractal and the number of caves, N,of length greater than l, is given by:

$$N(l) = N(l_0)\left(\frac{l}{l_0}\right)^{-D} \qquad (7)$$

where $N(l_0)$ is the number of caves with a length greater than a reference length l_0. Clearly, equation (7) is another form of equation (3) but it is included here to recognize the pioneering work of Curl not just in fractals in karst science but also as one of the first applications of fractals in general. Curl (1986) obtained, for most of the examined cases, a value of D around 1.4 (with values ranging from 1.2 to 1.6). Curl (1986) also showed that the conditional distribution of sizes of modular elements (caves limited by passages smaller than a given size) also has a fractal distribution; he obtained a value of 2.8 for the Little Bruce Creek cave in the United States. This value of 2.8 is close to the fractal dimension of a Menger sponge, which has a fractal dimension of log(20)/log(3) = 2.727 (Fig. 6A). Figure 6B shows a limestone slate that can be represented as a stochastic Menger sponge. The voids in Figure 6B are not caves (Curl, 1964, 1986) but porosity that can be regarded as micro-caves. In principle, these micro-caves could

be accessed and mapped by micro-electronic or other means. Thus, the fractal analysis of karst conduits is more general than the fractal analysis of proper caves (caves accessible by humans).

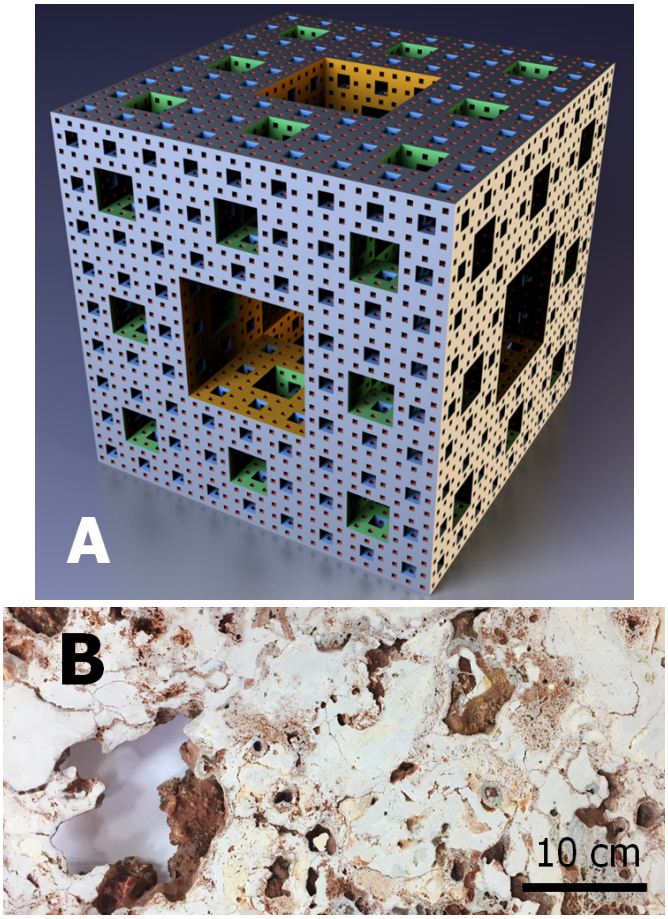

Fig. 6. A) Menger sponge, a deterministic fractal after four iterations in its construction. Figure from Wikipedia created and distributed by Niabot under the GNU Free Documentation Licence; B) Fragment of an Upper Miocene reef limestone slate that can be represented as a stochastic Menger sponge.

Karst conduits are formed from the dissolution of fractures and by bedding planes and other lithological or structural discontinuities in carbonate rocks. The exhaustive network of karst conduits is not observed and mapped by speleological exploration, which is limited to the mapping of accessible caves or accessible parts of caves. Additionally, speleological mapping is biased because not all existing passages have been found, not all the found passages have been explored and not all existing passages are accessible. Nevertheless, based on speleological data, Pardo-Igúzquiza et al. (2014a) used fractal extrapolation to estimate the conduit porosity of the Sierra de las Nieves Karst aquifer in Southern Spain. In addition, fractal dimension was proposed as a geo-morphometric descriptor of three-dimensional networks of karst conduits (Pardo-Igúzquiza et al., 2011) and the fractal character of these networks was used in Pardo-Igúzquiza et al. (2012) to generate realistic synthetic networks of karst conduits using a diffusion limited aggregation method. The fractal dimension of these networks has a typical value of 1.67 (Jeannin et al., 2007). However, in practice, smaller values are usually estimated. For example, experimental values of 1.65 for a karst network in France (Pardo-Igúzquiza et al., 2011), 1.50 for the Yukatan karst networks (Hendrick & Renard 2016a), 1.50 for a karst network in China (Pardo-Igúzquiza et al., 2012) and 1.23 and 1.63 for two different karst networks in Spain (Pardo-Igúzquiza et al., 2016, a, b). These smaller values may be due to the fact that some parts of the system are still unexplored, which suggests the possible use of the fractal dimension to estimate the percentage of a karst network that has not yet been discovered. The value of 1.67 (Jeannin et al., 2007) is the fractal dimension of a self-avoiding random walk (Havlin & Ben-Avraham, 1982). Other studies of the fractal dimension of cave systems can be found in Kusumayudha et al. (2000) and Verbovšek (2007) and a study of the fractal dimension of gypsum cave networks can be found in Andreychouk et al. (2013).

An example of the universality of fractals, with respect to these networks of caves, is provided in Figure 7 which shows the three-dimensional representation of the Shuanghe network (Bottazi, 2004; Pardo-Igúzquiza et al., 2012) and the projection of the network onto the horizontal plane. Figure 8A shows the projection of the Sakany network (Cassou y Bigot, 2007; Pardo-Igúzquiza et al., 2011) onto the horizontal plane, which can be compared with the map of the underground rail system of the city of Madrid (Fig. 8B). This is another example of fractal universality where very different physical processes (in 8A a natural process and in 8B a man-made structure) have similar spatial patterns, as can be qualitatively assessed by visual comparison of both figures. The network of karst conduits in Figure 8A is optimal for draining the water of a karst massif while the underground network in Figure 8B is optimal for the transportation and distribution of people in a large city. Nevertheless, it should be noted that the network of karst conduits is the result of a complex process that has taken place over a long (geological) time. During this time some parts of the system that were optimal for given climatic conditions may have become inactive but remain part of the network structure. Thus, the network of karst conduits is optimal in a global historical sense.

Adequately capturing the complexity of karst networks by mapping is the most challenging aspect of karst modelling especially for modelling and predicting flow and transport in karst media (Ford & Ewers, 1978; Kaufmann & Braun, 2000; Bakalowicz, 2005). Using a lumped model of a karst system and assuming a fractal structure for the karst media, Maramathas & Boudouvis (2006) show that the power law is the optimal relationship between certain parameters of a MODKARST spring model and gives the best agreement between field measurements and model-calculated values of chloride concentration.

FRACTALS IN KARST HYDROGEOLOGY

In a karst massif there are three types of coexisting porosity: rock matrix porosity, fracture porosity and conduit porosity. The three types of porosity have fractal behaviours. Conduit porosity is the ratio of the volume of conduit voids to the total volume and can

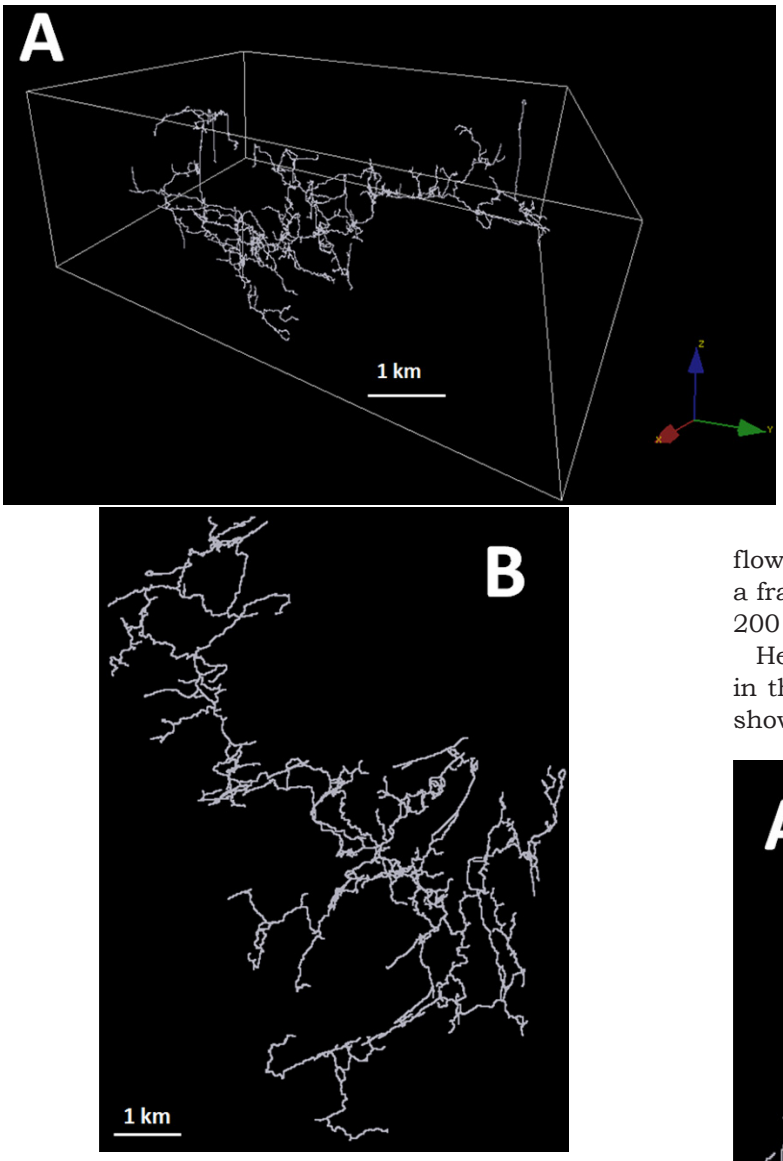

Fig. 7. A) the 130 km of karst conduits of the subtropical Shuanghe network in China; A) 3D view of the network in which the Z-axis scale has been magnified by a factor of 5; B) projection of the network onto the X–Y plane.

be calculated by fractal extrapolation using the fractal character of karst conduits (Pardo-Igúzquiza et al., 2014a). Fracture porosity is the ratio of the volume of fracture voids to the total volume and depends on the extent and apertures of fractures. The fractal character of fractures has been amply demonstrated in the literature (Berkowitz, 2002; Mace et al., 2005). Finally, matrix rock porosity can be observed in hand samples, such as the one shown in Figure 4B, and in thin-section photographs (Fig. 9). The internal surfaces of the pores are very rough due to dissolution and mineralization (Fig. 9). The fractal character of (general) porous media has been widely studied and reported (Katz & Thompson, 1985; Lenormand, 1997; Yu & Liu, 2004).

With respect to hydraulic conductivity, Worthington & Ford (2009) recognized the self-organized character of permeability in carbonate aquifers. This is due to the dissolution and enlargement of fractures, bedding planes and other rock discontinuities that occur along the entire length of pathways through carbonate aquifers, which results in a network of channels at all scales. The self-organization of this three-dimensional network implies a hierarchization of flow (Lauber et al., 2014), in the same way as there is hierarchization of surface flow in a river network (Rodríguez-Iturbe & Rinaldo, 2001), and this hierarchical network of karst conduits is fractal. This implies that there is no typical scale of permeability in carbonate aquifers; the scale increases with the observation scale (Ford & Williams, 2007, Fig. 5.2). This self-organization complexity is general in geomorphology as pointed out by Turcotte (2007).

Hergarten & Birk (2007) found that, during the recession of karst spring hydrographs, there is a power-law decrease of discharge over short times after a rainfall event. The discharge at short times after rainfall events involves fast flow through the network of karst conduits, which has a fractal geometry (Shevenell, 1996; Bacdk & Krothe, 2001).

Hendrick & Renard (2016a) use transport properties in the fractal characterization of karst networks and show that, for two large networks, conductivity scales

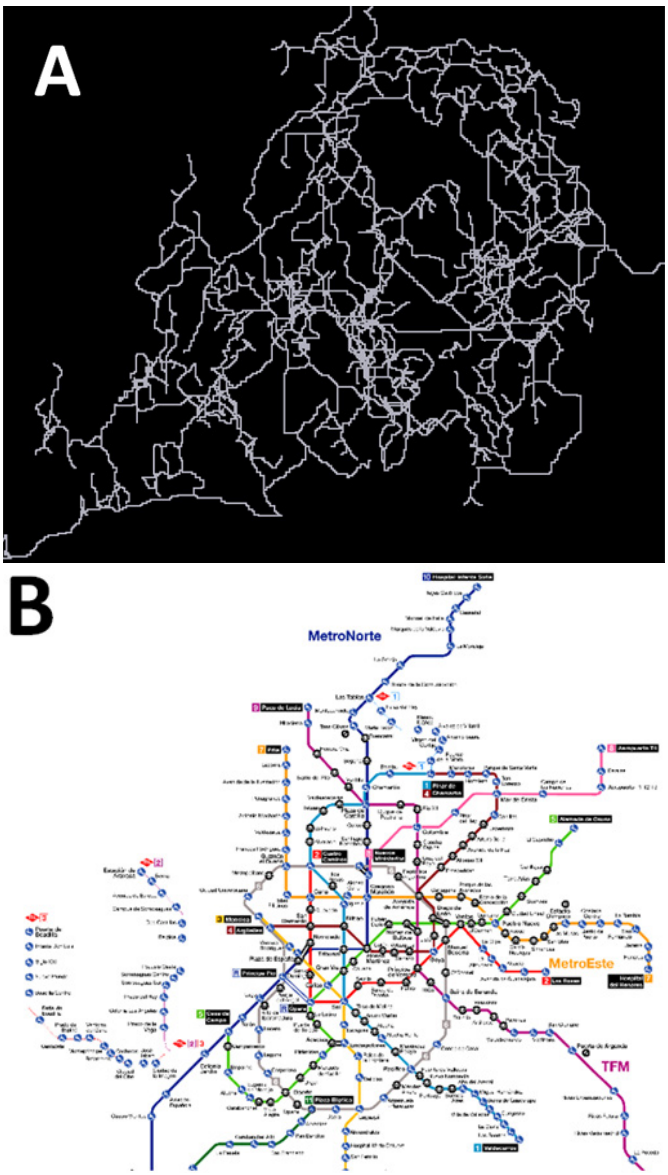

Fig. 8. A) Projection of the Sakany network (France) onto the X–Y plane; B) Underground rail map of the city of Madrid (Consorcio de Transportes Madrid, Comunidad de Madrid, Spain).

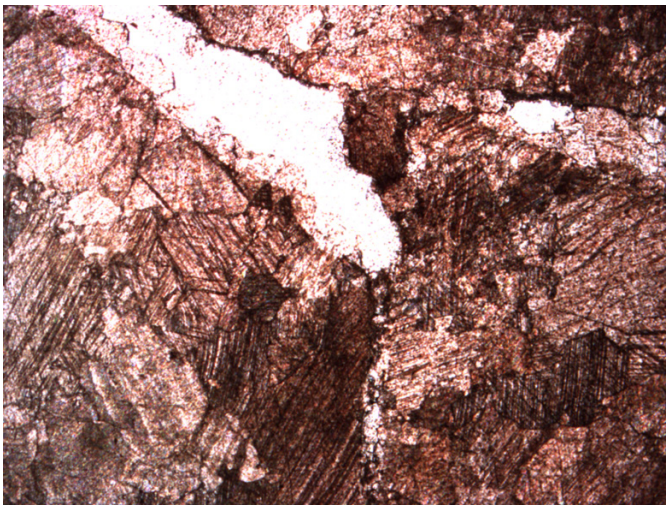

Fig. 9. Irregular pores in a thin-section of dolostone from the Sierra de las Nieves karst aquifer (Málaga, Spain). The width of the section is 2 cm.

as a power law. They analysed the mapped karst network as spatially embedded graphs and computed the fractal dimensions by using the scale-invariant re-normalisation procedure proposed by Song et al. (2005) for complex networks.

DISCUSSION

Many features of karst terrains exhibit fractal behaviour and several theoretical models have been proposed to explain why this should be so. Mandelbrot (1983) proposes a conjecture in relation to the power law of the size-distribution of lakes that can be applied to karst geoforms. He proposes that the underlying reason that the power-law is found in nature is its "resistance" to different forms of "torture"; for example, multiplying the multiplicand in the power law by an arbitrary multiplier does not change the form of the power law. The multiplicand may be determined by an initial state in which the terrain has a power law character and the multiplier can involve many geological and tectonic factors that affect the form of the karst features. In karst terrains, the initial state of the karst system before any extensive dissolution process takes place, is fractured carbonate rocks; and fracture networks have been shown to have a fractal character (Barton, 1995; Berkowitz, 2002; Kruhl, 2013). The multiplier is a measure of the interplay of all the processes involved in the formation of karst features (Ford & Williams, 2007), the product of which is fractal, as shown in the work presented here. This raises the obvious question of why fracture networks are fractals in the first place and a number of physical arguments have been provided and reviewed in Bonnet et al. (2001), in particular, the absence of characteristic length scales in the fracture growth process.

Multifractal analysis is a generalization of fractal analysis (Stanley & Meakin, 1988). It can identify cases in which the fractal dimension is not constant over all scales of variability. Thus, instead of a single fractal dimension, a complete range of values, the fractal spectrum, is estimated from the experimental data (Majone et al., 2002, 2004). However, multifractal analysis requires significantly more experimental data than fractal analysis, which may explain why it has not found many applications in karst studies.

CONCLUSIONS

Fractals are widespread in nature including karst geomorphology and karst hydrogeology. Although the fractal concept does not appear in standard textbooks of karst geomorphology and hydrogeology (Ford & Williams, 2007) and speleogenesis (Klimchouk et al., 2000), recent publications, discussed in this review, have shown that fractals in karst, far from being a mere scientific curiosity, have important practical applications that can contribute to advancing karst and cave science. There are many practical uses of the fractal analysis of karst features. For example, fractal extrapolation can be used to determine the number of small features that cannot be measured because of the fixed range of variation of the available data; fractal simulation can be used to generate realistic synthetic karst features that can be included in mathematical models (Pardo-Igúzquiza et al., 2012; Hendrick & Renard, 2016b); fractal indices can be used as geomorphometric parameters that can be linked to physical generation processes or used to compare different karst massifs. The best of fractal analysis in karst is still to come, as modern techniques (such as LIDAR) for mapping the karst landscape and laser mapping of cave interiors will provide the required high-resolution data. Fractal analysis will then provide a means of exploring and understanding high-detail features. We conclude with the open question of why nature in general, and karst systems in particular, tend to have fractal geometry and why natural variables tend to follow a fractal distribution. Physicists have started to address this question (Sornette, 2006) although many unknowns remain.

ACKNOWLEDGEMENTS

This work was supported by research project CGL2015-71510-R of the Ministerio de Economía, Industria y Competitividad of Spain. We thank Jean Bottazi (Plongée Spéléo Club Jeunes Années, PSCJA) for providing the data for the Shuanghe cave system. We thank Jean-Pierre Cassou (Groupe de Recherches et d'Activités Spéléo, Lourdes, France) for providing the Réssau de Sakany data. We thank the speleologists of the Grupo de Exploraciones Subterráneas from the Sociedad Excursionista de Málaga for providing the data from the Sierra de las Nieves cave system. We would like to thank the detailed comments of the anonymous reviewers that have helped to improve the final version of this paper.

REFERENCES

Andreychouk V., Blachowicz T. & Domino K., 2013 – *Fractal dimensions of gypsum cave-mazes of Western Ukraine*. Speleology and Karstology, **11**: 40-47. http://institute.speleoukraine.net/sk-issues-eng/issue11-eng

Avnir D., Biham O., Lidar D. & Malcai O., 1998 – *Is the geometry of nature fractal?* Science, **279**: 39-40. https://doi.org/10.1126/science.279.5347.39

Bacdk S.J. & Krothe N.C., 2001 – *Derivation of effective hydraulic parameters of a karst aquifer from discharge hydrograph analysis.* Water Resources Research, **37**: 13-19. https://doi.org/10.1029/2000WR900247

Bakalowicz M., 2005 – *Karst groundwater: a challenge for new resources.* Hydrogeology Journal, **13**: 148-160. https://doi.org/10.1007/s10040-004-0402-9

Barton C.C., 1995 – *Fractal analysis of scaling and spatial clustering of fractures.* In: Barton C.C. & La Pointe P.R. (Eds.), *Fractal in the earth sciences.* Plenum Press, New York, p. 141-178. https://doi.org/10.1007/978-1-4899-1397-5_8

Belmonte-Ribas A., 2004 – *Aportaciones a la geomorfología del macizo de Cotiella.* Lucas Mallada, **11**: 25-40.

Ben-Avraham D. & Havlin S., 2000 – *Diffusion and reactions in fractals and disordered systems.* Cambridge University Press, Cambridge, 332 p. https://doi.org/10.1017/CBO9780511605826

Berkowitz B., 2002 – *Characterizing flow and transport in fractured geological media: A review.* Advances Water Resources, **25**: 861-884. https://doi.org/10.1016/S0309-1708(02)00042-8

Bonnet E., Bour O., Odling N.E., Davy P., Main I., Cowie P. & Berkowitz B., 2001 – *Scaling of fracture systems in geological media.* Reviews of Geophysics, **39**: 347-383. https://doi.org/10.1029/1999RG000074

Borrough P.A., 1981 – *Fractal dimensions of landscapes and other environmental data.* Nature, **294**: 240-243. https://doi.org/10.1038/294240a0

Bottazzi J., 2004 – *Shuanghedongqun la plus longue grotte de Chine.* Spelunca, **93**: 13-28.

Bour O., Davy P., Darcel C. & Odling N., 2002 – *A statistical scaling model for fracture network geometry, with validation on a multiscale mapping of a joint network (Hornelen Basin, Norway).* Journal of Geophysical Research, **107**: 1-12. https://doi.org/10.1029/2001JB000176

Cassou J.-P. & Bigot J.-Y., 2007 – *Le labyrinthe de la grotte de Sakany (Quié, Ariège).* Actes de la 17# Recontre d'Octubre, Orgnac, p. 29-36.

Crovelli R.A. & Barton C.C., 1993 – *Fractals and the Pareto distribution applied to petroleum accumulation-size distributions.* U.S. Department of Interior. United States Geological Survey, Open-File Report 91-18, 29 p.

Crovelli R.A. & Barton C.C., 1995 – *Fractals and the Pareto distribution applied to petroleum accumulation-size distributions.* In: Barton C.C. & La Pointe P.R. (Eds.), *Fractals in petroleum geology and earth processes.* Plenum Press, New York, p. 59-72. https://doi.org/10.1007/978-1-4615-1815-0_4

Curl R.L., 1960 – *Stochastic models of cavern development.* Bulletin National Speleological Society, **22**: 66-76.

Curl R.L., 1964 – *On the definition of a cave.* Bulletin National Speleological Society, **26**: 1-6.

Curl R.L., 1966 – *Caves as a measure of karst.* Journal of Geology, **74**: 798-830. https://doi.org/10.1086/627212

Curl R.L., 1986 – *Fractal Dimensions and Geometries of Caves.* Mathematical Geology, **18**: 765-783. https://doi.org/10.1007/BF00899743

Dodds P.S. & Rothman D.H., 2000 – *Scaling, universality, and geomorphology.* Annual Review Earth Planetary Sciences, **28**: 571-610. https://doi.org/10.1146/annurev.earth.28.1.571

Falconer K.J., 1990 – *Fractal geometry: Mathematical foundations and applications.* John Wiley & Sons, Chichester (UK), 368 p.

Ford D.C. & Ewers R.O., 1978 – *The development of limestone cave systems in the dimensions of length and depth.* International Journal of Speleology, **10**: 213-244. https://doi.org/10.5038/1827-806X.10.3.1

Ford D.C. & Williams P., 2007 – *Karst hydrogeology and geomorphology.* John Wiley & Sons, Chichester, 562 p. https://doi.org/10.1002/9781118684986

Ghanbarian B. & Hunt A.G. (Eds), 2017 – *Fractals: concepts and applications in geosciences.* CRC Press, Boca Ratón, 352 p. https://doi.org/10.1201/9781315152264

Hutchinson J.E., 1991 – *Fractals and self-similarity.* Indiana University Mathematical Journal, **30**: 713-747. https://doi.org/10.1512/iumj.1981.30.30055

Havlin S. & Ben-Avraham D., 1982 – *Theoretical and numerical study of fractal dimensionality in self-avoiding walks.* Physical Review A, **26**: 1728-1734. https://doi.org/10.1103/PhysRevA.26.1728

Hendrick M. & Renard P., 2016a – *Fractal dimension, walk dimension and conductivity exponent of karst networks around Tulum.* Frontiers in Physics, **4**: 27. https://doi.org/10.3389/fphy.2016.00027

Hendrick M. & Renard P., 2016b – *Subnetworks of percolation backbones to model karst systems around Tulum, Mexico.* Frontiers in Physics, **4**: 43. https://doi.org/10.3389/fphy.2016.00043

Hergarten S. & Birk S., 2007 – *A fractal approach to the recession of spring hydrographs.* Geophysical Research Letters, **34 (11)**: L11401. https://doi.org/10.1029/2007GL030097

Huchra J.P., Macri L.M., Masters K.L., Jarrett T.H., Berlind P., Calkins M., Crook A.C., Cutri R., Erdoğdu P., Falco E., George T., Hutcheson C.M., Lahav O., Mader J., Mink J.D., Martimbeau N., Schneider S., Skrutskie M., Tokarz S. & Westover M., 2012 – *The 2MASS redshift survey – Description and data release.* The Astrophysical Journal Supplement Series, **199 (6)**: 1-22. https://doi.org/10.1088/0067-0049/199/2/26

Imre A.R. & Novotný J., 2016 – *Fractals and the Korcak-law: a history and a correction.* The European Physical Journal H, **41**: 69-91. https://doi.org/10.1140/epjh/e2016-60039-8

Jang J. & Jang Y.H., 2012 – *Spatial distributions of islands in fractal surfaces and natural surfaces.* Chaos, Solitons & Fractals, **45**: 1453-1459. https://doi.org/10.1016/j.chaos.2012.09.003

Jeannin P.-Y., Groves C. & Häuselaman P., 2007 – *Speleological investigations.* In: N. Goldscheider & D. Drew (Eds.), *Methods in karst hydrogeology.* Taylor & Francis, London, p. 25-44.

Katz A.J. & Thompson A.H., 1985 – *Fractal Sandstone Pores: Implications for Conductivity and Pore Formation.* Physical Review Letters, **54**: 1325. https://doi.org/10.1103/PhysRevLett.54.1325

Kaufmann G. & Braun J., 2000 – *Karst aquifer evolution in fractured, porous rocks.* Water Resources Research, **36**: 1381-1391. https://doi.org/10.1029/1999WR900356

Klimchouk A.B., Ford D.C., Palmer A.N. & Dreybrodt W. (Eds.), 2000 – *Speleogenesis. Evolution of karst aquifers,* National Speleological Society, Huntsville, 527 p.

Klinkenberg B. & Goodchild M.F., 1992 – *The fractal properties of topography: a comparison of methods.* Earth Surface Processes and Landforms, **17**: 217-234. https://doi.org/10.1002/esp.3290170303

Korvin G., 1992 – *Fractal models in earth sciences.* WH. Freeman, San Francisco, 424 p.

Kruhl J.H., 2013 – *Fractal-geometry techniques in the quantification of complex rock structures: A special view on scaling regimes, inhomogeneity and anisotropy.* Journal of Structural Geology, **46**: 2-21. https://doi.org/10.1016/j.jsg.2012.10.002

Kusumayudha S.B. & Zen M.T., Notosiswoyo S. & Gautama R.S., 2000 – *Fractal analysis of the Oyo River, cave systems, and topography of the Gunungsewu karst area, central Java, Indonesia*. Hydrogeology Journal, **8**: 271-278. https://doi.org/10.1007/s100400050014

Lauber U., Ufrecht W. & Goldscheider N., 2014. *Spatially resolved information on karst conduit flow from in-cave dye tracing*. Hydrology and Earth System Sciences, **18**: 435-445. https://doi.org/10.5194/hess-18-435-2014

Laverty M., 1987 – *Fractals in karst*. Earth Surface Processes and Landforms, **12**: 475-480. https://doi.org/10.1002/esp.3290120505

Lenormand R., 1997 – *Fractals and porous media. From pore to geological scales*. In: Carpinteri A. & Mainardi F. (Eds.), *Fractals and fractional calculus in continuum mechanics*. International Centre for Mechanical Sciences (Courses and Lectures), Springer-Verlag, Vienna, p. 173-222. https://www.springer.com/us/book/9783211829134

Liucci L. & Melelli L., 2017 – *The fractal properties of topography as controlled by the interactions of tectonic, lithological and geomorphological processes*. Earth Surface Processes and Landforms, **42**: 2585-2598. https://doi.org/10.1002/esp.4206

López-Chicano M., 1995 – *El paisaje kárstico de Sierra Gorda. Formas y evolución geodinámica reciente*. Espeleotemas, **5**: 31-50.

Mace R., Marrett R.A. & Hovorka S.D., 2005 – *Fractal scaling of secondary porosity in karstic exposures of the Edwards Aquifer*. In: Beck B.F. (Ed.), *Sinkholes and the engineering and environmental impacts of karst*. American Society Civil Engineers, Geotechnical Special Publication, No. 144, 10 p. https://doi.org/10.1061/40796(177)19

Mandelbrot B.B., 1967 – *How long is the coast of Britain? Statistical self-similarity and fractional dimension*. Science, **156**: 636-638. https://doi.org/10.1126/science.156.3775.636

Mandelbrot B.B., 1975 – *Stochastic models for the Earth's relief, shape and fractal dimension of coastlines, and number-area rule for islands*. Proceedings National Academy of Sciences USA, **72**: 3825-3838. https://doi.org/10.1073/pnas.72.10.3825

Mandelbrot BB., 1983 – *The fractal geometry of nature*. WH. Freeman, San Francisco, 460 p.

Maramathas A.J. & Boudouvis A.G., 2006. *Manifestation and measurement of the fractal characteristics of karst hydrogeological formations*. Advances in Water Resources, **29**: 112-116. https://doi.org/10.1016/j.advwatres.2005.06.003

Maire R., Jaillet S. & Hobléa F., 2003 – *Karren in Patagonia, a natural laboratory for hydroaeolian dissolution*. In: Ginés A., Knez M., Slabe T. & Dreybrodt W. (Eds.), *Karst rock features – Karren sculpturing*. Carsologica, Publication no. 9, Postojna-Ljubljana, p. 329-348.

Majone B., Bellin A. & Borsato A., 2002 – *Fractal and multifractal analysis of the hydraulic property variations of karst aquifers*. Proceedings of Calibration and Reliability in Groundwater Modelling: A Few Steps Closer to Reality ModelCARE 2002, Prague, Czech Republic, IAHS Publications **277**, 148-154.

Majone B., Bellin A. & Borsato A., 2004 – *Runoff generation in karst catchments: multifractal analysis*. Journal of Hydrology, **294**: 176-195. https://doi.org/10.1016/j.jhydrol.2003.11.042

Nikora V.I. & Sapozhnikov V.B., 1993 – *River network fractal geometry and its computer simulation*. Water Resources Research, **29**: 3569-3575. https://doi.org/10.1029/93WR00966

Pardo-Igúzquiza E., Durán-Valsero J.J. & Rodríguez-Galiano V., 2011 – *Morphometric analysis of three-dimensional networks of karst conduits*. Geomorphology, **132**: 17-28. https://doi.org/10.1016/j.geomorph.2011.04.030

Pardo-Igúzquiza E., Dowd P.A., Xu C. & Durán-Valsero J.J., 2012 – *Stochastic simulation of karst conduit networks*. Advances in Water Resources, **35**: 141-150. https://doi.org/10.1016/j.advwatres.2011.09.014

Pardo-Igúzquiza E., Durán J.J. & Dowd P.A., 2013 – *Automatic detection and delineation of karst terrain depressions and its application in geomorphological mapping and morphometric analysis*. Acta Carsologica, **42 (1)**: 17-24. https://doi.org/10.3986/ac.v42i1.637

Pardo-Igúzquiza E., Durán J.J., Robledo P., Guardiola C., Luque J.A. & Martos S., 2014a – *Fractal modelling of karst conduits*. In: Pardo-Igúzquiza E. Guardiola-Albert C., Heredia J., Moreno-Merino L., Durán J.J. & Vargas-Guzmán J.A. (Eds.), *Mathematics of Planet Earth*. Springer, Berlin, p. 217-220.

Pardo-Igúzquiza E., Durán J.J., Luque-Espinar J.A. & Martos-Rosillo S., 2014b – *Análisis del relieve kárstico mediante el modelo digital de elevaciones. Aplicaciones a la Sierra de las Nieves (provincia de Málaga)*. Boletín Geológico y Minero, **125**: 381-389.

Pardo-Igúzquiza E., Durán J.J. & Robledo-Ardila P.A., 2016a – *Modelado fractal de la distribución del tamaño de dolinas en el macizo kárstico de la Sierra de las Nieves (Málaga, España)*. Cuaternario y Geomorfología, **30**: 61-73.

Pardo-Igúzquiza E., Durán J.J., Robledo-Ardila P., Luque-Espinar J.A., Martos-Rosillo S., Guardiola-Albert C. & Pedrera A., 2016b – *The karst network system of the Sierra de las Nieves (Málaga, Spain). An example of a high relief Mediterranean karst*. Boletín Geológico y Minero, **127**: 193-204.

Pardo-Igúzquiza E., Pulido-Bosch A., López-Chicano M. & Durán J.J., 2016c – *Morphometric analysis of karst depressions on a Mediterranean karst massif*. Geografiska Annaler: Series A, Physical Geography, **98**: 247-263. https://doi.org/10.1111/geoa.12135

Pardo-Igúzquiza E., Durán J.J., Balart D., Borrás E.J., Ferreres J., Quiroga E., Guillén J., Garza X., Marqués F., Robador A., Cabrera A. & Robledo-Ardila P., 2016d – *Morfometría y control geológico de las depresiones kársticas de la Sierra de Tendeñera*. Geo-Temas, **16**: 303-306.

Pardo-Igúzquiza E. & Dowd P.A., 2018. *Fractal analysis of karst landscapes*. Submitted for publication.

Persson B.N.J., 2014 – *On the fractal dimension of rough surfaces*. Tribology Letters, **54**: 99-106. https://doi.org/10.1007/s11249-014-0313-4

Reams M.W., 1992 – *Fractal dimensions of sinkholes*. Geomorphology, **5**: 159-165. https://doi.org/10.1016/0169-555X(92)90063-T

Rodriguez-Iturbe I. & Rinaldo A., 2001 – *Fractal river basins: chance and self- organization*. Cambridge University Press, Cambridge, 549 p.

Sapoval B., 2001- *Universalités et fractals*. Flammarion, Paris, 276 p.

Schroeder M., 1991 – *Fractal, chaos, power laws. Minutes from an infinite paradise*. W.H. Freeman and Company, New York, 429 p.

Shevenell L., 1996. *Analysis of well hydrographs in a karst spring: estimates of specific yields and continuum transmissivities*. Journal of Hydrology, **174**: 331-355. https://doi.org/10.1016/0022-1694(95)02761-0

Song C., Havlin S. & Makse H.A., 2005 – *Self-similarity of complex networks*. Nature, **433**: 392-395. https://doi.org/10.1038/nature03248

Sornette D., 2006 – *Critical phenomena in natural sciences. Chaos, fractals, self-organization and disorder: Concepts and tools*. Springer Series in Synergetics, Berlín, 556 p.

Stanley H.E. & Meakin P., 1988 – *Multifractality phenomena in physics and chemistry*. Nature, **335**: 405-409. https://doi.org/10.1038/335405a0

Stoyan D. & Stoyan H.., 1994 – *Fractals, random shapes and point fields*. John Wiley & Sons, Chichester, 389 p.

Taud H. & Parrot J.-F., 2005 – *Measurement of DEM roughness using the local fractal dimension*. Géomorphologie: relief, processus, environment, **11**: 327-338.

Tarboton D.G., Bras R.L. & Rodríguez-Iturbe I., 1988 – *The fractal nature of river networks*. Water Resources Research, **24**: 1317-1322. https://doi.org/10.1029/WR024i008p01317

Telbisz T., Dragušica H. & Nagy b., 2009 – *Doline morphometric analysis and karst morphology of Biokovo Mt (Croatia) based on field observations and digital terrain analysis*. Croatian Geographical Bulletin, **71**: 2-22. https://doi.org/10.21861/HGG.2009.71.02.01

Turcotte D.L., 1997 – *Fractals and chaos in geology and geophysics*. Cambridge University Press, Cambridge, 398 p. https://doi.org/10.1017/CBO9781139174695

Turcotte D.L., 2007 – *Self-organized complexity in geomorphology: observations and models*. Geomorphology, **91**: 302-310. https://doi.org/10.1016/j.geomorph.2007.04.016

Verbovšek T., 2007 – Fractal analysis of the distribution of cave lengths in Slovenia. *Acta Carsologica*, **36**: 369-377. https://doi.org/10.3986/ac.v36i3.170

White W.B. & White E.L., 2003 – *Conduit fragmentation, cave patterns, and the localization of karst ground water basins: the Appalachians as a test case*. Speleogenesis and Evolution of Karst Aquifers, **1**: 1-15.

Worhington S.R.H. & Ford D.C., 2009 – Self-organized permeability in carbonate aquifers. Ground Water, **47**: 326-336. https://doi.org/10.1111/j.1745-6584.2009.00551.x

Xu T., Moore I.D. & Gallant J.C., 1993 – *Fractals, fractal dimensions and landscapes – a review*. Geomorphology, **8**: 245-262. https://doi.org/10.1016/0169-555X(93)90022-T

Yizhaq H., Ish-Shalom C., Raz E. & Ashkenazy Y., 2017 – *Scale-free distribution of Dead Sea sinkholes: Observations and modeling*. Geophysical Research Letters, **44**: 4944-4952. https://doi.org/10.1002/2017GL073655

Yu B. & Liu W., 2004 – *Fractal Analysis of Permeabilities for Porous Media*. American Institute of Chemical Engineers Journal, **50**: 46-57. https://doi.org/10.1002/aic.10004

International Journal of Speleology	48 (1)	21-32	Tampa, FL (USA)	January 2019

Available online at scholarcommons.usf.edu/ijs

International Journal of Speleology

Official Journal of Union Internationale de Spéléologie

ISOLUTION 1.0: an ISOtope evoLUTION model describing the stable oxygen ($\delta^{18}O$) and carbon ($\delta^{13}C$) isotope values of speleothems

Michael Deininger* and Denis Scholz

[1]Institut für Geowissenschaften, Johannes Gutenberg-Universität Mainz, Johann-Joachim-Becher-Weg 21, 55128 Mainz, Germany

Abstract: Stable oxygen and carbon isotope ratios ($\delta^{13}C$ and $\delta^{18}O$) are the most applied climate and environmental proxies in speleothems allowing to infer past changes in cave drip water $\delta^{13}C$ and $\delta^{18}O$ related to climate and environmental variations from above the cave. However, disequilibrium isotope fractionation processes can modify $\delta^{13}C$ and $\delta^{18}O$ values in speleothems, which is in most cases difficult to estimate due to inter-dependencies on various cave specific parameter. To better understand the effect of these disequilibrium isotope fractionation processes proxy system models were developed in recent years, such as the ISOLUTION model. Here the code of the ISOLUTION model is made available for the public and the speleothem community to be applied to research questions that arise from e.g. monitoring programs that investigate $\delta^{13}C$ and $\delta^{18}O$ values of in situ calcite precipitates on watch glasses or modern speleothem calcite, respectively. Another application of the ISOLUTION model is to investigate the dependence of calcite $\delta^{13}C$ and $\delta^{18}O$ on the variation of one or multiple cave specific parameter, such as cave air temperature, drip interval, cave air pCO_2, Ca^{2+} concentration of the drip water as well as on relative humidity and wind velocity. This allows to quantitatively estimate the effect of disequilibrium isotope fractionation processes in individual caves and drip sites on speleothem $\delta^{13}C$ and $\delta^{18}O$ values for modern and past climates and may help to further elucidate the complex interplay of kinetic and disequilibrium isotope fractionation.

Keywords: speleothems, proxy system model, ISOLUTION

Received 4 July 2018; Revised 6 November 2018; Accepted 8 November 2018

Citation: Deininger M. and Scholz D., 2019. ISOLUTION 1.0: an ISOtope evoLUTION model describing the stable oxygen ($\delta^{18}O$) and carbon ($\delta^{13}C$) isotope values of speleothems. International Journal of Speleology, 48 (1), 21-32. Tampa, FL (USA) ISSN 0392-6672
https://doi.org/10.5038/1827-806X.48.1.2219

INTRODUCTION

Speleothems are valuable continental archives of past climate and environmental change (Fairchild & Baker, 2012). Their greatest advantages are that they can be dated with very high precision by U-series disequilibrium methods (Richards & Dorale, 2003; Cheng et al., 2013) and that they preserve a variety of climate and environmental proxies, such as stable oxygen and carbon isotopes and trace elements (McDermott, 2004; Fairchild & Treble, 2009; Lachniet, 2009). The interpretation of these proxy time series is not always straightforward since the proxy signals in speleothems depend on a complex interplay of processes occurring in or between the atmosphere, the soil and karst above the cave as well as inside the cave (McDermott, 2004; Fairchild & Treble, 2009; Lachniet, 2009; Dreybrodt & Scholz, 2011). However, in most cases the variation of speleothem proxy time series can be linked to past climate changes when the signal-to-noise ratio is very high, i.e., the climate related signal in speleothems overprints any other variations, such as variations in oxygen isotope ratios to changes in the Asian Monsoon (Cheng et al., 2016) or the South American Monsoon (Cruz et al., 2005). Another example are the analyses of stable oxygen isotopes in Central European winter precipitation ($\delta^{18}O_p$), which depend on the North Atlantic Oscillation (Baldini et al., 2008b, Deininger et al., 2016) – the dominating mode of atmospheric climate variability in Europe in winter (Hurrell, 1995). Deininger et al. (2016) show that changes in $\delta^{18}O_p$ dominate speleothem $\delta^{18}O$ signals in Central Europe and that speleothems from Central Europe can be utilised to reconstruct the NAO.

In the last decades, various models have been developed quantitatively describing the processes of $CaCO_3$ dissolution and precipitation (both above

*michael.deininger@uni-mainz.de

and inside the cave, Hendy, 1971; Buhmann & Dreybrodt, 1985a, b; Dreybrodt, 1988), the processes that determine the growth rate and the shape of speleothems (Baker et al., 1998; Dreybrodt, 1999; Kaufmann, 2003; Kaufmann & Dreybrodt, 2004; Mühlinghaus et al., 2007; Romanov et al., 2008a) as well as the processes that determine the preserved stable isotope signals in speleothems (Mühlinghaus et al., 2007; Dreybrodt, 2008; Romanov et al., 2008b, Mühlinghaus et al., 2009; Scholz et al., 2009; Wackerbarth et al., 2010; Dreybrodt & Scholz, 2011; Fohlmeister et al., 2011a, b; Deininger et al., 2012; Dreybrodt & Deininger, 2014). The development of proxy system models that account for in-cave isotope fractionation processes was in large part performed by the speleothem research group DAPHNE (www.fg-daphne.de). The aim of DAPHNE was to improve the quantitative understanding of speleothem proxy signals with a focus on stable oxygen and carbon isotopes ($\delta^{18}O$ and $\delta^{13}C$) and their dependence on climate and environmental variations from above the cave as well as on cave specific parameters, such as cave air temperature, drip rate and soil and cave air pCO_2. DAPHNE conducted, amongst other activities, extensive cave monitoring programs (Riechelmann et al., 2011), performed experiments with synthetic carbonates (Wiedner et al., 2008; Polag et al., 2010) and developed proxy system models for carbon (^{13}C and ^{14}C) and oxygen (^{18}O) isotope signals in cave drip water (Wackerbarth et al., 2010; Fohlmeister et al., 2011a). A particular focus of DAPHNE was to gain a better understanding of the stable carbon and oxygen isotope fractionation processes during the formation of speleothems, i.e., during the precipitation of calcite, when the stable carbon and oxygen isotope signal of the cave drip water is preserved in the speleothem. In this context, a proxy system model was developed to describe the temporal evolution of the oxygen and carbon isotope ratios in a carbonic solution on the surface of a speleothem during calcite precipitation, the ISOtope evoLUTION model (ISOLUTION).

ISOLUTION is coded in MATLAB® and performs a variety of complex, iterative calculations (see below for details). So far, the results of the model have been made available to the community by corresponding publications (Mühlinghaus et al., 2007, 2009; Scholz et al., 2009; Deininger et al., 2012). These enable the reader to derive and understand the qualitative relationships resulting from the model (e.g., that a reduced drip rate – or an increased drip interval – results in increasing $\delta^{13}C$ and $\delta^{18}O$ values of speleothem calcite). However, quantitative information on specific questions are difficult to obtain from these publications alone. In addition, due to the complex interplay of the different processes, the response to a synchronous change in several parameters (e.g., soil pCO_2, cave pCO_2 and drip rate), which is usually the case in natural cave systems, is impossible to derive from the examples discussed in the literature.

Here we make the MATLAB® code of the ISOLUTION model available for the public and the speleothem community – but also to other scientific communities, such as climate modellers and researchers working on data-model comparison. In the following sections, we briefly discuss the basic equations of the model (geochemistry and isotope geochemistry) and the relationships between the individual parameters and the modelled stable oxygen and carbon isotope ratios.

DESCRIPTION OF THE ISOLUTION MODEL

The ISOLUTION model calculates the $\delta^{18}O$ and $\delta^{13}C$ values of the calcite precipitated at the tip of a stalagmite (i.e., at the growth axis of the stalagmite) from a carbonic solution (i.e., containing dissolved inorganic carbon, DIC) that is super-saturated with respect to calcite. This carbonic solution is fed by water that drips from the cave ceiling and is referred to as cave drip water in the following. ISOLUTION accounts for isotope fractionation processes during the precipitation of calcite that we refer to as disequilibrium isotope fractionation or effects in the following. We emphasise that disequilibrium isotope fractionation should not be confused with kinetic isotope fractionation. Kinetic isotope fractionation is – in comparison to equilibrium isotope fractionation – described by a different (kinetic) isotope fractionation factor, α_k. Kinetic isotope fractionation effects include for example the relationship of α_k for ^{18}O with the calcite precipitation rate and pH that is observed in beaker experiments by (Dietzel et al., 2009). In case of the dependence of α_k on the calcite precipitation rate alternative theoretical models are proposed inferring that the ratio of the calcite precipitation rate and the dissolution rate (DePaolo, 2011; Watkins et al., 2014) or the molecular diffusion of oxygen isotopes (Watson, 2004) in the calcite crystal are responsible for the observed relationships. In contrast, disequilibrium isotope fractionation accounts for all (chemical and isotope) reactions/processes between molecules participating in the reaction of calcite precipitation, which disturb the isotope equilibrium between the individual molecules. These include the conversion of HCO_3^- to CO_2, H_2O and $CaCO_3$ (calcite) during calcite precipitation (Eq. 1) (Mühlinghaus et al., 2009; Scholz et al., 2009), the oxygen isotope exchange between H_2O and HCO_3^- during the hydration and hydroxylation of CO_2 (Scholz et al., 2009) or the oxygen isotope fractionation during the evaporation and condensation of H_2O from the solution layer or the cave air, respectively (Deininger et al., 2012; Dreybrodt & Deininger, 2014). Thus, disequilibrium isotope effects can result in $\delta^{13}C$ and $\delta^{18}O$ values deviating from the value expected for isotope equilibrium. Theoretical and empirical studies infer that the degree to which disequilibrium isotope effects alter the equilibrium $\delta^{13}C$ and $\delta^{18}O$ values in speleothems in dependence on cave specific parameters varies with the drip interval (Mühlinghaus et al., 2009; Deininger et al., 2012; Riechelmann et al., 2013). Therefore, these effects are expected to be important for drip sites where the drip interval is long and/or varies between short and long values (see below for a detailed discussion).

This section is subdivided into two paragraphs: First, we briefly introduce the basics of the geochemistry of the CO_2-H_2O-$CaCO_3$-system (2.1.1) and the isotope

mass balance model (2.1.2). Then (2.2) we explain the individual functions of the ISOLUTION model. A list of parameters used by the ISOLUTION model and in the following text is given in Table 1.

Table 1. Nomenclature of parameters used by the ISOLUTION model.

Nomenclature		
	Variable	**Explanation**
Model variables	$\delta^{13}C$ $\delta^{18}O$ T_C	Carbon isotope ratio ($^{13}C/^{12}C$) of the drip water DIC (HCO_3^-) expressed in the delta-notation relative to VPDB [per mil] Oxygen isotope ratio ($^{18}O/^{16}O$) of the drip water (H_2O) expressed in the delta-notation relative to VSMOW [per mil] Cave air temperature [°C]
	d	Drip interval [s], i.e., the time between two subsequent drops dripping from the cave ceiling
	$pCO_{2.cave}$	$pCO_{2.cave}$ [ppmV]: CO_2 partial pressure of the cave air
	$pCO_{2.drip}$	$pCO_{2.drip}$ [ppmV]: the equivalent of the pCO_2 required to get the Ca^{2+} concentration of the cave drip water. This pCO_2 level can be calculated from the Ca^{2+} concentration [mol/l] prior to the application of ISOLUTION using the MATLAB function CALCPCO2.m. Note that no other ions, such as Sr^{2+} and Mg^{2+} are taken into account.
	Φ	The mixing parameter describes the mixing between the new, impacting drip and the existing solution on the surface of the speleothem. Due to splashing effects, the contribution of the new drop to the solution may be variable. A mixing parameter of 1 means that the new drop contributes 100% to the existing solution, i.e., it replaces the entire old solution. Φ = 0.5 means that the new solution contains 50% of the previous solution and 50% of the new drop (see Mühlinghaus et al., 2007; 2009, for details).
Other parameters used in the manuscript or by the ISOLUTION model	T_K	Cave air temperature [K]
	$^x\alpha_y$	$^x\alpha_y$ is the isotope fractionation factor between two species. x indicates the respective isotope system, i.e., 18 for oxygen isotopes and 13 for carbon isotopes. y describes the corresponding physical or chemical reaction. For instance, if y is calcite/H_2O, the fractionation factor refers to isotope fractionation between water and calcite.
	^xR_y	R denotes the isotope ratio. As for fractionation factors, x is 18 for the oxygen isotope system and 13 for the carbon isotope. y describes the corresponding physical or chemical reaction, e.g., $^{18}R_{HCO3^-}$ is the oxygen isotope ratio of bicarbonate (HCO_3^-).
	δ^xZ_y	δ^xZ_y is the expression of the isotope ratios in the delta notation ($\delta^xZ_y = {}^xR_y/{}^xR_{st} - 1$). $^{18}R_{st}$ is the value for internationally accepted standards (VPDB for all carbon bearing species and VSMOW for water). Note that δ^xZ_y is $\delta^{18}O_y$ for oxygen isotopes and $\delta^{13}C_y$ for carbon isotopes.
	N_y	N [mol] is the molar mass of species y
	n_y	n [mol/l] is the concentration of species y
	T	time [s]
	τ_P	$\tau_P = \delta/\lambda_P$ is calculated from the thickness, δ, of the solution layer on the speleothem surface and the rate constant λ_P. λ_P depends on temperature. This value are taken from Dreybrodt and Scholz (2011), based on calculations (Baker et al., 1998).
	τ_{OEX}	τ_{OEX} is the characteristic time constant for oxygen isotope exchange between water and HCO_3^- and is taken from Dreybrodt and Scholz (2011), based on experiments by Beck et al. (2005).

Theoretical background

Geochemistry

The ISOLUTION model is based on the chemical equations of the CO_2-H_2O-$CaCO_3$-system (e.g., Dreybrodt 1988) including the chemical equilibrium between Ca^{2+} and HCO_3^- with $CaCO_3$, CO_2, and H_2O (Eq. 1). This equation basically describes the precipitation (and dissolution) of $CaCO_3$ in case of a chemical disequilibrium between the right and left-hand side of the equation:

$$Ca^{2+} + 2HCO_3^- \rightleftharpoons CaCO_3 + CO_2 + H_2O \qquad (1)$$

Note that Eq. (1) is valid for the majority of cave systems, where the cave drip water has a pH-value of ca. 8 and the DIC mainly consists of HCO_3^-.

For calcite precipitation (i.e., stalagmite growth), the temporal evolution of the Ca^{2+} concentration of the cave drip water at the tip of the stalagmite is given by (Eq. 2) (Kaufmann, 2003):

$$Ca^{2+}(t) = \left(Ca^{2+}(t_0) - Ca^{2+}_{ap}\right) \cdot e^{-\tau_P t} + Ca^{2+}_{ap} \qquad (2)$$

whereat Ca^{2+} is the calcium concentration, Ca^{2+}_{ap} is the apparent Ca^{2+} concentration (both in mol/l), τ_P is the time constant for calcite precipitation and t is the time (both in seconds). The temporal evolution of the Ca^{2+} concentration depends on the initial Ca^{2+} concentration of the cave drip water, $Ca^{2+}(t_0)$, which is defined as the Ca^{2+} concentration at time t_0 = 0 s, when the drip impinges on the speleothem surface. The initial Ca^{2+} concentration is determined mainly by the available CO_2 during the $CaCO_3$ dissolution in the karst (Hendy, 1971), which is parameterised by the drip water CO_2 in ISOLUTION (i.e., the required CO_2 partial pressure in air to obtain an observed Ca^{2+} concentration in the cave drip water). The apparent Ca^{2+} concentration, Ca^{2+}_{ap}, denominates the 'equilibrium' Ca^{2+} concentration of the drip water with respect to the cave pCO_2 and inhibiting effects during calcite precipitation. It is calculated by

Ca^{2+}_{ap} = $Ca^{2+}_{eq}/\sqrt{0.8}$, whereat Ca^{2+}_{eq} is the Ca^{2+} concentration with respect to the cave air pCO_2 and the factor $1/\sqrt{0.8}$ accounts for the inhibiting effects (Dreybrodt et al., 1997; Kaufmann, 2003). Therefore, the amount of excess Ca^{2+} ($Ca^{2+}(t_0)$-Ca^{2+}_{ap}) that is available for calcite precipitation and speleothem formation, respectively, depends on the difference between the drip water pCO_2 and cave air pCO_2. The precipitation rate constant, λ_P, is approximated by a cubic spline (Eq. 3) using the values of Dreybrodt & Scholz (2011), which are based on the results of Baker et al. (1998) who used the theoretical model for calcite precipitation derived by Buhmann & Dreybrodt (1985a, b) and Dreybrodt (1988, 1999):

$$\lambda_p = \left(1.188 \cdot T_C^3 - 1.29 \cdot T_C^2 + 787.5 \cdot T_C + 4844\right) \cdot 10^{-11} \left[\frac{m}{s}\right] \quad (3)$$

T_C is the cave air temperature in °C. Typical values for τ_P are c. 2,000, 740, and 350 s for cave air temperature of 0, 10, and 20°C, respectively. These values are found to be in good agreement with empirical observations (Baker et al., 1998) and have been used also in other studies that investigate growth rate related effects in speleothem stable isotope time series (Baldini et al., 2008a).

A similar equation can be derived for the evolution of the HCO_3^- concentration by considering the condition of electro neutrality (Eq. 4):

$$HCO_3^-(t) = \left(HCO_3^-(t_0) - HCO_{3ap}^-\right) \cdot e^{-\tau_P t} + HCO_{3ap}^- \quad (4)$$

HCO_3^- is the HCO_3^- concentration of the solution (mol/l) and $HCO_{3\,ap}^-$ is the apparent HCO_3^- concentration (both in mol/l). The time constant of calcite precipitation (τ_P) is determined by Δ/λ_P: Δ is the thickness of the solution film at the tip of the stalagmite, and λ_P is the precipitation rate constant for a film thickness of 100 µm (Eq. 3). Both τ_P and time (t) are measured in seconds.

Carbon and oxygen isotope geochemistry

The calculation of speleothem calcite $\delta^{13}C$ and $\delta^{18}O$ values by the ISOLUTION model is based on a multi-box mass-balance approach, first described by Rayleigh (1902), which has been used to calculate the change of isotope ratios in various disciplines of isotope geochemistry (Mook & de Vries, 2000; Mook, 2006). The fundamental principle of this mass-balance approach is that the number (amount) of rare isotopes (e.g., ^{18}O or ^{13}C) is constant for the entire system at all times (i.e., a closed system) irrespective of the individual isotope fractionation (or its 'strength') processes and the geochemical reactions within the system. For calcite precipitation (Eq. 1), this means that even if the total number of ^{18}O atoms contained in the HCO_3^- reservoir changes with time during precipitation of calcite, the total number of ^{18}O atoms contained in the whole system (i.e., HCO_3^-, CO_2, H_2O, and $CaCO_3$) is constant. We note that the Rayleigh approach forming the basis of ISOLUTION has been a matter of debate for several years (Dreybrodt & Scholz, 2011; Dreybrodt, 2016; Dreybrodt & Romanov, 2016). However, the intention of this paper is to outline the basic principles of ISOLUTION and to make it available to the public rather than a critical discussion of its basics. In this context, the reader is referred to the corresponding publications (Dreybrodt & Scholz, 2011; Dreybrodt, 2016; Dreybrodt & Romanov, 2016).

In general, an isotope ratio, R, is defined as the ratio between the rare and the abundant isotope of the same element, which are in the case of stable oxygen and carbon isotopes, $^{18}R = {}^{18}O/{}^{16}O$ for oxygen and $^{13}R = {}^{13}C/{}^{12}C$ for carbon isotopes. These ratios are usually translated into the δ-notation by reporting the relative deviation of the isotope ratio from a standard (R_{st}): $\delta = (R/R_{st}-1)$. In case of the ISOLUTION model, the VPDB standards are used for carbonates, and the VSMOW standard for water.

Here we recall the very basic mass balance multi-box model, which only accounts for one process/reaction progressively removing molecules from a reservoir (e.g., evaporation of water from a pond; Eq. 5). This process is accompanied by isotope fraction described by the isotope fractionation factor α. Furthermore, the educt is assumed to be removed instantaneously to permit any further interaction with the reservoir. Note that it is not removed from the system because this would be a violation of the mass balance. Considering a reservoir of N molecules (e.g., H_2O or HCO_3^-) with an isotope ratio R_0 at time t_0 = 0 s, from which molecules are progressively removed at a specific rate dN (note that the rate can change with time as it is the case for calcite precipitation, Eq. 2) by a certain process or reaction (e.g., evaporation of water), the equation for the mass balance of the rare isotopes is given by:

$$\frac{R \cdot N}{1+R} = \frac{(R+dR)}{1+R+dR} - \frac{\alpha \cdot R \cdot dN}{1+\alpha \cdot R} \quad (5)$$

The term on the left-hand side of the equation is the number of rare isotopes before the mass or number of molecules, dN, has been removed from the reservoir, whereas the right-hand side is the sum of the number of rare isotopes remaining in the reservoir and the number of rare isotopes that were removed. To a good approximation, (1 + R + dR) and (1 + αR) are ≈(1 + R) because dR is much smaller than R and α is approximately 1. Further, if products of differentials are neglected, Eq. (5) can be simplified to Eq. 6a and 6b, respectively.

$$R \cdot N \approx R \cdot N + N \cdot dR + R \cdot dN + \alpha \cdot R \cdot (-dN) \quad (6a)$$

$$0 \approx N \cdot dR + R \cdot dN + \alpha \cdot R \cdot (-dN) \quad (6b)$$

The solution of this differential equation (Eq. 6b), which describes the temporal evolution of the isotope ratio, R, of the reservoir is then given by:

$$R(t) = R_0 \cdot \left(\frac{N(t)}{N_0}\right)^{\alpha-1} \quad (7)$$

Equation 7 describes the temporal evolution of the isotope ratio R of the reservoir, which depends on the isotope ratio and the number of molecules at time t = 0 s, R_0, and N_0, the temporal evolution of the number of molecules, N(t), whereat t is the time, and the isotope fractionation factor α. If the mass balance is more complicated than this example, which is the case for the CO_2-H_2O-$CaCO_3$-system, it is also possible from Eq. (6b) to calculate the change of the isotope

ratio of the reservoir, dR, and the new isotope ratio of the reservoir, R_{new}, as follows:

$$dR = (\alpha - 1) R_{old} \cdot \frac{dN}{N} \Rightarrow R_{new} = R_{old} + dR \qquad (8)$$

In Eq. 8, dR is the change in the isotope ratio of the molecules in the reservoir that is caused by the removal of molecules described by dN, which is accompanied by isotope fraction effects. The change of the isotope ratio dR depends on the isotope ratio before the removal of molecules, R_{old}, as well as on the relative change of the molecules (dN/N) and the isotope fractionation factor α. A similar approach can be inferred for the weighted mean isotope ratio of the fraction removed from the reservoir (e.g., the precipitated calcite) by summing up all fractions weighted by the number of molecules dN removed from the reservoir. This is necessary because the reaction/mass rates can change with time like it is the case for calcite precipitation, where dN progressively decreases with time (Eq. 2).

The previous example is the most simple mass balance model. However, it nicely shows the mathematical structure of the ISOLUTION model. ISOLUTION accounts for additional processes/reactions and has more reservoirs (Table 2). In detail, the current version of ISOLUTION includes reservoirs for HCO_3^-, liquid and vaporous H_2O ($H2O_l$ and $H2O_v$). The processes and reactions included in the ISOLUTION model are the precipitation of calcite (P1), the oxygen isotope exchange between $H2O_l$ and HCO_3^- (P2) and the evaporation of liquid water ($H2O_l$) as well as the condensation of water vapour ($H2O_v$) (P3). We refer to the original publications for a detailed derivation of the individual mass balance models for each reservoir and the discussion of the results (Mühlinghaus et al., 2007, 2009; Scholz et al., 2009; Deininger et al., 2012).

Table 2. Summary of reservoirs (R) and physical and chemical processes (P) potentially affecting the $\delta^{18}O$ and $\delta^{13}C$ value of calcite accounted for in the ISOLUTION model.

Number	Reservoirs and reactions/ processes	Relevance	Explanation	Publication
$^{18}R1$ $^{13}R1$	HCO_3^-	$\delta^{13}C$, $\delta^{13}O$	HCO_3^- reservoir	(Mühlinghaus et al., 2007) (only $\delta^{13}C$) (Mühlinghaus et al., 2009)
$^{18}R2$	H_2O_l	$\delta^{13}O$	Reservoir of liquid water	(Mühlinghaus et al., 2009) (Scholz et al., 2009) (Deininger et al., 2012)
$^{18}R3$	H_2O_v	$\delta^{13}O$	Reservoir of water vapour	(Deininger et al., 2012)
$^{18}P1.1$ $^{13}P1.1$	$HCO_3^- \rightarrow CaCO_3$	$\delta^{13}C$, $\delta^{13}O$	Conversion of HCO_3^- into calcite during precipitation of calcite	(Mühlinghaus et al., 2007) (only $\delta^{13}C$) (Mühlinghaus et al., 2009) (Scholz et al., 2009)
$^{18}P1.2$ $^{13}P1.2$	$HCO_3^- \rightarrow CO_2$	$\delta^{13}C$, $\delta^{13}O$	Conversion of HCO_3^- into dissolved CO_2 during precipitation of calcite	(Mühlinghaus et al., 2007) (only $\delta^{13}C$) (Mühlinghaus et al., 2009) (Scholz et al., 2009)
$^{18}P1.3$	$HCO_3^- \rightarrow H_2O_l$	$\delta^{13}O$	Conversion of HCO_3^- into liquid H_2O during precipitation of calcite	(Mühlinghaus et al., 2009) (Scholz et al., 2009)
$^{18}P2.1$	$HCO_3^- \rightarrow H_2O_l$	$\delta^{13}O$	Oxygen isotope exchange between HCO_3^- and liquid H_2O	(Mühlinghaus et al., 2009) (Scholz et al., 2009)
$^{18}P2.2$	$H_2O_l \rightarrow HCO_3^-$	$\delta^{13}O$	Oxygen isotope exchange between HCO_3^- and liquid H_2O	(Mühlinghaus et al., 2009) (Scholz et al., 2009)
$^{18}P3.1$	$H_2O_v \rightarrow H_2O_l$	$\delta^{13}O$	Condensation of vaporous H_2O	(Deininger et al., 2012)
$^{18}P3.1$	$H_2O_l \rightarrow H_2O_v$	$\delta^{13}O$	Evaporation of liquid H_2O	(Deininger et al., 2012)

The average isotope ratio of the calcite precipitated during a specific time interval (e.g., between two subsequent drops) is calculated as the weighted mean of the isotope ratio of the precipitated calcite that has been converted from HCO_3^- (Eq. 9):

$$\overline{R} = \frac{\sum_i dN(t_i) \cdot R_{calcite}(t_i)}{\sum_i dN(t_i)} \qquad (9)$$

The calcite isotope ratio at time t_i, $R_{calcite}(t_i)$ (Eq. 10), is calculated from the isotope ratio of HCO_3^-, R_{HCO3-}, and the isotope fractionation factor for the conversion of HCO_3^- to calcite ($\alpha_{calcite/HCO3-}$).

$$R_{calcite}(t_i) = \alpha_{calcite/HCO_3^-} \cdot R_{HCO_3}(t_i) = \\ = \alpha_{calcite/H_2O} \cdot \alpha_{H_2O/HCO_3^-} \cdot R_{HCO_3}(t_i) \qquad (10)$$

The isotope fractionation factor, $\alpha_{calcite/HCO3-}$, is derived from the combination of the isotope fractionation factors for $HCO_3^- \rightarrow H_2O$ ($\alpha_{H2O/HCO3-}$) and $H_2O \rightarrow$ calcite ($\alpha_{calcite/H2O}$). See section 2.2 for a more detailed discussion.

MATLAB-functions of the ISOLUTION model

The ISOLUTION model consists of nine individual functions (Table 3) programmed in MATLAB®. These are subdivided into different levels: level 0 functions start a routine, whereas higher level functions are invoked by lower level functions. In the following, the individual functions are briefly described.

CALCPCO2.m

Function CALCPCO2.m converts Ca^{2+} concentrations (given in mol/l) in a pCO_2-equivalent using the mass laws of the CO_2-H_2O-$CaCO_3$-system assuming a chemical equilibrium between all chemical species. CALCPCO2.m does not consider any other ions occurring in natural cave drip waters, such as Mg^{2+}. CALCPCO2.m firstly calculates the Ca^{2+} concentrations for pCO_2 values ranging from 0 to 1,000,000 ppmV subdivided into ten equidistant intervals (i.e., the Ca^{2+} concentration for 0, 100,000, 200,000 ppmV, etc.). In a second step, the function finds the interval mirroring

Table 3. ISOLUTION MATLAB® functions.

#	Function	Level
1	CALCPCO2.m	0
2	ISOLUTION.m	0
3	ISOTOPE_CALCITE.m	1
4	ISOTOPE_EVOLUTION.m	2
5	ISOTOPE_EVOLUTION_MEAN.m	2
6	CONCENTRATIONS.m	2, 3
7	CONSTANTS.m	2, 3
8	EVAPORATION.m	2, 3
9	FRACTIONATION_FACTORS.m	2, 3

the real Ca^{2+} concentration (e.g., the interval from 0 to 100,000 ppmV). Then step one and two are repeated until the real and the calculated Ca^{2+} concentration are similar, i.e., the pCO_2 interval mirroring the real Ca^{2+} concentration is again subdivided into ten equidistant intervals, and then step 2 is repeated.

ISOLUTION.m

ISOLUTION.m starts the ISOLUTION model and allows the user to choose between two different options: **1)** Calculation of a single calcite $\delta^{13}C$ and $\delta^{18}O$ value for a given set of input parameters (i.e., temperature, drip interval, drip water pCO_2 (calculated by CALCPCO2.m), cave air pCO_2, relative humidity, wind velocity, mixing parameter, initial drip water $\delta^{13}C$ (of the DIC) and $\delta^{18}O$ (of liquid H_2O) values prior to calcite precipitation). The user can enter these parameters into the MATLAB command window. The $\delta^{13}C$ and $\delta^{18}O$ values are calculated by the function ISOTOPE_CALCITE.m using the values of the input parameters. **2)** Calculation of the evolution (sensitivity) of calcite $\delta^{13}C$ and $\delta^{18}O$ values in dependence on a user-defined interval for one of the following input parameters: temperature, drip interval, drip water pCO_2, cave air pCO_2, relative humidity and wind velocity. The other input parameters are kept constant. The user again enters these values into the MATLAB command window. The calcite $\delta^{13}C$ and $\delta^{18}O$ values are again calculated by the function ISOTOPE_CALCITE.m.

2.2.3 ISOTOPE_CALCITE.m

ISOTOPE_CALCITE.m calculates a single calcite $\delta^{13}C$ and $\delta^{18}O$ value for a given set of input parameters. First, the equilibrium $\delta^{13}C$ and $\delta^{18}O$ values of the HCO_3^- at the tip of the stalagmite – which vary in dependence on the mixing parameter and other parameters – are calculated by the function ISOTOPE_EVOLUTION.m. These equilibrium values are usually established after a few drops, depending, however, on the mixing parameter (Mühlinghaus et al., 2009; Deininger et al., 2012). As a rule of thumb, the number of drops until isotope equilibrium has been established increases with decreasing mixing parameter, but is usually lower than 20. Based on these equilibrium isotope values, the temporal evolution of the $\delta^{13}C$ and $\delta^{18}O$ values of the HCO_3^- is then calculated for the user-defined drip interval by the function ISOTOPE_EVOLUTION_MEAN.m. This temporal evolution is used in turn to calculate the mean $\delta^{13}C$ and $\delta^{18}O$ values of the precipitated calcite.

ISOTOPE_EVOLUTION.m

ISOTOPE_EVOLUTION.m calculates the equilibrium $\delta^{13}C$ and $\delta^{18}O$ values of HCO_3^-, the concentration of HCO_3^- and the amount of liquid H_2O, which change in case of calcite precipitation and evaporation of water, respectively. The stable isotope and chemical equilibrium is usually established within 10 to 20 drops, respectively.

ISOTOPE_EVOLUTION_MEAN.m

ISOTOPE_EVOLUTION_MEAN.m calculates the weighted mean (Eq. 9) of the $\delta^{13}C$ and $\delta^{18}O$ values of HCO_3^- that is used to calculate the $\delta^{13}C$ and $\delta^{18}O$ values of the precipitated calcite using the isotopic and chemical equilibrium values estimated by ISOTOPE_EVOLUTION.m.

CONCENTRATIONS.m

Function CONCENTRATIONS.m calculates the equilibrium concentrations of the CO_2-H_2O-$CaCO_3$-system in dependence of a pCO_2 value and temperature based on equations of Dreybrodt (1988).

CONSTANTS.m

CONSTANTS.m lists all constants that are used, such as the stable oxygen and carbon isotope ratios of VPDB and VSMOW, respectively.

EVAPORATION.m

EVAPORATION.m calculates the evaporation rate in dependence of temperature, relative humidity and wind velocity (Deininger et al., 2012).

FRACTIONATION_FACTORS.m

FRACTIONATION_FACTORS.m lists all stable carbon and oxygen isotope fractionation factors used by ISOLUTION (See (Deininger et al., 2012) for detail). The original publication of ISOLUTION (Deininger et al., 2012) used the fractionation factor of (Kim & O'Neil, 1997) to describe equilibrium isotope fractionation between water and calcite, $\alpha_{calcite/H2O}$. The updated version of ISOLUTION.m described here allows the user in addition to choose between the $\alpha_{calcite/H2O}$ values of Johnston et al. (2013), Tremaine et al. (2011), and Coplen (2007). Although different fractionation factors result in different absolute temperatures, we note that the temperature sensitivity of all fractionation factors is very similar. Hence, if ISOLUTION is applied to estimate palaeo-temperatures, the calculated relative temperature changes should be very similar irrespective of the choice of $\alpha_{calcite/H2O}$.

RESULTS

Disequilibrium isotope fractionation effects

As outlined in the previous sections, ISOLUTION only uses equilibrium isotope fractionation factors. Thus, kinetic isotope effects, which most likely have a significant effect in many speleothems (Mickler et al., 2006; McDermott et al., 2011) are not accounted for. However, since progressive precipitation of $CaCO_3$ from the thin solution layer disturbs the initial carbon and oxygen isotope equilibrium (Scholz et al., 2009),

the modelled $\delta^{13}C$ and $\delta^{18}O$ values of the precipitated speleothem calcite are not in equilibrium with the drip water initially impinging on the speleothem surface (or the water collected in the framework of cave monitoring studies). In order to avoid the common mistake in the speleothem literature that this disequilibrium is related to kinetic isotope fractionation, we use the term disequilibrium isotope fractionation throughout this paper.

The degree of isotope disequilibrium introduced to the modelled speleothem $\delta^{18}O$ and $\delta^{13}C$ values strongly depends on the input parameters of the ISOLUTION model. The dependence of the $\delta^{18}O$ and $\delta^{13}C$ values of the precipitated calcite on the individual cave and drip site specific parameters can be deduced from sensitivity studies (Mühlinghaus et al., 2009; Deininger et al., 2012). Table 4 summarises the qualitative response of the $\delta^{18}O$ and $\delta^{13}C$ values on changes of the individual parameters. For most variables, the qualitative effect is similar for $\delta^{13}C$ and $\delta^{18}O$ values. For instance, if the drip interval increases, this results in increasing $\delta^{13}C$ as well as $\delta^{18}O$ values (Table 4). If the cave air pCO_2 increases (implying reduced supersaturation of the cave drip water with resepct to calcite, Eq. 2), the resulting values will be lower for both $\delta^{13}C$ and $\delta^{18}O$ (Table 4). The exception is temperature, which has opposing effect on the $\delta^{13}C$ and $\delta^{18}O$ values (Table 4). If cave air temperature increases, speleothem calcite $\delta^{18}O$ values will be lower, whereas calcite $\delta^{13}C$ values will increase.

Table 4. Compilation of the qualitative response of the $\delta^{18}O$ and $\delta^{13}C$ values of the precipitated calcite on changes of the individual cave parameters. Arrows pointing upwards (downwards) indicate increasing (decreasing) $\delta^{13}C$ and $\delta^{18}O$ values, respectively.

Change in corresponding parameter	Temperature for $\delta^{18}O$	Temperature for $\delta^{13}C$	Drip interval	Drip pCO_2	Cave air pCO_2	Rel. humidity	Wind velocity	F
↑	↓	↑	↑	↑	↓	↓	↑	↓
↓	↑	↓	↓	↓	↑	↑	↓	↑

Beside these qualitative responses, the ISOLUTION model can be used to evaluate the importance of individual cave-specific parameters for calcite $\delta^{13}C$ and $\delta^{18}O$ values at individual cave and drip sites, respectively. For example, cave air pCO_2 will not be important if it is constant (e.g., in case of little or no cave ventilation (Riechelmann et al., 2011). In contrast, if cave air pCO_2 varies on the order of 1000 ppmV throughout the year (Spötl et al., 2005; Mattey et al., 2008), it may have a significant effect on $\delta^{13}C$ and $\delta^{18}O$ values of speleothem calcite. To demonstrate the application of the ISOLUTION model for such questions, we investigate the dependence of speleothem $\delta^{18}O$ and $\delta^{13}C$ values for a cave with the following conditions: the cave air temperature is 10°C, we consider two drip sites with very different drip intervals of 100 (drip site 1) and 1500 s (drip site 2), drip water pCO_2 is 5,000 ppmV and cave air pCO_2 is 1,000 ppmV. Furthermore, relative humidity is 100%, and we assume no wind flow (wind velocity is 0 m/s). We also assume that no mixing between the solution film on the speleothem surface and the impinging drop occurs, which corresponds to a mixing parameter, ϕ, of 1.

To investigate the effect of changes in these parameters on the $\delta^{18}O$ and $\delta^{13}C$ values of the precipitated speleothem calcite, we vary them in reasonable intervals. For this simulation, we select option 2 of the ISOLUTION model and select the variable that is examined. The results are illustrated in Figure 1 (examples 1 and 2), Figure 2 (examples 3 and 4) and Figure 3 (example 5).

Example (1) Varying temperature: Cave air temperature can experience temporal variations ranging from diurnal, seasonal, annual or even longer time scales (Spötl et al., 2005; Tremaine et al., 2011). In addition, it may depend on the location inside the cave where it is recorded. We would expect that temperature vary considerably close to a cave entrance, while temperature changes in remote chambers of a cave should be small. This has, for instance, been observed in a monitoring study of Obir Cave, a dynamically ventilated cave, where the seasonal temperature change of a chamber closest to the entrance (12 meters) is about 4°C, whereas remote chambers only experience seasonal temperature changes that are less than 0.5°C (Spötl et al., 2005). ISOLUTION modelled changes in calcite $\delta^{18}O$ and $\delta^{13}C$ infer changes in $\delta^{18}O$ of approximately -0.2‰/°C, whilst the corresponding change in $\delta^{13}C$ is 0.05‰/°C (Fig. 1a and b). Hence, the observed temperature changes in Obir Cave would cause changes in $\delta^{18}O$ of about 0.8‰ in the entrance part and <0.1‰ in remote chambers. Changes in $\delta^{13}C$ are 0.2‰ and <0.025‰. We note again that the change in $\delta^{18}O$ is more or less invariant on the used fractionation factor $\alpha_{calcite/H2O}$, because the temperature dependence is nearly identical for all fractionation factors. Furthermore, while speleothem $\delta^{18}O$ and $\delta^{13}C$ values linearly respond to temperature changes for low drip intervals, the response is non-linear for long drip intervals (Fig. 1, the non-linearity cannot be resolved for $\delta^{18}O$). The reason for this non-linearity is the temperature dependence of the precipitation rate and other isotope fractionation effects during precipitation of calcite (Table 2) (Mühlinghaus et al., 2009; Deininger et al., 2012).

Example (2) Varying drip interval: Drip intervals can show by far the largest variability within caves (e.g., Genty et al., 2014), which is a result of the complexity of karst hydrology (e.g., Bradley et al., 2010) and the water balance of the atmosphere-soil-karst system, which may depend on rain- and snowfall, respectively, and evapo-transpiration – depending in turn on temperature, density and type of vegetation and soil thickness and permeability. The effect of the drip interval of different drip sites inside a single cave (short vs. long) has been shown

to directly affect the recorded speleothem $\delta^{18}O$ and $\delta^{13}C$ values (Riechelmann et al., 2013). The reason for the dependence of the $\delta^{18}O$ and $\delta^{13}C$ values on drip interval is related to the temporal evolution of the $\delta^{18}O$ and $\delta^{13}C$ values of the dissolved HCO_3^- during the precipitation of calcite. While calcite is progressively precipitated from the drip water, isotope fractionation effects (Table 2) result in increasing $\delta^{18}O$ and $\delta^{13}C$ values in HCO_3^- in turn causing increased calcite $\delta^{18}O$ and $\delta^{13}C$ values (Scholz et al., 2009). With increasing drip intervals, the influence of these processes becomes stronger and result in higher $\delta^{13}C$ and $\delta^{18}O$ values (Mühlinghaus et al., 2009; Deininger et al., 2012) (Figs. 1c and d). For very long drip intervals, the drip water may reach chemical equilibrium within the cave pCO_2, and the calcite $\delta^{18}O$ and $\delta^{13}C$ values converge to an upper value that depend also on the other cave parameters (Mühlinghaus et al., 2009).

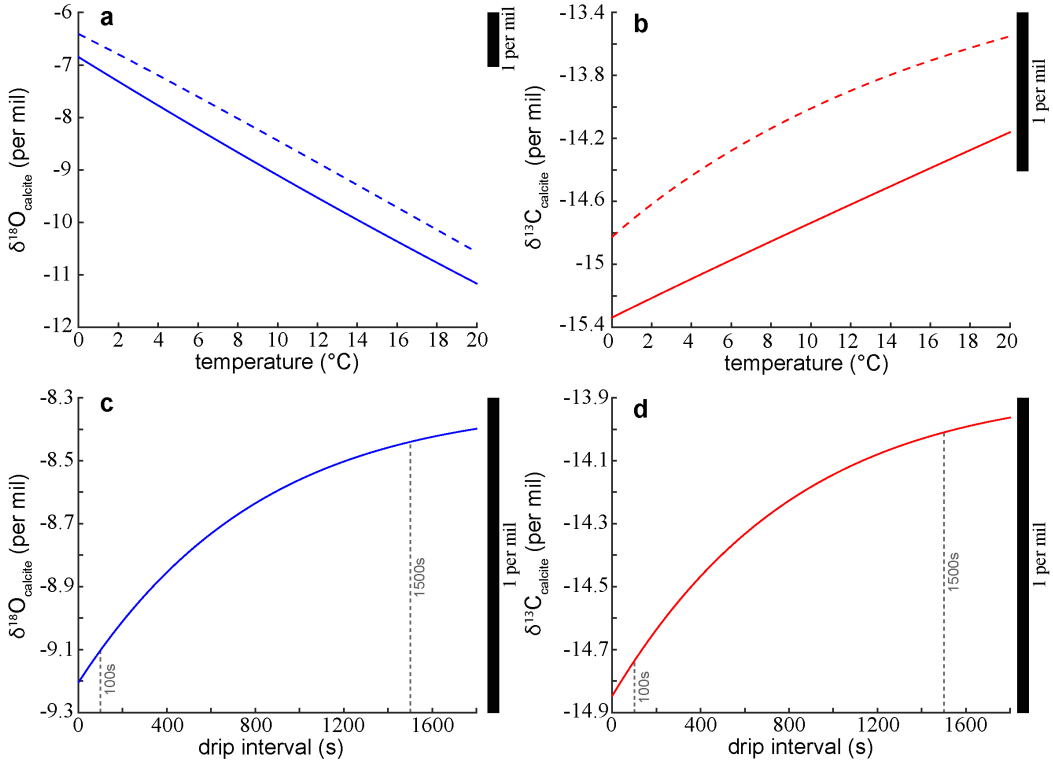

Fig. 1. Response of speleothem calcite $\delta^{18}O$ (blue) and $\delta^{13}C$ (red) values on changes in temperature and drip interval. For these experiments cave temperature is varied from 0 to 20°C (a and b) and the drip interval from 1 to 1,800 s (c and d). The drip water and cave air pCO_2 are kept constant at 5,000 and 1,000 ppmV, respectively. Furthermore, relative humidity is 100%, and we assume no wind flow (wind velocity is 0 m/s). Panels a) and b) illustrate the evolution of the $\delta^{18}O$ and $\delta^{13}C$ values in response to temperature changes for a drip interval of 100 (straight line) and 1,500 s (dashed line). Panels c) and d) show the evolution of the $\delta^{18}O$ and $\delta^{13}C$ values for varying drip interval. The black bar indicates a change of 1‰.

Examples (3) and (4) Varying Ca^{2+} concentration (drip water pCO_2) and cave air pCO_2: The excess Ca^{2+} concentration, which is equivalent to the difference of the Ca^{2+} concentrations for the drip water pCO_2 and the cave air pCO_2 (Eq. 2) determines the maximum amount of Ca^{2+} available for calcite precipitation and in turn speleothem formation. Hence, if the drip water pCO_2 increases while the cave air pCO_2 is constant the excess Ca^{2+} concentration increases whereas if the cave air pCO_2 increases at a constant drip water pCO_2 the excess Ca^{2+} concentration decreases; and vice versa for a decreased drip water pCO_2 and a decreased cave air pCO_2. Depending on the drip interval, the variations of the excess Ca^{2+} concentration can change the degree to which disequilibrium isotope effects modify calcite $\delta^{18}O$ and $\delta^{13}C$ values. In principle, if the drip interval is longer than approximately 4 times τ_p, the entire Ca^{2+} excess is precipitated resulting in the highest calcite $\delta^{18}O$ and $\delta^{13}C$ values ($\tau_p = \delta/\lambda_P$ whereat δ is the film thickness and λ_P the precipitation rate, see section 2 for detail). Therefore, for a higher Ca^{2+} excesses and longer drip intervals, higher $\delta^{18}O$ and $\delta^{13}C$ values are observed (Fig. 2). Hence, for a constant drip interval, an increasing Ca^{2+} concentration of the drip water or a higher drip water pCO_2, respectively, results in increasing calcite $\delta^{18}O$ and $\delta^{13}C$ values. In contrast, an increasing cave air pCO_2 provokes decreasing calcite $\delta^{18}O$ and $\delta^{13}C$ values and vice versa. Importantly, the effect of changes in the Ca^{2+} excess becomes stronger for longer drip intervals (Fig. 2).

Example (5) Mixing effects: The carbonic solution film at the tip of the stalagmite is constantly renewed by new drops falling from the cave ceiling keeping the carbonic solution super-saturated with respect to calcite, i.e., maintaining active speleothem formation. However, it is possible that the falling drop does not replace the entire carbonic solution at the tip of the stalagmite but only a fraction, which provokes mixing of the previous carbonic solution and the new drop. This affects, on the one hand, the equilibrium concentrations of the CO_2-H_2O-$CaCO_3$-system and, on the other hand, the mean carbon and oxygen isotope ratios of the dissolved bicarbonate (Mühlinghaus et al., 2009). For instance, if the impinging drop completely replaces the carbonic solution at the tip of the stalagmite (ϕ = 1), the initial Ca^{2+} (HCO_3^-)

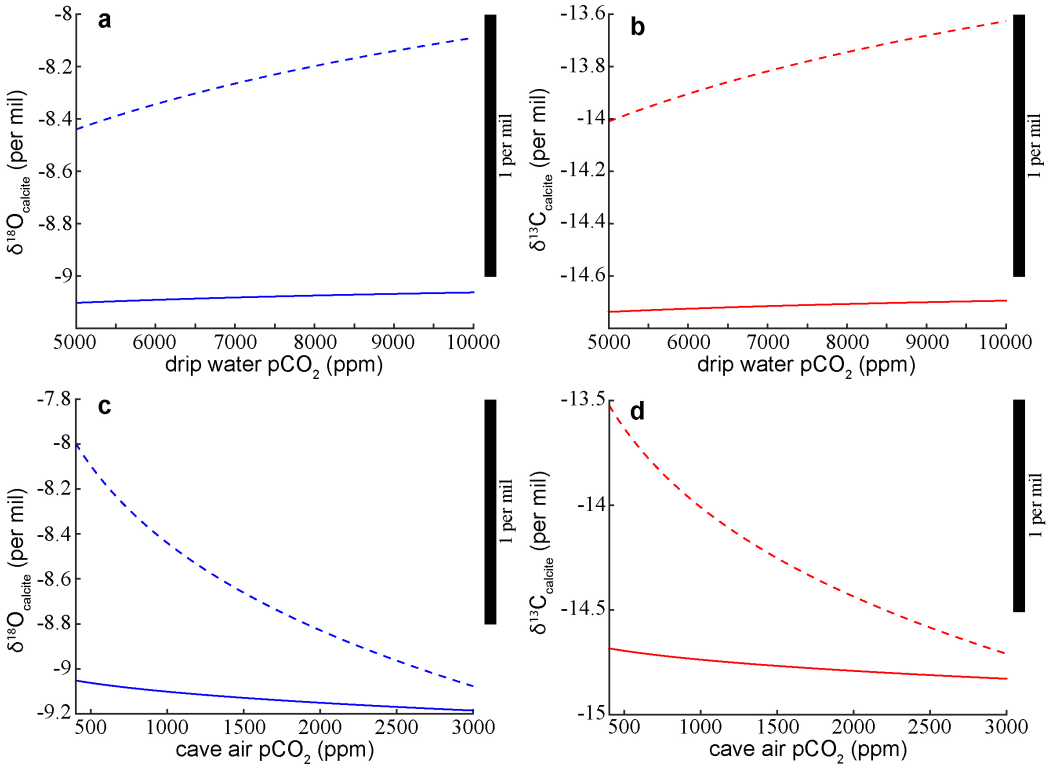

Fig. 2. Response of $\delta^{18}O$ (blue) and $\delta^{13}C$ (red) values of the precipitated calcite to changes in drip water (a and b) and cave air pCO_2 (c and d). For these experiments the drip water and cave air pCO_2 value are varied from 5,000 to 10,000 ppmV and 400 to 3,000 ppmV, respectively. The cave air temperature and the drip intervals are kept constant at 10°C and 100 s (straight line) and 1,500 s (dashed line), respectively. Furthermore, relative humidity is 100%, and we assume no wind flow (wind velocity is 0 m/s). The black bar indicates a change of 1‰.

concentration and the $\delta^{13}C$ and $\delta^{18}O$ values of the carbonic solution correspond to the respective values of the drip. If, however, due to splashing effects, only a specific fraction of the impinging drop contributes to the existing solution film at the tip of the speleothem (e.g., 50%, ϕ = 0.5), the new initial Ca^{2+} (HCO_3^-) concentration and the $\delta^{18}O$ and $\delta^{13}C$ values are determined by a mixture of the values of the drop and the existing carbonic solution. This results in stronger disequilibrium isotope fractionation effects because of the contribution of the existing carbonic solution, which has already been affected by progressive precipitation of calcite (Fig. 3). Note that for a very small contribution of the drip to the existing carbonic solution (e.g., ϕ = 0.1, heavy splashing), oxygen isotope exchange between H_2O and HCO_3^- and the resulting re-establishment of oxygen isotope equilibrium between H_2O and HCO_3^- causes an attenuation of the observed disequilibrium effects. This is particularly pronounced for large drip intervals (Fig. 3a) (Mühlinghaus et al., 2009; Deininger et al., 2012).

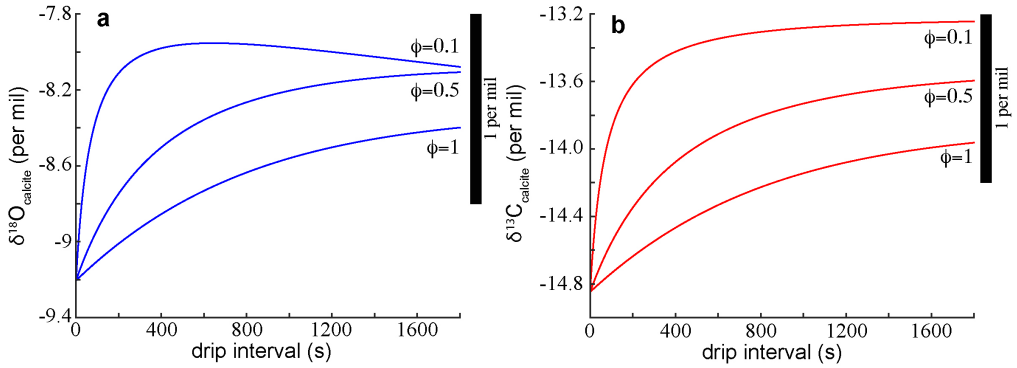

Fig. 3. Dependence of the $\delta^{18}O$ (a) and $\delta^{13}C$ (b) values of the precipitated calcite on the mixing parameter, ϕ. The black bar indicates a change of 1‰.

SUMMARY AND OUTLOOK

ISOLUTION is the most complex model describing stable oxygen and carbon isotope fractionation processes during the formation of speleothems currently available. Here we make the code available to the public, which enables other researchers to estimate the effect of various cave specific parameters, such as temperature, drip interval, cave pCO_2 or Ca^{2+} content of the drip water, on $\delta^{13}C$ and $\delta^{18}O$ values expected for speleothem calcite. We hope that this will result in more quantitative estimates of the effects of disequilibrium isotope fractionation in speleothem palaeoclimate studies, which are frequently mentioned to explain deviations as well as a larger variability in $\delta^{13}C$ and $\delta^{18}O$ values expected under conditions

of isotope equilibrium. Furthermore, we expect that the application of ISOLUTION to monitoring data (e.g., comparison of drip water data with the $\delta^{13}C$ and $\delta^{18}O$ values of recent calcite collected in situ inside the caves) will provide further information on the current potential and limitations of ISOLUTION. One shortcoming of the current version of ISOLUTION is that it does not account for uncertainties of the cave specific parameters that result either from measurements or regressions or simply because certain parameter couldn't be measured and were estimated only. However, these uncertainties can be visualised by repeating the sensitivity analyses with varied input parameters (e.g., the minimum and maximum of the range of a cave specific parameter, e.g., temperature).

ISOLUTION does not account for real, rate-dependent kinetic isotope fractionation effects (Dietzel et al., 2009; Watkins et al., 2014). If precise and accurate kinetic isotope fractionation factors as well as their dependence on the different cave parameters become available, ISOLUTION could be extended by accounting for these processes as well. Furthermore, ISOLUTION currently neither accounts for carbon and oxygen isotope exchange between the dissolved HCO_3^- and gaseous CO_2 (Dreybrodt & Romanov, 2016; Hansen et al., 2017) nor for isotope exchange with the calcite surface. For specific cave parameters (e.g., long drip intervals, high cave pCO_2 and low concentrations of HCO_3^-), these processes may have a significant effect on the temporal evolution of the $\delta^{13}C$ and $\delta^{18}O$ values of both the dissolved HCO_3^- and the precipitated calcite. These processes may also be included in future versions of ISOLUTION. Another extension of ISOLUTION in the future can be the generation of artificial speleothem $\delta^{13}C$ and $\delta^{18}O$ time series that includes also the growth rate model of Mühlinghaus et al. (2007). This would facilitate to investigate changes in the signal-to-noise-ratio of climate-related changes in e.g., $\delta^{18}O$ and $\delta^{13}C$ when for example seasonal CO_2 changes in the cave air occur or to study the effect of different $CaCO_3$ sampling strategies for isotope measurements, which can smooth the original $\delta^{18}O$ and $\delta^{13}C$ signal in dependence on the growth rate (Baldini et al., 2008a).

ACKNOWLEDGEMENTS

We thank two anonymous reviewers for comments that helped to improve this manuscript. MD and DS thank all members of the DFG-Forschergruppe 668, DAPHNE, for fruitful discussions (www.fg-daphne.de). DAPHNE was funded by the Deutsche Forschungsgemeinschaft (DFG). MD acknowledges funding by the DFG through grant DE 2398/3-1; DS acknowledged funding by the DFG through grant SCHO 1274/9-1.

SUPPLEMENTARY MATERIAL

1) User manual
2) ISOLUTION model code V1.0 for MATLAB

REFERENCES

Baker A., Genty D., Dreybrodt W., Barnes W.L., Mockler N.J. & Grapes J., 1998 – *Testing theoretically predicted stalagmite growth rate with recent annually laminated samples: Implications for past stalagmite deposition.* Geochimica et Cosmochimica Acta, **62 (3)**: 393-404. https://doi.org/10.1016/S0016-7037(97)00343-8

Baldini J.U.L., McDermott F., Hoffmann D.L., Richards D.A. & Clipson N., 2008a – *Very high-frequency and seasonal cave atmosphere PCO_2 variability: Implications for stalagmite growth and oxygen isotope-based paleoclimate records.* Earth and Planetary Science Letters, **272 (1)**: 118-129. https://doi.org/10.1016/j.epsl.2008.04.031

Baldini L.M., McDermott F., Foley A.M. & Baldini J.U.L., 2008b – *Spatial variability in the European winter precipitation $\delta^{18}O$-NAO relationship: Implications for reconstructing NAO-mode climate variability in the Holocene.* Geophysical Research Letters, **35 (4)**: L04709. https://doi.org/10.1029/2007GL032027

Beck W.C., Grossman E.L. & Morse J.W., 2005 – *Experimental studies of oxygen isotope fractionation in the carbonic acid system at 15, 25, and 40ºC.* Geochimica et Cosmochimica Acta, **69 (14)**: 3493-3503. https://doi.org/10.1016/j.gca.2005.02.003

Bradley C., Baker A., Jex C.N. & Leng M.J., 2010 – *Hydrological uncertainties in the modelling of cave drip-water $\delta^{18}O$ and the implications for stalagmite palaeoclimate reconstructions.* Quaternary Science Reviews, **29 (17-18)**: 2201-2214. https://doi.org/10.1016/j.quascirev.2010.05.017

Buhmann D. & Dreybrodt W., 1985a – *The kinetics of calcite dissolution and precipitation in geologically relevant situations of karst areas: 1. Open system.* Chemical Geology, **48 (1)**: 189-211. https://doi.org/10.1016/0009-2541(85)90046-4

Buhmann D. & Dreybrodt W., 1985b – *The kinetics of calcite dissolution and precipitation in geologically relevant situations of karst areas: 2. Closed system.* Chemical Geology, **53 (1)**: 109-124. https://doi.org/10.1016/0009-2541(85)90024-5

Cheng H., Edwards R.L., Sinha A., Spötl C., Yi L., Chen S., Kelly M., Kathayat G., Wang X. & Li X., 2016 – *The Asian monsoon over the past 640,000 years and ice age terminations.* Nature, **534**: 640-646. https://doi.org/10.1038/nature18591

Cheng H., Lawrence Edwards R., Shen C.-C., Polyak V.J., Asmerom Y., Woodhead J., Hellstrom J., Wang Y., Kong X., Spötl C., Wang X. & Calvin Alexander Jr E., 2013 – *Improvements in ^{230}Th dating, ^{230}Th and ^{234}U half-life values, and U–Th isotopic measurements by multi-collector inductively coupled plasma mass spectrometry.* Earth and Planetary Science Letters, **371-372**: 82-91. https://doi.org/10.1016/j.epsl.2013.04.006

Coplen T.B., 2007 – *Calibration of the calcite–water oxygen-isotope geothermometer at Devils Hole, Nevada, a natural laboratory.* Geochimica et Cosmochimica Acta, **71 (16)**: 3948-3957. https://doi.org/10.1016/j.gca.2007.05.028

Cruz F.W., Burns S.J., Karmann I., Sharp W.D., Vuille M., Cardoso A.O., Ferrari J.A., Dias P.L.S. & Viana O., 2005 – *Insolation-driven changes in atmospheric circulation over the past 116,000 years in subtropical Brazil.* Nature, **434 (7029)**: 63-66. https://doi.org/10.1038/nature03365

Deininger M., Fohlmeister J., Scholz D. & Mangini A., 2012 – *Isotope disequilibrium effects: The influence of evaporation and ventilation effects on the carbon and*

oxygen isotope composition of speleothems-A model approach. Geochimica et Cosmochimica Acta, **96**: 57-89. https://doi.org/10.1016/j.gca.2012.08.013

Deininger M., Werner M. & McDermott F., 2016 – *North Atlantic Oscillation controls on oxygen and hydrogen isotope gradients in winter precipitation across Europe; implications for palaeoclimate studies*. Climate of the Past, **2016**: 1-27. https://doi.org/10.5194/cp-12-2127-2016

DePaolo D.J., 2011 – *Surface kinetic model for isotopic and trace element fractionation during precipitation of calcite from aqueous solutions*. Geochimica et Cosmochimica Acta, **75 (4)**: 1039-1056. https://doi.org/10.1016/j.gca.2010.11.020

Dietzel M., Tang J., Leis A. & Köhler S.J., 2009 – *Oxygen isotopic fractionation during inorganic calcite precipitation—Effects of temperature, precipitation rate and pH*. Chemical Geology, **268 (1)**: 107-115. https://doi.org/10.1016/j.chemgeo.2009.07.015

Dreybrodt W., 1988 – *Processes in karst systems*. Springer, Berlin, 288 p. https://doi.org/10.1007/978-3-642-83352-6

Dreybrodt W., 1999 – *Chemical kinetics, speleothem growth and climate*. Boreas, **28 (3)**: 347-356. https://doi.org/10.1080/030094899422073

Dreybrodt W., 2008 – *Evolution of the isotopic composition of carbon and oxygen in a calcite precipitating H_2O–CO_2–$CaCO_3$ solution and the related isotopic composition of calcite in stalagmites*. Geochimica et Cosmochimica Acta, **72 (19)**: 4712-4724. https://doi.org/10.1016/j.gca.2008.07.022

Dreybrodt W., 2016 – *Letter: Problems in using the approach of rayleigh distillation to interpret the ^{13}C and ^{18}O isotope compositions in stalagmite calcite*. Acta Carsologica, **45 (3)**: 285-293. https://doi.org/10.3986/ac.v45i3.4698

Dreybrodt W. & Deininger M., 2014 – *The impact of evaporation to the isotope composition of DIC in calcite precipitating water films in equilibrium and kinetic fractionation models*. Geochimica et Cosmochimica Acta, **125**: 433-439. https://doi.org/10.1016/j.gca.2013.10.004

Dreybrodt W., Eisenlohr L., Madry B. & Ringer S., 1997 – *Precipitation kinetics of calcite in the system $CaCO_3$-H_2O-CO_2: The conversion to CO_2 by the slow process $H^+ + HCO_3^- > CO_2 + H_2O$ as a rate limiting step*. Geochimica et Cosmochimica Acta, **61 (18)**: 3897-3904. https://doi.org/10.1016/S0016-7037(97)00201-9

Dreybrodt W. & Romanov D., 2016 – *The evolution of ^{13}C and ^{18}O isotope composition of DIC in a calcite depositing film of water with isotope exchange between the DIC and a CO_2 containing atmosphere, and simultaneous evaporation of the water. Implication to climate proxies from stalagmites: A theoretical model*. Geochimica et Cosmochimica Acta, **195**: 323-338. https://doi.org/10.1016/j.gca.2016.07.034

Dreybrodt W. & Scholz D., 2011 – *Climatic dependence of stable carbon and oxygen isotope signals recorded in speleothems: From soil water to speleothem calcite*. Geochimica et Cosmochimica Acta, **75 (3)**: 734-752. https://doi.org/10.1016/j.gca.2010.11.002

Fairchild I.J. & Baker A., 2012 – *Speleothem science: from process to past environments*. John Wiley & Sons, 432 p. https://doi.org/10.1002/9781444361094

Fairchild I.J. & Treble P.C., 2009 – *Trace elements in speleothems as recorders of environmental change*. Quaternary Science Reviews, **28 (5)**: 449-468. https://doi.org/10.1016/j.quascirev.2008.11.007

Fohlmeister J., Kromer B. & Mangini A., 2011a – *The influence of soil organic matter age spectrum on the reconstruction of atmospheric 14C levels via stalagmites*. Radiocarbon, **53 (1)**: 99-115. https://doi.org/10.1017/S003382220003438X

Fohlmeister J., Scholz D., Kromer B. & Mangini A., 2011b – *Modelling carbon isotopes of carbonates in cave drip water*. Geochimica et Cosmochimica Acta, **75 (18)**: 5219-5228. https://doi.org/10.1016/j.gca.2011.06.023

Genty D., Labuhn I., Hoffmann G., Danis P.A., Mestre O., Bourges F., Wainer K., Massault M., Van Exter S. & Régnier E., 2014 – *Rainfall and cave water isotopic relationships in two South-France sites*. Geochimica et Cosmochimica Acta, **131**: 323-343. https://doi.org/10.1016/j.gca.2014.01.043

Hansen M., Scholz D., Froeschmann M.L., Schone B.R. & Spotl C., 2017 – *Carbon isotope exchange between gaseous CO_2 and thin solution films: Artificial cave experiments and a complete diffusion-reaction model*. Geochimica et Cosmochimica Acta, **211**: 28-47. https://doi.org/10.1016/j.gca.2017.05.005

Hendy C.H., 1971 – *The isotopic geochemistry of speleothems—I. The calculation of the effects of different modes of formation on the isotopic composition of speleothems and their applicability as palaeoclimatic indicators*. Geochimica et Cosmochimica Acta, **35 (8)**: 801-824. https://doi.org/10.1016/0016-7037(71)90127-X

Hurrell J.W., 1995 – *Decadal trends in the North Atlantic oscillation: Regional temperatures and precipitation*. Science, **269**: 676-679. https://doi.org/10.1126/science.269.5224.676

Johnston V.E., Borsato A., Spötl C., Frisia S. & Miorandi R., 2013 – *Stable isotopes in caves over altitudinal gradients: fractionation behaviour and inferences for speleothem sensitivity to climate change*. Climate of the Past, **9**: 99-118. https://doi.org/10.5194/cp-9-99-2013

Kaufmann G., 2003 – *Stalagmite growth and palaeo-climate: the numerical perspective*. Earth and Planetary Science Letters, **214 (1)**: 251-266. https://doi.org/10.1016/S0012-821X(03)00369-8

Kaufmann G. & Dreybrodt W., 2004 – *Stalagmite growth and palaeo-climate: an inverse approach*. Earth and Planetary Science Letters, **224 (3)**: 529-545. https://doi.org/10.1016/j.epsl.2004.05.020

Kim S.-T. & O'Neil J.R., 1997 – *Equilibrium and nonequilibrium oxygen isotope effects in synthetic carbonates*. Geochimica et Cosmochimica Acta, **61 (16)**: 3461-3475. https://doi.org/10.1016/S0016-7037(97)00169-5

Lachniet M.S., 2009 – *Climatic and environmental controls on speleothem oxygen-isotope values*. Quaternary Science Reviews, **28 (5)**: 412-432. https://doi.org/10.1016/j.quascirev.2008.10.021

Mattey D., Lowry D., Duffet J., Fisher R., Hodge E. & Frisia S., 2008 – *A 53 year seasonally resolved oxygen and carbon isotope record from a modern Gibraltar speleothem: reconstructed drip water and relationship to local precipitation*. Earth and Planetary Science Letters, **269 (1-2)**: 80-95. https://doi.org/10.1016/j.epsl.2008.01.051

McDermott F., 2004 – *Palaeo-climate reconstruction from stable isotope variations in speleothems: a review*. Quaternary Science Reviews, **23 (7)**: 901-918. https://doi.org/10.1016/j.quascirev.2003.06.021

McDermott F., Atkinson T.C., Fairchild I.J., Baldini L.M. & Mattey D.P., 2011 – *A first evaluation of the spatial gradients in $\delta^{18}O$ recorded by European Holocene speleothems*. Global and Planetary Change, **79 (3)**: 275-287. https://doi.org/10.1016/j.gloplacha.2011.01.005

Mickler P.J., Stern L.A. & Banner J.L., 2006 – *Large kinetic isotope effects in modern speleothems*. Geological Society of America Bulletin, **118 (1-2)**: 65-81. https://doi.org/10.1130/B25698.1

Mook W. & de Vries J., 2000 – *Environmental Isotopes in the Hydrological Cycle Principles and Applications-Volume I: Introduction-Theory*. Methods, Review, IAEA, Vienna.

Mook W.G., 2006 – *Introduction to isotope hydrology*. Taylor & Francio, London, 226 p.

Mühlinghaus C., Scholz D. & Mangini A., 2007 – *Modelling stalagmite growth and $\delta^{13}C$ as a function of drip interval and temperature*. Geochimica et Cosmochimica Acta, **71 (11)**: 2780-2790. https://doi.org/10.1016/j.gca.2007.03.018

Mühlinghaus C., Scholz D. & Mangini A., 2009 – *Modelling fractionation of stable isotopes in stalagmites*. Geochimica et Cosmochimica Acta, **73 (24)**: 7275-7289. https://doi.org/10.1016/j.gca.2009.09.010

Polag D., Scholz D., Mühlinghaus C., Spötl C., Schröder-Ritzrau A., Segl M. & Mangini A., 2010 – *Stable isotope fractionation in speleothems: Laboratory experiments*. Chemical Geology, **279 (1)**: 31-39. https://doi.org/10.1016/j.chemgeo.2010.09.016

Rayleigh L., 1902 – *LIX. On the distillation of binary mixtures*. The London, Edinburgh, and Dublin Philosophical Magazine and Journal of Science, **4 (23)**: 521-537. https://doi.org/10.1080/14786440209462876

Richards D.A. & Dorale J.A., 2003 – *Uranium-series chronology and environmental applications of speleothems*. Reviews in Mineralogy and Geochemistry, **52 (1)**: 407-460. https://doi.org/10.2113/0520407

Riechelmann D.F.C., Deininger M., Scholz D., Riechelmann S., Schröder-Ritzrau A., Spötl C., Richter D.K., Mangini A. & Immenhauser A., 2013 – *Disequilibrium carbon and oxygen isotope fractionation in recent cave calcite: Comparison of cave precipitates and model data*. Geochimica et Cosmochimica Acta, **103**: 232-244. https://doi.org/10.1016/j.gca.2012.11.002

Riechelmann D.F.C., Schröder-Ritzrau A., Scholz D., Fohlmeister J., Spötl C., Richter D.K. & Mangini A., 2011 – *Monitoring Bunker Cave (NW Germany): A prerequisite to interpret geochemical proxy data of speleothems from this site*. Journal of Hydrology, **409 (3)**: 682-695. https://doi.org/10.1016/j.jhydrol.2011.08.068

Romanov D., Kaufmann G. & Dreybrodt W., 2008a – *Modeling stalagmite growth by first principles of chemistry and physics of calcite precipitation*. Geochimica et Cosmochimica Acta, **72 (2)**: 423-437. https://doi.org/10.1016/j.gca.2007.09.038

Romanov D., Kaufmann G. & Dreybrodt W., 2008b - *$\delta^{13}C$ profiles along growth layers of stalagmites: Comparing theoretical and experimental results*. Geochimica et Cosmochimica Acta, **72 (2)**: 438-448. https://doi.org/10.1016/j.gca.2007.09.039

Scholz D., Mühlinghaus C. & Mangini A., 2009 – *Modelling $\delta^{13}C$ and $\delta^{18}O$ in the solution layer on stalagmite surfaces*. Geochimica et Cosmochimica Acta, **73 (9)**: 2592-2602. https://doi.org/10.1016/j.gca.2009.02.015

Spötl C., Fairchild I.J. & Tooth A.F., 2005 – *Cave air control on dripwater geochemistry, Obir Caves (Austria): Implications for speleothem deposition in dynamically ventilated caves*. Geochimica et Cosmochimica Acta, **69 (10)**: 2451-2468. https://doi.org/10.1016/j.gca.2004.12.009

Tremaine D.M., Froelich P.N. & Wang Y., 2011 – *Speleothem calcite farmed in situ: Modern calibration of $\delta^{18}O$ and $\delta^{13}C$ paleoclimate proxies in a continuously-monitored natural cave system*. Geochimica et Cosmochimica Acta, **75 (17)**: 4929-4950. https://doi.org/10.1016/j.gca.2011.06.005

Wackerbarth A., Scholz D., Fohlmeister J. & Mangini A., 2010 – *Modelling the $\delta^{18}O$ value of cave drip water and speleothem calcite*. Earth and Planetary Science Letters, **299 (3)**: 387-397. https://doi.org/10.1016/j.epsl.2010.09.019

Watkins J.M., Hunt J.D., Ryerson F.J. & DePaolo D.J., 2014 – *The influence of temperature, pH, and growth rate on the $\delta^{18}O$ composition of inorganically precipitated calcite*. Earth and Planetary Science Letters, **404**: 332-343. https://doi.org/10.1016/j.epsl.2014.07.036

Watson E.B., 2004 – *A conceptual model for near-surface kinetic controls on the trace-element and stable isotope composition of abiogenic calcite crystals*. Geochimica et Cosmochimica Acta, **68 (7)**: 1473-1488. https://doi.org/10.1016/j.gca.2003.10.003

Wiedner E., Scholz D., Mangini A., Polag D., Mühlinghaus C. & Segl M., 2008 – *Investigation of the stable isotope fractionation in speleothems with laboratory experiments*. Quaternary International, **187 (1)**: 15-24. https://doi.org/10.1016/j.quaint.2007.03.017

International Journal of Speleology	48 (1)	33-48	Tampa, FL (USA)	January 2019

Available online at scholarcommons.usf.edu/ijs

International Journal of Speleology

Official Journal of Union Internationale de Spéléologie

Fifty years of cave arthropod sampling: techniques and best practices

J. Judson Wynne[1*], Francis G. Howarth[2], Stefan Sommer[1], and Brett G. Dickson[3]

[1]Department of Biological Sciences, Merriam-Powell Center for Environmental Research, Northern Arizona University, Box 5640, Flagstaff, Arizona 86011, USA
[2]Department of Natural Sciences, Bernice P. Bishop Museum, 1525 Bernice St., Honolulu, Hawaii, 96817, USA
[3]Conservation Science Partners, 11050 Pioneer Trail, Suite 202, Truckee, CA 96161 and Lab of Landscape Ecology and Conservation Biology, Landscape Conservation Initiative, Northern Arizona University, Box 5694, Flagstaff, Arizona 86011, USA

Abstract: Ever-increasing human pressures on cave biodiversity have amplified the need for systematic, repeatable, and intensive surveys of cave-dwelling arthropods to formulate evidence-based management decisions. We examined 110 papers (from 1967 to 2018) to: (i) understand how cave-dwelling invertebrates have been sampled; (ii) provide a summary of techniques most commonly applied and appropriateness of these techniques, and; (iii) make recommendations for sampling design improvement. Of the studies reviewed, over half (56) were biological inventories, 43 ecologically focused, seven were techniques papers, and four were conservation studies. Nearly one-half (48) of the papers applied systematic techniques. Few papers (24) provided enough information to repeat the study; of these, only 11 studies included cave maps. Most studies (56) used two or more techniques for sampling cave-dwelling invertebrates. Ten studies conducted ≥10 site visits per cave. The use of quantitative techniques was applied in 43 of the studies assessed. More than one-third (42) included some level of discussion on management. Future studies should employ a systematic study design, describe their methods in sufficient detail as to be repeatable, and apply multiple techniques and site visits. This level of effort and detail is required to obtain the most complete inventories, facilitate monitoring of sensitive cave arthropod populations, and make informed decisions regarding the management of cave habitats. We also identified naming inconsistencies of sampling techniques and provide recommendations towards standardization.

Keywords: systematic sampling, repeatability, conservation, pitfall trapping

Received 8 October 2018; Revised 23 January 2019; Accepted 24 January 2019

Citation: Wynne J.J., Howarth F.G., Sommer S. and Dickson B.G., 2019. Fifty years of cave arthropod sampling: techniques and best practices. International Journal of Speleology, 48 (1), 33-48. Tampa, FL (USA) ISSN 0392-6672 https://doi.org/10.5038/1827-806X.48.1.2231

INTRODUCTION

With mounting anthropogenic threats to cave ecosystems, it is increasingly important to systematically and efficiently collect data on cave-dwelling arthropods, so that informed management decisions can be made or adjusted on a regular basis. Cave ecosystems face numerous human impacts globally including land cover conversion (Culver, 1986; Trajano, 2000; Howarth et al., 2007; Silva et al., 2015), mining (Elliott, 2000; Silva et al., 2015; Sugai et al., 2015), groundwater pollution (Aley, 1976; Notenboom et al., 1994; Graening & Brown, 2003; Whitten, 2009), water extraction and water impoundments (Lisowski, 1983; Ubick & Briggs, 2002; Olson, 2005), invasive species (Elliott, 1992; Reeves, 1999; Taylor et al., 2003; Howarth et al., 2007; Wynne et al., 2014), global climate change (Chevaldonné & Lejeune, 2003; Badino, 2004; Mammola et al., 2018), and recreational use (Culver, 1986; Howarth & Stone, 1993; Pulido-Bosch et al., 1997). These threats have significant implications for conservation because caves are highly sensitive habitats, often serving as hotspots of endemism and subterranean biodiversity (Culver et al., 2000; Culver & Sket, 2000; Eberhard et al., 2005).

Because of their restricted distributions and life history traits, many populations of troglomorphic (subterranean-adapted) species are considered highly sensitive or imperiled and thus high priority targets for protective management (Culver et al., 2000; Niemiller & Zigler, 2013; Niemiller et al., 2017). Troglomorphic species are often endemic to a single cave or region (Reddell, 1994; Culver et al., 2000; Christman et al., 2005; Gao et al., 2018) and characterized by

*jut.wynne@nau.edu

small populations (Mitchell, 1970). Thus, effectively sampling caves to detect troglobionts should be a priority of cave biological inventories.

The fauna of most of the world's caves remain unknown or, at best, incompletely surveyed (Howarth, 1983; Whitten, 2009; Gibert & Deharveng, 2002; Deharveng & Bedos, 2000; Encinares & Lit, 2014; Gilgado et al., 2015). In addition, accurate information on the taxonomy, genetics, distribution, and environmental requirements of cavernicoles will be necessary to make rigorous ecological inference, as well as to develop appropriate recommendations for monitoring and protecting cave animals (Wynne et al., 2018).

Numerous researchers (e.g., Weinstein & Slaney, 1995; Howarth et al., 2007; Krejca & Weckerly, 2007; Zagmajster et al., 2008; Wynne et al., 2018) have emphasized the difficulties of sampling terrestrial cavernicolous arthropods, which present challenges for effectively inventorying, and managing sensitive cavernicolous arthropod communities. Caves are highly diverse habitats with constricted, maze-like interconnected passageways, uneven terrain, loose rocks and boulders, deep fissures and pits. This diverse array of habitats often requires technical climbing and rope work for access. Additionally, temporal and spatial heterogeneity of cave habitats (Kane & Poulson, 1976; Chapman, 1983; Pellegrini & Ferriera, 2013; Trontelj et al., 2013) often requires considerable pre-planning and on-site evaluations prior to sampling.

Furthermore, research emphasis should be placed on identifying and surveying nutrient resource sites that support troglomorphic animals (Howarth et al., 2007; Wynne, 2013; Wynne et al., 2018). For example, Peck & Wynne (2013) showed a cave cricket roost (Family Rhaphidophoridae), within the type locality of the troglomorphic leiodid beetle (*Ptomaphagus parashant*), provided an important substrate (frass and decaying carcasses) for the growth of fungi – a primary food source for this beetle. Additionally, Stone et al. (2012) and Wynne (2013) underscored the importance of root curtains as both microhabitats and a nutrient source for subterranean-adapted animals in Hawai'i and New Mexico, respectively. Wynne & Shear (2016), Wynne et al. (2014), and Benedict (1979) identified vegetation and moss within entrances and beneath cave skylights as key habitat for relictual species.

In this study, we (i) examine how cave-dwelling invertebrates have been sampled (from 1967 to 2018); (ii) provide both a summary of techniques most commonly applied and their appropriateness, and; (iii) make recommendations for sampling design improvement. We also identify naming inconsistencies of sampling techniques and provide recommendations towards standardization.

METHODS AND MATERIALS

We reviewed the literature (from 1967 to 2018) by obtaining articles through a Web of Science search using combinations of the following search terms 'cavernicole', 'troglobiont,' 'troglobite,' 'cave arthropod,' 'cave invertebrate,' 'inventory,' and 'ecology.' We augmented our search using Google Scholar (with the same search terms), examining titles and abstracts of all papers published in both the International Journal of Speleology (1967-2018) and National Speleological Society Bulletin, now Journal of Cave and Karst Studies (years 1967-1995 and 1996-2018, respectively), and working 'backwards' into the literature by reviewing the literature cited of all of the articles considered. As most of the work in cave biology has been published in English and to a lesser extend in French, Spanish, and Portuguese, we assert the papers assembled in this review are representative of the work conducted over the past ~50 years.

Papers were selected for inclusion or exclusion using the following decision rules: (1) papers focused on inventorying cave-dwelling terrestrial invertebrate communities and/or investigating an aspect of cave arthropod community ecology; (2) for studies using an all taxa approach (i.e., terrestrial and aquatic invertebrate sampling and vertebrate sampling), only terrestrial invertebrate techniques were examined; (3) only multi-taxon inventories were included; single species or single taxonomic group studies were excluded; and (4) because reviews and synthesis papers of specific geographic regions rarely include sampling methods, these papers were not included. When possible, we examined the original studies that included field methods.

We evaluated each article on cave-dwelling invertebrates using the following questions and criteria. (1) Were systematic techniques (i.e., techniques consistently applied throughout a given cave or across cave study sites) employed (yes, no, or not known)? (2) Was sufficient information provided to enable repeatability of data collection and/or the experiment (yes or no)? (3) To further facilitate repeatability, did the researchers include cave maps with plotted sample locations and/or use the information from cave maps as part of their experimental design (yes or no)? (4) Did the workers apply multiple sampling techniques (yes, no, not stated)? If yes, how many? (5) Did the researchers conduct multiple site visits (yes, no; if yes, how many?)? (6) Were the data analyzed using statistical techniques? (7) Finally, did the authors provide conservation and management implications for their work (yes or no)? We also summarized the techniques encountered in the literature, discussed the functional groups each technique is best suited for capturing, and provided recommendations for best practices.

RESULTS

We assessed nearly 300 papers on terrestrial cave-dwelling arthropods. Of these, 110 articles (Appendix I, Supplemental Information) met our decision rules and were included in this review. More than half of these articles (67) were based upon work conducted in the Western Hemisphere - United States (36), Latin America, the Galapagos, and the Caribbean (31; Fig. 1).

Papers reviewed were parsed into four categories (inventory, ecology, techniques, and conservation).

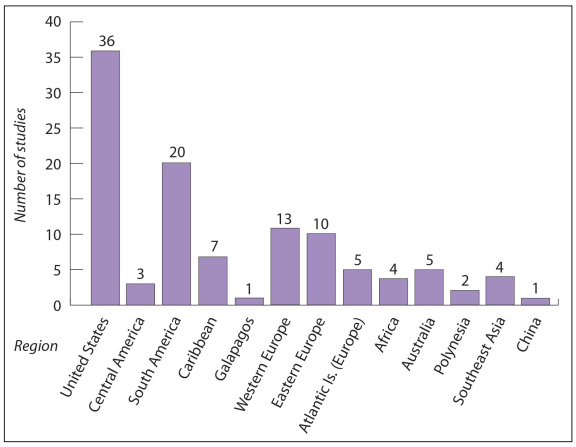

Fig. 1. Summary of 110 studies reviewed per geographic region. Number totals 111, as Wynne et al. (2018) had study areas in both the United States and Polynesia.

We used these categories to frame how the evaluative criteria were applied. Slightly over half of the studies (56) examined were biological inventories, 43 advanced ideas and hypotheses on various aspects of cave ecology, seven examined the efficacy of sampling/analytical techniques, and four studies were conservation focused. For the ecological studies, 17 examined the distribution and assembly of communities within caves, 11 investigated the influence of habitat on arthropod diversity, eight probed how nutrients affected community structure, four explored the influence of seasonality on diversity, and three analyzed the evolution and colonization of subterranean-adapted arthropods (Fig. 2).

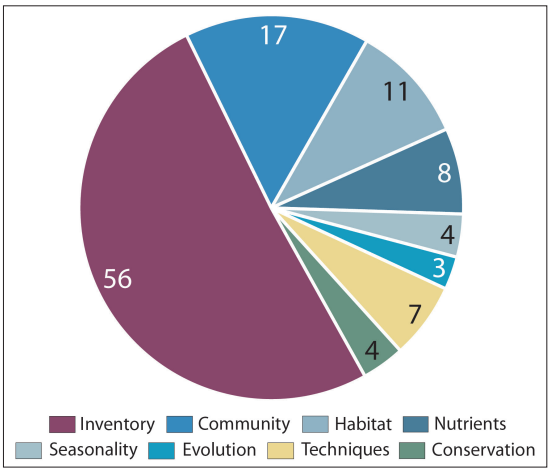

Fig. 2. Pie chart describing the reviewed articles by study type. Numbers associated with each "pie slice" represent the number of papers per study type. Subdivisions of ecology (community, habitat, nutrients, seasonality and evolution) are dipicted in hues of blue. Legend reads left to right; pie chart reads clockwise starting with the largest slice.

Five studies addressed all seven of our evaluative criteria. For ecological studies, four (Chapman, 1982; Martín & Oromí, 1986; Ferreira et al., 2000; Iskali & Zhang, 2015) of 43 papers addressed all of the criteria. Schneider et al. (2011) met all but one criterion – the inclusion of cave maps with plotted sample locations to further enhance repeatability. An additional four ecological studies (Chapman, 1983; Herrera 1995; Prous et al., 2004; Tobin et al., 2014) met all criteria with the exception of discussing conservation implications. One techniques paper (Wynne et al., 2018) met all evaluative criteria. None of the conservation studies or biological inventories met all evaluative criteria. However, one inventory study (Northup et al., 1994) used a systematic and repeatable sampling design, applied multiple sampling techniques, and provided conservation implications.

Systematic sampling

Overall, 48 studies incorporated systematic sampling into their study design, 50 did not, and 12 studies did not provide enough information to make this determination. Of the 43 ecologically focused papers, 26 of these studies applied systematic techniques, 15 did not, and two studies did not provide enough information to make this determination. For the 56 inventory studies, 15 applied systematic techniques, while 32 did not; for nine inventory studies, this could not be determined. Five of seven techniques studies applied systematic techniques. Two (Borges et al., 2012; Howarth et al., 2007) of four conservation papers applied systematic techniques.

Repeatability

Most of the studies (86) did not provide enough information to replicate the study. The twenty-four repeatable studies included 15 ecological projects, five biological inventories, and four techniques papers. For nearly half of the repeatable studies, maps were included or referenced; this included seven ecological studies (Chapman, 1982, 1983; Martín & Oromí, 1986; Herrera, 1995; Tobin et al., 2014; Iskali & Zhang, 2015; Lunghi et al., 2014), two techniques papers (Kozel et al., 2017; Wynne et al., 2018) and two biological inventories (Lamprinou et al., 2009; Dumnicka et al., 2015). Additionally, a total of 36 studies (which included both repeatable and unrepeatable) provided cave maps with plotted sampling locations or employed maps to establish sampling intervals. The combination of both repeatable sampling techniques and cave maps enables future workers to replicate those studies with the highest level of accuracy.

Multiple techniques

Multiple sampling techniques were applied in ~51% of the studies (56 of the 110), while 11 papers did not provide information on number of techniques used. Of the 56 studies, 32 applied two techniques, 18 used three techniques, four employed four techniques, and two studies applied six techniques (Fig. 3).

Notably, three techniques papers (Weinstein & Slaney, 1995; Encinares & Lit, 2014; Wynne et al., 2018) found that applying multiple methods maximized the completeness of the survey. Weinstein & Slaney (1995) descriptively compared four sampling techniques: pitfall trapping (baited and unbaited), leaf litter traps (wet and dry), timed searches with interval spacing on transect, and timed direct intuitive searches in a tropical Australian cave. When comparing the performance of each technique against total diversity and abundance values, they found wet leaf litter traps to be most effective and uniquely detected two species. Encinares & Lit (2014), when sampling a tropical Philippine cave by environmental zone, discovered that a combined wet and dry leaf

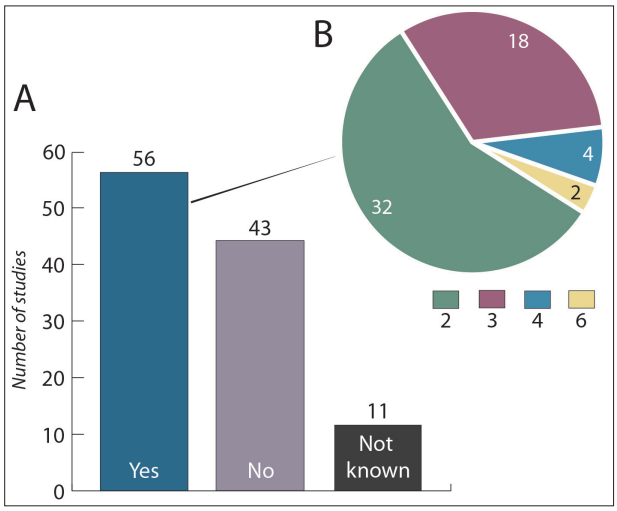

Fig. 3. A) Breakdown of studies using multiple techniques (Yes), one technique (No), and Not known number of techniques. The 'Not Known' category was used in the case of three studies where the authors did not provide an explanation of the methods used. Of the studies employing multiple techniques, the pie chart (B) represents the total number of studies per number of techniques (numbers within each pie slice and color coded in the legend). Legend reads clockwise starting with largest slice.

litter trap approach was required to maximize the number of species detected.

Wynne et al. (2018) applied three techniques (live capture baited pitfall trapping, timed constrained searches around traps before and after deployment, and opportunistic searches) across 26 study caves in the American Southwest and Easter Island, and applied three additional techniques in selected caves (bait sampling and timed searches within a 1-m^2 grid established within cave deep zones, timed searches in nutrient resource sites – moss-fern/ moss gardens in cave entrances and root curtains in cave deep zones). They revealed that each method uniquely detected species, and thus applying multiple techniques (with multiple site visits) optimized the number of species detected – in particular, management concern species.

Multiple site visits

Overall, seven studies conducted one site visit, 43 studies applied two or more site visits, eight studies used a non-standardized approach whereby the number of site visits varied per cave, and 52 studies did not disclose the number of site visits. For studies applying multiple site visits, these were: 15 studies at two visits, 18 studies between three to eight visits, nine studies between 10 and 36 visits, and one study with more than 100 site visits.

For the 43 studies specifically addressing ecological questions, three studies applied one site visit, 12 conducted two site visits, 10 studies between three to eight visits, three studies between used 10 and 23 visits, and one study with more than 100 site visits. Additionally, two studies employed a non-standardized approach where the number of visits varied across the caves sampled, while 12 studies did not disclose how many site visits were conducted.

Quantitative techniques

We found 43 of the 110 studies included some sort of quantitative analytical framework. Most of the ecological studies (34 of 43), three of four conservation papers, six of seven techniques studies applied quantitative techniques. None of the 56 inventory papers included quantitative analysis.

Conservation and management

Most studies (68) did not mention conservation or management. The 42 papers that discussed conservation were: 16 of 43 ecological studies, all four conservation papers, five of seven techniques studies, and 17 of 56 inventory papers. When we examined this by decade, we found that none of the papers from 1967 through 1979 discussed conservation; however, for the last two decades, most of the papers (per decade) addressed conservation issues and impending human impacts (Fig. 4).

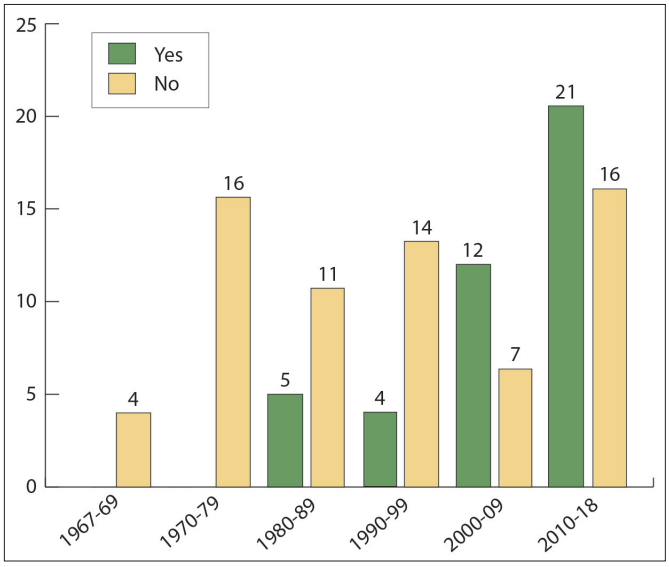

Fig. 4. Frequency in which 'conservation' and/ or 'management' were mentioned or fully developed by decade for the papers analyzed. Green bars represent the papers in which these topics were discussed (Yes), yellow bars indicate the absence of any discussion on conservation and management (No).

Study design

Cave biologists applied a wide array of techniques for sampling invertebrate populations. We examined the most commonly published study designs and techniques. Based upon our experience, we also provided information on advantages and disadvantages of each technique.

Dividing the total length of the cave into sampling increments occurred in three forms: environmental zones, predefined intervals, and quadrats. As caves are strongly zonal habitats, this is often a useful approach for dividing the cave into more manageable sampling units. Four principal zones are recognized: two photic (light and twilight) and two aphotic (transition and deep; Howarth, 1980). Howarth & Stone (1990) described a fifth environmental zone, the "bad air" zone, which is beyond, and technically a subdivision of, the deep zone. Overall, 25 studies applied a zonal approach – concentrating on three or more zones, a variation on this theme, or specifically on the dark (i.e., deep) zone, which breaks down as follows: 10 of 43 ecological studies, one of four conservation studies, five of seven techniques studies, and 9 of 56 inventory studies (Table 1). Only two studies (Howarth

Table 1. Summary of publications where sampling was conducted by environmental zone.

Purpose of study	# (%)	References
Ecological	9/43 (21%)	Howarth & Stone, 1990; Ashmole et al., 1992; Reeves & McCreadie, 2001; Dao-Hong, 2006; Silva et al., 2013; Sendra et al., 2014; Iskali & Zhang, 2015; Araujo & Peixoto, 2015; Růžička et al., 2016
Conservation	1/4 (25%)	Borges et al., 2012
Techniques	5/7 (71%)	Weinstein & Slaney, 1995; Schneider & Culver, 2004; Krejca & Weckerly, 2007; Encinares & Lit, 2014; Wynne et al., 2018
Inventory	10/56 (18%)	Barr & Reddell, 1967; Peck & Lewis, 1978; Lewis, 1983; Peck, 1989; Oromí et al., 1990; Northup & Welbourn, 1997; Buhlmann, 2001; Wynne & Pleytez, 2005; Serrano & Borges, 2010; Wynne & Voyles, 2014

& Stone, 1990; Borges et al., 2012) applied a study design examining all four environmental zones. The remaining studies applied some variation on sampling by zone.

Interval spacing was applied primarily in four ways: (1) the cave was sampled at a specific predefined interval (e.g., sampling at every 5-m); (2) the cave was subdivided at arbitrary predefined intervals (e.g., 20-m, 150-m, 225-m, 310-m); (3) a percentage of the cave's length was used to define the sampling interval; or, (4) transects were established along the length of each cave, and sampled at predefined intervals. Overall, interval spacing was applied in nine studies. These consisted of five ecological studies including one habitat (Prous et al., 2004), two community studies (Peck, 1976; Novak et al., 2012) and two nutrients studies (Chapman, 1983; Campbell et al., 2011), as well as two techniques (Kozel et al., 2017; Wynne et al., 2018) and two inventory studies (Braack, 1989; Sharratt et al., 2000).

Seven studies (all ecologically focused) applied a quadrat approach sampling one cave by: establishing sampling grids along mud banks to examine arthropod response to augmented nutrients and water (Humphreys, 1991); dividing habitat types or substrates into sampling quadrats (Herrera, 1995; Zepon & Bichuette, 2017); dividing each study cave into 3-m quadrats along the length of the cave (Lunghi et al., 2014); apportioning the cave into five quadrats (Tobin et al., 2014); establishing sample quadrats/stations along the length of the study cave (Kur et al., 2016); and, creating 418 4-m^2 grids (surface to aphotic zone) to examine distribution of arthropods (Prous et al., 2015).

Sampling techniques

Cave biologists applied an array of methods for capturing arthropods including direct intuitive searching, opportunistic collecting, visual searching, timed and untimed searches, several types of pitfall trapping, substrate sampling, and using a variety of baits and leaf litter to attract arthropods (Fig. 5; Appendix II and III, Supplemental Information; Table 2). We also provided information on studies that applied each technique, their methodological limitations, and functional groups each technique was most likely to target (Appendix III, Supplemental Information).

Direct Intuitive Searching (DIS): Direct intuitive searches (i.e., specifically targeting a microhabitat and/or environmental zone to address a research question(s) and/or increase the likelihood of maximizing number of species detected) were applied in 34 studies. These microhabitats included flood detritus, penetrating tree roots hanging from ceilings/walls, guano deposits, edges of drip pools and ponds, muddy banks, animal and/or insect carcasses. These areas were targeted because they were likely to support high diversity or contained specific functional groups (e.g., guanophiles). Additionally, researchers applied this approach to specific environmental cave zones (typically, the cave deep zone). This method may be either timed or untimed DIS with defined or undefined search radius.

Of the 34 studies applying DIS, 16 examined specific microhabitats, seven studies sampled bat guano deposits, seven studies searched for subterranean-adapted arthropods in deep zones, and four studies used DIS across multiple environmental zones. Eight studies were timed DIS, while 26 were untimed DIS. For timed DIS, Ferreira et al., (2000) searched each bat guano pile encountered within a cave for 30 minutes; search radius was not defined. Additionally, Wynne et al. (2018) applied a one-hour DIS in moss-fern/moss gardens and root curtains without defining a search radius, and one timed DIS within selected cave deep zones (10 minutes within an estimated 1-m^2 area).

Thirteen of 34 studies employed DIS within selected habitats as their only technique. Of these, six were designed to address ecological questions (Hill, 1981; Trajano, 2000; Silva et al., 2011, 2013; Zampaulo, 2015; Bento et al., 2016), two studies were conservation focused (Simões et al., 2014; Silva & Ferreira, 2015), one was a techniques paper (Gallão & Bichuette, 2015), and four studies were inventories (Barr & Reddell, 1967; Holsinger, et al., 1976; Edington, 1984; Drost & Blinn, 1997).

Visual Searches: Studies applying this technique explicitly stated "hand collection," "visible searches," "collecting," and "direct searches;" visual searching was employed in 29 studies (22 inventory and seven ecological studies). Overall, hand collecting and/or using instruments (e.g., aspirators) to facilitate collection was applied in 13 studies, visual search, direct search or visual inspection (in none of the cases was this clearly defined) was applied in six studies, and some variation on hand collection or visual search (e.g., "make collections", "basic collecting", "collecting," etc.) was applied in seven studies, and visual counting was used in three studies. This method was combined with other sampling techniques in four ecological studies and 12 inventory studies.

Table 2. Descriptions of the nine primary cave-dwelling arthropod sampling techniques within four methodological groups (hand sampling, trapping, substrate sampling, and attractants). We recommend standardizing to this terminology and providing more complete descriptions of all techniques used. Note: Multiple sampling techniques were applied in half the studies reviewed; thus, the "Times Applied" will total more than 110 (i.e., the number of papers reviewed).

Group / Method	Description	Times applied
Hand Sampling		
Direct Intuitive Search (DIS)	Surveys targeted to habitats likely to yield highest diversity, which include flood detritus, edges of pools, streams and flowstone, bat guano and other animal feces, carrion and/ or cave deep zones; applied in conjunction with a grid/ quadrat system or without defining size of search area; may be timed or untimed; arthropods collected by hand, aspirator, forceps, or paint brushes.	34
Visual search	Category created due to a lack of information provided; this category is probably DIS, opportunistic collecting or both; workers described this approach as "visual searching", "hand collecting", "direct searching", or simply "collecting" with no additional information provided.	29
Opportunistic collecting	Collecting arthropods as encountered while walking through the cave and/or conducting other tasks.	5
Timed search	Searches were timed and centered around pitfall trapping, leaf litter trap-like structures (with or without defining search area around traps), or within grids/ quadrats; arthropods were collected via same methods as DIS by examining the cave floor and/or adjacent wall, and searching beneath rocks and other objects.	16
Untimed search	Same as timed searches, but without allocating or reporting a standardized time spent searching per area.	10
Trapping		
Pitfall trapping	A container or tube-like apparatus counter sunk into the cave floor, left *in situ* for a specific period of time (typically no more than several days), then traps and contents are retrieved. The four primary pitfall trap types are baited with or without a preservative (e.g., alcohol, ethylene, or propylene glycol) and unbaited with or without a preservative; various baits may be used, refer to text for more information.	41
Leaf litter	Cleaned (autoclaved recommended), arthropod-free brown leaves from surface placed upon a wire mesh/ window screen or directly on cave floor, and typically in damp areas; water delivery systems may be used for xeric areas within caves.	4
Extraction		
Substrate sampling	Direct removal of cave sediment, bat guano, leaf litter, and/or flood detritus; arthropods are subsequently extracted using Berlese/ Tullgren funnels, sorting and removing by hand, sieving, or a combination thereof.	36
Attractants		
Bait	Deployed in specific habitats (typically in cave deep zones to attract troglobionts), left *in situ* for a few days, then baits and arthropods selectively removed; baits typically placed on the cave floor and within cracks and crevices of walls and ceiling; a variety of baits may be used to attract different feeding guilds, refer to text for more information.	14

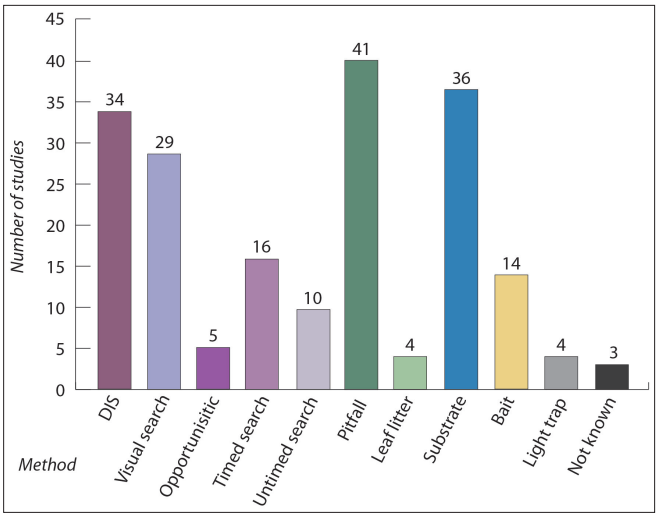

Fig. 5. Total number of times each sampling technique was applied for the 110 studies reviewed. Because multiple techniques were used for more than half of the studies reviewed, the contents of this graph total more than 110. Hand collecting (DIS through Untimed Search in purple hues), and trapping (pitfall and leaf litter in green hues). Variants of same color were used to convey similarities across techniques. DIS refers to 'direct intuitive search' (which combined timed and untimed applications).

Visual searching was employed as a single technique in nine inventory studies and one ecological study. Additionally, in three cases, arthropods were "visually counted" (two ecological and one inventory); most of these studies applied visual counting in combination with other techniques.

Phrases such as "hand collecting", "visual searching", "direct searching", or simply "collecting" were used to describe this technique. This category likely represents studies applying direct intuitive searches, opportunistic collecting, or a combination of the two; unfortunately, there was not sufficient information provided to confidently make this determination. This approach is particularly useful for targeting some predators (in particular, spiders and harvestmen). Additionally, some negatively phototactic arthropods will retreat from the observers' light and may not be detected.

Opportunistic collecting: Five studies applied what we considered 'opportunistic collecting'. With the exception of two cases (Wynne & Pleytez, 2005; Ferreira et al., 2000), the remaining studies specifically stated

arthropods were collected opportunistically (refer to Reeves et al., 2000; Wynne & Voyles, 2014; Wynne et al., 2018). This technique involves researchers walking through the cave, examining rock walls, floors, and ceilings, and collecting arthropods as they are encountered (e.g., Wynne et al., 2018).

Timed searches: This adds a systematic component to visual searches for cave-dwelling arthropods. Timed searches (TS) may be applied to improve the thoroughness of trapping or baiting, as well as for sampling arthropods by cave environmental zone, at predetermined intervals or within quadrats. When applied in concert with trapping or baiting, we recommend further standardizing this approach by using a fixed grid or radius around the trap or bait.

Timed searches were applied in 16 of the 110 papers examined. This technique included several variations *viz*: coupled TS with pitfall trapping (3 studies); conducted TS within defined quadrats (5 studies); applied TS by cave environmental zone (4 studies); conducted TS at standard intervals (1 study); applied a total amount of time spent per cave searching (1 study); and two studies did not provide enough information to determine how the TS was applied. For the studies using pitfall trapping, two (Campbell et al., 2011; Wynne et al., 2018) used fixed radius TS around the traps prior to deployment and removal, while Peck (1976) applied an undefined radius, one-minute search prior to trap deployment and removal.

For 11 studies, timed searches were employed within study designs using cave environmental zones, quadrat, or interval sampling approach. Wynne & Voyles (2014) and Oromí et al. (1990) used TS in the three primary environmental zones (entrance, twilight, and "dark"), while Ashmole et al. (1992) applied TS at selected locations within the twilight and "dark" zones. Prous et al. (2004) searched for ≥25 minutes at 2-m intervals. Lunghi et al. (2014), Sharratt et al. (2000) and Tobin et al. (2014) performed TS using quadrat sampling at 7.5 minutes, 10 to 25 minutes, and 30 minutes per quadrat, respectively. Weinstein and Slaney (1995) employed a TS approach along five transects, which encompassed the twilight, transition, and deep zones; their results were compared to the results of other systematically applied techniques. Christiansen & Bullion (1978) applied TS most broadly; whereby they searched for 30 to 120 minutes along the length of each of their 58 study caves. Both Sendra & Reboleira (2012) and Sendra et al. (2014) performed one-hour searches within selected areas, but were not specific about where these searches occurred.

An added benefit of this technique, when combined with baited pitfall trapping, is detection of animals attracted by the bait but not ensnared by the trap. If consistently applied, it also allows comparisons of relative population density between caves – at least for species that are common and whose behavior is well known (e.g., Wynne et al., 2018).

Untimed searches: Untimed searches (UTS) were employed in 10 studies and applied in similar circumstances as timed searches. For five cases, this protocol was applied in conjunction with either pitfall or leaf-litter trapping, two studies employed UTS within a multi-technique sampling frame (not related to pitfall or leaf litter trapping), and three studies used UTS as a single technique. For studies coupling this technique with trapping, three of these studies used this method both before trap deployment and prior to trap removal (Poulson & Culver, 1969; Martín & Oromí, 1986; Wynne & Voyles, 2014), while two studies (Schneider & Culver, 2004 and Humphreys, 1991) applied this technique to pitfall traps and leaf litter traps, respectively, upon trap removal only. Martín & Oromí (1986) were the only study to define a search radius (1 to 5-m) around trapping stations.

The remaining studies used untimed searches within a quadrat, zonal or zonal sampling design. Krejca & Weckerly (2007), Dao-Hong (2006) and Prous et al. (2015) applied UTS as a single technique. Prous et al. (2015) and Kur et al. (2016) employed this technique in concert with other sampling methods.

Pitfall trapping: Pitfall trapping (PT) was the most commonly employed technique (41 of 110 studies; Fig. 5). Four approaches were used including baited with or without a preservative (e.g., alcohol, ethylene, or propylene glycol), and unbaited with or without a preservative. Traps with preservative result in 100% take (i.e., kill) of animals that fall into the trap. Traps without a preservative maintain captured animals alive until examined by researchers. However, captured animals may escape, be eaten by other animals, or die and begin to decompose before retrieval (Weeks & McIntyre, 1997). Weinstein & Slaney (1995) used glass jars with a constricted mouth since the curved neck should limit escape.

Pitfall traps were typically counter-sunk within the cave sediment and/or rocky substrate to minimize an exposed lip that might prevent capture of arthropods. When this was not possible, researchers built ramps around each trap using local materials (e.g., rocks, wooden debris, etc.) to provide invertebrates with easier access to the trap (e.g., Ashmole et al., 1992; Wynne & Voyles, 2014; Wynne et al., 2018). Campbell et al. (2011) developed a ramped PT design (trap was placed on the ground surface with plastic ramps leading to PT). Růžička et al. (2016) applied a free-hanging PT design, which attached to the walls of a vertical deep pit; these traps consisted of a ramp leading from the wall onto a platform with PT at center.

Of the 41 papers reporting on the use of pitfall traps, one study used both baited and unbaited traps (without preservative), 17 studies applied baited traps without preservative, 13 used bait with a preservative, three studies applied unbaited traps, five employed traps with preservative only, and two studies stated only that traps were used (Fig. 6). Various types of bait were used including rotten liver, cheese, banana, and peanut butter (Table 3). Four studies suspended baits (either cheese or liver) over a "Turquin" liquid, which served as both an attractant and preservative. Serrano & Borges (2010) described Turquin as a mixture of 1000-ml of dark beer, 5-ml acetic acid, 5-ml formalin, and 10-g of chloral hydrate. One study used PT with a "variety

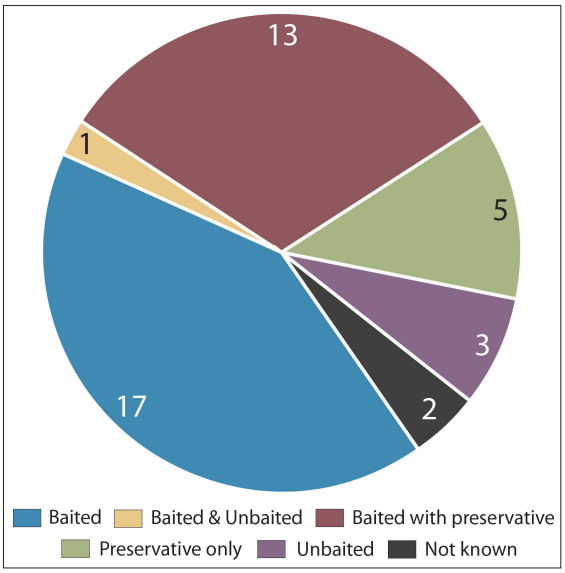

Fig. 6. Application of pitfall trapping across the 41 studies employing this technique. Legend reads left to right; pie chart reads clockwise starting with largest slice at bottom.

of attractants" (Araujo & Peixoto, 2015). Two studies used PT with only a preservative – formalin (Dessen et al., 1980) and a 50/50 water/ethanol mixture (Iskali & Zhang, 2015). Two studies (Reeves, 2001; Deleva & Georgiev, 2015) used ethylene glycol, which served as both an attractant and preservative. One study used cheese and ethylene glycol as a bait/ attractant (Isaia et al., 2011). Wynne & Voyles (2014) used live capture baited and unbaited PT and Wynne et al. (2018) used live capture PT; both studies baited with peanut butter.

Functional groups most often captured in PT include detritivores and omnivores, as well as some predators and other functional groups. However, some cavernicoles, especially many troglomorphic species, do not enter pitfalls (Kuštor & Novak, 1980; Bell et al., 2007). Both Barber (1931) and Valentine (1941) favored baited PT for capturing cavernicolous, omnivorous, and carrion beetles due to its quick return rate. Wynne et al. (2018) reported that most (70% of beetle morphospecies) were detected with baited traps. Conversely, spiders and volant species may escape from live capture pitfalls.

Other considerations include anticipating possible disturbance by rats or other mammals (including humans), as well as mitigating the potential harmful effects of this method on the cave resources. Placing cages around each trap may limit rodent disturbance, but may also prevent access by targeted animals. To limit human disturbance, hiding traps or deploying in cryptic areas may help. Importantly, efforts must be made to prevent disturbance to other cave resources (e.g., archaeological, cultural, geologic, and paleontological) when placing and removing traps. In some cases, physically disturbing the cave floor or sediments to install traps may be prohibited. Additionally, many preservatives applied in the past (e.g., picric acid, choral hydrate, and formalin) are now regulated chemicals and considered dangerous to use in caves. Propylene glycol with the proper mixture of ethanol to break the surface tension is a preferred preservative for most invertebrates and is considered environmentally safe.

Substrate sampling: Substrate sampling involves collecting samples of sediment (e.g., soil, guano, or organic material), and then extracting specimens using a variety of techniques. The most common extraction methods include using Berlese or Tullgren funnels, floating in a liquid, and sieving. Thirty-six studies applied this approach including: 16 studies examined bat guano; eight studies sampled sediment; five sampled "organic debris" or "detritus;" two studies sampled leaf litter; one study examined both sediment and bat guano; one study sampled oilbird (*Steatornis caripensis* Humboldt, 1817) seed beds and bat guano deposits; and, three studies did not state clearly what substrate was sampled.

Seventeen studies sampled substrate systematically. Of note, researchers applied the following methods: (i) a percentage or specific quantity of sediment (Welbourn, 1978; Northup et al., 1994; Lamprinou et

Table 3. Summary of bait types used in pitfall traps.

Bait type	References
Rotten liver	Poulson & Culver, 1969; Richards, 1971; Peck, 1976; Welbourn, 1978; Martín & Oromí, 1986; Ferreira et al., 2000
Cheese	Richards, 1971; Chapman, 1980; Oromí et al., 1990; Ashmole et al., 1992; Lewis et al., 2003; Schneider & Culver, 2004; Serrano & Borges, 2010; Sendra & Reboleira, 2012; Sendra et al., 2014
Peanut butter	Wynne & Voyles, 2014; Phillips et al., 2016; Wynne et al., 2018
Mixture of rice, fish, and meat	Chapman, 1982
Combination of meat, cheese, tinned fish, damp biscuits, jam, bird carcasses, human feces	Chapman, 1980
Ripe banana	Weinstein & Slaney, 1992
Beef liver, banana	Campbell et al., 2011
Oats, sugar, margarine	Reddell & Veni, 1996
Cheese and mushrooms	Howarth et al., 2007
Rotten beef with apple and cherry/ maraschino essence	Kozel et al., 2017
"Bone"	Bertolana et al., 1994

al., 2009; Dumnicka et al., 2015) or bat guano (Braack, 1989; Pellegrini & Ferriera, 2013; Iskali & Zhang, 2015) was collected; (ii) sediment (Herrera, 1995) or guano samples (Negrea & Negrea, 1971) were divided into subsamples by depth; and, (iii) a percentage of each bat guano pile was sampled (Ferreira & Martins, 1999; Ferreira et al., 2000). The remaining six studies applied a systematic design, but did not provide the quantities of materials collected.

Substrate sampling is used primarily for collecting microarthropods. However, if samples are not handled properly and processed in a timely manner, they can become damaged resulting in few to no animals extracted. Animals most likely to be detected are guanophiles, edaphobites, detritivores, and their predators.

Bait sampling: Typically, bait sampling involves deployment of baits directly onto cave floors, walls, and ceilings, as well as within cracks and fissures, and is typically applied to detect subterranean-limited (i.e., troglomorphic) species. Fourteen studies reported using baits. These included baits: used in cave deep zones only in six studies (Peck, 1989; Buhlmann, 2001; Howarth et al., 2007; Faille et al., 2015; Kur et al., 2016; Wynne et al., 2018); deployed along the length of caves in three studies (Peck, 1982; Reeves & McCreadie, 2001; Pape & O'Connor, 2014); employed in select cave zones in one study (Howarth & Stone, 1990); and, placed at the bottom of vertical pits in another study (Schneider et al., 2011). Three studies did not provide specific details on the placement of baits.

Baits are often chosen based on their potential to attract specific taxa of interest. A variety of baits have been used including liver-based cat food (Buhlmann, 2001), chicken liver (Reeves & McCreadie, 2001), sweet potato (Howarth & Stone, 1990), wooden blocks (plant species not defined; Pape & O'Connor, 2014), dung and carrion (type of carrion not identified; Peck & Peck, 1981; Peck, 1989), liver and "carrion" (type not defined; Holsinger & Peck, 1971), carrion and cheese (types not defined; Peck, 1982), cottage cheese with bread (Kur et al., 2016), commercially-purchased dead "white lab rats" (Schneider et al., 2011), sweet potato, native tree branches, chicken liver and fish entrails (Wynne et al., 2018), cat food, chicken liver, dung, rotten apples and cheese (Reeves et al., 2000), sweet potato, blue cheese, mushroom and oatmeal (Howarth et al., 2007), and moss, rotten wood and cheese (types not described; Faille et al., 2016). For all bait types, efforts should be made to remove residues once sampling is completed.

Leaf litter attractant: Leaf litter was used both as an attractant and habitat substrate in four studies. The litter serves as habitat, cover and nutrient source for fungivores, detritivores, omnivores and their predators. Three studies (Humphreys, 1991; Weinstein & Slaney, 1995; Encinares & Lit, 2014) placed leaf litter within a trap structure, while Schneider et al. (2011) placed leaf litter directly on the cave floor. Humphreys (1991) used leaf litter traps with a water delivery system to keep the litter wet and facilitate leaf decomposition; he examined the effects of nutrient subsidies to caves. Whereas, Weinstein & Slaney (1995) and Encinares & Lit (2014) compared the efficacy of using wet and dry leaf traps. If using a water drip system, checking and maintaining traps will depend upon the amount of time water can be actively delivered before the water runs out. Schneider et al. (2011) reported that millipedes and collembolans were most abundantly detected groups in their study.

Leaf litter should be cleaned before deployment in caves. Encinares & Lit (2014) used a Berlese funnel to extract arthropods prior to using bamboo. However, autoclaving leaves would ensure the material does not harbor harmful and unwanted organisms, such as *Beauveria bassiana* (Bals.-Criv.) Vuill. (1912) (Gunde-Cimerman et al.,1998) and *Metarhizium anisopliae* (Metschnikoff, 1879) Sorokin, 1883 (Zhang et al., 2017), which are entomopathogens; both have broad host ranges and are widely used for pest control in surface environments. Insect predators (Howarth & Moore, 1984) and alien species competitors (Wynne et al., 2014) may also be introduced. Failure to apply this cleaning step may also result in captured surface arthropods being incorrectly classified as cavernicoles. For reference, Slaney & Weinstein (1996) provided an illustration of their trap design.

Light trapping & Dry ice: Three studies used incandescent white light trapping (McClure et al., 1967; Chapman, 1980; Peck, 1984). Peck (1984) indicated his light suction trap designed to specifically target Diptera was unsuccessful. While this technique may be useful in attracting some arthropods like certain species of Diptera, Lepidoptera, and Coleoptera, using full spectrum lighting to attract arthropods hasn't resurfaced in the literature (at least based upon our review) in over 30 years. However, Reeves (2001) employed both black lights and dry ice for trapping arthropods, although there was no discussion specifically stating the efficacy of these techniques.

DISCUSSION

As cavernicolous arthropod inventories and question-driven research projects are conducted in the future, we recommend structuring these studies in a manner that maximizes scientific inference and provides the information necessary to make evidence-based management decisions. To this end, future studies should include the following elements: systematic experimental design; repeatability (in that the methods are thoroughly reported); use of multiple techniques; and use of multiple site visits (Wynne et al., 2018).

Most of the studies reviewed did not include a clearly discernable *a priori* systematic study design. Culver & Sket (2002) even questioned the utility of such an approach for both sampling and monitoring cavernicolous arthropods. Certainly, low population densities and the heterogeneous nature in which microhabitats and nutrients are distributed within caves, as well as the seasonal influx of nutrients (e.g., bat guano and flood detritus), have presented researchers with challenges for both optimal sampling and monitoring. Nonetheless, for cave biology to

progress, systematically applied experimental design and sampling efforts are necessary both to make results comparable across caves and to advance hypothesis-driven studies. For monitoring cave-dwelling arthropod species of concern, the U.S. Fish and Wildlife Service has partially addressed the heterogeneity issue by requiring a suite of environmental conditions be met and surveys conducted during the most appropriate season, as well as providing a checklist of suitable conditions for troglomorphic arthropods (USFWS, 2006). We recommend that sampling also include an intensive systematic approach to optimally detect the greatest number of species, as well as potentially detect more cryptic animals (such as troglobionts; Wynne et al., 2018).

Only 24 studies were repeatable (i.e., workers clearly documented their sampling techniques and experimental design). For cave arthropod studies to more solidly advance our understanding of cave communities both temporally and spatially, researchers should thoroughly document how their field data were collected. Without this step, meaningful quantitative comparisons across caves and regions cannot be made and evidence-based conservation planning and monitoring of sensitive taxa and/or communities cannot be assured.

We recognize that optimal sampling methods change over time as technology and our understanding of cave ecology advances; therefore, we hope that this paper will serve to advance future work. We realize the methods applied must be appropriate to fulfill the objectives of the particular study. Thus, one set of protocols will unlikely be suitable for all cave studies. Furthermore, the complexity of caves often requires that study designs be modified in the field to address local cave conditions.

That said, we recommend further standardization of sampling terminology (refer to Table 2). The most substantial gray areas in our review were the lack of clarity on use of the terms: visual searches, direct searches, opportunistic collecting, and direct intuitive searches. 'Visual searching' was either 'opportunistic collecting' or 'direct intuitive searching;' however, because there was not sufficient information to explain what the workers meant by 'visual searching,' we created the visual search category. Furthermore, we also found inconsistencies in how direct searches were described. Thus, when information was lacking, studies using direct searches were included in the visual search category. Providing a sufficient description of the sampling methods applied will be critical to avoiding confusion in the future.

Clear descriptions of the study design and the sampling methods can be further enhanced by including figures of sampling locations plotted on cave maps for the sake of repeatability. Given that most journals offer archiving of data as online supplemental information, this is a methodological perk available to most researchers, often at no extra cost. Thus, inclusion of this information will enable future workers to know the precise locations of past sampling efforts, and may use this information for both replicating experiments and establishing future monitoring strategies for resource management. However, researchers must adhere to federal and local agencies and regulations in the countries in which they work regarding the publication of potentially sensitive information (e.g., USC, 1988). Research permits for cave access often include a nondisclosure clause regarding the dissemination of sensitive data (e.g., cave names and in some cases, cave maps). When such guidance is not provided, we recommend using a decision tree like the one developed by Tulloch et al. (2018) to examine the risks and benefits associated with disclosing potentially sensitive information.

Of the papers included in this analysis, 10 studies conducted 10 or more site visits per cave. We recognize many biological inventories are designed to visit as many caves as possible in a short time to establish a baseline for site specific or regional diversity. Unfortunately, in most cases it is unlikely enough site visits were conducted to reasonably characterize arthropod diversity or community structure. For example, Wynne et al. (2018) intensively sampled 26 caves (10 caves each in two southwestern U.S. national monuments and six caves at Rapa Nui National Park, Easter Island, Chile), where they conducted between two to six site visits per cave. For each region, they pooled data across all caves and generated species accumulation curves – none of the curves for any of the regions exhibited signs of asymptotic behavior (Wynne et al., 2018). Thus, while biological inventories are of critical importance in establishing baseline information, as well as being helpful as a hypothesis generating exercise for future work, these data are typically quite limited in their ability to fully characterize arthropod communities.

Multiple site visits may be especially critical to more thoroughly inventory troglomorphic arthropods. For a cave in Williamson County, Texas, Krejca & Weckerly (2007) reported that despite intensive surveys by trained cave biologists an undescribed pseudoscorpion species was discovered upon the 40th visit to the cave. While not directly applicable to terrestrial cave-dwelling invertebrates, Sket (1981) and Culver et al. (2004) reported a new stygobiont (belonging to a new genus) after over one hundred site visits to a well studied cave in Slovenia. Granted it may be impossible for most studies to conduct 40 to 100 site visits per cave, but these examples underscore the need to conduct multiple site visits to most thoroughly define cave communities.

When sampling techniques are applied singly, the study may (a) fail to identify species of potential management concern (e.g., troglobionts and relict species), and (b) not be effective for long-term monitoring to detect changes related to anthropogenic impacts or stochastic events. Through their work, Wynne et al. (2018) found that the six techniques uniquely identified morphospecies; had multiple techniques not been applied, eight new species of presumed cave-restricted arthropods on Easter Island (Wynne et al., 2014), and the range expansions of two species of two tiphiid wasps in west-central New Mexico, would not have been detected (Wynne, 2013). In general, numerous studies (e.g., Muma,

1945; Ashmole & Ashmole, 1987; Basset et al., 1996; Wynne et al., 2018) have shown that applying multiple techniques resulted in the detection of a greater number of individuals and species than studies employing only one technique.

While it is often quite difficult to identify the number of site visits and the suite of techniques required to best capture cave arthropod diversity, Wynne et al. (2018) recommended applying as many sampling techniques and conducting as many site visits as possible. Species accumulation curves and species richness estimators (see Magurran, 2004) are also recommended tools for both gauging the efficacy of sampling efforts, and identifying areas requiring additional inventories. In most cases, Wynne et al. (2018) reported that species accumulation curves were more asymptotic (i.e., flatter) for all techniques combined (they applied a total of six techniques) than for curves generated using data from single techniques. Schneider & Culver (2004), who focused their efforts on troglomorphic arthropods, reported none of their species accumulation curves neared asymptotic behavior. Reporting similar non-asymptotic behavior, Gallão & Bichuette (2015) emphasized that sensitive subterranean-adapted species may be overlooked due to limited sampling; this could result in making incorrect management decisions based upon incomplete information.

To address the dilemma of incomplete surveys, Howarth & Ramsay (1989) recommended the use of 'indicator species' as a proxy for making management decisions. Specifically, discovering a cave passage with suitable environmental conditions associated with one or more significant cavernicoles may be sampled to gain inference into whether the cave warrants protective management or should be more fully studied.

While most of papers examined (~62%; or 68 of 110) did not discuss conservation and management implications, we acknowledge recommendations may have been made directly to resource managers and thus were not reported in the peer-reviewed publications we reviewed. Furthermore, conservation may simply not have been a goal of some studies, especially for those papers published before the amendment to the U.S. Endangered Species Act in 1978, which expanded the Act to include invertebrate species (USC, 1973). Subsequently, our review may underestimate the contributions made by some of these studies to conservation. However, with the rising anthropogenic impacts facing cave ecosystems globally, we maintain that inclusion of this information in the published literature is essential to aid in further developing the field of cave biology and promoting improved management and policy strategies.

Given the sensitivity of most cave communities and troglomorphic species to human disturbance, conservation and management should be at the forefront of cave biology. Through improvements in methodological reporting, systematic sampling designs using multiple techniques, and reliance on species accumulation curves to guide the number of site visits required to establish a reasonable baseline, cave biologists will both strengthen their ability to make more robust statistical inference and develop sound management recommendations based upon the best available data and resultant science.

ACKNOWLEDGEMENTS

We sincerely thank Jeffery Foster and Thomas Sisk of Northern Arizona University for providing comments and editorial suggestions. David Culver and Matthew Niemiller peer-reviewed this paper. Melanie W. Gregory and Alan Campbell offered fructuous discussions on color schemes for figures. Their contributions greatly improved the quality of this manuscript.

REFERENCES

Aley T.J., 1976 – *Hydrology and surface management*. In: *The National Cave Management Symposium Proceedings*. Albuquerque, New Mexico, p. 44-45.

Araujo A.V. & Peixoto R.S., 2015 – *The impact of geomorphology and human disturbances on the faunal distributions in Tiquara and Angico Caves of Campo Formoso, Bahia, Brazil*. Ambient Science, **2**: 25-30. https://doi.org/10.21276/ambi.2015.02.1.ra04

Ashmole M.J. & Ashmole N.P., 1987 – *Arthropod communities supported by biological fallout all recent lava flows in the Canary Islands*. Entomologica Scandinavica Supplement, **32**: 67-88.

Ashmole N.P., Oromí P., Ashmole M.J. & Martín J.-L., 1992 – *Primary faunal succession in volcanic terrain: lava and cave studies on the Canary Islands*. Biological Journal of the Linnean Society, **46**: 207-234. https://doi.org/10.1111/j.1095-8312.1992.tb00861.x

Badino G., 2004 – *Cave temperatures and global climate change*. International Journal of Speleology, **33**: 103-114. https://doi.org/10.5038/1827-806X.33.1.10

Barber H.S., 1931 – *Traps for cave inhabiting insects*. Journal of the Mitchell Society, **46**: 259-266. https://www.jstor.org/stable/24332344

Barr T.C., Jr. & Reddell J.R., 1967 – *The arthropod cave fauna of Carlsbad Caverns Region, New Mexico*. The Southwestern Naturalist, **12**: 253-273. https://doi.org/10.2307/3669113

Basset Y., Springate N.D., Aberlenc H.P. & Delvare G., 1996 – *A review of methods for sampling arthropods in tree canopies*. In: Stork N.E., Adis J. & Didham R.K. (Eds.), *Canopy arthropods*. Chapman and Hall, London, p. 27-52.

Bell W.J, Roth L.M. & Nalepa C.A., 2007 – *Cockroaches: Ecology, behavior and natural history*. Johns Hopkins University Press, Baltimore, 248 p.

Benedict E.M., 1979 – *A new species of Apochthonius Chamberlin from Oregon (Pseudoscorpionida, Chthoniidae)*. Journal of Arachnology, **7**: 79-83. https://www.jstor.org/stable/3704956

Bento D.D.M., Ferreira R.L., Prous X., Souza-Silva M., Bellini B.C. & Vasconcellos A., 2016 – *Seasonal variations in cave invertebrate communities in the semiarid Caatinga, Brazil*. Journal of Cave and Karst Studies, **78**: 61-71. https://doi.org/10.4311/2015LSC0111

Bertolana R., Manicardi G.C. & Rebecchi L., 1994 – *Faunistic study in the karst complex of Frasassi (Genga, Italy)*. International Journal of Speleology, **23**: 61-77. https://doi.org/10.5038/1827-806X.23.1.9

Borges P.A.V., Cardoso P., Amorim I.R., Pereira F.E.A.P., Constância J.P., Nunes J.C., Barcelos P., Costa P.,

Gabriel R. & Dapkevicius M.L., 2012 – *Volcanic caves: priorities for conserving the Azorean endemic troglobiont species*. International Journal of Speleology, **41**: 101-112. https://doi.org/10.5038/1827-806X.41.1.11

Braack L.E.O., 1989 – *Arthropod inhabitants of a tropical cave "island" environment provisioned by bats*. Biological Conservation, **48**: 77-84. https://doi.org/10.1016/0006-3207(89)90027-X

Buhlmann K.A., 2001 – *A biological inventory of eight caves in northwestern Georgia with conservation implications*. Journal of Cave and Karst Studies, **63**: 91-98.

Campbell J.W., Woods M., Ball H.L., Pirkle R.S., Carey V. & Ray C.H., 2011 – *Terrestrial macroinvertebrates captured with a baited ramp-pitfall trap from five limestone caves in North Alabama and Georgia (USA) and their association with soil organic matter*. Journal of Natural History, **45**: 2645-2659. https://doi.org/10.1080/00222933.2011.597884

Chapman P., 1980 – *The biology of caves in Gunung Mulu National Park, Sarawak*. Transactions of the British Cave Research Association, **7**: 141-149.

Chapman P., 1982 – *The ecology of caves in the Gunung Mulu National Park, Sarawak*. Transactions of the British Cave Research Association, **9**: 142-163.

Chapman P., 1983 – *Quantitative analysis of cave-dwelling invertebrates in Estado Falcón, Venezuela*. National Speleological Society Bulletin, **45**: 40-44.

Chevaldonné P. & Lejeune C., 2003 – *Regional warming-induced species shift in northwest Mediterranean marine caves*. Ecology Letters, **6**: 371-379. https://doi.org/10.1046/j.1461-0248.2003.00439.x

Christiansen K. & Bullion M., 1978 – *An evolutionary and ecological analysis of the terrestrial arthropods of caves in the Central Pyrenees*. National Speleological Society Bulletin, **40**: 103-117.

Christman M.C., Culver D.C., Madden M.K. & White D., 2005 – *Patterns of endemism of the eastern North American cave fauna*. Journal of Biogeography, **32**: 1442-1452. https://doi.org/10.1111/j.1365-2699.2005.01263.x

Culver D.C., 1986 – *Cave faunas*. In: Soulé M. (Ed.), *Conservation biology*. Sinauer Associates, Inc., Sunderland, p. 427-443.

Culver D.C. & Sket B., 2002 – *Biological monitoring in caves*. Acta Carsologica, **31**: 55-64. https://doi.org/10.3986/ac.v31i1.403

Culver D.C., Master L.L., Christman M.C. & Hobbs H.H. III., 2000 – *Obligate cave fauna of the 48 contiguous United States*. Conservation Biology, **14**: 386-401. https://doi.org/10.1046/j.1523-1739.2000.99026.x

Culver D.C., Christman M.C., Sket B. & Trontelj P., 2004 – *Sampling adequacy in an extreme environment: species richness patterns in Slovenia caves*. Biodiversity and Conservation, **13**: 1209-1229. https://doi.org/10.1023/B:BIOC.0000018153.49280.89

Dao-hong L., 2006 – *Correlation between the animal community structure and environmental factors in Dongbei Cave and Shuijiang Cave of Guizhou Province*. Zoological Research, **27**: 481-488.

Deleva S. & Georgiev D., 2015 – *Quantitative comparison of the complexes of terrestrial arthropods (Arthropoda) in two caves, located in different karst regions in Western Rhodopes mountains, Bulgaria*. Historia Naturalis Bulgarica, **21**: 257-266.

Dessen E.M.B., Eston V.R., Silva M.S., Temperini-Beck M.T. & Trajano E., 1980 – *Levantamento preliminar da fauna de cavernas de algumas regiões do Brasil*. Ciência e Cultura, **32**: 714-725.

Deharveng L. & Bedos A., 2000 – *The cave fauna of Southeast Asia: Origin, evolution and ecology*. In: Wilkens H., Culver D.C. & Humphreys W.F. (Eds.), *Ecosystems of the World 30: Subterranean ecosystems*. Elsevier, Amsterdam, p. 603-632.

Drost C.A. & Blinn D.W., 1997 – *Invertebrate community of Roaring Springs Cave, Grand Canyon National Park, Arizona*. The Southwestern Naturalist, **42**: 497-500. https://www.jstor.org/stable/30055318

Dumnicka E., Galas J., Karlikowska J. & Sznober N., 2015 – *Temporary co-existence of aquatic and terrestrial invertebrates in shallow periodically flooded and frozen cave*. Biologia, **70**: 1201-1209. https://doi.org/10.1515/biolog-2015-0142

Eberhard S.M., Halse S.A. & Humphreys W.F., 2005 – *Stygofauna in the Pilbara region, northwest Western Australia: a review*. Journal of the Royal Society of Western Australia, **88**: 167-176.

Edington M.A., 1984 – *Biological observation on the Ogbunike Cave System, Anambra State, Nigeria*. Studies in Speleology, **5**: 31-38.

Elliott W.R., 1992 – *Fire ants invade Texas caves*. American Caves: Winter **13**.

Elliott W.R., 2000 – *Conservation of the North American cave and karst biota*. In: Wilkens H., Culver D.C. & Humphreys W.F. (Eds.), *Ecosystems of the World 30: Subterranean ecosystems*. Elsevier, Amsterdam, p. 665-689.

Encinares J.M.A. & Lit I.L. Jr., 2014 – *Evaluation of leaf litter baits for sampling insects in Bulalon Cave, Burdeos, Pollilo Island, Quezon Province, Philippines*. Philippine Entomologist, **28**: 76-89.

Faille A., Bourdeau C. & Deharveng L., 2015 – *Weak impact of tourism activities on biodiversity in a subterranean hotspot of endemism and its implications for the conservation of cave fauna*. Insect Conservation and Diversity, **8**: 205-215. https://doi.org/10.1111/icad.12097

Ferreira R.L. & Martins R.P., 1999 – *Trophic structure and natural history of bat guano invertebrate communities, with special reference to Brazilian caves*. Tropical Zoology, **12**: 231-252. https://doi.org/10.1080/03946975.1999.10539391

Ferreira R.L., Martins R.P. & Yanega D., 2000 – *Ecology of bat arthropod communities in a Brazilian cave*. Ecotropica, **6**: 105-116.

Gallão J.E. & Bichuette M.E., 2015 – *Taxonomic distinctness and conservation of a new high biodiversity subterranean area in Brazil*. Anais da Academia Brasileira de Ciências, **87**: 209-217. https://doi.org/10.1590/0001-3765201520140312

Gao Z., Wynne J.J. & Zhang F., 2018 – *Two new species of cave-adapted pseudoscorpions (Pseudoscorpiones, Neobisiidae, Chthoniidae) from Guangxi, China*. Journal of Arachnology, **46**: 345-354. https://doi.org/10.1636/JoA-S-17-063.1

Gibert J. & Deharveng L., 2002 – *Subterranean ecosystems: a truncated functional biodiversity*. BioScience, **52**: 473-481. https://doi.org/10.1641/0006-3568(2002)052[0473:SEATFB]2.0.CO;2

Gilgado J.D., Enghoff H., Tinaut A. & Ortuno V.M., 2015 – *Hidden biodiversity in the Iberian Mesovoid Shallow Substratum (MSS): New and poorly known species of the millipede genus Archipolydesmus Attems, 1898 (Diplopoda, Polydesmidae)*. Zoologischer Anzeiger-A Journal of Comparative Zoology, **258**: 13-38. https://doi.org/10.1016/j.jcz.2015.06.001

Graening G.O. & Brown A.V., 2003 – *Ecosystem dynamics and pollution effects in an Ozark cave stream*. Journal of the American Water Resources Association, **39**: 1497-1507. https://doi.org/10.1111/j.1752-1688.2003.tb04434.x

Gunde-Cimerman N., Zalar P. & Jeram S., 1998 – *Mycoflora of cave cricket* Troglophilus neglectus *cadavers*. Mycopathologia, **141**: 111-114. https://doi.org/10.1023/A:1006947524503

Herrera F.F., 1995 – *Las comunidades de arthropodos del guano de guacharos en la cueva del guacharo, Venezuela*. Boletim da Sociedad Venezoelana de Espeleologia, **29**: 39-46.

Hill S.B., 1981 - *Ecology of Balo guano in Tamana Cave, Trinidad, W.I.* In: Beck B.F. (Ed.), *Proceedings of the 8th International Congress of Speleology*, Bowling Green, KY, **1**: 243-246.

Holsinger J.R. & Peck S.B., 1971 – *The invertebrate cave fauna of Georgia*. National Speleological Society Bulletin, **33**: 23-44.

Holsinger J.R., Baroody R.A. & Culver D.C., 1976 – *The invertebrate cave fauna of West Virginia*. West Virginia Speleological Survey Bulletin, **7**: 1-82.

Howarth F.G., 1980. *The zoogeography of specialized cave animals: A bioclimatic model*. Evolution, **34**: 394-406. https://doi.org/10.1111/j.1558-5646.1980.tb04827.x

Howarth F.G., 1983 – *Ecology of cave arthropods*. Annual Review of Entomology, **28**: 365-389. https://doi.org/10.1146/annurev.en.28.010183.002053

Howarth F.G. & Moore J., 1984 – *The land nemertine* Argonemertes dendyi *(Dakin) in Hawaii (Nemertinea: Hoplonemertinea: Prosorhochmidae)*. Pacific Science, **37**: 141-144.

Howarth F.G. & Ramsay G.W., 1991 – *The conservation of island insects and their habitats*. In: Collins N.M. & Thomas J.A. (Eds.), *The Conservation of Insects and their Habitats, 15th Symposium of the Royal Entomological Society of London*. Academic Press, p. 71-107. https://doi.org/10.1016/B978-0-12-181370-3.50010-5

Howarth F.G. & Stone F.D., 1990 – *Elevated carbon dioxide levels in Bayliss Cave, Australia: Implications for the evolution of obligate cave species*. Pacific Science, **44**: 207-218.

Howarth F.G. & Stone F.D., 1993 – *Conservation of Hawaii's speleological resources*. In: Halliday W.R. (Ed.), *Proceedings of the third international symposium on volcanospeleology, Bend, Oregon, 1982*. International Speleological Foundation, Seattle, p. 124-126.

Howarth F.G., James S.A., McDowell W., Preston D.J. & Imada C.T., 2007 – *Identification of roots in lava tube caves using molecular techniques: implications for conservation of cave arthropod faunas*. Journal of Insect Conservation, **11**: 251-261. https://doi.org/10.1007/s10841-006-9040-y

Humphreys W.F., 1991 – *Re-establishment of pulse-driven populations in a terrestrial troglobite community*. Journal of Animal Ecology, **60**: 609-623. https://doi.org/10.2307/5301

Isaia M., Giachino P.M., Sapino E., Casale A. & Badino G., 2011 – *Conservation value of artificial subterranean systems: A case study in an abandoned mine in Italy*. Journal for Nature Conservation, **19**: 24-33. https://doi.org/10.1016/j.jnc.2010.04.002

Iskali G. & Zhang Y., 2015 – *Guano subsidy and the invertebrate community in Bracken Cave: the world's largest colony of bats*. Journal of Cave and Karst Studies, **77**: 28-36. https://doi.org/10.4311/2013LSC0128

Kane T.C. & Poulson T.L., 1976 – *Foraging by cave beetles: spatial and temporal heterogeneity of prey*. Ecology, **57**: 793-800. https://doi.org/10.2307/1936192

Kozel P., Pipan T., Šajna N., Polak S. & Novak T., 2017 – *Mitigating the conflict between pitfall-trap sampling and conservation of terrestrial subterranean communities in caves*. International Journal of Speleology, **46**: 359-368. https://doi.org/10.5038/1827-806X.46.3.2123

Krejca J.K. & Weckerly B., 2007 – *Detection probabilities of karst invertebrates*. In: Elliott W.R. (Ed.), *Eighteenth national cave and karst management symposium (St. Louis, Missouri, USA, 8-12 October 2007)*. Texas Parks and Wildlife Department, Austin, p. 283-289.

Kur J., Radwański J.M. & Mioduchowska M., 2016 – *Investigation of the fauna in the Szmaragdowa/ Szeptunów Cave in Poland: an example of short time colonization process*. Acta Zoologica Cracoviensia, **59**: 153-162. https://doi.org/10.3409/azc.59_2.153

Kuštor V. & Novak T., 1980 – *Individual differences in trapping activity of two underground beetle species*. Mémoires de Biospéologie, **7**: 77-84.

Lamprinou V., Pantazidou A., Papadogiannaki G., Radea C. & Economou-Amill A., 2009 – *Cyanobacteria and associated invertebrates in Leontari Cave, Attica (Greece)*. Fottea, **9**: 155-164. https://doi.org/10.5507/fot.2009.014

Lisowski E.A., 1983 – *Distribution, habitat, and behavior of the Kentucky cave shrimp Palaemonias ganteri Hay*. Journal of Crustacean Biology, **3**: 88-92. https://doi.org/10.2307/1547855

Lunghi E., Manenti R. & Ficetola G.F., 2014 – *Do cave features affect underground habitat exploitation by non-troglobite species?* Acta Oecologica, **55**: 29-35. https://doi.org/10.1016/j.actao.2013.11.003

Magurran A.E., 2004 – *Measuring biological diversity*. Blackwell Publishing, Malden, Massachusetts.

Mammola S, Goodacre S.L. & Isaia M., 2018 – *Climate change may drive cave spiders to extinction*. Ecography, **41**: 233-243. https://doi.org/10.1111/ecog.02902

Martín J.-L. & Oromí P., 1986 – *An ecological study of Cueva de los Roques lava tube (Tenerife, Canary Islands)*. Journal of Natural History, **20**: 375-388. https://doi.org/10.1080/00222938600770281

McClure H.E., Lim B.-L. & Winn S.E., 1967 – *Fauna of the Dark Cave, Batu Caves, Kuala Lumpur, Malaysia*. Pacific Insects, **9**: 400-428.

Mitchell R.W., 1970 – *Total number and density estimates of some species of cavernicoles inhabiting Fern Cave, Texas*. Annales de Spéléologie, **25**: 73-90.

Muma M.H., 1945 – *Note on collecting cave spiders*. National Speleological Society Bulletin, **7**: 49.

Negrea A. & Negrea Ş., 1971 – *Sur la synusie du guano des grottes du Banat (Roumanie)*. Travaux de l'Institut de Spéologie "Émile Racovitza", **10**: 81-122.

Niemiller M.L. & Zigler K.S., 2013 – *Patterns of cave biodiversity and endemism in the Appalachians and Interior Plateau of Tennessee, USA*. PLoS One, **8**: e64177. https://doi.org/10.1371/journal.pone.0064177

Niemiller M.L., Zigler K.S., Ober K.A., Carter E.T., Engel A.S., Moni G., Philips T.K. & Stephen C.D., 2017 – *Rediscovery and conservation status of six short-range endemic* Pseudanophthalmus *cave beetles (Carabidae: Trechini)*. Insect Conservation and Diversity, **10**: 495-501. https://doi.org/10.1111/icad.12263

Northup D.E., Carr D.L. & Crocker M.T., 1994 – *Biological investigations in Lechuguilla Cave*. National Speleological Society Bulletin, **56**: 54-63.

Notenboom J., Plénet S. & Turquin M.-J., 1994 – *Groundwater contamination and its impact on groundwater ecosystems*. In: Gilbert J., Danielopol

D.L. & Stanford J.A. (Eds.), *Groundwater ecology*. Academic Press Limited, London, p. 477-504. https://doi.org/10.1016/B978-0-08-050762-0.50025-5

Novak T., Perc M., Lipovsek S. & Janzekovic F., 2012 – *Duality of terrestrial subterranean fauna*. International Journal of Speleology, **41**: 181-188. https://doi.org/10.5038/1827-806X.41.2.5

Olson R., 2005 – *The ecological effects of Lock and Dam No. 6 in Mammoth Cave National Park*. In: Harmon D. (Ed.), *People, places, and parks: Proceedings of the 2005 George Wright Society conference on parks, protected areas, and cultural sites*. Hancock, Michigan, p. 294-299.

Oromí P., Martin J.L., Ashmole N.P. & Ashmole M.J., 1990 – *A preliminary report on the cavernicolous fauna of the Azores*. Mémoires de Biospéologie, **17**: 97-105.

Pape R.B. & O'Connor B.M., 2014 – *Diversity and ecology of the macro-invertebrate fauna (Nemata and Arthropoda) of Kartchner Caverns, Cochise County, Arizona, United States of America*. Check List, **10**: 761-794. https://doi.org/10.15560/10.4.761

Peck S.B., 1976 – *The effect of cave entrances on the distribution of cave-inhabiting terrestrial arthropods*. International Journal of Speleology, **8**: 308-321. https://doi.org/10.5038/1827-806X.8.4.1

Peck S.B., 1982 – *Invertebrate faunas and zoogeographic significance of lava tube caves in Arizona and New Mexico*. Great Basin Naturalist, **42**: 405-412. https://www.jstor.org/stable/41711943

Peck S.B., 1984 – *The invertebrate faunas of tropical American caves, Part 6: Jumandi Cave, Ecuador*. International Journal of Speleology, **14**: 1-8. https://doi.org/10.5038/1827-806X.14.1.1

Peck S.B., 1989 – *The cave fauna of Alabama: part I: the terrestrial invertebrates (excluding Insects)*. National Speleological Society Bulletin, **40**: 39-63.

Peck S.B. & Kukalova-Peck J., 1981 – *The subterranean fauna and conservation of Mona Island (Puerto Rico)*. National Speleological Society Bulletin, **43**: 59-68.

Peck S.B. & Wynne J.J., 2013 – *Ptomaphagus parashant new species (Coleoptera: Leiodidae: Cholevinae: Ptomaphagini): the most troglomorphic cholevine beetle known from Western North America*. The Coleopterists Bulletin, **67**: 309-317. https://doi.org/10.1649/0010-065X-67.3.309

Pellegrini T.G. & Ferreira R.L., 2013 – *Structure and interactions in a cave guano-soil continuum community*. European Journal of Soil Biology, **57**: 19-26. https://doi.org/10.1016/j.ejsobi.2013.03.003

Poulson T.L. & Culver D.C., 1969 – *Diversity in terrestrial cave communities*. Ecology, **50**: 153-158. https://doi.org/10.2307/1934678

Prous X., Ferreira R.L. & Martins R.P., 2004 – *Ecotone delimitation: epigean–hypogean transition in cave ecosystems*. Austral Ecology, **29**: 374-382. https://doi.org/10.1111/j.1442-9993.2004.01373.x

Prous X., Ferreira R.L. & Jacobi C.M., 2015 – *The entrance as a complex ecotone in a Neotropical cave*. International Journal of Speleology, **44**: 177-189. https://doi.org/10.5038/1827-806X.44.2.7

Pulido-Bosch A., Martín-Rosales W., López-Chicano M., Rodríguez-Navarro C.M. & Vallejos A., 1997 – *Human impact in a tourist karstic cave (Aracena, Spain)*. Environmental Geology, **31**: 142-149. https://doi.org/10.1007/s002540050173

Reddell J.R., 1994 – *The cave fauna of Texas with special reference to the western Edwards Plateau*. In: Elliott W.R. & Veni G. (Eds.), *The caves and karst of Texas*. National Speleological Society, Huntsville, p. 31-50.

Reddell J.R. & Veni G., 2001 – *Biology of the Chiquibul Cave System, Belize and Guatemala*. Journal of Cave and Karst Studies, **58**: 131-138.

Reeves W.K., 1999 – *Exotic species of North American caves*. In: Henderson K. (Ed.), *Proceedings of the 1999 National Cave and Karst Management Symposium*. Chattanooga, p. 164-166.

Reeves W.K., 2001 – *Invertebrate and slime mold cavernicoles of Santee Cave, South Carolina, USA*. Proceedings of the Academy of Natural Sciences of Philadelphia, **151**: 81-85. https://doi.org/10.1635/0097-3157(2001)151[0081:IASMCO]2.0.CO;2

Reeves W.K. & McCreadie J.W., 2001 – *Population ecology of cavernicoles associated with carrion in caves of Georgia, USA*. Journal of Entomological Science, **36**: 305-331. https://doi.org/10.18474/0749-8004-36.3.305

Reeves W.K., Jensen J.B. & Ozier J.C., 2000 – *New faunal and fungal records from caves in Georgia, USA*. Journal of Cave and Karst Studies, **62**: 169-179.

Richards A.M., 1971 – *An ecological study of the cavernicolous fauna of the Nullarbor Plain, Southern Australia*. Journal of Zoology, **164**: 1-60. https://doi.org/10.1111/j.1469-7998.1971.tb01297.x

Růžička V., Mlejnek R., Juřičková L., Tajovský K., Šmilauer P. & Zajíček P., 2016 – *Invertebrates of the Macocha Abyss (Moravian Karst, Czech Republic*). Acta Carsologica, **45**: 71-84. https://doi.org/10.3986/ac.v45i1.896

Schneider K. & Culver D.C., 2004 – *Estimating subterranean species richness using intensive sampling and rarefaction curves in a high density cave region in West Virginia*. Journal of Cave and Karst Studies, **66**: 39-45.

Schneider K., Christman M.C. & Fagan W.F., 2011 – *The influence of resource subsidies on cave invertebrates: results from an ecosystem-level manipulation experiment*. Ecology, **92**: 765-776. https://doi.org/10.1890/10-0157.1

Sendra A. & Reboleira A.S.P.S., 2012 – *The world's deepest subterranean community – Krubera-Voronja Cave (Western Caucasus)*. International Journal of Speleology, **41**: 221-230. https://doi.org/10.5038/1827-806X.41.2.9

Sendra A., Garay P., Ortuño V.M., Gilgado J.D., Teruel S. & Reboleira A.S.P.S., 2014 – *Hypogenic versus epigenic subterranean ecosystem: lessons from eastern Iberian Peninsula*. International Journal of Speleology, **43**: 253-264. https://doi.org/10.5038/1827-806X.43.3.2

Serrano A.R.M. & Borges P.A.V., 2010 – *The cave-adapted arthropod fauna from Madeira archipelago*. Arquipelago: Life and Marine Sciences, **27**: 1-7.

Sharratt N.J., Picker M.D. & Samways M.J., 2000 – *The invertebrate fauna of the sandstone caves of the Cape Peninsula (South Africa): patterns of endemism and conservation priorities*. Biodiversity and Conservation, **9**: 107-143. https://doi.org/10.1023/A:1008968518058

Silva M.-S. & Ferreira R.L., 2015 – *Cave invertebrates in Espírito Santo state, Brazil: a primary analysis of endemism, threats and conservation priorities*. Subterranean Biology, **16**: 79-102. https://doi.org/10.3897/subtbiol.16.5227

Silva M.S., Martins R.P. & Ferreira R.L., 2011 – *Cave lithology determining the structure of the invertebrate communities in the Brazilian Atlantic Rain Forest*. Biodiversity and Conservation, **20**: 1713-1729. https://doi.org/10.1007/s10531-011-0057-5

Silva M.-S., Júnior A.S. & Ferreira R.L., 2013 – *Food resource availability in a quartzite cave in the Brazilian*

montane Atlantic Forest. Journal of Cave and Karst Studies, **75**: 177-188. https://doi.org/10.4311/2010JCKS0158

Silva M., Martins R.P. & Ferreira R.L., 2015 – *Cave conservation priority index to adopt a rapid protection strategy: a case study in Brazilian Atlantic rain forest*. Environmental Management, **55**: 279-295. https://doi.org/10.1007/s00267-014-0414-8

Simões M.H., Silva M.-S., & Ferreira R.L., 2014 – *Cave invertebrates in northwestern Minas Gerais state, Brazil: endemism, threats and conservation priorities*. Acta Carsologica, **43**: 159-174. https://doi.org/10.3986/ac.v43i1.577

Sket B., 1981 – *Niphargobates orophobata n.g., n.sp. (Amphipoda, Gammaridae s.l.) from cave waters in Slovenia (NW Yugoslavia)*. Biološki Vestnik, **29**: 105-118.

Slaney D.P. & Weinstein P., 1996 – *Leaf litter traps for sampling Orthopteroid insects in tropical caves*. Journal of Orthoptera Research, **5**: 51-52. https://doi.org/10.2307/3503579

Stone F.D., Howarth F.G., Hoch H. & Asche M., 2012 – *Root communities in lava tubes*. In: White W.B. & Culver D.C. (Eds.), *Encyclopedia of caves (2nd Ed.)*. Academic Press, Cambridge, p. 658-664. https://doi.org/10.1016/B978-0-12-383832-2.00097-9

Sugai L.S.M., Ochoa-Quintero J.M., Costa-Pereira R. & Roque F.O., 2015 – *Beyond above ground*. Biodiversity and Conservation, **24**: 2109-2112. https://doi.org/10.1007/s10531-015-0918-4

Taylor S.J., Krejca J., Smith J.E., Block V.R. & Hutto F., 2003 – *Investigation of the potential for red imported fire ant (Solenopsis invicta) impacts on rare karst invertebrates at Fort Hood, Texas: a field study. Illinois Bexar County Karst Invertebrates Draft Recovery Plan Natural History Survey*. Center for Biodiversity Technical Report 2003, **28**: 1-153.

Tobin B.W., Hutchins B.T. & Schwartz B.F., 2014 – *Spatial and temporal changes in invertebrate assemblage structure from the entrance to the deep-cave zone of a temperature marble cave*. International Journal of Speleology, **42**: 203-214. https://doi.org/10.5038/1827-806X.42.3.4

Trajano E., 2000 – *Cave faunas in the Atlantic tropical rain forest: composition, ecology and conservation*. Biotropica, **32**: 882-893. https://doi.org/10.1111/j.1744-7429.2000.tb00626.x

Trontelj P.A., Blejec A. & Fišer C., 2013 – *Ecomorphological convergence of cave communities*. Evolution, **66**: 3852-3865. https://doi.org/10.1111/j.1558-5646.2012.01734.x

Tulloch A.I., Auerbach N., Avery-Gomm S., Bayraktarov E., Butt N., Dickman C.R., Ehmke G., Fisher D.O., Grantham H., Holden M.H. & Lavery T.H., 2018 – *A decision tree for assessing the risks and benefits of publishing biodiversity data*. Nature Ecology & Evolution, **2**: 1209-1217. https://doi.org/10.1038/s41559-018-0608-1

Ubick D. & Briggs T.S., 2002 – *The harvestman family Phalangodidae 4. A review of the genus Banksula (Opiliones, Laniatores)*. Journal of Arachnology, **30**: 435-451. https://doi.org/10.1636/0161-8202(2002)030[0435:THFPAR]2.0.CO;2

[USC] United States Code, 1973. Endangered Species Act of 1973, Chapter 16, Conservation, Public Law 93-205; July 24, 1973; 16 U.S.C. ch. 35 §1531 et seq. & as amended through 1982 (Public Law 97-304, 96 Stat. 1411).

USC, 1988. Federal Cave Resources Protection Act of 1988, Chapter 16, Conservation (Public Law 100-691; November 18, 1988; 16 U.S.C. 4301 through 4309) and as emended through 1999 (Public Law 106-170).

[USFWS] U.S. Fish and Wildlife Service., 2006 – USFWS Section 10(a) (1) (A) Scientific Permit Requirements for Conducting Presence/Absence Surveys for Endangered Karst Invertebrates in Central Texas. Fish and Wildlife Service, 10711 Burnet Road, Suite 200, Austin, Texas 78758, 21 p.

Valentine J.M., 1941 – *Trapping for cave beetles*. National Speleological Society Bulletin, **2**: 4-7.

Weeks R.D. Jr. & Mclntyre N.E., 1997. – *A comparison of live versus kill pitfall trapping techniques using various killing agents*. Entomologia Experimentalis et Applicata, **82**: 267-273. https://doi.org/10.1046/j.1570-7458.1997.00140.x

Weinstein P. & Slaney D., 1995 – *Invertebrate faunal survey of Rope Ladder Cave, Northern Queensland: a comparative study of sampling methods*. Journal of the Australian Entomological Society, **34**: 233-236. https://doi.org/10.1111/j.1440-6055.1995.tb01329.x

Welbourn W.C., 1978 – *Biology of Ogle Cave with a list of the cave fauna of Slaughter Canyon*. National Speleological Society Bulletin, **40**: 27-34.

Whitten T., 2009 – *Applying ecology for cave management in China and neighbouring countries*. Journal of Applied Ecology, **46**: 520-523. https://doi.org/10.1111/j.1365-2664.2009.01630.x

Wynne J.J., 2013 – *Inventory, conservation and management of lava tube caves at El Malpais National Monument*. Park Science, **30**: 45-55.

Wynne J.J. & Pleytez W., 2005 – *Sensitive ecological areas and species inventory of Actun Chapat Cave, Vaca Plateau, Belize*. Journal of Cave and Karst Studies, **67**: 148-157.

Wynne J.J. & Voyles K.D., 2014 – *Cave-dwelling arthropods and vertebrates of North Rim Grand Canyon, with notes on ecology and management*. Western North American Naturalist, **74**: 1-17. https://doi.org/10.3398/064.074.0102

Wynne J.J. & Shear W.A., 2016 – *A new millipede (*Austrotyla awishashola*, n. sp., Diplopoda, Chordeumatida, Conotylidae) from New Mexico, USA, and the importance of cave moss gardens as refugial habitats*. Zootaxa, **4084**: 285-292. https://doi.org/10.11646/zootaxa.4084.2.8

Wynne J.J., Bernard E.C., Howarth F.G., Sommer S., Soto-Adames F.N., Taiti S., Mockford E.L., Horrocks M., Pakarati L. & Pakarati-Hotus V., 2014 – *Disturbance relicts in a rapidly changing world: the Rapa Nui (Easter Island) factor*. BioScience, **64**: 711-718. https://doi.org/10.1093/biosci/biu090

Wynne J.J., Sommer S., Howarth F.G., Dickson B.G. & Voyles K.D., 2018 – *Capturing arthropod diversity in complex cave systems*. Diversity and Distributions, **24**: 1478-1491. https://doi.org/10.1111/ddi.12772

Zagmajster M., Culver D.C. & Sket B., 2008 – *Species richness patterns of obligate subterranean beetles (Insecta: Coleoptera) in a global biodiversity hotspot – effect of scale and sampling intensity*. Diversity and Distributions, **14**: 95-105. https://doi.org/10.1111/j.1472-4642.2007.00423.x

Zampaulo R.D.A., 2015 – *Diversidade de espécies troglóbias em cavidades ferríferas do Parque Estadual da Serra do Rola Moça (PESRM), Minas Gerais*. ANAIS do 33° Congresso Brasileiro de Espeleologia Eldorado SP, 15-19 de julho de 2015 – Sociedade Brasileira de Espeleologia, p. 87-97.

Zepon T. & Bichuette M.E., 2017 – *Influence of substrate on the richness and composition of Neotropical cave fauna*. Anais da Academia Brasileira de Ciências, **89**: 1615-1628. https://doi.org/10.1590/0001-3765201720160452

Zhang Z.F., Liu F., Zhou X., Liu X.Z., Liu S.J. & Cai L., 2017 – *Culturable mycobiota from Karst caves in China, with descriptions of 20 new species*. Persoonia, **39**: 1-31. https://doi.org/10.3767/persoonia.2017.39.01

International Journal of Speleology	48 (1)	49-61	Tampa, FL (USA)	January 2019

Available online at scholarcommons.usf.edu/ijs

International Journal of Speleology

Official Journal of Union Internationale de Spéléologie

Cyanobacterial and algal abundance and biomass in cave biofilms and relation to environmental and biofilm parameters

Slađana Popović[1], Nataša Nikolić[2], Jelena Jovanović[3], Dragana Predojević[2], Ivana Trbojević[2], Ljiljana Manić[2], and Gordana Subakov Simić[2]

[1]University of Belgrade, Scientific Institution, Institute of Chemistry, Technology and Metallurgy, National Institute, Center for Ecology and Technoeconomics, Njegoševa 12, 11000 Belgrade, Serbia
[2]University of Belgrade, Faculty of Biology, Institute of Botany and Botanical Garden "Jevremovac", Takovska 43, 11000 Belgrad, Serbia
[3]Institute of Public Health of Serbia Dr Milan Jovanovic Batut, Dr Subotića 5, 11000 Belgrade, Serbia

Abstract: Due to life in extreme environments, cyanobacteria and algae from cave biofilms that form at the entrances or deep inside the cave around artificial lights are of increasing interest to many scientists. It is well-known that many phototrophic microorganisms are first to colonize exposed substrata and produce the organic matter on which other biofilm constituents relly. Many studies dealing with phototrophic microorganisms from biofilms focus on the diversity and community composition of cyanobacteria and algae, while quantitative assessments are rarely implemented. Biofilm sampling was conducted in Degurić and Vernjikica Cave located in Western and Eastern Serbia, respectively. Ecological parameters (temperature, relative humidity, light intensity) and distance from the entrance were measured. Additionally, chlorophyll content, as well as biofilm parameters (water content, organic and inorganic matter) were determined. The abundance of phototrophic microorganisms was assessed on microscope slides which contained 1 mg of biofilm that was dehydrated for a short period of time and homogenized prior to slide preparation, and then rehydratated. The biomass of recorded cyanobacterial and algal taxa was calculated by applying geometric approximations and standard mathematical formulas. In Degurić Cave, at the sampling site where the highest biomass was documented, the higher diversity, water content and chlorophyll values were also recorded, while in Vernjikica Cave a high content of organic matter was documented. According to the multivariate analyses performed, the biomass of simple trichal Cyanobacteria, Bacillariophyta, and Xanthophyta was positively correlated with the content of organic matter in biofilm and light intensity, while coccoid and heterocytous Cyanobacteria and Chlorophyta showed a positive correlation with water content in the biofilm, relative humidity and distance from the entrance. The total biomass was positively correlated with the chlorophyll content, organic matter and light intensity, and negatively with the distance from the entrance.

Keywords: cyanobacteria, biofilm, quantitative assessment, abundance and biomass, algae

Received 5 August 2018; Revised 8 February 2019; Accepted 13 February 2019

Citation: Popović S., Nikolić N., Jovanović J., Predojević D., Trbojević I., Manić Lj. and Subakov Simić G., 2019. Cyanobacterial and algal abundance and biomass in cave biofilms and relation to environmental and biofilm parameters. International Journal of Speleology, 48 (1), 49-61. Tampa, FL (USA) ISSN 0392-6672 https://doi.org/10.5038/1827-806X.48.1.2224

INTRODUCTION

Biofilms that develop on surfaces exposed to air consist of different microorganisms, among which are aerophytic cyanobacteria and algae. This interesting group of microorganisms is nowadays studied worldwide (Albertano, 2012). Those inhabiting caves, as one of the extreme environments, are of special interest and thus studied from different aspects, due to their specificity, ecology and physiology, form of the adaptation to the extreme environment, the potential discovery of new taxa, lampenflora management, etc. This refers both to taxa that live at the cave entrances and deep inside the cave, at places surrounding artificial lights (i.e. Rajczy, 1986; Abdelahad, 1989; Sant'Anna et al., 1991; Garbacki et al., 1999; Pentecost & Zhaohio, 2001; Poulíčkova & Hašler, 2007; Selvi & Altuner, 2007; Smith & Olson, 2007; Lamprinou et al., 2009; Vinogradova et al., 2009; Martinez & Asencio, 2010; Mulec et al., 2012; Borderie et al., 2014; Sallstedt et al., 2014; Tofilovska et al., 2014; Czerwik-Marcinkowska et al.,

*spopovic.bio@gmail.com

2015; Popović et al., 2015a, b; 2016a, b, c; Pflender et al., 2017; Popović et al., 2017a, b; Pflender et al., 2018a, b;). Numerous studies focus on the diversity of taxa in caves or the qualitative analysis of biofilm samples which give us information about community composition. Nevertheless, quantitative analyses of phototrophic biofilms exposed to air aren't oftenly represented in scientific research.

The quantitative assessment of cyanobacteria and algae – the study of their abundance and biomass, is a quite common tool in monitoring of different water bodies. It is frequently used in the assessment of water quality and ecological status of rivers and lakes. However, the quantification of these parameters in biofilm that is exposed to air is quite rare, in general. The counting of cyanobacterial and algal cells on opaque surfaces can be, e.g., carried out directly by using the epifluorescence microscope (Welton et al., 2005), which is a fast and non-destructive method based on chlorophyll fluorescence. The abundance of microorganisms can also be assessed using certain scales (based on the frequency in which they appear in the sample). Some scales for the assessment of relative abundance of organisms in water samples are represented in Breitig and Tümpling (1982) and European standard for water quality (BS EN 15708:2009). Following this approach, we tried to use a scale from 1 to 5 in the study Popović et al. (2015a). Using this approach, we cannot precisely determine the share of each taxon in the community. Some researchers reported the use of different sedimentation chambers (often used in phytoplankton analyses) for determining the cyanobacterial and algal abundance in biofilm samples. The preparation of biofilm for sedimentation implies proper biofilm sampling from the substrate, homogenization in water, followed by sedimentation and counting of cyanobacterial and algal cells (Welton et al., 2005). One of the novel approaches that is easy-to-use and represents a fast method for biofilm characterization (qualitative and quantitative) and detection of biofilm community structure changes is flow cytometry. This method is mostly used for biofilms that originate from water ecosystems, for pro- and eukaryotic microorganism cells (Sgier et al., 2016; Wilson et al., 2017). However, there are also some attempts at studying the aerophytic biofilms: Borderie et al. (2016) investigated the microbial composition of biofilms proliferating in a show cave (both heterotrophic prokaryotes and autotrophic microorganisms) using this approach.

The aim of this study was to quantitatively assess cyanobacteria and algae in biofilm samples, i.e. to determine the abundance and biomass of cyanobacteria and algae from cave biofilms, as well as to relate biomass to environmental and biofilm parameters. For abundance and biomass determination, microscope slides containing biofilm of known mass, that was shortly dehydrated and homogenized prior to slide preparation, and then rehydrated, were made.

MATERIALS AND METHODS

Sampling sites

The Degurić Cave (Fig. 1a) is located in Western Serbia, in the municipality of Valjevo, on the right side of the Gradac River, 216 m above the sea level. This is an active spring cave with a continuous flow of the Degurićka River (Đurović, 1998). Speleologists are still exploring this cave and according to the latest data that revealed the presence of many side channels, as well as five siphons, this is the longest cave of the Lelić karst (Milanović, 2012). The entrance is 5 m wide and 3 m high (Petrović, 1976) and the main channel is uniform from the beginning to the end of the cave. The cave is poor in cave formations, bearing in mind that only few groups of stalactites and stalagmites are observed (Đurović, 1998).

Vernjikica Cave (Fig. 1b, c) is located on the left side of the Lazareva River canyon, in the municipality of Bor, about 5 km from the village Zlot. The upper entrance is located at an altitude of 454 m, about 150 m above the Lazareva River. The length of the explored channels is 1015 m. The cave consists of one descending cascade channel that connects several halls, with the circular hall of 50-60 m in diameter and the largest height reaching 50 m. This is a typical dry cave formed in dry limestones which influenced the formation of diverse cave structures that decorate the halls: stalactites, stalagmites, pillars and draperies (Petrović, 1976; Đurović, 1998; Milanović, 2012).

Fig. 1. Degurić Cave (a) and Vernjikica Cave (b and c).

Environmental parameters

Prior to biofilm sampling, the measurement of ecological parameters was performed. Temperature, relative humidity and light intensity, were measured three times at each sampling site using the Temperature Humidity Meter, Extech, USA and DMV 1300 Luxmeter, Velleman, Belgium.

Biofilm sampling

Five sampling sites with different biofilm (different color and appearance, i.e., gelatinous, dry, powdered, etc.) were chosen for sampling in Degurić Cave, as well as in Vernjikica Cave. All sampling sites were located at the cave wall on vertical surfaces (left or right from the cave entrance). The distance of every sampling site from the cave entrance was measured and expressed in meters. In order to provide adequate qualitative and quantitative data, two methods of biofilm sampling were applied: non-destructive adhesive-tape method (Gaylarde & Gaylarde, 1998; Urzì & de Leo, 2001) and scraping biofilm directly from the stone substrata using flame-sterilized scalpel (Popović et al., 2015a; 2017a). As proposed in studies by Gaylarde & Gaylarde (1998); Urzì & de Leo (2001), and described in Popović et al. (2015a), tape strips were put and gently pressed to the stone surfaces with biofilm, then removed and placed on microscope slides. Adhesive tape strips with biofilm content were fixed with a drop of glycerol and stored in microscope slide boxes, while biofilm samples were transported to the laboratory in labeled sterile polyethylene bags. For the determination of chlorophyll (Chl) content, water content and content of inorganic/organic matter in biofilm samples it was necessary to take biofilm samples from exactly known surface. For that purpose, a round metal matrix covering a surface of 3.14 cm^2 was used as described in Popović et al. (2017a). The round metal matrix is carefully pressed on the stone surface (if it is possible flat one) and turned clockwise or counterclockwise to mark the area from which the biofilm will be sampled. Biofilm is sampled using scalpel and placed in a sterile polyethylene bags to be transported to the laboratory.

Determination of Chl and biofilm content

The concentration of Chl was determined based on the modified phytoplankton formula and standard ISO 10260: 1992, as described in Popović et al. (2015a) and expressed as μg Chl cm^{-2}. Since for chlorophyll extraction ethanol, acetone and methanol can be used, Pápista et al. (2002) re-examined the ISO 10260: 1992 and compared the extraction yields of these three solvents and concluded that extraction with methanol provide both the highest extraction yield and the lowest standard error value. However, due to the toxicity of methanol, this solvent is not widely used, and instead, ethanol is adopted as a safe alternative (Nagarkar & Williams, 1997). Water content and content of inorganic/organic matter in biofilm samples were determined following the procedure described in Popović et al. (2017a).

Quantitative algological analyses

Prior to the quantitative analysis, qualitative analysis of phototrophic microorganisms from biofilm samples was performed using light microscope Zeiss Axio-Imager M.1 with software AxioVision 4.8. The adhesive strips were directly observed. Considering biofilm samples, permanent microscope slides in triplicate were made using the sample mixed with glycerol. Cyanobacteria and algae were identified using the standard literature: Krieger & Gerloff (1962), Starmach (1972), Komárek & Fott (1983), Komárek & Anagnostidis (1998), John et al. (2003), Komárek & Anagnostidis (2005), Hofmann et al. (2013) and Komárek (2013).

Since there is no precisely defined method that is adequate for the assessment of the abundance of aerophytic cyanobacteria and algae in aerophytic biofilm samples, the quantitative analysis was performed using microscope slides prepared as described bellow. For the preparation of these slides, well-homogenized biofilm was needed. In order to make homogenization easier, part of each biofilm sample was first dried at 105°C for 1 minute, after which it was carefully homogenized using a glass stick. Subsequently, 0.001 g (1 mg) of each dry biofilm sample was measured using the analytical scale and placed on a microscope slide. The biofilm was first mixed with a drop of water to be rehydrated, then carefully and equally mixed with a drop of glycerine, after which cover glass was put over it and fixed with nail polish.

The counting of cyanobacteria and algae was performed in randomly selected transects on microscope slides using magnification of 400x or 630x. One transect (arrows on Fig. 2) along which the counting was performed, represented the path from the left edge of the cover glass (marked as “d” on Fig. 2) to the right edge or vice versa. According to the upper scale (marked as “b” on Fig. 2) on the microscope stand (Fig. 2), one transect accounted for 20 sections. We first randomly chose a place on the microscope slide from which to start the count (usually from left to the right) and marked on which line the upper scale is. By moving the microscope slide, part of the scale marked as “a” also moves enabling us to see how much scale lines we have passed. We have counted until we reached 500 individuals in each biofilm sample. During the counting, we would either pass only a part of the selected transect (corresponding to the certain number of lines on the upper scale), or more transects, depending on the sample. One cover glass may have a different number of transects depending on the magnification used. If we passed only a part of the transect, we first calculate how many individuals and cells of phototrophic microorganisms there are in one transect, according to the upper scale. This number is then multiplied with the number of transects to obtain how many individuals and cells are beneath the whole cover glass or in the weight of 0.001 g of biofilm.

Biomass was calculated taking into account the dimensions and abundance of each taxon. First, each taxon was assigned a certain geometric body, considering that cells can have the form of simple geometric bodies, or complex shapes that are built from several simple shapes. Geometric bodies that were observed in our study were sphaere, halfsphaere,

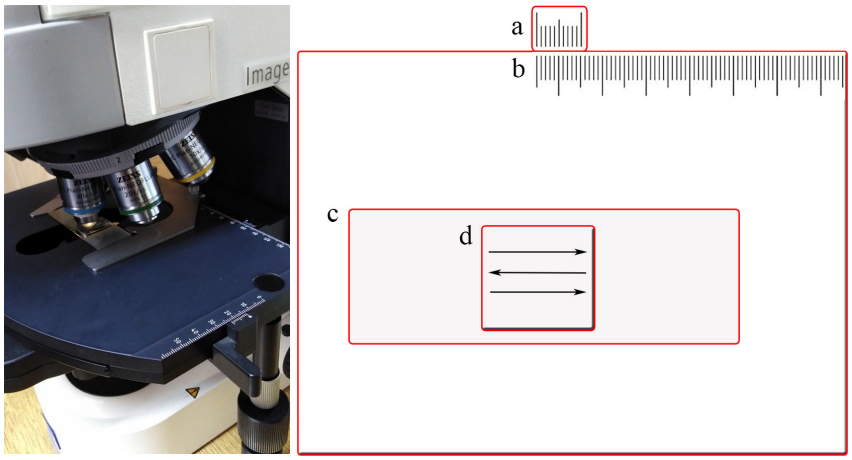

Fig. 2. The illustration that explains counting of cyanobacteria and algae and calculating the number of these microorganisms beneath the cover glass (in the known biofilm weight). a) the scale that moves when microscope slide moves; b) the upper scale on the microscope stand; c) microscope slide; d) cover glass; arrows – transects along the counting was performed.

ellipsoid, half of the elliptical prism, roller and cuboid. The biomass for each taxon was determined using geometric approximations and standard mathematical formulas according to Hillebrand et al. (1999) and Sun & Liu (2003).

Dimensions of the cells are measured taking into account 25 individuals of the same taxon from each sample, and the average value was used in mathematical formulas. Biomass of each taxon was used to calculate the total biomass of cyanobacteria and algae within the biofilm sample:

$$V_{total} = \Sigma (N \times V)$$

Vtotal – the total biomass of cyanobacteria and algae in biofilm sample ($\mu m^3/mg$);
N – number of cells of a certain taxon in 1 mg (0.001 g) biofilm sample;
V – average volume of a certain taxon cell ($\mu m^3/mg$).

The final biomass value is expressed in $\mu m^3/mg$ (for phytoplankton $\mu m^3/L$). Assuming that the cell density is 1, values of the phytoplankton biomass are expressed in µg/L, using the following conversion: $\mu m^3/L = 10^{-6} \mu g/L$. According to this, the final biomass of cyanobacteria and algae in the biofilm samples is expressed in µg/mg.

Statistical analyses

Principal component analysis (PCA) and detrended correspondence analysis (DCA) analyses were performed to illustrate the relationship of quantitative parameters – abundance and biomass, with following ecological and biofilm parameters: temperature (T), relative humidity (RH), light intensity (LI), water content in biofilm (WC), the content of organic matter (OM), the content of inorganic matter (IM), the distance from the entrance and the concentration of Chl. PCA represents the relationship of the mentioned ecological and biofilm parameters and the total biomass, number of cells and individuals, while DCA focus on the relationship between the same parameters and the biomass of every algal and cyanobacterial group separately. Software Canoco for Windows, version 5, was used (Ter Braak & Šmilauer, 2012).

RESULTS

The values of measured ecological parameters are presented in Table 1, as well as the data referring to the distance of the sampling site from the entrance of caves expressed in meters. Temperature did not vary a lot between sampling sites in Degurić Cave, but in Vernjikica Cave, sampling site V4 and V5 had 4˚C higher temperature from the rest. Relative air humidity also did not show big variations. It is worth mentioning that the highest value in Degurić Cave was recorded at sampling site D5, and in Vernjikica Cave at V1. Light intensity showed the highest variation in both caves.

Table 1. The values of measured ecological parameters (T: temperature, RH: relative humidity, LI: light intensity), and distance from the cave entrance. D1–D5: sampling sites in Degurić Cave; V1–V5: sampling sites in Vernjikica Cave.

	Sampling site	T (˚C)	RH (%)	LI (Lux)	Distance (m)
Degurić Cave	D1	22.4 ± 0.11	62.0 ± 3.0	108 ± 9	3.0
	D2	20.8 ± 0.10	63.0 ± 2.0	250 ± 8	3.5
	D3	20.4 ± 0.10	69.0 ± 2.0	140 ± 6	4.5
	D4	20.0 ± 0.05	67.0 ± 3.0	111 ± 7	5.0
	D5	19.7 ± 0.08	82.0 ± 1.0	241 ± 5	1.0
Vernjikica Cave	V1	17.1 ± 0.10	68.0 ± 1.0	67 ± 4	2.0
	V2	17.3 ± 0.10	65.0 ± 2.0	210 ± 7	2.3
	V3	17.1 ± 0.10	67.0 ± 2.0	380 ± 8	2.5
	V4	21.1 ± 0.15	56.0 ± 1.0	230 ± 9	2.5
	V5	21.3 ± 0.10	53.0 ± 2.0	780 ± 10	1.7

The concentration of Chl (Fig. 3) was high at sampling site D1 in Degurić Cave, and at V2 in Vernjikica Cave. On the rest of the sampling sites in both caves, similar values of this parameter were measured, except for V4 where the lowest concentration was determined.

In all biofilm samples from Degurić Cave, water content had the highest values, followed by the content of inorganic matter (Fig. 3). On the other side, inorganic matter had the highest values in all samples taken from Vernjikica Cave, except at V3 where water content was high. Organic matter in Degurić Cave had higher values at D1 and D5 compared to other sampling sites, and in Vernjikica Cave at V2 and V5. D5 and V5 are also sampling sites with higher measured light intensity.

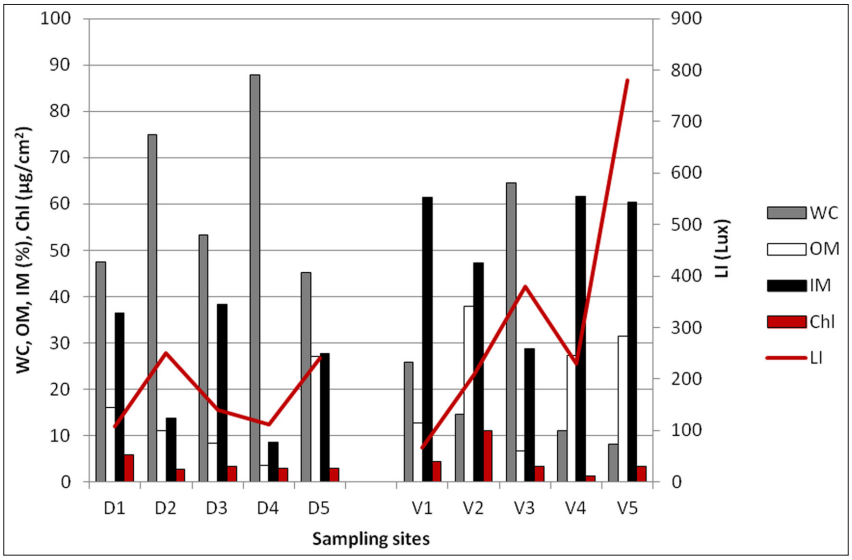

Fig. 3. The concentration of Chl in Degurić and Vernjikica caves, the content of inorganic (IM), organic matter (OM) and water content (WC) in biofilm samples – primary axis and light intensity (LI) – secondary Y-axis, from Degurić and Vernjikica caves. IM, OM, and WC are expressed in percentages for each biofilm sample.

The results of the quantitative analysis (the number of individuals, cells and biomass) of cyanobacteria and algae from biofilm samples of Degurić and Vernjikica caves are given in Tables 2 and 3.

The highest number of individuals in 1 mg of biofilm sample at D1 is calculated for *Desmococcus olivaceus*, the highest number of cells for *Leptolyngbya tenuis*, and biomass for *Chroococcus ercegovicii. Gloeobacter violaceus* is accounted for the highest number of individuals and cells at D2. Biomass was quite low for almost all taxa, only *Asterocapsa* cf. *purpurea* had somewhat higher values. On the other side, this coccoid cyanobacterium was absolutely dominant at D3 when all three parameters were considered (the number of individuals, cells and biomass). Also, at D4, this taxon had the highest number of individuals, but the highest number of cells was assigned to *Gloeocapsa nigrescens,* and biomass to *Nostoc commune.* However, at D5, the highest biomass was calculated for *Gloeocapsa nigrescens,* while the highest number of individuals and cells was observed for species *Chroococcus varius* (Table 2).

At V1, *Trebouxia* sp. was dominant when the number of individuals and cells were considered, although the highest biomass was assigned to *Orthoseira roseana.* However, *Trebouxia* sp. was dominant at V2, and *Desmococcus olivaceus* at V4, considering all parameters. Sampling site V3 was characterized by the greatest number of individuals of taxon *Gloeocapsa reicheltii*, and the highest estimated biomass and number of cells for *Aphanothece* cf. *bullosa. Chroococcidiopsis* sp. had the highest number of individuals, *Phormidium* sp.1 was the most abundant taxon regarding number of cells, while unidentified representative of Xanthophyta had the highest calculated biomass at V5 (Table 3).

The total number of individuals, cells and biomass in biofilm samples considering both caves is more precisely represented in Figure 4. The total number of individuals and cells, as well as biomass in Degurić Cave had the highest values at D1, and lowest at D2. In Vernjikica Cave, the highest number of individuals and cells were calculated for biofilm at V4, whereas the biomass had it's peak at V5.

It is worth mentioning that, as seen in Fig. 5a, total biomass showed a positive correlation with Chl, content of organic matter in biofilm and light intensity, and it was negatively correlated with the distance from the entrance. When more detailed analysis that include relation of biomass separately for different algal and cyanobacterial groups along with other parameters was considered, it revealed the following: simple trichal Cyanobacteria, Bacillariophyta and Xanthophyta showed a positive correlation to light intensity and content of organic matter in biofilm, while coccoid and heterocytous Cyanobacteria, as well Chlorophyta were positively correlated to water content in biofilm, relative air humidity and distance from the entrance (Fig. 5b).

DISCUSSION

As mentioned, one of the ways for quantitative assessment of biofilm is the use of the sedimentation chambers. Welton et al. (2005) used the Helber's chamber, which is usually used for the counting of

Table 2. The number of individuals, cells (in 1 mg of biofilm) and biomass (expressed in µg/mg) of cyanobacterial and algal taxa recorded in Degurić Cave.

	D1			D2			D3			D4			D5		
Taxon	IND	CEL	BIO	IND	CEL	BIO	IND	CEL	BIO	IND	CEL	BIO	IND	CEL	BIO
Cyanobacteria															
Aphanocapsa muscicola	1440	28800	0.26				83	1744	0.02						
Aphanocapsa sp.	1800	33840	0.08	50	1550	0.00	138	4153	0.02	540	4482	0.02	498	22596	0.05
Aphanothece cf. *bullosa*							27	166	0.004						
Asterocapsa cf. *purpurea*	34560	57600	1.56	1804	3074	0.19	6341	10467	0.41	12660	16794	0.99	10966	17280	0.18
Asterocapsa sp.1													1329	1329	0.01
Asterocapsa sp.2	360	720	0.03							27	54	0.003			
Chroococcidiopsis sp.	8280	18720	0.06							780	1350	0.01			
Chroococcus cohaerens										480	540	0.005			
Chroococcus ercegovicii	19080	37440	15.34				110	193	0.07				166	166	0.06
Chroococcus varius										10890	11772	0.06	26916	57987	0.46
Chocooccus sp.	360	720	0.06										332	664	0.05
Cyanothece aeruginosa							249	249	0.08						
Eucapsis sp.	1800	7200	0.05							540	648	0.002			
Gloeobacter violaceus				6149	11562	0.08									
Gloeocapsa alpina	2160	16920	0.85	76	330	0.01	996	5316	0.40	1620	2484	0.10			
Gloeocapsa atrata	9360	26280	0.47	813	2058	0.04	858	2076	0.17	70	108	0.002			
Gloeocapsa biformis	20520	62640	0.37				1190	2436	0.02				20270	26584	0.26
Gloeocapsa compacta	720	4320	0.05										830	4984	0.07
Gloeocapsa nigrescens	3240	17280	0.23	1905	7267	0.09				11440	21870	0.89	3489	31070	1.79
Gloeocapsa punctata	8640	28080	0.14												
Gloeocapsa reicheltii	14760	27000	0.16												
Gloeocapsa sanguinea							27	166	0.004				664	830	0.02
Gloeocapsa sp.	720	12960	0.22												
Gloeothece confluens				50	203	0.01	526	2963	0.07	70	108	0.003			
Gloeothece fusco-lutea	360	1440	0.12				1107	2215	0.19						
Heterocytous Cyanobacteria	1080	5400	0.40												
Leptolyngbya foveolarum	2880	45360	0.04	25	355	0.0002	55	1024	0.001						
Leptolyngbya perforans	11520	18720	0.03												
Leptolyngbya sp.				101	1473	0.003	27	110	0.0003	810	1458	0.005	166	664	0.002
Leptolyngbya tenuis	13320	164520	0.35				858	8418	0.08						
Nostoc commune	360	2520	0.27							5400	21600	1.89			
Nostoc microscopicum							55	1273	0.11						
Nostoc punctiforme										540	2970	0.22			
Nostoc sp.							27	249	0.01	4050	7722	0.42			
Pseudocapsa dubia										540	1080	0.02	498	8806	0.15
Chlorophyta															
Gloeocystis vesiculosa				25	50	0.01									
Desmococcus olivaceus	48240	65160	3.79	1041	1194	0.15				5650	7236	0.87	8473	9304	0.70
Sum	205560	683640	24.91	12045	29121	0.59	12683	43227	1.66	56107	102276	5.50	74603	182270	3.81

Table 3. The number of individuals, cells (in 1 mg of biofilm) and biomass (expressed in µg/mg) of cyanobacterial and algal taxa recorded in Vernjikica Cave.

	V1			V2			V3			V4			V5		
Taxon	IND	CEL	BIO	IND	CEL	BIO	IND	CEL	BIO	IND	CEL	BIO	IND	CEL	BIO
Cyanobacteria															
Aphanocapsa sp.	38	2545	0.04	27	378	0.00	540	11802	0.03				375	9766	0.02
Aphanothece cf. *bullosa*							5091	53460	0.62						
Aphanothece saxicola							77	462	0.00						
Chroococcidiopsis sp.	1581	2777	0.01				4474	8948	0.03	6440	15120	0.05	16810	29206	0.10
Chroococcus sp.							1157	2391	0.09						
Eucapsis sp.							385	2160	0.01						
Gloeocapsa atrata													187	1126	0.03
Gloeocapsa biformis							154	1234	0.01						
Gloeocapsa kuetzingiana							3471	5168	0.09						
Gloeocapsa nigrescens										280	560	0.01			
Gloeocapsa punctata							3085	8640	0.04						
Gloeocapsa reicheltii							10800	17125	0.24						
Gloeocapsopsis sp.							77	848	0.01						
Leptolyngya foveolarum	77	810	0.00	27	243	0.00							469	9203	0.01
Leptolyngbya perforans													93	751	0.00
Leptolyngbya sp.				27	189	0.00	231	2314	0.01				93	563	0.00
Nostoc punctiforme													93	1502	0.10
Nostoc sp.							77	1465	0.07						
Phormidium sp.1													4883	78511	8.21
Chlorophyta															
Desmococcus olivaceus	4397	5168	0.05	486	1053	0.06	2237	4242	0.12	109760	146440	2.93	14368	19815	0.28
Trebouxia sp.	10722	10915	0.83	11475	11475	4.08									
Bacillariophyta															
Hantzschia abundans													93	93	1.62
Nitzschia sp.													281	281	0.27
Orthoseira roseana	77	115	1.76	27	27	2.01									
Xanthophyta															
Xanthophyta													939	2347	12.84
Sum	16894	22332	2.69	12069	13365	6.16	31860	120265	1.36	116480	162120	2.99	38692	153172	23.48

bacteria (Collins & Lyne, 2004). This technique is even more suitable for enumeration of algal cells or fungal spores, given that it can be performed at higher magnification. Furthermore, to assess the abundance of phototrophs from biofilm developed near thermal springs, Debnath et al. (2009) performed counting in Sedgwick-Rafter chamber. In their research, according to the abundance, descriptive characters were assigned – rare (less than 1%), present (1-10%) or very abundant (more than 30%). Also, Bryanskaya et al. (2006) used the Goryaev chamber for the determination of the abundance and biomass. In this study, primary attempt was to implement Utermöhl method (1958), frequently used quantitative phytoplankton analysis as a standard method (EN 15204:2008). As suggested by Welton et al. (2005), biofilm samples of known mass were homogenized within certain water volume and the part of a solution was then sedimented in a counting chamber. However, biofilm dissolving was not entirely possible because of the adhesive properties of extracellular polymeric substances (EPS) that binds microorganisms cells together (Rossi & De Philippis, 2015). Microorganism cells were also retained on the sedimentation chamber wall that caused the loss of sample. Counting of microorganisms was difficult not only due to glued cells, but also because of the presence of organic and inorganic particles that dissimulate the phototrophic microorganisms.

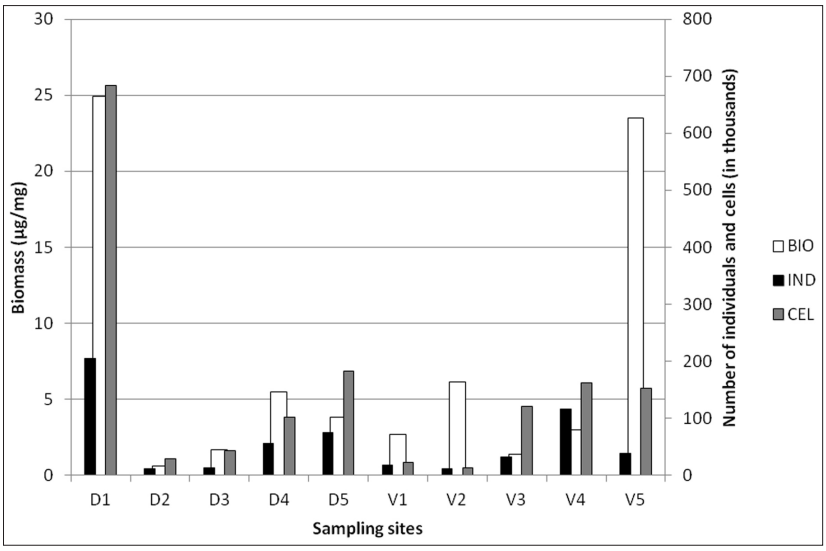

Fig. 4. The total number of individuals (IND), cells (CEL), and biomass (BIO) per sampling site in 1 mg biofilm.

Ordinary slides for taxa identification slides are prepared in a simple way: part of a biofilm of the unknown weight is put on a slide, mixed with a drop of water or glycerol, homogenized as much as possible and observed under the microscope. Microscope slides prepared in such a manner are only suitable for taxa identification, but not for their counting as in many places on the slide, biofilm can be thick or cells of the microorganism can be glued together due to the EPS properties. Additionally, unknown biofilm mass is used during the preparation of the slides. In this regard, in order to count taxa and determine their biomass, a biofilm sample of a certain mass is needed; homogenization of biofilm has to be better performed, so microorganisms could be viewed more easily, and it is necessary to reduce "glue effect".

EPS can contain up to 95% of water and can be in a form of gel or in a colloidal form, which depends on chemical composition and temperature. Internal and external polysaccharides in the form of a gel stabilize macromolecular constituents of the cell and the cell structure, as well. In this regard, it is suggested that they form hydrogen bonds with proteins, membrane lipids and DNA. Due to the presence of uronic acids, EPS has sticky properties that binds cells to the substrate, as well as together (Potts et al., 1994; Stal, 2012). According to Pan et al. (2016), heating can be effectively used as one of the extraction physical methods and can cause hydrolysis of EPS and disrupt cells. The way of biofilm preparation in this study that included drying of a larger amount of biofilm (short-term heating) which caused easier detachment of cells one from another, allowed biofilm to be equally distributed on the microscope slide. This served as a tool that enabled us easier counting and separation of biofilm constituents, which was one of the advantages. The counting of cells was harder only when organic and inorganic particles masked microorganisms. However, it is possible that biofilm preparation which includes short-term drying can alter the cells, slightly influencing their shape. Nevertheless, those changes are minor and within the limits of cell variability that naturally exists in samples: after rehydration (which occurred within a few minutes) they are not even easily observed under the microscope on the used magnification. The dehydration process in this study lasted for only one minute and was only temporary, not long lasting as e.g., many cyanobacteria and algae experience in nature habitat conditions after which they still recover very quickly. Cyanobacteria as the oldest phototrophic microorganisms can handle a wide spectrum of different extreme and unfavorable conditions and stresses among which is desiccation. Frequent and fast changing hydration/dehydration cycles are very common in all terrestrial/aerophytic cyanobacteria, and thanks to different mechanisms, these phototrophs respond almost immediately to such events. Many of them can reverse their

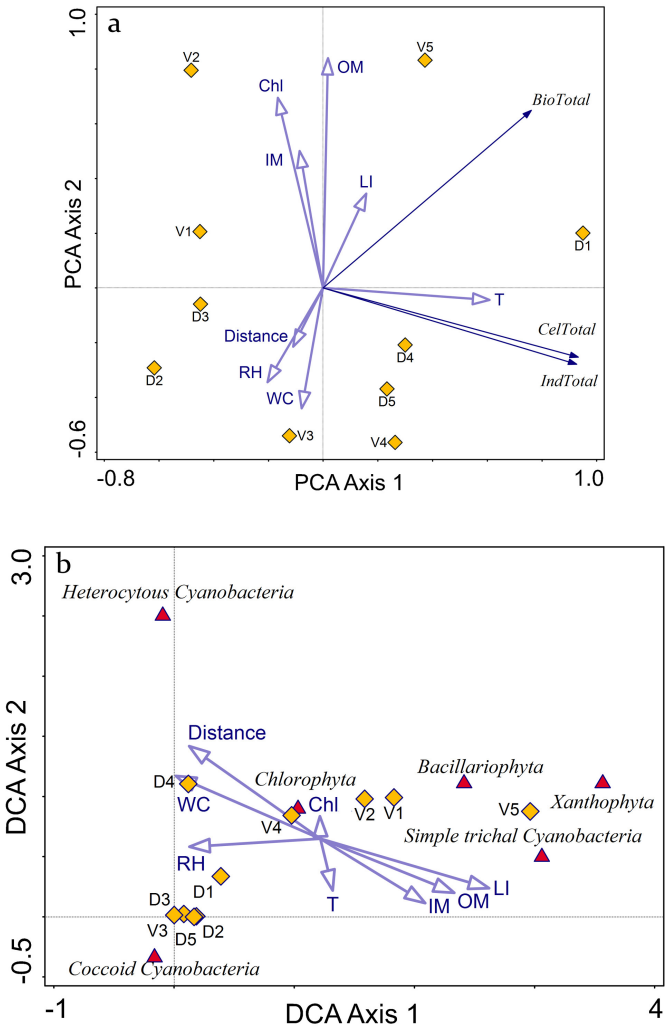

Fig. 5. a) PCA showing the relationship between ecological and biofilm parameters and the total biomass, number of cells and individuals; b) DCA showing the relationship between ecological and biofilm parameters and the biomass of every algal and cyanobacterial group separately. IM: the content of inorganic matter in biofilm; OM: the content of organic matter in biofilm; WC: the content of water in biofilm; Chl: chlorophyll; T: temperature; LI: light intensity; RH: relative air humidity; V1 – V5: sampling sites in Vernjikica Cave; D1 – D2: sampling sites in Degurić Cave. IM, OM and, WC are represented per surface area (mg/cm^2).

metabolism rapidly and hold back metabolic activity during dehydration (Potts, 1994). Cyanobacteria in desert crusts e.g. have the ability to resume metabolic activity upon rehydration within minutes (Garcia-Pichel & Belnap, 1996; Potts, 1994). According to Gray et al. (2007), similar response of desiccated microalgae is observed in terrestrial, as well as in marine representatives (indicating that not only desert Cyanobacteria have those mechanisms). The rehydration response starts 1–2 min after adding water, while the reactivation of photosynthesis occurs after 13 min (Chennu et al., 2015). As mentioned, the EPS plays a role in desiccation tolerance, but some studies report on an intracellular mechanism that copes with this stressful factor (Shirkey et `al., 2000).

Regarding homogenization, it is observed that in nonhomogenized biofilm, non-representative part of the community can be taken for counting (e.g., part of a biofilm where few taxa dominate). Nevertheless, homogenization significantly reduce that error, as higher quantity of biofilm is mixed prior to separation of the subsample for microscopy.

In rare occasions, the same taxon in biofilm sample had the highest number of cells, individuals and the highest biomass. It happened only in cases where taxon was exclusively dominant in biofilm sample, such as *Asterocapsa* cf. *purpurea* at D3, *Trebouxia* sp. at V2 and *Desmococcus olivaceus* at V4. At sampling sites D1 and D4, different taxa had the highest values for the number of individuals, cells and biomass. For example, the highest number of individuals at D4 site had *Asterocapsa* cf. *purpurea*, unicellular cocoid cyanobacteria that often appears as unicellular, while in rare occasions stadiums containing more cells enveloped with the same sheath are present. On the other hand, *Gloeocapsa nigrescens* representatives mostly consisted of more cells enveloped with the same sheath, so the number of individuals was lower, in comparison to cell number. And finally, the highest biomass was recorded for *Nostoc commune*, a colonial cyanobacterium which formed very big colonies containing many cells. At V1, *Trebouxia* sp. was dominant when number of individuals and cells was observed, but the highest documented biomass was for diatom *Orthoseira roseana* due to the large volume of its cells.

At D1 where the highest biomass in the cave was determined, the higher diversity, water content in biofilm, as well as the highest Chl values were recorded. The high water content is the consequence of the presence of many coccoid cyanobacteria such as representatives of *Gloeocapsa, Chroococcus* and *Aphanocapsa* with very well developed EPS at this sampling site. On the other hand, at the sampling site with the highest determined biomass in Vernjikica cave, originating predominantly from one representative of Xanthophyta group, content of organic matter had rather high values.

As seen from Fig. 5a, Chl concentration and the total biomass were correlated and both showed a positive correlation with OM and LI, but were not correlated with the distance from the entrance. According to this, Chl concentration and biomass gave us similar information when primary production was taken into consideration. This was interesting given that, while trying to correlate light with diversity of phototrophic microorganisms, the correlation was almost non-existent. From this results the positive side of biomass determination for aerophytic canobacteria and algae in hypogenic habitat can be seen. The advantage in calculating biomass from biofilm sample is in the biomass estimation for every taxa or different groups of algae separately. As seen in Figure 5b, different groups of Cyanobacteria, as well as various algal taxa, showed correlation with different parameters. Firstly, the biomass of coccoid and heterocytous cyanobacteria showed a positive correlation with the content of water in biofilm. This is expected since representatives of these cyanobacterial groups have very well developed and thick sheaths. Furthermore, these groups also showed a correlation with the distance from the entrance, while simple trichal forms were negatively correlated with this parameter. According to some authors, coccoid forms of cyanobacteria are more tolerant to low light intensity and are found in the

deeper part of the cave (Asencio & Aboal, 2001; Mulec & Kosi, 2008; Mulec et al., 2008; Martinez & Asencio, 2010), thus representing the dominant phototrophic microorganisms in these environments (Mulec et al., 2008). On the other hand, simple trichal forms are usually found on better illuminated places (Asencio & Aboal, 2001; Martinez & Asencio, 2010). Compared with Cyanobacteria, Bacillariophyta prefer more illuminated sites, which is concluded when the data about the vertical stratification of these groups in biofilm were taken into consideration (Roldán & Hernández-Mariné, 2009). The primary production of green algae is higher at cave entrances (Piano et al., 2015) and diversity of Bacillariophyta is also connected with the proximity of the cave entrance (Falasco et al., 2014). As seen in Figure 5b, biomass of diatoms correlates with light.

Quantitative analysis enables us to precisely determine the dominant, subdominant and rare taxa in sample, their abundance and biomass. This is one of the main advantages compared to the determination of Chl content, because Chl can have similar values for samples where the difference in the dominance of certain algal groups can be observed. Thus, based on quantitative analysis, the influence of different environmental parameters and changes in community composition can be monitored in more detailed manner.

Many caves worldwide represent a natural phenomenon characterized with enormous beauty, aesthetic value, attractive cave formations, with many of them being historically and culturally significant. Due to all this they are very attractive sites for people and many of them have thus been adapted for tourist visits. However, the adaptation of a cave can have a negative impact on the cave ecosystem in general: changes in this fragile environment occur, leading to the disturbance of previously stabile microclimate conditions. By introducing light, caves become a suitable environment for the development of phototrophic microorganisms, cyanobacteria and algae. The development of these microorganisms on places around artificial lighting, the microorganism community called lampenflora, can alter rock substrate leading to the destruction of cave formations. Thus, lampenflora should be monitored, qualitatively and quantitatively assessed and treated. Physical and/or chemical treatments that involve the eradication of all phototrophic microorganisms should be used if needed (Gunn, 2004; Borderie at al., 2014; Hebelka, 2014). We believe that future research should focus on the study of physiology and deteriogenic capability of each taxon present in lampenflora. The determination of biomass for each taxon separately can help to better understand their ecology and physiology. The deteriogenic capability can differ from one taxa to another and possibly could be higher in those taxa that are not dominant, but subdominant or rare in the biofilm. Looking at the biofilm under a microscope, it can always be seen which taxa are dominant if cell numbers are taken into account. However, as it was demonstrated, biomass of taxa that have a lot of cells could be lower than those taxa that appear sporadically due to the larger cell dimensions.

CONCLUSIONS

Biofilm sampling was conducted in Degurić and Vernjikica caves in Western and Eastern Serbia. The distance from the entrance and ecological parameters (temperature (T), relative humidity (RH) and light intensity (LI)) were measured. Chlorophyll content, as well as biofilm parameters (water content (WC), organic (OM) and inorganic (IM) matter) were also determined. The values of ecological parameters, except of LI, were similar at all sampling sites in one cave. The concentration of Chl was high at the sampling site D1 in Degurić Cave, and at V2 in Vernjikica Cave. Considering the biofilm parameters, the highest values were accounted for WC, followed by the IM, in the biofilm samples from Degurić Cave. In Vernjikica Cave, IM showed the highest values in all biofilm samples, except at V3 where WC was high. Higher values of OM in Degurić Cave were at D1 and D5, and in Vernjikica Cave at V2 and V5. Quantitative analyses of biofilms are rarely performed in scientific investigations. The counting of cyanobacteria and algae using sedimentation chambers (Utermöhl method) was not successful in this study. Microscope slides designed as described, that included biofilm dehydration and homogenization, followed by rehydration, were suitable and showed an advantage, when compared to the sedimentation method. At D1 where the highest total biomass in Degurić Cave was determined, high diversity, WC in biofilm (due to the presence of many coccoid Cyanobacteria), as well as the highest Chl values were also recorded. On the other hand, the highest determined biomass in Vernjikica Cave (at V5), which originated from one representative of Xanthophyta group, was at a sampling site where OM had high values. In general, the total biomass showed a positive correlation with Chl, OM, and LI, and it was negatively correlated with the distance from the entrance. When observed in more details, the biomass of simple trichal Cyanobacteria, Bacillariophyta, and Xanthophyta showed a positive correlation to LI and OM, while the biomass of coccoid and heterocytous Cyanobacteria, as well Chlorophyta, were positively correlated to WC, RH, and distance from the entrance.

ACKNOWLEDGEMENTS

The authors want to thank the anonymous reviewers for valuable suggestions and comments that significantly improved the clarity and quality of this manuscript. This research was supported by the Ministry of science and technological development, Republic of Serbia, projects no. 176018 and 176020.

REFERENCES

Abdelahad N., 1989 – *On four* Myxosarcina*-like species (Cyanophyta) living in the Inferniglio Cave (Italy).* Archiv für Hydrobiology Algological Studies, **54**: 3-13.

Albertano P., 2012 – *Cyanobacterial biofilms in monuments and caves*. In: Whitton B.A. (Ed.), *Ecology of Cyanobacteria II: Their diversity in space and time*. Springer, Dordrecht, 752 p. https://doi.org/10.1007/978-94-007-3855-3_11

Asencio A.D. & Aboal M., 2001 – *Biodeterioration of wall paintings in caves of Murcia (SE Spain) by epilithic and chasmoendolithic microalgae. Archiv fur Hydrobiologie*. Supplementband: Algological Studies, **140**: 131-142.

Borderie F., Tête N., Cailhol D., Alaoui-Sehmer L, Bousta F, Rieffel D., Aleya L. & Alaoui-Sossé B., 2014 – *Factors driving epilithic algal colonization in show caves and new insights into combating biofilm development with UV-C treatments*. Science of the Total Environment, **484**: 43-52. https://doi.org/10.1016/j.scitotenv.2014.03.043

Borderie F., Denis M., Barani E.A., Alaoui-Sossé B. & Aleya L., 2016 – *Microbial composition and ecological features of phototrophic biofilms proliferating in the Moidons Caves (France): investigation at the single-cell level*. Environmental Science and Pollution Research, **23 (12)**: 12039-12049. https://doi.org/10.1007/s11356-016-6414-x

Breitig G. & Tümpling W., 1982 – *Ausgewählte Methoden der Wasseruntersuchung (Band 2). Biologische, mikrobiologische und toxikologische Methoden*. Jena VEB Gustav Fischer Verlag, 580 p.

Bryanskaya A.V., Namsaraev Z.B., Kalashnikova O.M. & Barkhutova D.D., 2006 – *Biogeochemical processes in the algal–bacterial mats of the Urinskii alkaline hot spring*. Microbiology, **75**: 611-620. https://doi.org/10.1134/S0026261706050122

BS EN, 15708: 2009. *Water quality. Guidance standard for the surveying, sampling and laboratory analysis of phytobenthos in shallow running water*.

Chennu A., Grinham A., Polerecky L., de Beer D. & Al-Najjar M.A.A., 2015 – *Rapid Reactivation of Cyanobacterial Photosynthesis and Migration upon Rehydration of Desiccated Marine Microbial Mats*. Frontiers in Microbiology, **6**: 1472. https://doi.org/10.3389/fmicb.2015.01472

Czerwik-Marcinkowska J., Wojciechowska A. and Massalski A., 2015 – *Biodiversity of limestone caves: aggregations of aerophytic algae and cyanobacteria in relation to site factors*. Polish Journal of Ecology, **63**: 481-499. https://doi.org/10.3161/15052249PJE2015.63.4.002

Collins C.H. & Lyne P.M., 2004 – *Microbiological methods (8th Ed)*. Butterworths, London, 465 p.

Debnath M., Mandal N.C. & Ray S., 2009 – *The study of cyanobacterial flora from geothermal springs of Bakreswar, West Bengal, India*. Algae, **24**: 185-193. https://doi.org/10.4490/ALGAE.2009.24.4.185

EN 15204: 2008. Water quality - Guidance standard on the enumeration of phytoplankton using inverted microscopy (Utermöhl technique). https://www.iss.rs/standard/?natstandard_document_id=19282

Falasco E., Ector L., Isaia M., Wetzel C.E., Hoffmann L. & Bona F., 2014 – *Diatom flora in subterranean ecosystems: a review*. International Journal of Speleology, **43 (3)**: 231-251. https://doi.org/10.5038/1827-806X.43.3.1

Garbacki N., Ector L., Kostikov I. & Hoffmann L., 1999 – *Contribution à l'étude de la flore des Grottes de Belgique*. Belgian Journal of Botany, **132 (1)**: 43-76. https://www.jstor.org/stable/20794440

Garcia-Pichel F. & Belnap J., 1996 – *Microenvironments and microscale productivity of cyanobacterial desert crusts*. Journal of Phycology, **32 (5)**: 774-782. https://doi.org/10.1111/j.0022-3646.1996.00774.x

Gray D.W., Lewis L.A. & Cardon Z.G., 2007 – *Photosynthetic recovery following desiccation of desert green algae (Chlorophyta) and their aquatic relatives*. Plant Cell Environment, **30**: 1240-1255. https://doi.org/10.1111/j.1365-3040.2007.01704.x

Gunn J., 2004 – *Encyclopedia of caves and karst science*. Taylor & Francis, London, 902 p.

Hebelka J., 2014 – *Methodology of lampenflora removal in caves accessible for tourists*. The Cave Administration of the Czech Republic, Czech Republic.

Đurović P., 1998 – *Speleološk atlas Srbije*. Srpska akademija nauka i umetnosti, Beograd.

Hillebrand H., Dürselen C.D., Kirschtel D., Pollingher U. & Zohary T., 1999 – *Biovolume calculation for pelagic and benthic microalgae*. Journal of Phycology, **35 (2)**: 403-424. https://doi.org/10.1046/j.1529-8817.1999.3520403.x

Hofmann G., Werum M. & Lange-Bertalot H., 2013 – *Diatomeen im Süßwasser - Benthos von Mitteleuropa. Bestimmungsflora Kieselalgen für die ökologische Praxis. Über 700 der häufigsten Arten und ihre Ökologie*. Koeltz Scientific Books, Königstein.

ISO 10260: 1992. Water quality - Measurement of biochemical parameters Spectrometric determination of the chlorophyll-a concentration. https://www.iso.org/standard/18300.html

Lamprinou V., Pantazidou A., Papadogiannaki G., Radea C. & Economou-Amilli A., 2009 – *Cyanobacteria and associated invertebrates in Leontari Cave, Attica (Greece)*. Fottea, **9**: 155-164. https://doi.org/10.5507/fot.2009.014

John D.M., Whitton B.A. & Brook A.J., 2003 – *The freshwater algal flora of the British Isles: an identification guide to freshwater and terrestrial algae*. Cambridge University Press, Cambridge, 702 p.

Komárek J., 2013 – *Cyanoprokaryota 3. Teil/3rd Part: Heterocystous genera*. In: Budel B., Gärtner G., Krienitz L. & Schagerl M. (Eds.), *Süsswasserflora von Mitteleuropa*. Springer Spektrum, Heidelberg, 1130 p.

Komárek J. & Anagnostidis K., 1998 – *Cyanoprokariota. 1. Teil: Chroococcales*. In: Ettl H., Gärtner G., Heynig H. & Mollenhauer D. (Eds.), *Süßwasserflora von Mitteleuropa*. Spektrum Akademischer Verlag, Heidelberg, 548 p.

Komárek J. & Anagnostidis K., 2005 – *Cyanoprokaryota. 2. Teil: Oscillatoriales*. In: Büdel B., Gärtner G., Krienitz L. & Schagerl M. (Eds.), *Süßwasserflora von Mitteleuropa*. Spektrum Akademischer Verlag, Heidelberg, 759 p.

Komárek J. & Fott B., 1983 – *Chlorophyceae (Gr¨unalgen). Ordnung: Chlorococcales. Das Phytoplankton d^es Süßwassers, Systematik und Biologie*. In: Elster H.J. & Ohle W. (Eds.), *Die Binnengewässer XVI,, 7 (1)*. Stuttgart, Schweizerbart'sche Verlagsbuchhandlung, 1044 p.

Krieger W. & Gerloff J., 1962 – *Die gattung Cosmarium*. Verlag Von J. Cramer, Weinheim, 112 p.

Martınez A. & Asencio A.D., 2010 – *Distribution of cyanobacteria at the Gelada Cave (Spain) by physical parameters*. Journal of Cave and Karst Studies, **72**: 11-20. https://doi.org/10.4311/jcks2009lsc0082

Milanović S., 2012 – *Speleologija i speleoronjenje u hidrogeologiji karsta*. Rudarskogeološki fakultet, Beograd, 315 p. http://www.karst.edu.rs/documents/pdf/biblioteka/monografija/S-Milanovic-RGF_2012_Speleologija-i-speleoronjenje-u-hidrogeologiji-karsta.pdf

Mulec J. & Kosi G., 2008 – Algae *in the aerophytic habitat of Račiške Ponikve Cave (Slovenia)*. Natura Sloveniae, **10 (1)**: 39-49. http://eprints.gozdis.si/id/eprint/1036

Mulec J., Kosi G. & Vrhovšek D., 2008 – *Characterization of cave aerophytic algal communities and effects of irradiance levels on production of pigments*. Journal of Cave and Karst Studies, **70 (1)**: 3-12.

Mulec J., Krištůfek V. & Chroňákova A., 2012 – *Comparative microbial sampling from eutrophic caves in Slovenia and Slovakia using RIDA COUNT test kits*. International Journal of Speleology, **41 (1)**: 1-8. https://doi.org/10.5038/1827-806X.41.1.1

Nagarkar S. & Williams G.A., 1997 – *Comparative techniques to quantify cyanobacteria dominated epilithic biofilms on tropical rocky shores*. Marine Ecology Progress Series, **154**: 281-291. https://doi.org/10.3354/meps154281

Pan M., Zhu L., Chen L., Qiu Y. & Wang J., 2016 – *Detection techniques for extracellular polymeric substances in biofilms: A review*. BioResources, **11 (3)**: 8092-8115. https://doi.org/10.15376/biores.11.3.8092-8115

Pápista E., Ács E. & Böddi B., 2002 – *Chlorophyll-a determination with ethanol – a critical test*. Hydrobiologia, **485**: 191-198. https://doi.org/10.1023/A:1021329602685

Pentecost A. & Zhaohui Z., 2001 – *The distribution of plants in Scoska Cave, North Yorkshire, and their relationship to light intensity*. International Journal of Speleology, **30 A (1-4)**: 27-37. https://doi.org/10.5038/1827-806X.30.1.3

Pfendler S., Einhorn O., Karimi B., Bousta F., Cailhol D., Alaoui-Sosse L., Alaoui-Sosse B. & Aleya L., 2017 – *UV-C as an efficient means to combat biofilm formation in show caves: evidence from the La Glacière Cave (France) and laboratory experiments*. Environmental Science and Pollution Research, **24 (31)**: 24611-24623. https://doi.org/10.1007/s11356-017-0143-7

Pfendler S., Karimi B., Maron P.-A., Ciadamidaro L., Valot B., Bousta F., Alaoui-Sosse L., Alaoui-Sosse B. & Aleya L., 2018a – *Biofilm biodiversity in French and Swiss show caves using the metabarcoding approach: First data*. Science of the Total Environment, **615**: 1207-1217. https://doi.org/10.1016/j.scitotenv.2017.10.054

Pfendler S., Alaoui-Sossé B., Alaoui-Sossé L., Bousta F. & Aleya L., 2018 – *Effects of UV-C radiation on Chlorella vulgaris, a biofilm-forming alga*. Journal of Applied Phycology, **30 (3)**: 1607-1616. https://doi.org/10.1007/s10811-017-1380-3

Piano E., Bona F., Falasco E., La Morgia V., Badino G. & Isaia M., 2015 – *Environmental drivers of phototrophic biofilms in an Alpine show cave (SWItalian Alps)*. Science of the Total Environment, **536**: 1007-1018. https://doi.org/10.1016/j.scitotenv.2015.05.089

Popović S., Subakov Simić G., Stupar M., Unković N., Predojević D., Jovanović J. & Ljaljević Grbić M., 2015a – *Cyanobacteria, algae and microfungi present in biofilm from Božana Cave (Serbia)*. International Journal of Speleology, **44 (2)**: 141-149. https://doi.org/10.5038/1827-806X.44.2.4

Popović S., Subakov Simić G., Stupar M., Unković N., Predojević D., Blagojević A. & Ljaljević Grbić M., 2015b – *Cyanobacteria, algae and microfungi from Degurić Cave, west Serbia*. 6th Balkan Botanical Congress, September 14-18, University Campus Rijeka, Croatia, 100 p.

Popović S., Subakov Simić G., Korać A., Golić I. & Komárek J., 2016a – *Nephrococcus serbicus, a new coccoid cyanobacterial species from Božana Cave, Serbia*. Phytotaxa, **289 (2)**: 135-146. https://doi.org/10.11646/phytotaxa.289.2.3

Popović S., Jovanović J., Predojević D., Trbojević I., Blagojević A. & Subakov Simić G., 2016b – *Phototrophic microorganisms in biofilm samples from Vernjika Cave, Serbia*. Geophysical Research Abstracts, **18**: EGU2016-16064.

Popović S., Jovanović J., Predojević D., Trbojević I., Blagojević A., Jakovljević O. & Subakov Simić G., 2016c – *Cyanobacteria and algae from biofilms: the comparison of phototrophic microorganism community from cave entrance and lampenflora - Lazareva Cave, Serbia*. 5th Congress of Ecologists of Macedonia, Macedonia (Ohrid) 19–22, October, 125 p.

Popović S., Subakov simić G., Stupar M., Unković N., Krunić O., Savić N. & Ljaljević Grbić M., 2017a – *Cave biofilms: characterization of phototrophic cyanobacteria and algae and chemotrophic fungi from three caves in Serbia*. Journal of Cave and Karst Studies, **79 (1)**: 10-23. https://doi.org/10.4311/2016MB0124

Popović S., Jovanović J., Blagojević A., Trbojević I., Predojević D., Nikolić N., Vidović M. & Subakov Simić G., 2017b – *Diversity of epilithic and endolithic cyanobacteria and green algae at the entrance of two caves in Serbia*. 11th International Phycological Congress, Szczecin, Poland, p. 13.

Potts M., 1994 – *Desiccation tolerance of prokaryotes*. Microbiological Review, **58**: 755-805. https://mmbr.asm.org/content/58/4/755

Pouličková A. & Hašler P., 2007 – *Aerophytic diatoms from caves in central Moravia (Czech Republic)*. Preslia, **79**: 185-204.

Prieto B., Silva B. & Lantes O., 2004 – *Biofilm quantification on stone surfaces: comparison of various methods*. Science of the Total Environment, **333**: 1-7. https://doi.org/10.1016/j.scitotenv.2004.05.003

Rajczy M., Buczkó K. & Komáromy P., 1986 – *Contributions to the flora of the Hungarian caves I. Flora of the entrances of the caves Lők-völgyi-barlany and Szeleta-barlany*. Studia Botanica Hungarica, **9**: 79-88.

Roldán M. & Hernández-Mariné M., 2009 – *Exploring the secrets of the threedimensional architecture of phototrophic biofilms in caves*. International Journal of Speleology, **38 (1)**: 41-53. https://doi.org/10.5038/1827-806X.38.1.5

Rossi F. & De Philippis R., 2015 – *Role of Cyanobacterial exopolysaccharides in phototrophic biofilms and in complex microbial mats*. Life, **5 (2)**: 1218-1238. https://doi.org/10.3390/life5021218

Sallstedt T., Ivarsson M., Lundberg J., Sjöberg R., Ramón J. & Romani V., 2014 – *Speleothem and biofilm formation in a granite/dolerite cave, Northern Sweden*. International Journal of Speleology, **43 (3)**: 305-313. https://doi.org/10.5038/1827-806X.43.3.7

Sant'Anna C., Branco L. & Silva S., 1991 – *A new species of Gloeothece (Cyanophyceae, Microcystaceae) from São Paulo State, Brazil*. Algological Studies, **92**: 1-5.

Selvi B. & Altuner Z., 2007 – *Algae of Ballıca Cave (Tokat-Turkey)*. International Journal of Natural and Engineering Sciences, **1 (3)**: 99-103.

Sgier L., Freimann R., Zupanic A. & Kroll A., 2016 – *Flow cytometry combined with viSNE for the analysis of microbial biofilms and detection of microplastics*. Nature Communications, **7**: 11587. https://doi.org/10.1038/ncomms11587

Shirkey B., Kovarcik D.P., Wright D.J., Wilmoth G., Prickett T.F., Helm R.F., Gregory E.M. & Potts M., 2000 – *Active Fe-containing superoxide dismutase and abundant sodF mRNA in Nostoc commune (Cyanobacteria) after years of desiccation*. Journal of Bacteriology **182**: 189-197. https://doi.org/10.1128/JB.182.1.189-197.2000

Smith T. & Olson R., 2007 – *A taxonomic survey of Lamp Flora (Algae and Cyanobacteria) in electrically lit passages within Mammoth Cave National Park, Kentuky*. International Journal of Speleology, **36 (2)**: 105-114. https://doi.org/10.5038/1827-806X.36.2.6

Stal L.J., 2012 – *Cyanobacterial Mats and Stromatolites*. In: Whitton B.A. (Ed.), *Ecology of Cyanobacteria II: Their diversity in space and time*. Springer Science, Dordrecht, 752 p. https://doi.org/10.1007/978-94-007-3855-3_4

Starmach K., 1972 – *Chlorophyta III. Zielenice nitkowate: Ulotrichales, Ulvales, Prasiolales, Sphaeropleales, Cladophorales, Trentepohliales, Sipholales, Dichotomosiphonales*. Warszawa and Krakow, Panstwowe Wyadwnictwo Naukowe, series Flora slodkowodna Polski 10, 750 p.

Sun J. and Liu D., 2003 – *Geometric models for calculating cell biovolume and surface area for phytoplankton*. Journal of Plankton Research, **25 (11)**: 1331-1346. https://doi.org/10.1093/plankt/fbg096

Ter Braak C.J.F. & Šmilauer P., 2012 – *Canoco Reference Manual and User's Guide: Software for Ordination, version 5.0*. Ithaca, USA, Microcomputer Power, 496 p.

Tofilovska S., Wetzel C.E., Ector L. & Levkov Z., 2014 – *Observation on Achnanthes Bory sensu stricto (Bacillariophyceae) from subaerial habitats in Macedonia and comparison with the type material of A. coarctata (Brébisson ex W. Smith) Grunow A. coarctata var. sinaensis Hustedt and A. intermedia Kützing*. Fottea, **14 (1)**: 15-42. https://doi.org/10.5507/fot.2014.002

Utermöhl H., 1958 – *Zur vervolkmmung der quantitativen phytoplankton methodik. Verhandlungen der Internationalen Vereinigung für Theoretische und Angewandte*. Limnologie, **9**: 1-38.

Vinogradova O.N., Nevo E. & Wasser S.P., 2009 – *Algae of the Sefunum Cave (Israel): species diversity affected by light, humidity and rock stresses*. International Journal on Algae, **11**: 99-116. https://doi.org/10.1615/InterJAlgae.v11.i2.10

Welton R.G., Ribas Silva M., Gaylarde Ch., Herrera L.K., Anleo X., De Belie N. & Modry S., 2005 – *Techniques applied to the study of microbial impact on building matherials*. Matherials and Structures, **38 (10)**: 883-893. https://doi.org/10.1007/BF02482255

Wilson C., Lukowicz R., Merchant S., Valquier-Flynn H., Caballero J., Sandoval J., Okuom M., Huber C., Durham Brooks T., Wilson E., Clement B., Wentworth C.D. & Holmes A.E., 2017 – *Quantitative and qualitative assessment methods for biofilm growth: a mini-review*. Research & Reviews: Journal of Engineering and Technology, **6 (4)**: 1-25.

International Journal of Speleology	48 (1)	63-74	Tampa, FL (USA)	January 2019

Available online at scholarcommons.usf.edu/ijs

International Journal of Speleology

Official Journal of Union Internationale de Spéléologie

Cave dripwater isotopic signals related to the altitudinal gradient of Mount-Lebanon: implication for speleothem studies

Carole Nehme[1,2,3*], Sophie Verheyden[2,4], Fadi H. Nader[5], Jocelyne Adjizian-Gerard[6], Dominique Genty[7], Kevin De Bondt[2], Benedicte Minster[7], Ghada Salem[3], David Verstraeten[2], and Philippe Claeys[2]

[1]Laboratoire IDEES UMR 6266 CNRS, University of Rouen Normandy, rue Thomas becket, 76821, Mont-Saint Aignan Cedex, France
[2]Analytical, Environmental & Geo-Chemistry, Department of Chemistry, Vrije Universiteit Brussel, Pleinlaan 2, 1050 Elsene, Brussels, Belgium
[3]ALES, Association Libanaise d'Etudes Speleologiques, Mansourieh El-Matn, Lebanon
[4]Directorate of Earth and Quaternary, Royal Belgian Institute of Natural Sciences (RBINS), rue Vautier 29, 1000, Brussels, Belgium
[5]Energie France Pétrole-Nouvelles, 4, avenue de Bois-Préau, 92852, Rueil-Malmaison Cedex, France
[6]CREEMO, Saint-Joseph University of Beirut, Faculty of Human Sciences, Rue de Damas, BP 17-5208, Beirut, Lebanon
[7]Laboratoire des Sciences du Climat et de l'Environnement (LSCE/IPSL), UMR 8212 CEA/CNRS/UVSQ, F-91191, Gif sur Yvette Cedex, France

Abstract: An important step in paleoclimate reconstructions based on vadose cave carbonate deposits or speleothems is to evaluate the sensitivity of the cave environment and speleothems to regional climate. Accordingly, we studied four caves, located at different altitudes along the western flank of Mount-Lebanon (Eastern Mediterranean). The objectives of this study are to identify the present-day variability in temperature, pCO_2, and water isotopic composition and to assess the possible influence of the altitudinal gradient on cave drip waters and cave streams. We present here an overview of the spatial variability of rainwater based on local and regional data, and we compare these data with our results, i.e., temperature, air pCO_2, and the isotopic composition of cave water and modern cave calcite collected in 2011 and 2014. The results show that the rainwater isotopic signal is generally preserved in the cave dripwater isotopic composition with some exceptions in large caves with high ceilings where evaporation effects may influence its isotopic composition. The altitude effect observed in rainwater isotopic composition seems to be transferred to the cave dripwater. Different $\delta^{18}O$/100 m gradients between dripwater and rainwater (0.13‰ and 0.21‰, respectively) are noted. This is mainly attributed to the $\delta^{18}O$/100 m value of the dripwater which is site-specific and dependent on i) local processes within the epikarst/soil, ii) the relation to the precipitation altitude gradient and iii) the extension of the defined infiltration basin.

Keywords: drip water, isotopic signal, Lebanon, caves, altitude gradient

Received 8 February 2019; Revised 26 February 2019; Accepted 26 February 2019

Citation: Nehme C., Verheyden S., Nader F.B., Adjizian-Gerard J., Genty D., De Bondt K., Minster B., Salem G., Verstraeten D. and Claeys P., 2019. Cave dripwater isotopic signals related to the altitudinal gradient of Mount-Lebanon: implication for speleothem studies. International Journal of Speleology, 48 (1), 63-74. Tampa, FL (USA) ISSN 0392-6672
https://doi.org/10.5038/1827-806X.48.1.2253

INTRODUCTION

Speleothems, which are secondary cave carbonate deposits that precipitate from cave drip water are increasingly used to reconstruct changes in regional climate and vegetation. Their isotopic composition, $\delta^{18}O$, and $\delta^{13}C$ is influenced mainly by respectively the isotope signature of rainwater linked to temperature (Clarck & Fritz, 1997; Lachniet, 2009) and by the carbon isotopic composition of dissolved carbon influenced by the soil bioactivity ($\delta^{13}C$), linked to vegetation and thus to temperature and water availability (Hellstrom et al., 1998; Genty et al., 2006). Rainwater and dissolved carbon circulate through the unsaturated zone, i.e. the upper part of the epikarst, which is affected by dissolution and is characterized by a mainly vertical transfer of percolation water to the cave (Hendy, 1971; Bar-Matthews et al., 1996; Ford & Williams, 2007; Fairchild & Baker, 2012).

Several cave monitoring programs have been conducted worldwide, providing information on the role of local cave environment and hydrology that possibly influence stalagmite-based palaeoclimate proxy records (Bar-Matthews et al., 1996; Spotl et al., 2005; Baldini et al., 2006; Verheyden et al., 2008a; Mattey et al., 2010; Miorandi et al., 2010; Tremaine

*carole.nehme@univ-rouen.fr

et al., 2011; Johnston et al., 2013; Genty et al., 2014; Deininger et al., 2014; Van Rampelbergh et al., 2014; Suric et al., 2016; Beddows et al., 2016). These studies aim at understanding better the registration of the nowadays climatic signal in speleothems in order to more precisely constrain the past climatic records.

In the Levant region, although speleothems from Palestine/Israel are well studied and proxy interpretations well-supported by monitoring programs, the rest of the region is still understudied in terms of speleothem-based paleoclimate studies (Nader et al., 2007, Verheyden et al., 2008b, Cheng et al., 2015, Nehme et al., 2015; 2018). Nearly no cave monitoring information is available and only limited rainwater isotopic data is available (Aouad-Rizk et al., 2005; Gat el al., 2005, Abou Zakhem & Hafez, 2010). Aouad-Rizk et al. (2005) and Koeniger & Margane (2014) each defined a local meteoric water line (LMWL) based on data from central Mount-Lebanon. Both studies display some differences which will be further discussed in the paper. The Levant (East-Mediterranean) is characterized by abrupt temperature and rainfall gradients, due to its current location on the arid/semi-arid boundary and to its steep topography between coastal and inland areas.

In a first attempt to understand the local environmental conditions, four Lebanese caves were investigated for their temperature, *p*CO2 concentration, and dripwater isotopic composition. Here, modern changes in the rainwater isotopic composition across the steep altitudinal trend of Mount-Lebanon, are compiled based on a literature review, and compared with the observed changes in modern cave drip waters. The main objectives of this paper are to discuss if rainwater signal is generally preserved in the cave dripwaters and to assess the possible influence of the altitudinal gradient on cave drip waters and cave streams. This study will help also verify the ability of cave waters in Lebanon to transfer spatial changes in isotopic composition of rainwaters and by extension of spatial and temporal changes in regional climate.

THE STUDY AREA: REGIONAL CLIMATIC CONTEXT AND SITE DESCRIPTION

The Levant region in general is mainly influenced by the mid-latitude westerlies (Fig. 1A), which originate from the Atlantic Ocean, forming a series of subsynoptic low-pressure systems (Gat et al., 2003; Ziv et al., 2010) across the Mediterranean Sea. In winter, cold air plunging south over the relatively warm Mediterranean enhance cyclogenesis, creating the Cyprus Low (Alpert et al., 2005). This low-pressure system drives moist air onshore, generating intense orographic rainfall across the mountains of the northern Levant. The duration, intensity, and track of these storm systems strongly influence the rainfall amount in this region. In summer, the westerly belt is shifted to the north, following the northern shift of the North-African subtropical high pressures, and the region experiences hot and dry conditions with more southward winds. In Lebanon (Fig. 1B and 1C), the annual rainfall varies between 700 and 1000 mm along the coastline and more than 1400 mm in higher mountains with 4 months snow coverage (Shabaan et al., 2015). As a consequence of the above circulation system, the climate is seasonal with wet winters (November to February) and dry, hot summers (May to October). A general N-S gradient in rainfall amount and mirrored by the isotopic signal ($\delta^{18}O$ and $\delta^{2}H$) is clearly evident from northern Syria (Abou Zakhem & Hafez, 2010), to southern Israel/ Palestine (Gat et al., 2005). A West-East gradient, i.e. from the Levantine coastline to inner regions (Fig. 1A), is also visible as a consequence of the continental and/or altitudinal effects related to the Rayleigh distillation processes (Dansgaard, 1964; Rozanski et al., 1993).

Four caves are selected at different altitudes along a transect from the coast to the Makmel Mountain, which is the highest peak in the Mount-Lebanon range (Fig. 2). These are: Kanaan Cave (96 m above sea level - asl), Jeita Cave (98 m asl), Mabaage Cave (770 m asl), and Qadisha Cave (1720 m asl).

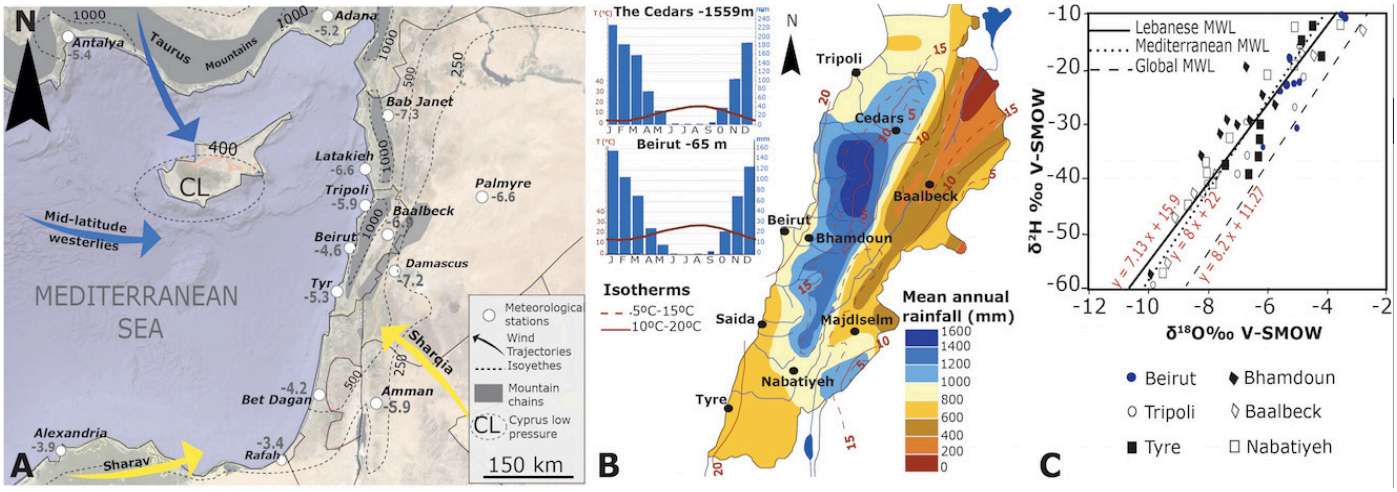

Fig. 1. Climate and geographic setting of the study area. A) Eastern Mediterranean map showing the position of the mid latitude winds (http://iridl.ldeo.columbia.edu/Maproom), NS and EW precipitation gradients and $\delta^{18}O$ mean values NS and EW precipitation gradients, of rainwater stations over coastal and inner cities (Kailani et al., 2003; El-Asrag, 2004; Aouad-Rizk et al., 2005; Dirican et al., 2005; Gat el al, 2005; Saad et al., 2005; Abou Zakhem & Hafez, 2010; GNIP database); B) Precipitation gradients of Lebanon and histograms of Beirut and the Cedars with mean annual rainfall and temperature (Abi-Saleh & Safi, 1988; http://fr.climate-data.org); C) Rainwater isotope graph with several published meteoric waterlines: the Lebanese MWL in Saad et al. (2005), the Global MWL in Rozanski et al. (1993), and the Mediterranean MWL in Gat (1980).

Except for Qadisha Cave which is developed mainly in Quaternary deposits and Cretaceous limestones (Dubertret, 1975), Mabaage, Jeita and Kanaan caves develop in the middle Jurassic Kesrouane Formation, a faulted micritic limestone and dolomite sequence (Walley, 1998). The studied caves (Table 1) are located in the western flank of Mount-Lebanon (Fig. 1) along a N-S altitudinal transect. All four caves were previously studied for their speleothem content (Verheyden et al., 2008a; Cheng et al., 2015; Nehme et al., 2015, 2018).

Kanaan Cave (162 m long) is located 15 km northeast of Beirut. This fossil cave was discovered after quarrying activity in the late 1990s (Nehme et al., 2009). The Jeita multi-level system cave, located at 4.5 km distance from the coast, hosts a series of dry and active galleries (Karkabi, 1990), a permanent stream with a discharge of 1 to 25 m^3/s (Doummar, 2012) and is the most visited show cave in Lebanon. A 75 m deep canyon connects fossil galleries with the lower galleries in the downstream extremity of the 10 km karstic network, making the cave a well-ventilated system (Fig. 2). Mabaage Cave 400 m long, located at 40 km northeastern of Beirut and in the inner part to the Fidar valley (Jabbour-Gedeon & Zaatar, 2013) was recently transformed into a touristic cave during summer but closes in winter due to flooding of the cave stream. Finally, Qadisha Cave, located in the northern part of Mount-Lebanon, hosts a permanent spring with a discharge rate up to 1 m^3/s (Edgell, 1997). Qadisha cave was partially transformed into a touristic cave in 1934.

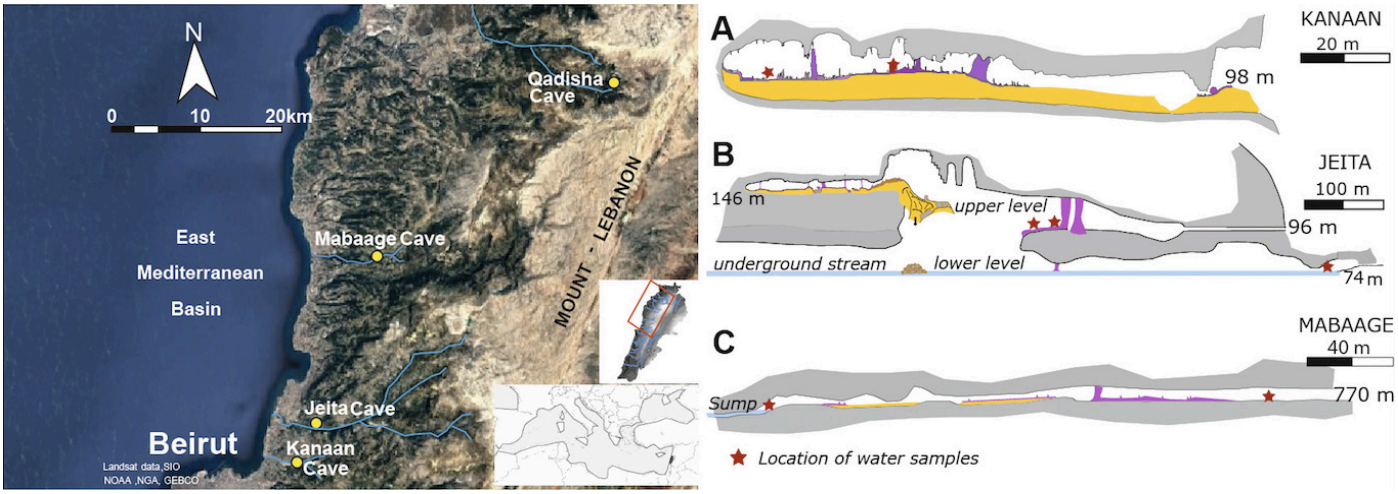

Fig. 2. The study area and cross-sections of A) Kanaan Cave (Nehme et al., 2013); B) Jeita Cave (Karkabi, 1990; Nehme, 2013); C) Mabaage Cave (Zaatar et al., 2013). For the cross-sec`tion of Qadisha Cave, see Tawk et al. (2008). Red stars indicate the location of water samples taken inside each cave and cave elevations are in m above sea level (asl). Refer to Table 1 for additional cave site data.

The vegetation cover above the caves mainly develops in shallow Mediterranean soil. Between 100 and 800 m asl, the vegetation consists of densely evergreen shrubs (juniper, oaks, and partially pine trees) growing on calcareous slopes above Kanaan, Jeita and Mabaage caves. The vegetation cover above Qadisha Cave (1720 m asl) is composed of sparse herbs, shrubs, and conifers (Table 1).

Table 1. Locations, morphology of the studied caves, and their soil characteristics.

Cave	Coordinates	Cave type	Entrance (m)	Infiltration basin elevation (m)	Aspect	Length (m)	Host Rock	Vegetation type
Kanaan	33°54'25"N; 35°36'25"E	Horizontal, relict	98	547	SE-NW	162	J4-J5	dense garrigue, pine forest
Jeita upper	33°56'35"N; 35°38'48"E	Horizontal, relict	96	1067	N-S	1300	J4-J5	dense garrigue, pine forest
Jeita Lower	33°56'35"N; 35°38'48"E	Horizontal, active	60	1669	E-W	8750	J4-J6	dense garrigue, pine forest
Mabaage	34°06'25"N; 35°46'01"E	Descending cave	770	1379	E-W	400	J6	sparse garrigue, oaks, pine
Qadisha	34°14'38"N; 36°02'11"E	horizontal, spring	1720	2244	NE-SW	1076	Q; C4	Sparse hurbs, shrubs, conifer

SAMPLES AND METHODS

A total of 35 cave drip water and 12 underground stream water samples were collected in the Jeita and Qadisha caves for $\delta^{18}O$ and $\delta^{2}H$ analyses, respectively. The samples were obtained during two sampling campaigns: a first one held in September 2011 in Jeita and Qadisha caves and a second one between September and November 2014 in Jeita, Qadisha, Mabaage, and Kanaan caves.

Temperature and pCO_2 of cave air were measured using a hand thermometer with a precision of 0.5°C and a Dräger pump system (σ ± 50 ppmv), respectively. Continuous temperature monitoring using a Niphargus (Burlet et al., 2015) temperature logger (precision of 0.1°C and resolution of 0.05°C)

was pursued from December 2015 to March 2017 in Qadisha and Jeita caves with one measurement every 20 minutes.

Isotopic analyses of cave waters collected in 2014 were carried out using a PICARRO L2130-i Cavity Ring-Down Spectrometer (CRDS) at the Vrije Universiteit Brussel. Measured values were corrected using three house standards calibrated against the international VSMOW2, GISP, and SLAP2 standards following the method described in De Bondt et al., (2018). Analytical uncertainties (2σ) equal 0.06‰ for $\delta^{18}O$ values and 0.3‰ for $\delta^{2}H$ values. Water samples collected were analyzed in 2011 at the Laboratoire des Sciences du Climat et de l'Environnement (LSCE-CEA), Paris. Hydrogen isotopes were measured on an ISO-PRIME mass spectrometer and a PICARRO CRDS with a 1 sigma error of ±0.7‰. Oxygen isotopes were analyzed using a Finnigan MAT 252 by equilibration with CO_2. The 2 sigma error of the $\delta^{18}O$ is ±0.05‰. All values obtained from both laboratories are calibrated against and reported in permill (‰) relative to Vienna Standard Mean Ocean Water (V-SMOW2).

To calculate the altitudinal gradient of the cave dripwaters with respect to the altitude of the entrance and the infiltration basin of the studied caves, the infiltration basin elevation (Table 1) was derived after plotting the georeferenced caves maps on a Digital Elevation Model (DEM) using a Geographical Information System (ArcGIS). The infiltration watershed area of the cave is defined by considering the altitudes between the cave entrance and the limit of the surface watershed. The underground waterflow main directions identified in Hakim (1985) and Hakim et al. (1988) for the Lebanese karst basins were considered to derive the most significant infiltration surface above the caves. The mean altitude is then calculated for the delimited infiltration basin for each cave using the DEM. Note that the Jeita Cave develops on two-levels (an upper fossil and a lower active gallery) thus has two different infiltration elevations.

RESULTS

Cave air temperature and pCO_2

Cave air and underground stream temperatures, measured at different sites inside each cave (see Supplementary Data), a fairly constant (Fig. 3A) with variations of less than 1°C over the sampling period. The measured air temperatures in Kanaan (19°C ± 0.5), Jeita upper (20°C ± 0.5), Mabaage (13°C ± 0.5), and Qadisha caves (9°C ± 0.5) all display autumn values roughly in agreement with the outside mean temperature (Fig. 3B) data (Karam, 2002), despite the small offset compared to the surface temperature trendline and some small internal changes (up to 0.3°C) as shown by the continuous monitoring data in Jeita and Qadisha (Fig. 3C).

As for the pCO_2 concentrations in each cave, the measured values reached 3,600 and 8,000 ppmv in Jeita and Mabaage caves respectively, whereas low values (600 ppmv) close to the atmospheric concentrations are detected in Qadisha Cave (see Supplementary Data).

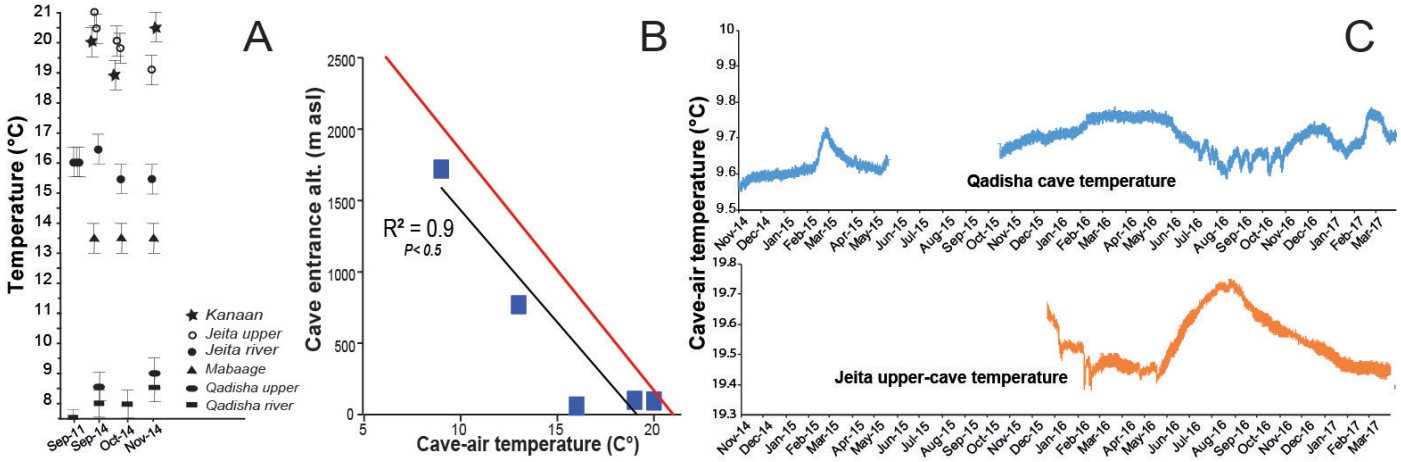

Fig. 3. A) Cave-air and underground stream temperature measurements collected each month in both 2011 and 2014 171 campaigns; B) cave-air temperature trendline (black line) vs the cave entrance altitude. The air-temperature trendline from compiled data of Lebanese meteorological stations (Karam, 2002) is represented in red line; C) continuous cave-air temperature monitoring from November 2014 to March 2017 for Qadisha and from January 2016 to March 2017 for Jeita Cave.

Cave dripwater $\delta^{18}O$ and $\delta^{2}H$

Cave dripwaters and stream waters $\delta^{18}O$ and $\delta^{2}H$ are summarized in Table 2 and detailed in the Supplementary Data. Jeita Cave dripwaters exhibit an average of -5.7 ± 1.1‰ for $\delta^{18}O$ and –26.6 ± 6.9‰ for $\delta^{2}H$ (Table 2), with an amplitude of 2.9 and 20.5‰, respectively. As for Kanaan Cave, measurements show an average of -5.40 ± 0.04‰ for $\delta^{18}O$ and –24.0 ± 0.2‰ for $\delta^{2}H$ (Table 2), with an amplitude of 0.2 and 0.5‰ respectively. Mabaage Cave located at higher altitude (770 m) shows an average of -7.2 ± 0.6‰ for $\delta^{18}O$ and –36.6 ± 6.2‰ for $\delta^{2}H$, whereas the amplitude varies between 1.8 and 14.0‰, respectively.

Qadisha Cave, located at the highest altitude in our study area, shows an average of -8.48 ± 0.05‰ for $\delta^{18}O$ and –46.1 ± 0.31‰ for $\delta^{2}H$ with an amplitude of 0.2 and 1.1‰, respectively. The variability of the dripwater oxygen isotopic signal in Kanaan (avg. -5.4‰) and Qadisha (avg. -8.5‰) does not exceed ±0.1‰ (Table 2). Drip water values in both Jeita and Qadisha caves show lower isotopic values than Jeita (avg. -7.2‰) and Qadisha (avg. -9.0‰) stream waters. However, the difference is much higher between dripwater and stream water isotopic values in Jeita Cave (~1.5‰) than those of Qadisha Cave (~0.4‰).

Table 2. Summary of the isotopic results of the drip and stream waters collected from the studied caves. Note that Jeita upper is the fossil cave and Jeita lower in the active cave with a permanent stream. (n) is the number of samples and oxygen isotopic composition ranges. The mean (avg.), maximum and minimum values of the $\delta^{18}O$ drip and stream water and mean (avg.) of the $\delta^{2}H$ of the autumn values, are reported in ‰ VSMOW.

Fossil Caves	***n***	**Dripwater $\delta^{18}O$ (‰ VSMOW)**				**Dripwater $\delta^{2}H$ (‰ VSMOW)**	
		min	**max**	**avg.**	**2s**	**avg.**	**2s**
Kanaan	6	-5.48	-5.37	-5.43	±0.04	–24	± 0.2
Jeita Upper	11	-6.92	-4.05	-5.71	±1.11	–26.6	± 6.9
Mabaage	8	-8.28	-6.64	-7.18	±0.66	-36.6	± 6.2
Qadisha	10	-8.55	-8.38	-8.48	±0.05	-46.1	± 0.3
Cave Streams	***n***	**Stream water $\delta^{18}O$ (‰ VSMOW)**				**Stream water $\delta^{2}H$ (‰ VSMOW)**	
		min	**max**	**avg.**	**2s**	**avg.**	**2s**
Jeita lower	6	-7.35	-7.17	-7.28	±0.06	-35.73	± 0.48
Qadisha	6	-8.96	-8.92	-8.95	±0.02	-49.24	± 0.26

DISCUSSION

In order to determine if the current spatial gradients in rainwater isotopic composition are recorded in the cave dripwater, we discuss *i)* the available meteoric water lines of Lebanon and their altitudinal trends, *ii)* the cave waters $\delta^{18}O/\delta^{2}H$ signals compared to the available $\delta^{18}O/\delta^{2}H$ rainwater data, and *iii)* the altitudinal trend in rainwater $\delta^{18}O/\delta^{2}H$ and the potential altitudinal trends in cave water $\delta^{18}O$ to test for their agreement.

Rainwater data of Lebanon: different meteoric water lines and altitudinal trends

Several studies on the rainwater isotopic signal in Lebanon (Aouad-Rizk et al., 2005; Saad et al., 2005; Saad and Kazpard, 2007; Koeniger & Margane, 2014; Koeniger et al., 2017) exist in the literature (Table 3). The trendline slopes of the MWL (Lebanon, Mount-Lebanon, etc.) are different than that of the Mediterranean MWL, due mainly to a secondary evaporation effect during rainfall events (Saad et al., 2005; Saad & Kazpard, 2007). The evaporation occurs mostly during hot (dry) seasons and is particularly impacting light rains. Consequently, this process will determine the lowering of the slope and the "d-excess" value of the rain sample (Clark & Fritz, 1997).

In general, the constructed Lebanese Meteoric water lines based on $\delta^{18}O$ and $\delta^{2}H$ data of rainwater are roughly in agreement with a general depletion trend with elevation. However, the local MWL (Koeniger & Margane, 2014; Koeniger et al., 2017) for the Kelb basin, the Mount-Lebanon (Aouad-Risk et al., 2005) and the general Lebanese MWL (Saad et al., 2005; Saad & Kazpard, 2007) are calculated based on different locations of the meteorological stations (Fig. 4A).

Table 3. Summary of the Global MWL and the MWLs previously calculated for the Mediterranean, Lebanon and Kelb basin.

Meteoric water line	**Equation**	**Author**
Global meteoric water line	**$\delta^{2}H = 8 * \delta^{18}O + 10$**	Craig, 1961
Mediterranean water line	**$\delta^{2}H = 8 * \delta^{18}O + 22$**	Gat, 1980; Gat et al., 2003
Lebanese water line	**$\delta^{2}H = 7.13 * \delta^{18}O + 15.98$**	Saad et al., 2005 ; Saad & Kazpard, 2007
Mount-Lebanon water line	**$\delta^{2}H = 6.3 * \delta^{18}O + 8.2$**	Aouad-Rizk et al., 2005
Kelb basin water line (Local)	**$\delta^{2}H = 6.04 * \delta^{18}O + 8.45$**	Koeniger & Margane, 2014; Koeniger et al., 2017

The MWL after Aouad-Risk et al. (2005) referred here as the Mount-Lebanon MWL, is constructed using data from meteorological stations which display the same E-W trend than the stations used for the MWL of the Kelb basin (Koeniger & Margane, 2014). Indeed, the MWL after Aouad-Risk et al. (2005) and the local MWL after Koeniger & Margane (2014) show the same gradient (Table 3).

The altitudinal trendline (Fig. 4B) used in this study is constructed after the latest rainwater data (Koeniger & Margane, 2014; Koeniger et al., 2017) from stations located in the Kelb basin (central Mount-Lebanon) since the collected data covers an elevation range up to 1600 m (Chabrouh station) close to the basin altitude of the studied caves and includes snowfall isotopic signals. This altitudinal trendline show a linear $\delta^{18}O$-altitude relation of -0.13‰/100 m in West Mount-Lebanon (Fig. 4B), i.e., a decrease in rainwater $\delta^{18}O$ of 0.13‰ per 100 meters altitudinal increase.

Cave waters $\delta^{18}O/\delta^{2}H$ signals compared to the available $\delta^{18}O/\delta^{2}H$ rainwater data

The isotopic results of cave waters (drip and stream) of the four studied caves fall well on the Mount Lebanon MWL (Aouad-Risk et al., 2005), except for some of the Jeita Cave dripwaters (Fig. 4C). In general, Kanaan, Jeita, Mabaage and Qadisha $\delta^{18}O_{water}$ (drip and stream) values seems to fall more closely to the Mount Lebanon and Lebanese MWL than the regional Mediterranean MWL (Gat, 1980; Gat et al., 2003).

The $\delta^{18}O_{drip}$ values of Kanaan Cave are at the lower part of both Lebanese and Mount-Lebanon MWLs whereas Mabaage $\delta^{18}O_{drip}$ values are located at the center. $\delta^{18}O_{drip}$ values of Qadisha cave correspond to the highest part on both MWLs. Both Qadisha and Jeita $\delta^{18}O_{drip}$ results of 2014 fall generally close to the Lebanese MWL trend. Jeita $\delta^{18}O_{drip}$ results of 2011 show a distinct displacement to the right of the Mount Lebanon MWL, that clearly indicates evaporation

processes (Saad & Kazpard, 2007). The positive $\delta^{18}O_{drip}$ values of the 2011 campaign in Jeita Cave (Fig. 4C) suggest several processes and factors that might explain this particularity. Mickler et al. (2004) and Day and Handerson (2011) showed that the evaporation effect often occurs in caves with higher cave-air temperatures, which is the case for Jeita Cave (20°C), and less so for Qadisha Cave (9°C). Another possibility is related to other cave environment parameters which include enhanced ventilation (Muhlinghaus et al., 2009; Deininger et al., 2012) that would lead to enhanced out-of-equilibrium processes.

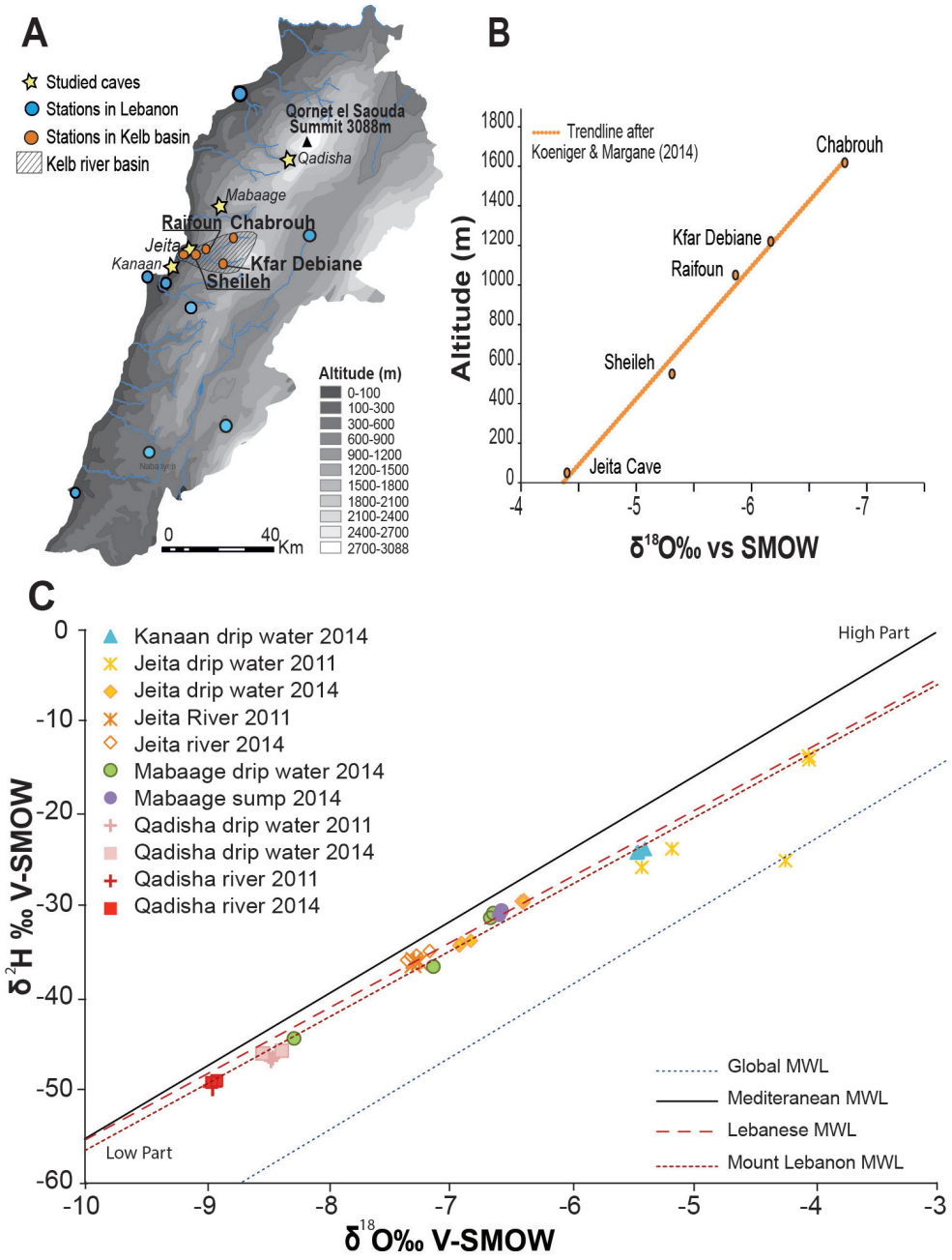

Fig. 4. Summary of major cave drip and stream water $\delta^{18}O$ and $\delta^{2}H$ values plotted on the available meteoric water lines (MWL) with the location of their meteorological stations. A) location of the studied caves (yellow stars) and the meteorological stations (blue circles) in Saad et al. 2005 and Saad & Kazpard, 2007 and (orange circles) in Koeniger & Margane, 2014; B) the altitudinal trendline used in this study and derived from the Local MWL of 222 the Kelb basin (Koeniger & Margane, 2014); C) $\delta^{18}O$ and $\delta^{2}H$ values of 47 dripwater and stream samples plotted on the available MWLs.

The $\delta^{18}O$ values for stream waters in the Qadisha and Jeita caves plot along the Mount Lebanon and Lebanese MWLs. The Qadisha stream water displays $\delta^{18}O$ values close to the drip water isotopic signal of the same cave suggesting a similar water infiltration source for the vadose and the karst aquifer (phreatic) zones. However, the isotopic signal of Jeita stream exhibits higher values than the drip water isotopic signal in Jeita upper cave advocating for different infiltration reservoir for the unsaturated and saturated zones. Indeed, the Jeita underground stream exhibits a $\delta^{18}O$ signal which is very close to the average $\delta^{18}O$ signal of the highest karstic springs feeding the Kelb basin: Nabaa el-Labane spring at 1647 m (avg. -7.26‰) and Nabaa al-Assal spring at 1528 m (avg. -7.32‰) (Aouad-Rizk et al., 2005; Koeniger et al., 2017). The isotopic signals are also in agreement with the well-known infiltration basin (or recharge area) for the Jeita underground stream situated at a mean altitude of 1669 m asl (Table 1).

The spread of the isotopic values cave waters along the Mount Lebanon MWL is related to the variability in $\delta^{18}O$ and $\delta^{2}H$ in rainwater and therefore in cave drip water. This is mainly due to the spatial variability, inter-seasonal, or interannual variations in isotopic composition of rain. It suggests that all sampled dripwaters in the caves, especially in Jeita and less in Qadisha may be related to rainwater from different seasons or even years depending on the residence time of the water in the vadose, here epikarst zone.

The deuterium excess (d-excess) value is calculated from $\delta^{18}O$ values and $\delta^{2}H$ using this equation:

$$\text{d-excess} = \delta^{2}H - 8 * \delta^{18}O$$

The d-excess, an indicator for the source and trajectories of atmospheric moisture (Rozanski, 1993; Sharp, 2007), is associated with evaporation at the moisture source. The comparison of d-excess_{drip} vs d-excess_{rain} is necessary to understand if the measured cave waters are controlled by a similar vapor source than the rainwater. The Eastern Mediterranean source waters have d-excess values ranging from 14‰ to 19‰ (Kattan, 1997), whilst they reach 15‰ (Frot et al., 2007) for Western Mediterranean sourced waters, and are close to 10‰ for Atlantic-sourced moisture. The Lebanese MWL exhibit a d-excess of 15.98‰ which is within the range of the Eastern Mediterranean waters' values (Kattan, 1997). The d-excess for the dripwater in cave indicate a value of 16.25, which is close to the one defined by the Lebanese MWL (Aouad-Rizk et al., 2005; Saad & Kazpard, 2007; Koeniger & Margane, 2014).

Altitudinal trends in cave water $\delta^{18}O$

The Mediterranean air masses arriving from the west are orographically uplifted as they reach the Mount-Lebanon range. As the air rises and cools, the rainwater with a heavier isotope falls first, resulting in rainwater exhibiting more negative isotopic values with altitude (Bowen & Wilkinson, 2002). Globally, the average change in $\delta^{18}O_{rain}$ is -0.2‰ per 100 m elevation gain (Rozanski et al., 1993). Locally, we determined this trend as -0.13‰/100 m (Fig. 4B). In order to understand the altitude effect on the isotopic composition of cave water (drip and stream), the $\delta^{18}O$ cave water values are plotted first against altitude of the cave entrances (Fig. 5A).

Only the $\delta^{18}O_{drip}$ and $\delta^{18}O_{stream}$ values that fall closely on the local MWL were retained for the altitudinal trend analysis (Fig. 5A). Figure 5A clearly shows a poor altitudinal trend when considering only the altitude of the cave entrance. However, there is a clear altitudinal trend with a regression coefficient $R^2 = 0.86$ ($P < 0.001$) when considering the mean altitude of the infiltration basin (or recharge area) of these caves (Fig. 5B and 5C). Indeed, the basin from where water infiltrates is at higher elevation relative to the cave entrance due to the thick limestone overburden and the topography above the caves entrance. The $\delta^{18}O_{water}$ values of Jeita stream are a clear example of that particularity, showing that the underground water originates from an infiltration basin at a higher altitude (avg. alt. 1669 m) than the cave entrance (60 m) (Doummar, 2012; Koeniger et al., 2017).

With the infiltration basin altitude (Table 1) taken into consideration here, all points fall within the 95% confidence interval (Fig. 5B and 5C) except one point, which represent cave waters taken from Mabaage Cave at the end of August 2014. All drip and stream waters $\delta^{18}O$ values reach 0.2‰ per 100 m (Fig. 5B) with an overall offset of 0.07‰ compared to the rainwater trend of 0.13‰ per 100 m calculated form the trendline (Fig. 4B) after Koeniger & Margane (2014).

Comparable studies in the Mediterranean region showed different small offsets between altitudinal gradients for precipitation and dripwater $\delta^{18}O$ values. In the steep northern Italian Alps, eight caves aligned along two transects, show slightly different gradients of 0.15 and 0.08‰ in dripwater (Johnston et al., 2013). In the eastern Adriatic coast and Dinaric mountains (Croatia), the offset reaches up to 0.2‰ (Suric et al., 2016) similar to the offset measured in Mount-Lebanon cave waters.

Clearly, the $\Delta\delta^{18}O$/100 m value of the dripwater (Fig. 5C) is site-specific, mainly due to: *i)* local processes that influence the $\delta^{18}O_{drip}$ on its way to the cave, such as those within the litter, soil, and epikarst (Beddows et al., 2016), *ii)* the relation to the precipitation altitude gradient (rainfall quantity, patterns, and frequencies above the cave infiltration

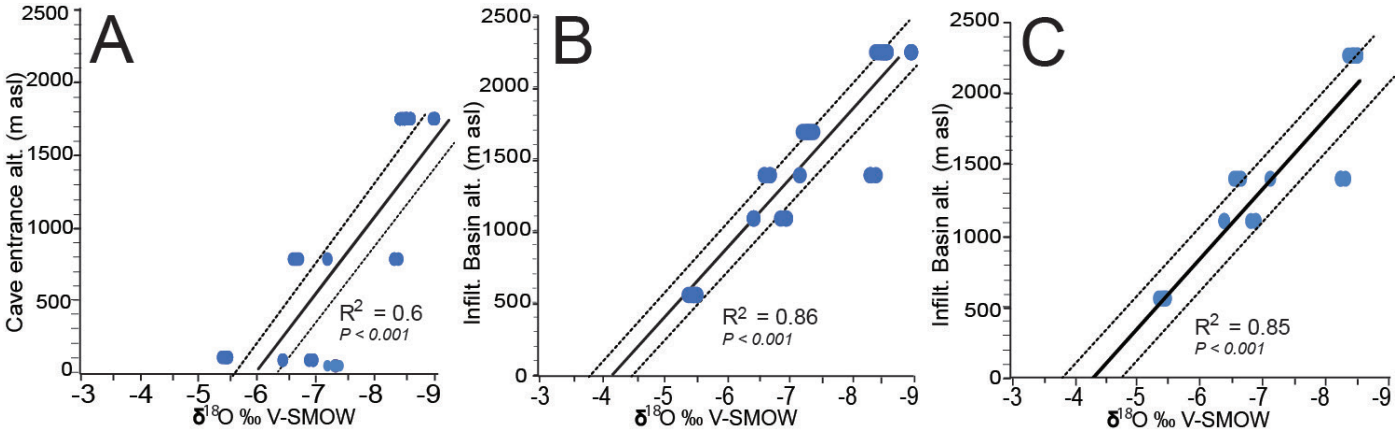

Fig. 5. Altitudinal trends in cave water $\delta^{18}O$ (drips and streams). A) Adjusted linear regression between the $\delta^{18}O_{cave\ water}$ and the altitude of the cave entrance; B) $\delta^{18}O_{cave\ water}$ and the altitude of the infiltration basin; C) Plot showing the $\delta^{18}O_{dripwater}$ trendline only vs the infiltration basin altitude. The calculated interval of confidence (dashed line) for each linear regression is 95% and the significance p-value for all three graphs is $P < 0.001$.

basin), or *iii)* the hilly topography above the cave and the limits of the calculated infiltration basin defined herein.

Figure 6A compares the offset between altitudinal gradients for precipitation and dripwater $\delta^{18}O$ values. Within the limit of the 95% confidence interval of the precipitation $\delta^{18}O$ trendline and considering the 2σ sigma error of the dripwater, the drip $\delta^{18}O$ values fall generally close to the precipitation $\delta^{18}O$ trendline except for Qadisha Cave. There is, however, a minor negative offset (0.2‰ at low altitude to 1.2‰ at high altitude) between the dripwater and the precipitation $\delta^{18}O$ trendline.

This offset, similar to the one observed for the Adige, Valsugana valleys, northern Italy (Johnston et al., 2013), the Adriatic coast (Suric et al., 2016), and Vancouver, Canada (Beddows et al., 2016) represents a bias due to the infiltration effects of rainwater. In winter, the infiltrated water from rainfall/snowmelt with lower $\delta^{18}O$ values reaches the cave, while in summer seasons, ^{18}O (^{2}H)-enriched water will partially evaporate in the unsaturated zone, especially when shallow overburden exists above the cave (Wackerbarth et al., 2010, 2012). The cave waters are therefore normally biased towards lower/lighter $\delta^{18}O/\delta^{2}H$ values compared to the rainwater isotopic signal (Wackerbarth et al., 2012).

Generally, cave dripwaters in Lebanon are mostly the result of percolation happening during the wet season (from autumn to spring snowmelt), with a longer infiltration period at higher altitudes due to snowmelt. For Qadisha Cave, which is located at a higher altitude, the offset between the precipitation $\delta^{18}O$ trendline and the dripwaters isotopic signals is the most negative when compared to the other studied caves. This is explained by the infiltration of winter water enhanced by a negative isotopic value of winter snow, especially at higher altitudes (Aouad-Rizk et al., 2005) and contributing into the vadose water budget.

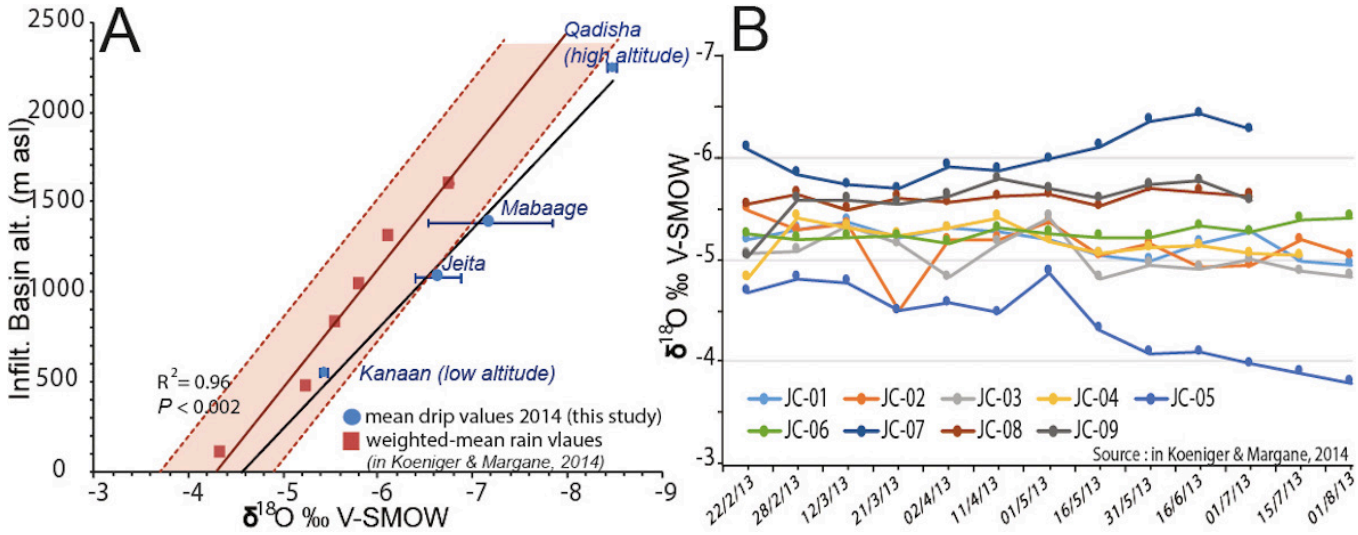

Fig. 6. Cave dripwaters $\delta^{18}O$ values in Lebanese caves compared to $\delta^{18}O_{rain}$: A) trendline showing the mean $\delta^{18}O_{dripwater}$ (blue dots) of each cave (this study) compared to the altitudinal trendline used in this study (red rectangles) and derived from the Local MWL ($\delta^{18}O$ weighted-mean rainwater values) after Koeniger & Margane (2014). The calculated interval of confidence (dashed line) for the $\delta^{18}O$ weighted-mean rainwater regression is 95% and the significance p-value is P < 0.002; B) $\delta^{18}O_{dripwater}$ measured at nine different sampling sites (JC-01to 09) in Jeita Cave on a yearly basis (data in Koeniger & Margane, 2014).

Regarding the altitudinal effect on the ^{18}O- and ^{2}H-depleted dripwater, our study shows that $\delta^{18}O_{drip}$ values decrease up to 3‰ between Kanaan and Qadisha caves (Fig. 6A). This amplitude attributed to the altitudinal effect could theoretically be increased by variations in the $\delta^{18}O_{drip}$ values related to site-specific characteristics or to a seasonal bias between winter and summer dripwaters values transferred by the rainwater seasonal variations. Indeed, rainwater $\delta^{18}O$ values in Lebanon show clearly a seasonal bias with a variation up to 5‰ (Saad & Kazpard, 2007; Koeniger & Margane, 2014) between early-winter and winter-spring seasons. In fact, seasonal variations in meteoric precipitation may range up to >15‰ for $\delta^{18}O$ (Genty et al., 2014). However, the majority of cave sites studied around the world (Genty et al., 2014; Beddows et al., 2016) demonstrated that drip waters typically show little or no isotopic seasonality compared to the variations in meteoric precipitation. For instance, the $\delta^{18}O_{drip}$ variability of caves in Vancouver Island, Canada is reduced in amplitude by 60–90% compared to the Victoria rainfall records of the same year. In Villars, Chauvet, and Orgnac caves, southern France, the $\delta^{18}O_{drip}$ values stayed stable for 15 years with little seasonal variations compared to drip rate measurement. In Lebanon, our $\delta^{18}O_{drip}$ data, even though stable during the autumn season prevent us from assessing a seasonal variability for all four cave sites. However, a previous campaign on dripwater isotopic measurement completed at nine drip sites in Jeita Cave (Koeniger & Margane, 2014) show little variability at each drip site over a complete rainy and early-summer season (Fig. 6B), but rather a spatial variability between each drip site. Indeed, the maximum seasonal variability of 1‰ is only recorded in JC-05 site (Fig. 6B). The $\delta^{18}O_{drip}$ yearly average is -5.24‰ in Jeita cave showing a low seasonal variability with a standard deviation of ±0.48. Therefore, the seasonal variations in cave dripwaters as seen in Jeita $\delta^{18}O_{drip}$ measurement, account less in the altitudinal effect on the lowering of the dripwater isotopic values.

Implications for future speleothems-based paleoclimate studies

The isotopic signal of the dripwater in Lebanese caves located on the western flank of Mount-Lebanon falls generally on the local MWL (Koeniger & Margane, 2014) as well as the Mount-Lebanon MWL (Aouad-Rizk et al., 2005). This implies: *i)* an identical source of water being derived from rain forming over the Mediterranean basin as indicated by similar d-excess values of the water, *ii)* a reduced evapotranspiration effect, observable on only some samples with a clear offset to the right of the MWL, probably due to increased cave ventilation, and *iii)* a longer infiltration period occurring in the unsaturated zone at higher altitudes.

Whilst some exceptions might occur as seen in some drip water in Jeita Cave during the 2011 campaign, which were more exposed to ventilation at some locations, most of the cave dripwater exhibits a similar $\delta^{18}O$ and $\delta^{2}H$ signal as the local rainwater. However, a slight offset towards lower 'winter values' may occur due to a preferential water recharge during winter months, including the recharge by melting snow.

Regarding the altitudinal trend observed in the rainwater over the Mount-Lebanon range (Fig. 4B), the isotopic signal in dripwater exhibits an altitudinal trend, but with a slightly different gradient (-0.21‰ per 100 m) than the rainwater (-0.13‰ per 100 m). This is however, more significant when the dripwater isotopic signal is compared to the altitude of the infiltration basin of each cave (Fig. 5C).

CONCLUSION

The preliminary dripwater isotopic measurements and temperature conducted on four caves located in the western flank of Mount-Lebanon, revealed the following important conclusions for future speleothem-based interpretation of paleoclimate changes at both local and regional scales:

- Despite for some water samples influenced by evaporative processes, the drip water exhibits isotopic values in agreement with the local rainwater. Therefore, stalagmites for paleoclimatic reconstructions (or fluid inclusion analysis) should be preferentially chosen outside a possible ventilation-influenced area of the cave.
- The altitudinal trend confirmed previously in the rainwater isotopic composition on the western flank of Mount-Lebanon is demonstrated also in cave drip water indicating the transfer to the cave through the vadose zone of the spatial isotopic signals of the rainwater. The isotopic composition of the dripwaters, however, exhibits a slightly higher negative $\delta^{18}O$/100 m gradient for cave drip water due to slower infiltration of winter waters. The isotopic dripwater signal represents therefore mostly a lower limit of the isotopic signal of the corresponding rain/snow melt.
- The results of this study can further help in the interpretation of past altitudinal trends based on speleothems. Additional future cave water and calcite monitoring with automated logging equipment (pCO_2, temperature, humidity, etc.) will continue to refine the interpretations that have been based on the initial monitoring findings presented here.
- To build further on this study, the altitudinal trend signal should be confirmed by modern calcite from the same caves, in which the trend should have a similar gradient.

ACKNOWLEDGMENTS

This study was funded by the 2014 mobility fellowship program of the Belgian Federal Scientific Policy (BELSPO), co-funded by the Marie Curie Actions of the European Commission, and the European Union's Horizon 2020 Research. Laboratory analysis conducted at LSCE-Paris were funded under the MISTRALS research program. We acknowledge the assistance of St-Joseph University of Beirut for facilitating the access to caves with the help of ALES (Association Libanaise d'Etudes Spéléologiques) and SCL (Spéléo-Club du Liban) and the support of both caving club members who collected water and calcite samples during field campaigns. The authors are grateful to Bogdan Onac for his editorial handling of the manuscript and endless patience and especially to the two anonymous reviewers for their constructive comments and revisions that considerably improved the quality of the manuscript.

REFERENCES

Abi-Saleh B. & Safi S., 1988 – *Carte de la végétation du Liban.* Ecologia Mediterranea, **14**: 123-141.

Abou Zakhem A. & Hafez R., 2010 – *Climatic factors controlling chemical and isotopic characteristics of precipitation in Syria.* Hydrological Processes, **24**: 2641-2654. https://doi.org/10.1002/hyp.7646

Aouad-Rizk A., Job J.O., Khalil S., Touma T., Bitar C., Bocquillon C. & Najem W., 2005 – *$\delta^{18}O$ and $\delta^{2}H$ contents over Mount-Lebanon related to mass trajectories and local parameters.* In: *Isotopic composition of precipitation in the Mediterranean Basin in relation to air circulation patterns and climate.* IAEA-TECDOC, **1453**: 75-82.

Alpert P., Price C., Krichak S.O., Ziv B., Saaroni H., Osetinsky I. & Kishcha P., 2005 – *Tropical teleconnections to the Mediterranean climate and weather.* Advances in Geosciences, **2**: 157-160. https://doi.org/10.5194/adgeo-2-157-2005

Baldini J.U.L., McDermott F. & Fairchild I.J., 2006 – *Spatial variability in cave drip water hydrochemistry: Implications for stalagmite paleoclimate records.* Chemical Geology, **235**: 390-404. https://doi.org/10.1016/j.chemgeo.2006.08.005

Baker A., Barnes W. & Smart P., 1997 – *Variations in the discharge and organic matter content of stalagmite drip waters in Lower Cave, Bristol.* Hydrological Processes, **11**: 1541-1555. https://doi.org/10.1002/(SICI)1099-1085(199709)11:11%3C1541::AID-HYP484%3E3.0.CO;2-Z

Bar-Matthews M., Ayalon A., Matthews A., Sass E. & Halicz L., 1996 – *Carbon and oxygen isotope study of the active water-carbonate system in a karstic Mediterranean*

cave: implications for paleoclimate research in semiarid regions. Geochimica Cosmochimica Acta, **60**: 337-347. https://doi.org/10.1016/0016-7037(95)00395-9

Bar-Matthews M., Ayalon A., Gilmour M., Matthews A. & Hawkesworth C.J., 2003 – *Sea-land oxygen isotopic relationships from planktonic foraminifera and speleothems in the Eastern Mediterranean region and their implication for paleorainfall during interglacial intervals*. Geochimica Cosmochimica Acta, **67**: 3181-3199. https://doi.org/10.1016/S0016-7037(02)01031-1

Beddows P.A., Mandic M., Ford D.C. & Schwarcz H.P., 2016 – *Oxygen and hydrogen isotopic variations between adjacent drips in three caves at increasing elevation in a temperate coastal rainforest, Vancouver Island, Canada*. Geochimica Cosmochimica Acta, **172**: 370-386. https://doi.org/10.1016/j.gca.2015.08.017

Bowen G.J. & Wilkinson B., 2002 – *Spatial distribution of $\delta^{18}O$ in meteoric precipitation*. Geology, **30**: 315-318. https://doi.org/10.1130/0091-7613(2002)030%3C0315:SDOOIM%3E2.0.CO;2

Burlet C., Vanbrabant Y., Piessens K., Welkenhuysen K. & Verheyden S., 2015 – *Niphargus: a silicon band-gap sensor temperature logger*. Computers & Geosciences, **74**: 50-59. https://doi.org/10.1016/j.cageo.2014.10.009

Cheng H., Sinhac A., Verheyden S., Nader F.H., Li X.L., Zhang P.Z., Yin J.J., Yi L., Peng Y.B., Rao Z.G., Ning Y.F. & Edwards R.L., 2015 – *The climate variability in northern Levant over the past 20,000 years*. Geophysical Research Letters, **42**: 8641-8650. https://doi.org/10.1002/2015GL065397

Day C.C. & Henderson G.M., 2011 – *Oxygen isotopes in calcite grown under cave-analogue conditions*. Geochimica Cosmochimica Acta, **75**: 3956-3972. https://doi.org/10.1016/j.gca.2011.04.026

Dansgaard W., 1964 – *Stable isotopes in precipitation*. Tellus, **16**: 438-468. https://doi.org/10.3402/tellusa.v16i4.8993

Deininger M., Fohlmeister J., Scholz D. & Mangini A., 2012 – *Isotope disequilibrium effects: The influence of evaporation and ventilation effects on the carbon and oxygen isotope composition of speleothems - A model approach*. Geochimica Cosmochimica Acta, **96**: 57-79. https://doi.org/10.1016/j.gca.2012.08.013

De Bondt K., Seveno F., Petrucci G., Rodriguez F., Joannis C. & Claeys P., 2018 – *Potential and limits of stable isotopes ($\delta^{18}O$ and $\delta^{2}H$) to detect parasitic water in sewers of oceanic climate cities*. Journal of Hydrology: Regional Studies, **18**: 119-142. https://doi.org/10.1016/j.ejrh.2018.06.001

Dirican A., Unal S., Acar Y. & Demircan M., 2005 – *The temporal and seasonal variation of $\delta^{2}H$ and $\delta^{18}O$ in atmospheric water vapour and precipitation from Ankara, Turkey in relation to air mass trajectories at Med. Basin*. In: *Isotopic composition of precipitation in the Mediterranean Basin in relation to air circulation patterns and climate*. IAEA-TECDOC, **1453**: 191-214.

Doummar J., 2012 – *Identification of indicator parameters for the quantitative assessment of vulnerability in karst aquifers*. Unpublished Thesis, University of Gottingen, Gottingen, 116 p.

Dubertret L., 1975 – *Introduction à la carte géologique au 1/50000^{e} du Liban*. Notes et Mémoires sur le Moyen-Orient, **23**: 345-403.

El-Asrag A.M., 2005 – *Effect of synoptic and climatic situations on fractionation of stable isotopes in rainwater over Egypt and east Mediterranean*. In: *Isotopic composition of precipitation in the Mediterranean Basin in relation to air circulation patterns and climate*. IAEA-TECDOC, **1453**: 51-73.

Edgell H.S., 1997 – *Karst and hydrogeology of Lebanon*. Carbonates and Evaporites, **12 (2)**: 220-235. https://doi.org/10.1007/BF03175419

Frot E., Van Wesemael B., Vandenschrick G., Souchez R. & Benet A.S., 2007 – *Origin and type of rainfall for recharge of a karstic aquifer in the western Mediterranean: a case study from the Sierra de Gador-Campo de Dalias (southeast Spain)*. Hydrological Processes, **21**: 359-368. https://doi.org/10.1002/hyp.6238

Fairchild I.J. & Baker A., 2012 – *Speleothem science: from process to past environments*. Wiley-Blackwell, Chichester, 450 p. https://doi.org/10.1002/9781444361094

Friedman I. & O'Neil J.R., 1977 – *Data of geochemistry: Compilation of stable isotope fractionation factors of geochemical interest*. United States Geological Survey, Washington, USA, 170 p.

Fohlmeister J., Scholz D., Kromer B. & Mangini A., 2011 – *Modelling carbon isotopes of carbonates in cave drip water*. Geochimica Cosmochimica Acta, **75**: 5219-5228. https://doi.org/10.1016/j.gca.2011.06.023

Ford D. & Williams P., 2007 – *Karst hydrogeology and geomorphology*. John Wiley & Sons, Chichester, 562 p. https://doi.org/10.1002/9781118684986

Frisia S. & Borsato A., 2010 – *Karst*. In: Alonso-Zarza A.M. & Tanner L.H. (Eds.), *Developments in sedimentology, carbonates in continental settings*. Elsevier, Amsterdam, p. 269-318. https://doi.org/10.1016/S0070-4571(09)06106-8

Gat J., 1980 – *The isotopes of hydrogen and oxygen in precipitation*. In: Fritz P. & Fontes J.Ch. (Eds.), *Handbook of environmental isotope geochemistry*, **1**: 22-48.

Gat J.R., Klein B., Kushnir Y., Roether W., Wernli H., Yam R. & Shemesh A., 2003 – *Isotope composition of air moisture over the Mediterranean Sea: an index of the air–sea interaction pattern*. Tellus, Series B-Chemical & Physical Meteorology, **55 (5)**: 953-965. https://doi.org/10.1034/j.1600-0889.2003.00081.x

Gat J.R., Ben-Mair R., Yama R., Yakir D. & Wernli H., 2005 – *The Isotope Composition of Atmospheric Waters in Israel's Coastal Plain*. In: *Isotopic composition of precipitation in the Mediterranean Basin in relation to air circulation patterns and climate*. IAEA-TECDOC, **1453**: 99-114.

Genty D., Blamart D., Ghaleb B., Plagnes V., Causse C.h., Bakalowicz M., Zouari K., Chkir N., Hellstrom J., Wainer K. & Bourges F., 2006 – *Timing and dynamics of the last deglaciation from European and North African $\delta^{13}C$ stalagmite profiles– comparison with Chinese and South Hemisphere stalagmites*. Quaternary Science Reviews, **25**: 2118-2142. https://doi.org/10.1016/j.quascirev.2006.01.030

Genty D., Labuhn I., Hoffmann G., Danis P.A., Mestre O., Bourges F., Wainer K., Massault M., Van Exter S., Régnier E., Orengo Ph., Falourd S. & Minster B., 2014 – *Rainfall and cave water isotopic relationships in two South-France sites*. Geochimica Cosmochimica Acta **131**: 323-343. https://doi.org/10.1016/j.gca.2014.01.043

Hellstrom J., McCulloch M. & Ston J., 1998 – *A detailed 31.000-year record of climate and vegetation change, from the isotope geochemistry of two New Zealand speleothems*. Quaternary Research, **50**: 167-178. https://doi.org/10.1006/qres.1998.1991

Hendy C.H., 1971 – *The isotopic geochemistry of speleothems-I: The calculations of the effects of different modes of formation on the isotopic composition*

of speleothems and their applicability as paleoclimate indicators. Geochimica Cosmochimica Acta, **35**: 801-824. https://doi.org/10.1016/0016-7037(71)90127-X

Hendy C.H., Wilson A.T., Popplewell K.B. & House D.A., 1977 – *Dating of geochemical events in Lake Bonney, Antarctica, and their relation to glacial and climate changes*. New Zealand Journal of Geology & Geophysics, **20 (6)**: 1103-1122. https://doi.org/10.1080/00288306.1977.10420698

Hakim B., 1985 – *Recherche hydrologiques et hydrochimiques sur quelques karsts méditerranéens: Liban, Syrie, Maroc*. PhD thesis, Lebanese University Beirut, Lebanon, 700 p.

Hakim B. & Karakabi S., 1988 – *Coloration du gouffre de Faouar Dara et de la grotte de Kassarat*. Al-Ouate-Ouate Spéléo-Club du Liban, **3**: 18-33.

International Atomic Energy Agency/World Meteorological Organization (2008) Global network of isotopes in precipitation. The GNIP Database. https://nucleus.iaea.org/Pages/GNIPR.aspx (Accessed date: May 2016)

Jabbour-Gedeon B. & Zaatar J., 2013 – *Mgharet Mabaage: nouvelles découvertes et aménagement touristique "surprenant"*. Spéléorient, Association libanaise d'Etudes spéléologiques, **6**: 61-67.

Johnston V.E., Borsato A., Spötl C., Frisia S. & Miorandi R., 2013 – *Stable isotopes in caves over altitudinal gradients: fractionation behaviour and inferences for speleothem sensitivity to climate change*. Climate of the Past, **9**: 99-118. https://doi.org/10.5194/cp-9-99-2013

Karam F., 2002 – *Climate change and variability in Lebanon: impact on land use and sustainable agriculture development*. Proceedings of the 1st technical workshop of the "Mediterranean" component of CLIMAGRI project on climate change and agriculture, FAO, Rome, 25-27.

Karkabi S., 1990 – *Cinquantenaire de la spéléologie libanaise*. Al-Ouate-Ouate, special edition, 138 p.

Kattan Z., 1997 – *Environmental isotope study of the major karst springs in Damascus limestone aquifer systems: case of the Figeh and Barada springs*. Journal of Hydrology, **193 (1-4)**: 161-182. https://doi.org/10.1016/S0022-1694(96)03137-X

Koeniger P. & Margane A., 2014 – *Stable isotope investigations in the Jeita Spring catchment*. BGR, Special report on protection of Jeita Spring, **12**, 48 p.

Koeniger P., Margane A., Abi-Rizk J. & Himmelsbach T., 2017 – *Stable isotope based mean catchment altitudes of springs in the Lebanon Mountains*. Hydrological Processes, **21**: 3708-3718. https://doi.org/10.1002/hyp.11291

Luetscher M. & Jeannin P.-Y., 2004 – *Temperature distribution in karst systems: the role of air and water fluxes*. Terra Nova, **16**: 344-350. https://doi.org/10.1111/j.1365-3121.2004.00572.x

Lachniet M.S., 2009 – *Climatic and environmental controls on speleothem oxygen isotope values*. Quaternary Science Reviews, **28**: 412-432. https://doi.org/10.1016/j.quascirev.2008.10.021

Mattey D., Fairchild I., J. Atkinson T.C., Latin J.-P., Ainsworth M. & Durell R., 2010 – *Seasonal microclimate control of calcite fabrics, stable isotopes and trace elements in modern speleothem from St Michaels Cave, Gibraltar*. In: Pedley H.M. & Rogerson M. (Eds.), *Tufas and speleothems: Unravelling the microbial and physical controls*. Geological Society, London, Special Publications, **336**: 323-344. https://doi.org/10.1144/SP336.17

McDonald J. & Drysdale R., 2007 – *Hydrology of cave drip waters at varying bedrock depths from a karst system in southeastern Australia*. Hydrological Processes, **21**: 1737-1748. https://doi.org/10.1002/hyp.6356

Mickler P.J., Banner J.L., Stern L., Asmerom Y., Edwards R.L. & Ito E., 2004 – *Stable isotope variations in modern tropical speleothems: Evaluating equilibrium vs. kinetic isotope effects*. Geochimica Cosmochimica Acta, **68**: 4381-4393. https://doi.org/10.1016/j.gca.2004.02.012

Miorandi R., Borsato A., Frisia S., Fairchild I.J. & Richter D.K., 2010 – *Epikarst hydrology and implications for stalagmite capture of climate changes at Grotta di Ernesto (NE Italy): results from long-term monitoring*. Hydrological Processes, **24**: 3101-3114. https://doi.org/10.1002/hyp.7744

Mhawej M., Faour G., Fayad A. & Shaban A., 2014 – *Towards an enhanced method to map snow cover areas and derive snow-water equivalent in Lebanon*. Journal of Hydrology, **513**: 274-282. https://doi.org/10.1016/j.jhydrol.2014.03.058

Muhlinghaus C., Scholz D. & Mangini A., 2009 – Modelling fractionation of stable isotopes in stalagmites. Geochimica Cosmochimica Acta, **73**: 7275-7289. https://doi.org/10.1016/j.gca.2009.09.010

Nehme C., Jabbour-Gedeon B., Gerard P.-C., Sadier B. & Delannoy J.J., 2009 – *Reconstitution sepéléogénique de la grotte de Kanaan (Antelias, Liban): contribution à la morphogenèse du Nahr Antélias*. Karstologia, **54**: 21-30.

Nehme C., Verheyden S., Noble S.R., Farrant A.R., Sahy D., Hellstrom J., Delannoy J.J. & Claeys P., 2015 – *Reconstruction of MIS 5 climate in the central Levant using a stalagmite from Kanaan Cave, Lebanon*. Climate of the Past, **11**: 1785-1799. https://doi.org/10.5194/cp-11-1785-2015

Nehme C., Verheyden S., Breitenbach S.F., Gillikin D.P., Verheyden A., Cheng H., Edwards R.L., Hellstrom J., Noble S.R., Farrant A.R. & Sahy D., 2018 – *Climate dynamics during the penultimate glacial period recorded in a speleothem from Kanaan Cave, Lebanon (central Levant)*. Quaternary Research, **90 (1)**: 1-16. https://doi.org/10.1017/qua.2018.18

Peel M.C., Finlayson B. & McMahon Th., 2007 – *Updated world map of the Köppen-Geiger climate classification*. Hydrological and Earth Systems Sciences Discussions, **4 (2)**: 439-473. https://doi.org/10.5194/hessd-4-439-2007

Rozanski K., Araguas-Araguas L. & Gonfiantini R., 1993 – *Isotopic patterns in modern global precipitation*. Geophysical Monographical Series, **78**: 1-36. https://doi.org/10.1029/GM078p0001

Saad Z., V. Kazpard A.G. Samrani El. & Slim K., 2005 – *Chemical and isotopic composition of rainwater in coastal and highland regions in Lebanon*. Journal of Environmental Hydrology, **13**: 1-11.

Saad Z. & Kazpard V., 2007 – *Seasonal effect on the isotopic pattern of rainwater in Lebanon*. Journal of Environmental Hydrology, **15**: 1-15.

Sharp Z., 2007 – *Principles of stable isotope geochemistry*. Pearson Prentice Hall, New Jersey, 344 p.

Scholz D., Muhlinghaus C. & Mangini A., 2009 – *Modelling $\delta^{13}C$ and $\delta^{18}O$ in the solution layer on stalagmite surfaces*. Geochimica Cosmochimica Acta, **73**: 2592-2602. https://doi.org/10.1016/j.gca.2009.02.015

Spotl C., Fairchild I.J. & Tooth A.F., 2005 – *Cave air control on dripwater geochemistry, Obir Caves (Austria): Implications for speleothem deposition in dynamically ventilated caves*. Geochimica Cosmochimica Acta, **69**: 2451-2468. https://doi.org/10.1016/j.gca.2004.12.009

Suric M., Loncaric R., Loncar N., Buzjak N., Bajo P. & Drysdale R., 2017 – *Isotopic characterization of cave environments at varying altitudes on the eastern Adriatic coast (Croatia) – Implications for future speleothem-based studies*. Journal of Hydrology, **545**: 367-380. https://doi.org/10.1016/j.jhydrol.2016.12.051

Tawk J. & Kaasamani H., 2014 – *La grotte de Qadisha - première grotte touristique du Liban*. Al-Ouate-Ouate, Spéléo-club du Liban, **14**: 36-41.

Tremaine D.M., Froelich P.N. & Wang Y., 2011 – *Speleothem calcite farmed in situ: Modern calibration of $\delta^{18}O$ and $\delta^{13}C$ paleoclimate proxies in a continuously monitored natural cave system*. Geochimica Cosmochimica Acta, **75**: 4929-4950. https://doi.org/10.1016/j.gca.2011.06.005

Van Geldern R. & Barth-Johannes A.C., 2012 – *Optimization of instrument setup and post-run corrections for oxygen and hydrogen stable isotope measurements of water by isotope ratio infrared spectroscopy (IRIS)*. Limnology Oceanography Methods, **10**: 1024-1036. https://doi.org/10.4319/lom.2012.10.1024

Verheyden S., Genty D., Deflandre G., Quinif Y. and Keppens E., 2008a – *Monitoring climatological, hydrological and geochemical parameters in the Père Noël cave (Belgium): implication for the interpretation of speleothem isotopic and geochemical time-series*. International Journal of Speleology, **37 (3)**: 221-234. https://doi.org/10.5038/1827-806X.37.3.6

Verheyden S., Nader F.H., Cheng H.J., Edwards L.R. & Swennen R., 2008b – *Paleoclimate reconstruction in the Levant region from the geochemistry of a Holocene stalagmite from the Jeita cave, Lebanon*. Quaternary Research, **70**: 368-381. https://doi.org/10.1016/j.yqres.2008.05.004

Wackerbarth A., Langebroek P.M., Werner M., Lohmann G., Riechelmann S., Borsato A. & Mangini A., 2012 – *Simulated oxygen isotopes in cave drip water and speleothem calcite in European caves*. Climate of the Past, **8**: 1781-1799. https://doi.org/10.5194/cp-8-1781-2012

Wackerbarth A., Scholz D., Fohlmeister J. & Mangini A., 2010 – *Modelling the $\delta^{18}O$ value of cave drip water and speleothem calcite*. Earth and Planetary Science Letters, **299 (3-4)**: 387-397. https://doi.org/10.1016/j.epsl.2010.09.019

White B., 1988. Geomorphology and hydrology of *karst terrains*. Oxford University Press, New York, 464 p.

Ziv B., Dayan U., Kuschnir Y., Roth C., Enzel Y., 2006 – *Regional and global atmospheric patterns governing rainfall in the southern Levant*. International Journal of Climatology, **26**: 55-73. https://doi.org/10.1002/joc.1238

Ziv B., Saaroni H., Romem M., Heifetz E., Harnik N. & Baharad. A., 2010 – *Analysis of conveyor belts in winter Mediterranean cyclones*. Theoretical Applied Climatology, **99**: 441-455. https://doi.org/10.1007/s00704-009-0150-9

International Journal of Speleology	48 (1)	75-105	Tampa, FL (USA)	January 2019

Available online at scholarcommons.usf.edu/ijs

International Journal of Speleology

Official Journal of Union Internationale de Spéléologie

Guano-related phosphate-rich minerals in European caves

Philippe Audra[1*], Jo De Waele[2], Ilham Bentaleb[3], Alica Chroňáková[4], Václav Krištůfek[4], Ilenia M. D'Angeli[2], Cristina Carbone[5], Giuliana Madonia[6], Marco Vattano[6], Giovanna Scopelliti[6], Didier Cailhol[7], Nathalie Vanara[8], Marjan Temovski[9], Jean-Yves Bigot[10], Jean-Claude Nobécourt[11], Ermanno Galli[12], Fernando Rull[13], and Aurelio Sanz-Arranz[13]

[1]Polytech'Lab EA 7498, University of Nice Sophia-Antipolis, 930 route des Colles, 06903 Sophia-Antipolis, France
[2]Department of Biological, Geological and Environmental Sciences, University of Bologna, Via Zamboni 67, 40127 Bologna, Italy
[3]Institute des Sciences de l'Évolution Montpellier, University of Montpellier, Montpellier, Cédex 5, France
[4]Biology Centre CAS, Inst. Soil Biology, Na Sadkach 7, 370 05 Ceske Budejovice, Czech Republic
[5]DISTAV, Dipartimento di Scienze della Terra, dell'Ambiente e della Vita, Università di Genova, Corso Europa 26, Genova, Italy
[6]Dipartimento di Scienze della Terra e del Mare, University of Palermo, Via Archirafi 22, 90123 Palermo, Italy
[7]Laboratoire EDYTEM, University Savoie – Mont-Blanc, CNRS, Pôle Montagne, 73376 Le Bourget-du-Lac, France
[8]Laboratoire TRACES, UMR 5608 / Université Paris 1 – Panthéon-Sorbonne, France
[9]Isotope Climatology and Environmental Research Centre, Institute of Nuclear Research, Hungarian Academy of Sciences, Bem tér 18/C, 4026 Debrecen, Hungary
[10]Association Française de Karstologie (AFK), 21 rue des Hospices, 34090 Montpellier, France
[11]Crespe, 06140 Vence, France
[12]Università degli Studi di Modena e Reggio Emilia, Dipartimento di Scienze Chimiche e Geologiche, Campus Scientifico, via Giuseppe Campi, 103, 41125 Modena, Italy
[13]Unidad Asociada UVA-CSIC al Centro de Astrobiología, University of Valladolid, Parque Tecnológico Boecillo, 47151 Valladolid, Spain

Abstract: Guano is a typical deposit found in caves derived from the excretions of bats and in minor cases of birds. These organic deposits decompose and form a series of acid fluids and gases that can interact with the minerals, sediments, and rocks present in the cave. Over sixty phosphates are known and described from caves, but guano decay also often leads to the formation of nitrates and sulfates. In this study twenty-two European caves were investigated for their guano-related secondary minerals. Using various analytical techniques, seventeen phosphates, along with one sulfate (gypsum), were recognized as secondary products of guano decay. Among those minerals, some are very rare and result from the interaction of guano leachates with clays, fluvial deposits, or pyrite. Some of these minerals are even found only in the studied caves (spheniscidite, robertsite). The most common minerals belong to the apatite group. The common mineral association present in fresh decaying guano is brushite-ardealite-gypsum, minerals that usually are not present in older deposits because of their higher solubility. Most minerals are in hydrated form because of the wet cave environment; however, some specific dry conditions may favor the presence of dehydrated minerals, such as berlinite, formed during guano combustion. Investigation on the acidity of guano piles shows pH values as low as 3.5 with an increase of acidity with age and depth. Finally, cave guano deposits should be better studied in the future because of their role in paleoenvironmental and paleoclimatic reconstructions and because it is important to better understand the origin of guano-related minerals, especially the phosphates and sulfates. Among all of the caves studied, Corona 'e sa Craba (Italy) and Domica-Baradla Cave (Slovakia-Hungary) are considered to be outstanding sites with respect to their phosphate mineralogy.

Keywords: secondary cave minerals, phosphates, minerogenesis, limestone caves, bat guano

Received 1 February 2019; Revised 7 March 2019; Accepted 7 March 2019

Citation: Audra P., De Waele J., Bentaleb I., Chroňáková A., Krištůfek V., D'Angeli I.M., Carbone C., Madonia G., Vattano M., Scopelliti G., Cailhol D., Vanara N., Temovski M., Bigot J.-Y., Nobécourt J.-C., Galli E., Rull F. and Sanz-Arranz A., 2019. Guano-related phosphate-rich minerals in European caves. International Journal of Speleology, 48 (1), 75-105. Tampa, FL (USA) ISSN 0392-6672 https://doi.org/10.5038/1827-806X.48.1.2252

INTRODUCTION

Phosphate minerals are commonly found in caves containing guano accumulations from bat colonies (e.g., Martini, 1996; Hill, 1999; Onac & Vereş, 2003) or in caves which contain a large quantity of bone deposits (Goldberg & Nathan, 1975; Karkanas et al., 2002). The phosphates result from the interaction between guano-derived leachates with cave bedrock, generally limestone, (calcite) speleothems or cave sediments

*audra@unice.fr

(detrital clay deposits). A review of cave phosphate minerals was first published by Hill & Forti (1997), reporting a total of fifty-two mineral species. The minerogenetic mechanisms forming cave phosphates are microbial decay, dissolution, double replacement, and redox reactions (Onac & Forti, 2011b). Around 60 cave phosphate minerals are currently known (Onac & Forti, 2011a), with five of common occurrence: hydroxylapatite, brushite, ardealite (Schadler, 1932; Pogson et al., 2011), taranakite (Hill & Forti, 1997), and variscite (Onac et al., 2004). They usually display as crusts, nodules, lenses, and earthy or powdery masses (Onac, 2012). Some cave phosphate minerals are very rare, such as tinsleyite (Marincea et al., 2002), foggite and churchite-(Y) (Onac et al., 2005a), hydroxylellestadite (Onac et al., 2006a), and berlinite (Onac & White, 2003; Marincea & Dumitraş, 2005; Onac & Effenberger, 2007; Sauro et al., 2014). Others have been found only in a limited number of caves around the world, such as vashegyite (Forti et al., 2000), stercorite (Frost & Palmer, 2011), newberyite (Bridge, 1977; Frost et al., 2011), and crandallite (Kaye, 1959; Frost et al., 2012).

Through microbial activity the breakdown of guano produces strong acids (sulfuric, phosphoric), whereas degradation of bat urea yields nitric and other weak organic acids. All processes contribute to increase acidity toward the base of the guano accumulation, with pH as low as 2-4 (Martini, 1993; Hill & Forti, 1997; Martini, 2000; Forti, 2001). Nitrogen and sulfur can also be active above the guano accumulation on the ceiling and walls, through their gaseous phases (NH_3 and H_2S, respectively). These gases rise through warm air convections produced by exothermic guano breakdown or by bat colonies, then oxidize, often through microbial mediation, into nitric and sulfuric acids, respectively, and together with CO_2 eventually strongly corrode the limestone host rock and calcite speleothems (Hill & Forti, 1997; Martini, 2000; Audra et al., 2016; Onac, 2019). Contrary to sulfur and nitrogen, phosphorus does not have a gaseous phase at ambient temperature.

With time and increase of guano accumulation depth, organic matter decays, and the organic compounds gradually transform into secondary mineral deposits. The oxidation of organic phosphorous into PO_4^{3-} ion seems to be at least partly driven by microorganisms (Forti, 2001; Chang et al., 2010). Very soluble nitrogen is washed away, as ammonium phosphate $(NH_4)_2HPO_4$ transforms into calcium phosphate $(CaHPO_4)_2$ allowing the ammonium ion (NH_4^+) to be carried away, according to the following reaction (Frost & Palmer, 2011):

$$(NH_4)_2HPO_4 + Ca^{2+} + 2H_2O \rightarrow CaHPO_4{\cdot}2H_2O + 2NH_4^+$$

After nitrogen, easily soluble sulfur, in the form of H_2SO_4, produced by sulfo-oxidant bacteria (Yoshimura et al., 1989) is consumed thereby producing gypsum, whereas phosphate (PO_4^{3-}) and cations (Fe^{2+}, Fe^{3+}, Al^{3+}, K^+) gradually increase by relative enrichment, making the P/S and P/N ratios increase with depth (and age) of the guano pile (Hill & Forti, 1997; Shahack-Gross et al., 2004; Onac, 2012). Within the guano accumulation, sulfuric acid reacts with the bedrock and with speleothems and produces sulfates, mainly gypsum (Hill & Forti, 1997), whereas the reaction with phosphoric acid produces phosphates (Onac & Vereş, 2003). Both gypsum and phosphates are the only stable compounds in such acidic environment (Pogson et al., 2011). At the base of guano accumulations, after leaching of alkali ions (Onac, 2012), the interaction with limestone bedrock (or calcite speleothems) reduces acidity to a pH close to 6-7 and produces Ca-rich stable phosphates such as hydroxylapatite and brushite (Hill & Forti, 1997). Fluorine (F^-) can easily replace the hydroxyl ion (OH^-) generating almost pure fluorapatite (Onac, 2012). The contact with clay materials allows cation exchange (such as Fe^{2+}, Fe^{3+}, Al^{3+}, and K^+) with production of other phosphate minerals, mainly taranakite and variscite, or less frequent mineral species (see Hill & Forti, 1997). Deeper in the sediment, still acidic conditions allow the vertical leaching of Mn compounds that form a black accumulation horizon marking the boundary of the phosphatization front with the unaltered sediment (Martini, 1993).

Environmental conditions play a key-role in the formation or inhibition of phosphate minerals (Onac & Vereş, 2003; Shahack-Gross et al., 2003; Puşcaş et al., 2014). From a Romanian cave study, Onac & Vereş (2003) stated that pH, humidity, alkali content, and Ca/P ratio are the major parameters controlling the mineral assemblages. Variscite, taranakite, and brushite are stable under acidic conditions, whereas hydroxylapatite indicates less acidic conditions. In low-humidity conditions (and higher temperature), dehydration occurs, causing new minerals to form (i.e., berlinite). In arid regions with extremely dry conditions, very soluble species may precipitate around guano accumulation through evaporation, producing sylvite and nitrate minerals such as saltpeter (Martini, 1993). On the contrary, in damp places, the complete breakdown of guano at very low pH (2-4) leads to pure gypsum displayed as candy-floss (Martini, 1993). Therefore, phosphate minerals, combined with stable isotope analyses on guano, can be considered as good proxies of past environmental conditions, at both regional and local scales (Onac et al., 2014).

Gypsum often occurs together with secondary phosphate minerals and can be considered in most cases a by-product of guano decay. This mineral probably always forms because of the interaction of sulfuric acid with the carbonate host rock (often limestone) or with the Ca-rich dripping water, but in humid conditions it is generally dissolved away by seeping waters. Gypsum, and more generally sulfates, are thus mainly found in drier cave conditions in which they can persist (do not go into solution) and where evaporation processes dominate.

This paper reports the mineralogical findings of guano-related minerals (phosphates and sulfates) in a variety of European caves, from Hungary, Slovak Republic, France, Macedonia, and Italy, along with the processes and environmental conditions that control their occurrences.

METHODS

Sampling. Samples were taken in separate containers or plastic bags, scraping or scratching from the walls or rocks with a chisel, or collecting enough material with a clean spatula. In some cases, physical environmental parameters, temperature (T), relative humidity (RH) and CO_2 concentration were measured using a pSENSE RH from SENSEAIR AB, with a precision of ±0.6°C, ±3-5% RH, ±30 ppm CO_2.

pH. The pH of guano deposits was determined using a pH meter in a 1:5 proportional guano: distilled water suspension.

X-ray diffraction. Samples were analyzed on different diffractometers: a Philips PW 1050/25 (40 kV and 20 mA, CuKα radiation, Ni filter) at the University of Modena and Reggio Emilia, Italy; a Philips (40 kV and 20 mA, CoKα radiation, Graphite filter) at the CEREGE – CNRS, Aix-Marseille University, France; a Philips PW3710 (40 kV and 20 mA, CoKα radiation, Fe filter) interfaced with Philips High Score software package for data acquisition and processing at the DISTAV (Genoa University); a Bruker Analytical X-Ray System, D8 Endeavor (50 kV and 40 mA, CuKα radiation, Ni filter) at the University of South Florida; and a Panalytical Xpert Pro (60 kV and 200 mA, Cu Kα radiation) at CINaM – CNRS and Aix-Marseille University. All samples were scanned from 5° to 75° 2θ with a step increment of 0.02°, a scan speed of 0.5 s/step. Mineral identification and abundance were evaluated semi-quantitatively by determining peak intensities (peak height) of the X-ray diffraction results with the DIFFRAC^{Plus} EVA V.8.0 software and compared to the ICDD-PDF2 database for phase identification.

^{14}C radiometric dating. Sixteen bat guano samples and a piece of wood found at the base of the Raganeous guano heap were radiocarbon dated by means of accelerator mass spectrometry (AMS) in the Poznań Laboratory (Poland). Additionally, thirteen other bat guano samples were dated by the ARTEMIS Radiocarbon Laboratory Facility (LMC14, Saclay France) and one sample was dated at the Centre de Datation de Radiocarbone (CDRC) in Lyon (France). Radiocarbon calibrated ages were obtained using the online program CALIB 7.10 (Stuiver and Reimer, 1993) with the IntCal13 atmospheric calibration curve (Reimer et al., 2013). All radiocarbon ages (2σ), including those from previous studies, are reported in calibrated years as cal yr. AD and BC. In addition, we used 6 results from previous studies (Krištůfek et al., 2008).

Micro-Raman spectroscopy. Since XRD spectra are sometimes less relevant for certain phosphate minerals, further information was obtained from micro-Raman spectroscopy. These analyses were carried out at the Unidad Asociada UVA-CSIC at the Centro de Astrobiología, University of Valladolid (Valladolid, Spain). Up to 11 Raman spectra were taken from different areas of each sample. The excitation source was a Laser Research Electro-Optics (REO) working at 632.8 nm. The KOSI HoloSpec f/1.8i spectrometer from Kaiser Optical covered a spectral range of 150–3,800 cm^{-1} and a spectral resolution of 5 cm^{-1}, while the CCD (charge coupled device) employed was a DV420A-OE-130 model from Andor. The Raman head used was KOSI MKII, HFPH-FC-S-632.8 model from Kaiser Optical Systems coupled by optical fiber to a Nikon Eclipse E600 microscope, which in turn, was attached to a JVC TK-C1381EG video camera for visual analysis and precise control of the measured spots. An objective of 50× allowed microanalyses of 15 µm diameter spots. The laser power on the sample was maintained around 15 mW (corresponding irradiance of 76 kW/cm^2) to ensure no thermal damage occurred to the samples. Typical integration time for spectral acquisition was 10 s and 10 accumulations were done. The sample was manually scanned, whereas the height of focus adjusted in order to optimize the intensity of the spectra signals.

In Isturitz Cave, an in-situ mineral characterization was carried out by the Departamento de Química Analítica, Universidad del País Vasco, using a portable Raman spectrometer innoRam (B & WTEKINC., Newark, USA), equipped with a 785 nm excitation laser (with 225 mW of nominal power), with a measurement area of about 100 µm. The Raman signals are collected by a refrigerated CCD detector using the Peltier effect. The spectrometer allows analyzing a fixed spectral range between 100 and 3,500 cm^{-1}, with an average spectral resolution of 3 cm^{-1}. Twenty measures by point were taken for representativity of the analysis. Spectra were produced using BWSpecTM v.4.02_15 (B & WTEKINC., Newark, USA) and data processed using Omnic 7.2 (Nicolet).

Scanning electron microscopy (SEM). Scanning electron microprobe analyses were performed with a SEM VEGA3 TESCAN (DISTAV, Genoa University) operated at 20 kV and equipped with the EDAX-APOLLO_X DPP3 energy-dispersive (EDS) X-ray spectrometer having an ultrathin polymer window and with resolutions for Manganese Kα = 126 eV and typically ranging detection for chemical elements of atomic number greater than 5 (Boron). Data acquisition and elaboration were performed with the TEAM Enhanced Version: V4.2.2 EDS software. Qualitative chemical analyses were also carried out on a Philips XL40 environmental scanning electron microscope (ESEM) equipped with an energy dispersive spectrometer (EDS-EDAX 9900) at the C.I.G.S. (Centro Interdipartimentale Grandi Strumenti) of the Modena and Reggio Emilia University.

Subsequently, elemental characterization by Energy Dispersive X-ray Fluorescence (EDXRF) was carried out using XMET5100 (Oxford Instruments), equipped with a Rhodium X-ray tube having a maximum voltage of 45 kV and a high-resolution silicon detector (SDD) with a spectral resolution of 20 eV and an energy resolution of 150 eV (measured with the K-alpha transition of manganese at -20°C). Each point was measured at least three times. Some samples of the Grotta dei Personaggi and Salnitro cave (Sicily) were analyzed with a SEM LEO 440 equipped with a EDS Oxford ISIS system with a Si (Li) PENTAFET detector (DiSTeM, Palermo University).

CAVES AND SAMPLING SITES DESCRIPTION

We studied 22 caves systems in Europe where guano deposits and bat colonies are or were present: one on the border between the Slovak Republic and Hungary, seven in France, three in Macedonia, and the remaining eleven in Italy (eight of which on the island of Sicily).

Domica-Baradla (Kečovo, Slovakia and Aggetlek, Jósvafő, Hungary)

The Domica-Baradla cave system contains 21 km of passages developing across the Slovakian and Hungarian border (Fig. 1). It has been included in the UNESCO World Heritage List since 1995. Domica Cave has its main entrance at 339 m asl, whereas the mountains range from 180 to 947 m asl (Gallay et al., 2015). The cave is formed in the Middle Triassic (Ladinian) lagoon limestones of Wetterstein type (Gaál & Vlček, 2011). The main cave displays large passages of up to 25 m diameter. It is fed by multiple sinking rivers that bring sediments (mainly clay) from outside. Cosmogenic (Al-Be) nuclide dating (3.47 ± 0.78 Ma) of the oldest gravels in the upper level shows that the cave originated in or before middle Pliocene (Bella et al., 2019). Relative humidity ranges from 95 to 98%, and temperature from 10.2 to 11.4°C, placing the cave among the warmest in Slovakia according to its latitude and altitude (Bella & Lalkovič, 2001). The partial pressure of CO_2 of the cave air is 1700-1800 ppm (July 2015). Vegetation above the cave comprises shrub and deciduous forest. The cave is equipped for tourist visits with 1.6 km of foot trails and it attracts 30,000 visitors per year.

Past records of bat species mention the presence of *Rhinolophus hipposideros, R. euryale, Plecotus auritus, Myotis myotis, M. emarginatus, M. natterei,* and *Eptesicus discolor* (Kettner, 1948). Currently, a colony of up to 1,500-2,500 individuals of Mediterranean horseshoe bats (*R. euryale*) use Domica Cave during their pre-hibernation stage (Kováč et al., 2014). Due to the large extension and dimension of passages, bats are settling up to more than 1 km away from the closest entrance. Many guano deposits are present as small accumulations from individual bats, or as large guano heaps. Some cone-shaped heaps are actively accumulating such as in *Prales* Chamber or in *Palmový háj*, which basal radiocarbon date is at about AD 990 (Krištůfek et al., 2008). Other guano accumulations are not active anymore such as in *Libanon-hegy* in Baradla Cave. Previous phosphate studies mention the occurrence of gypsum, brushite, and "apatite" (Kettner, 1948). The soluble brushite, associated to rims of calcite, deposited as wall crusts from leachates through above-lying guano deposits only when dry conditions were present. Gypsum, associated with brushite was identified at the base of guano piles, in guano pots (small depressions on the cave floor created by guano and its acids), and at the top of large stalagmites that collected bat droppings. In *Palmový háj*, Kereskényi (2014) identified brushite and traces of ardealite at the guano surface, and taranakite, gypsum, and hydroxylapatite at depth. In Baradla Cave, the same author identified hydroxylapatite and taranakite.

The following three sites were sampled: in *Prales* Chamber (Fig. 1A), close to the show cave entrance of Domica, guano corrosion pots on top of some stalagmites originating from guano drops of individual bats were found to contain some secondary mineral deposits (Fig. 2A). Below the fresh guano, we sampled a whitish-yellowish paste (Sample Pr. B) covering weathered limestone (Pr. A). In *Teknösbéka* (Turtle Gallery; Fig. 1B), close to the show cave entrance of Baradla, ceiling cupolas are covered with patches of dark brown crusts (BA 3 in Fig. 2B). *Libanon-Hegy* is a chamber located at about 1.5 km from Baradla Cave entrance (Fig. 1C), where we found some recent guano deposits. The BA 4 guano accumulation is old and no longer active; it displays a dark brown compact and sticky material, about 50 cm thick (Fig. 2C). Here we sampled a white pasty wet layer (BA 4a), another white layer located above clay (BA 4b), a sticky black layer at the contact of the limestone base (BA 4c), and a wet pasty pure white deposit also at the contact with the limestone base (BA 4d) at 5 cm above the base of the guano deposit.

Julio Cave (Saint-Étienne-d'Albagnan, Hérault, France)

Julio Cave is located in the *Montagne Noire*, a southern segment of the French *Massif Central*. The cave opens along the *Jaur* Valley, at 205 m asl. It is a several hundred meters long maze, developed along a steep dip (about 60°) of the Lower Devonian limestone (Fig. 3). The lower levels contain large cobbles introduced by the *Jaur* River. Decantation silts and fine sands are present up to the top of the cave, 73 m above the entrance. They contain abundant allogenic minerals (quartz, mica, feldspars) from past flooding events. The cave was mined for guano in the early 20th century. A recent study regarding important bat colonies mentions *Miniopterus schreibersii* (3,000 individuals), *Rhinolophus euryale* (800 individuals), *Myotis capaccinii*, and *R. ferrumequinum* (Nemoz, 2008). The cave is included in a Natura 2000 protected area. In its upper part, old and fresh guano cover the silty-sandy sediments that are entirely weathered to a grey or white toothpaste-like material. We sampled the lower grey layer (Vezelle 3) and the upper white one (Vezelle 2).

Isturitz-Oxocelhaya Caves (Isturitz and Saint-Martin-d'Arberoue, Pyrénées-Atlantiques, France)

The Isturitz-Oxocelhaya caves are located on the NW piedmont of the Pyrenees Range. The *Gatzelu* Hill (209 m asl) is built of Lower Cretaceous (Aptian) limestones surrounded by marls and appearing as a rocky spur blocking the *Arberoue* Valley. The homonymous river crossed the *Gatzelu* Hill forming through-caves and leaving fluvial sediments within them. Four tiers are arranged over an altitudinal range of 75 m, the lowest one still active (Fig. 4). The caves were once intensively used as shelters by animals, mainly bears and bats, and by humans since the Middle Paleolithic,

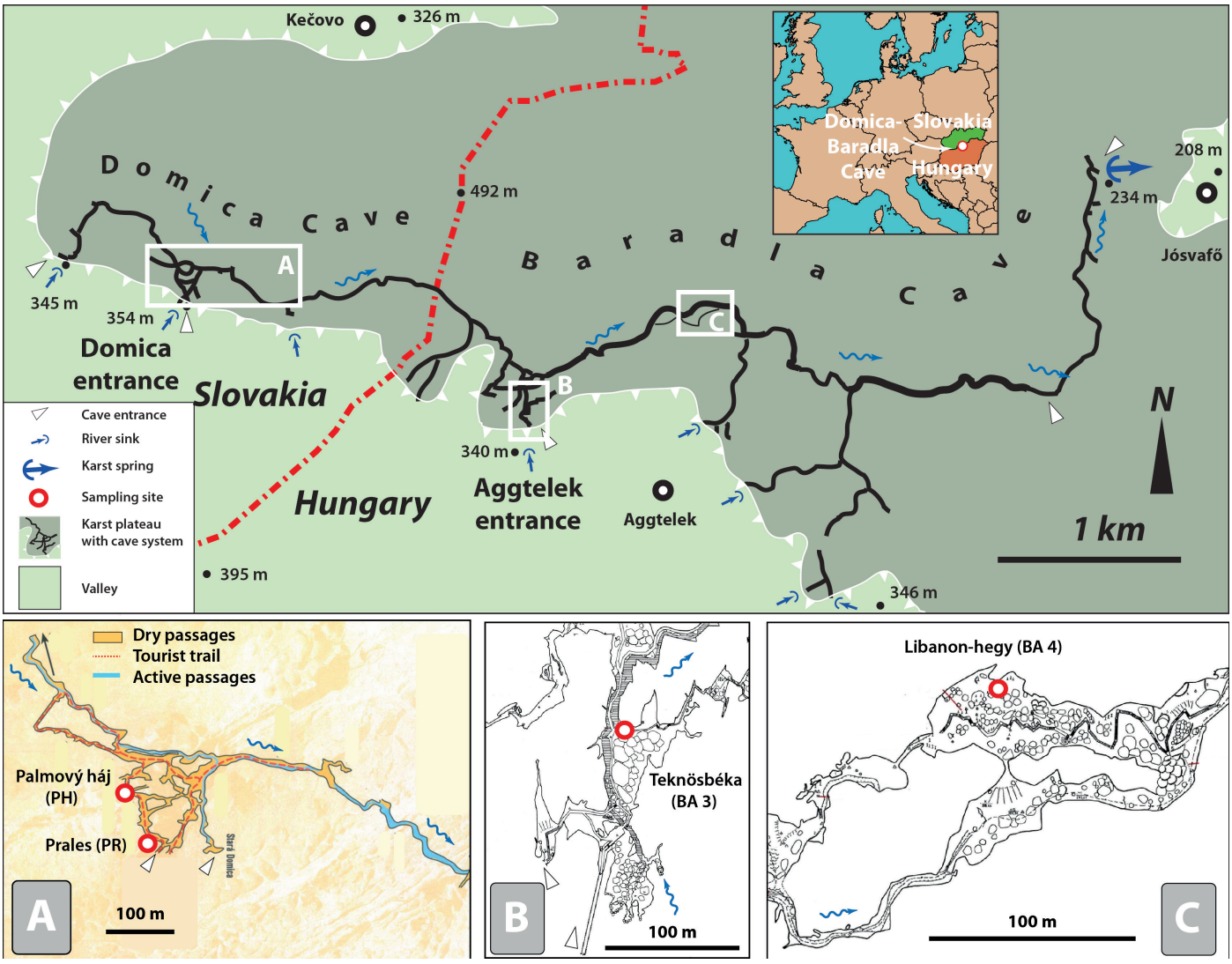

Fig. 1. Plan view of Domica-Baradla cave system in Slovakia and Hungary, with location (A-C) of studied places (redrawn after Ország et al., 1989). Detailed survey of Domica Cave after Slovak Cave Association (http://www.ssj.sk/en/jaskyna/7-domica-cave) and of Baradla Cave after Ország et al. (1989).

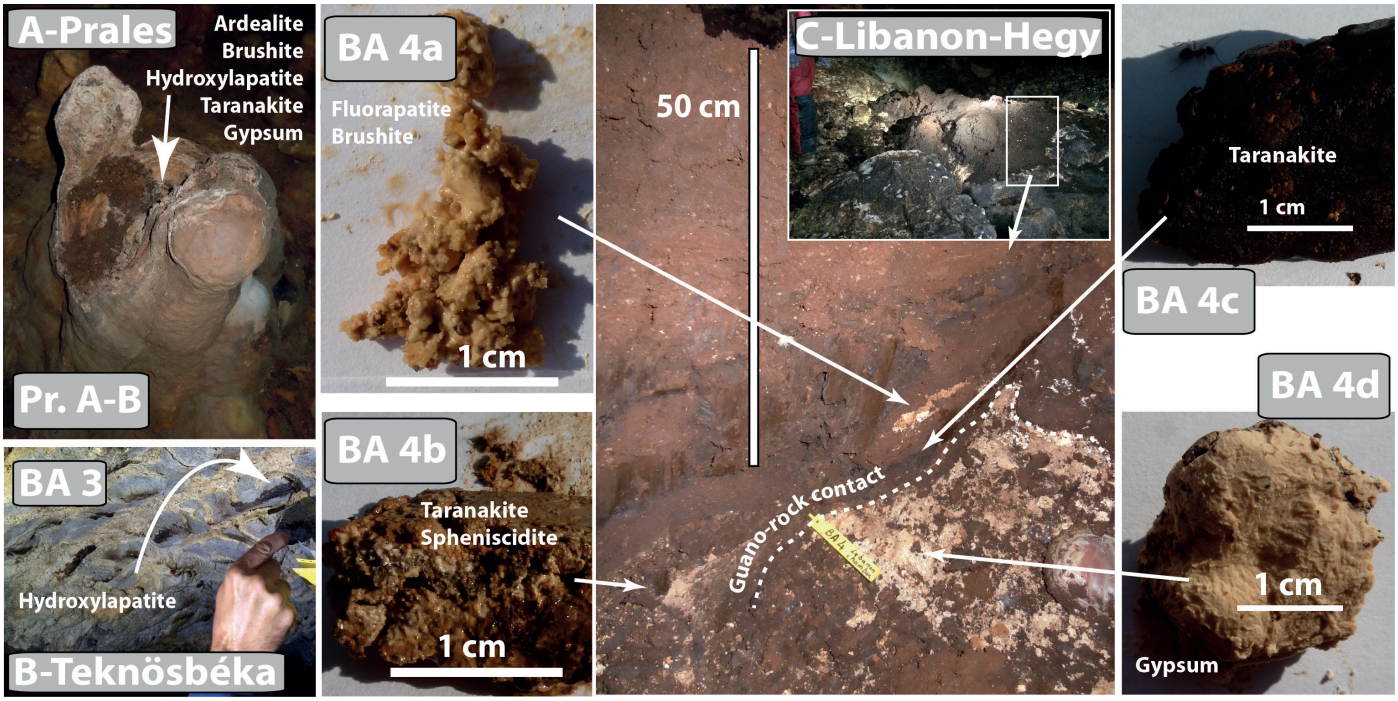

Fig. 2. Samples in Domica-Baradla Cave. A) *Prales* Chamber in Domica Cave. Guano-corroded stalagmite showing calcite layers in the guano pot that perforates its upper part. Below the guano, a whitish-yellowish paste (Pr. B) covering weathered limestone (Pr. A) was sampled (photo by V. Krištůfek); B) *Teknösbéka* (Turtle Gallery) in Baradla Cave. Dark brown apatite crusts (BA 3) on the ceiling of a cupola (Photo by A. Chroňáková); C) The guano accumulation in *Libanon-Hegy*, Baradla Cave (Photo by V. Krištůfek) with the location and mineralogy of BA 4 samples (Photos by P. Audra).

as shown by major art testimonies such as paintings and engravings (Garate et al., 2013). Also, guano and phosphates were intensively mined during the second half of the 19th century. After being classified as a Historical Monument in 1953 and opened as a show cave, all its entrances were closed. Consequently, bat colonies (mainly *Myotis myotis*) disappeared. Currently, only a couple of bats are still present (*Rhinolophus hipposideros*, *R. ferrumequinum*).

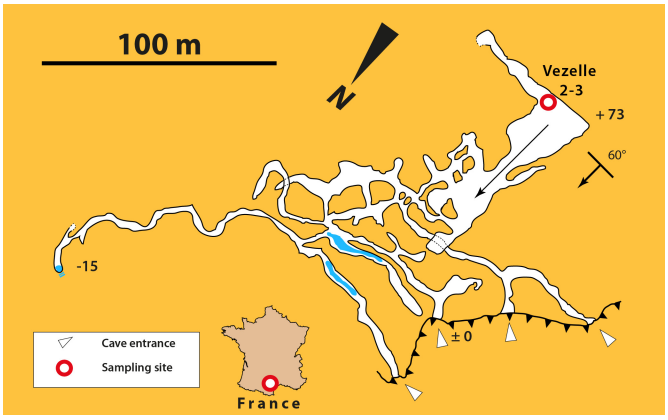

Fig. 3. Plan view of the Julio Cave with sampling-site locations (Survey after J. Fauré, SC Béziers, 1981, redrawn).

Four sites were investigated in-situ using portable Raman spectrometer and XRF (Figs. 4-5). An artificial tunnel allows the connection of the Isturitz upper level with the Oxocelhaya middle level. Before the tunnel enters the host rock it cuts and displays the entire sediment filling of Isturitz Cave along the staircase ("Staircase" sample, Fig. 5A). The lower part of the sediment filling resting on the rocky floor consists of fine colored sands (yellow, orange) separated by a dark layer. The floor of the *Rhinolophes* Chamber, located in Isturitz Cave, is covered by boulders. Boulders are partly covered by white crusts ("*Rhinolophes*" sample, Fig. 5B). Below these crusts, the limestone rock is weathered and has a powdery appearance. The "Great Pilar" is a huge calcite column, deeply corroded by condensation niches linked to aerial corrosion above guano (Audra et al., 2016). We analyzed dark crusts and corroded white surfaces ("Great Pilar" sample, Fig. 5C). At the *Lithophone* site, a guano corrosion pot (depression formed by acid guano corrosion) is covered by fresh guano and white deposits ("*Lithophone*" sample, Fig. 5D).

Raganeous Cave (Saint-Benoît, Alpes-de-Haute-Provence, France)

Raganeous Cave opens in a cliff along the *Coulomp* Valley at 698 m asl in the Southern French Alps. Together with neighboring *Radar* and *Théoriciens* caves, they constitute a system of maximal altitude difference of 54 m and of more than 1 km of mainly large galleries (Fig. 6). The cave is developed in a 30-50 m-thick, steeply dipping (30-70°), fossiliferous (Nummulites sp.) limestone bed, resting on Cretaceous marls and partly covered by Upper Eocene (Priabonian) marls. The cave was an important underground drain, which developed as a phreatic lift in a *per ascensum* way, following the Pliocene aggradation in *Coulomp* Valley; the current entrances acted as springs (Mocochain et al., 2011). Underground flow carried fine sandy-clayey sediments into the cave, having originated from the weathering of Priabonian marls and Annot sandstones that were brought in through sinkholes. The caves were "discovered" by climbers in 2012. However, artifacts of Neolithic and Middle Age show that the cave was known and used for over millennia by local inhabitants. Currently, a colony of >1000 bats uses the cave for reproduction, roosting, transit, and hibernation. Seven species are present (*Rhinolophus ferrumequinum, R. hipposideros, R. euryale, Miniopterus schreibersii, Myotis blythii, M. myotis,* and *M. emarginatus)* (obs. M.-Cl. Lankester).

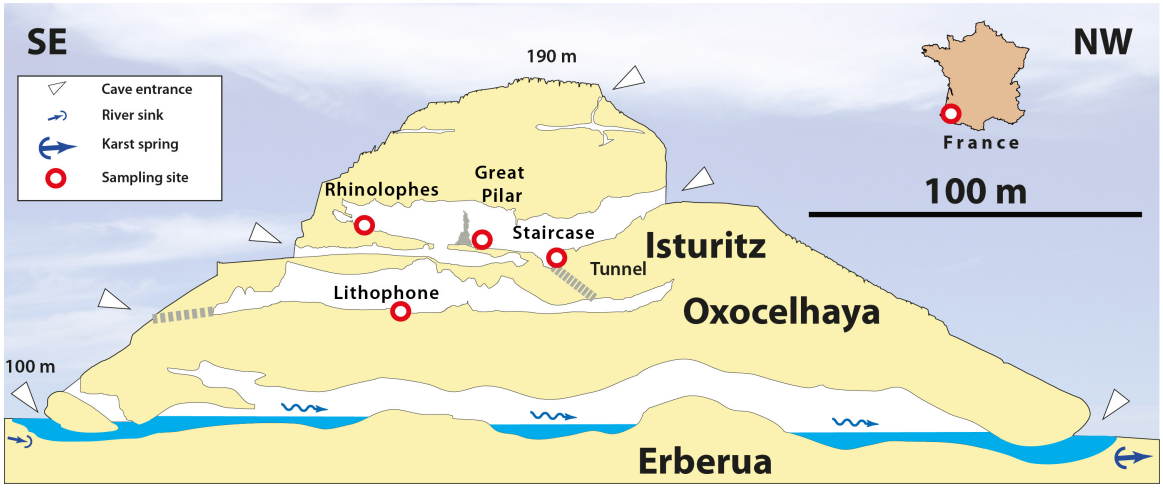

Fig. 4. Profile of Isturitz-Oxocelhaya caves with location of the sampling sites (survey after J.-D. Larribau & Y. Bramoullé). Horizontal passages correspond to successive-lowering river levels, which were utilized by prehistoric people and bats after each passage drained.

Guano deposits are important in different places. Some are still active and occur as soft accumulations of dry pellets, whereas other deposits are older and appear as dark sticky layers. Two sites were sampled (Fig. 6A). A 1.8 m-high cone is made of dry and poorly compacted material, which is composed of loose guano pellets showing alternating brown-white layers (Raga, Fig. 6B). White and brown layers have been sampled for mineralogy both on top and at the base of the guano cone. Additionally, 10 samples of guano were collected for radiocarbon dating, along with an old wooden torch found close to the bottom of the guano cone. The cave

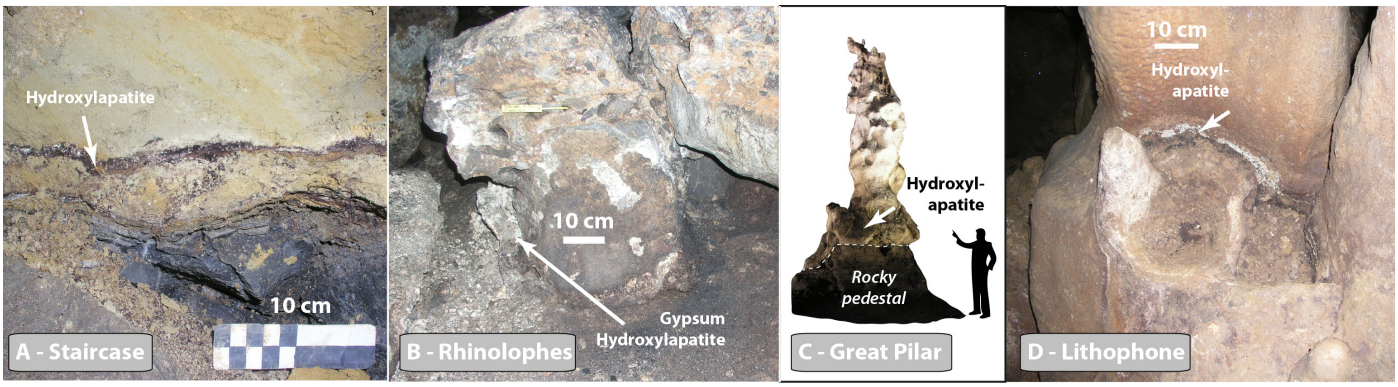

Fig. 5. Studied sites in the Isturitz-Oxocelhaya caves. A) Staircase profile corresponding to the base of the Isturitz Cave filling. Above the rocky floor, layers of yellow and orange stratified fine sands are separated by a dark layer; B) *Rhinolophes* Chamber. Blocks covered with dark crusts and thick detaching white crusts; C) The Great Pilar. Its surface is either bare, light-colored calcite or it is covered with dark deposits; D) *Lithophone* site. Guano corrosion pot showing an aureole of soft white material at the contact with the calcite (Photos by J.-Y. Bigot).

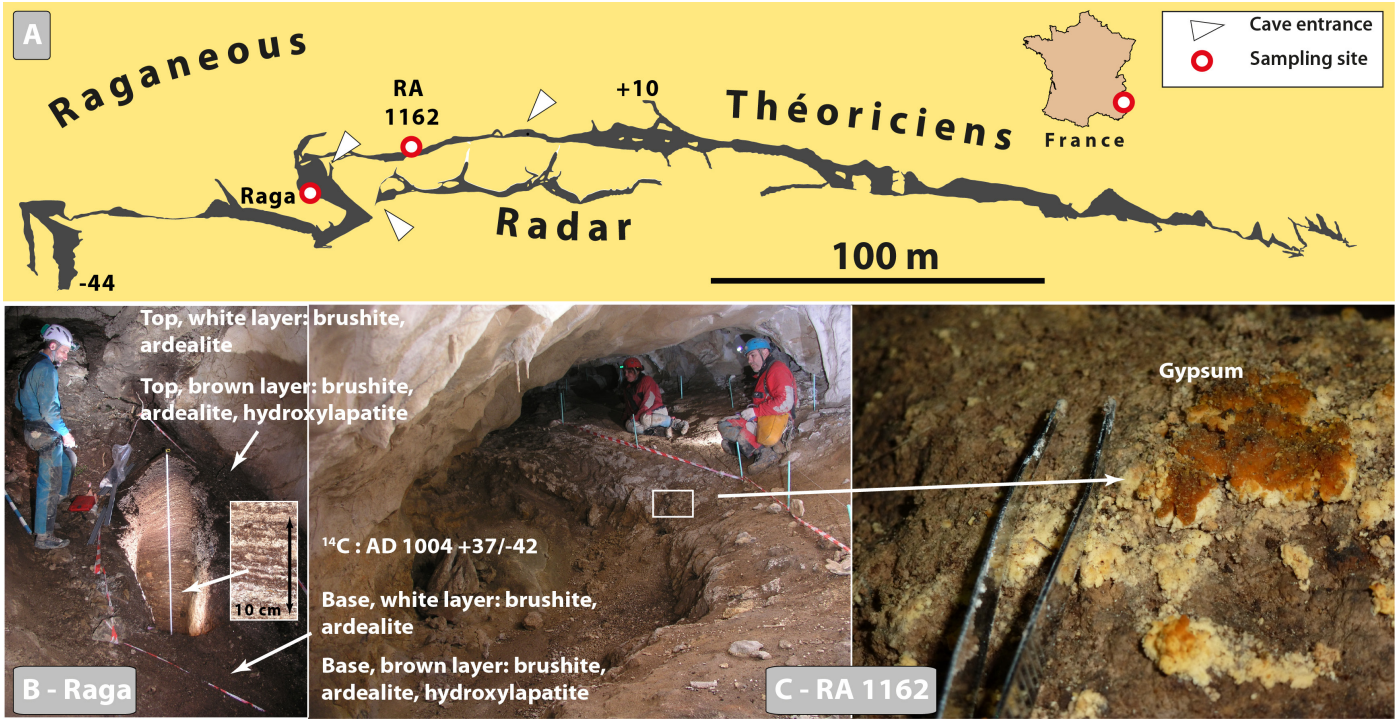

Fig. 6. A.) Profile view of the Raganeous Cave and the neighboring cave systems indicating the sampling sites (Survey: Ph. Audra). B) The 1.8 m guano profile (Raga). It displays a laminated deposit made of alternating brown and white layers (photo by J.-Y. Bigot); C) yellow-orange crust (RA 1162) covering old guano and clay-sand sediments (photos by J.-Y. Bigot and Ph. Audra).

was probably entirely mined for fertilizers at the time when the torch was abandoned; the present cone built up since the mining days. In the main gallery, clay-sand sediments are covered by old guano, which in turn is veneered by a yellow-orange crust (RA 1162) (Fig. 6C).

Guano Cave (Saint-Cézaire, Alpes-Maritimes, France)

The Guano Cave opens at the foot of the cliff in the *Siagne* Gorge, 350 m asl, in *Alpes-Maritimes*, France. It is developed in dolomitic and calcareous Bajocian-Bathonian carbonates. The 280 m-long horizontal looping passage harbors numerous features of extreme corrosion, such as corroded blocks, ceiling cupolas, potholes, and weathered walls. Extensive guano deposits were mined by the owner of the cave. A large bat colony (300 individuals) uses the cave for reproduction. Seven species are present (*Rhinolophus ferrumequinum, R. hipposideros, R. euryale, Miniopterus schreibersii, Myotis blythii, M. myotis,* and *M. capaccinii).* The cave is protected for this specific biotope. About 100 m from the entrance, a narrow passage isolates the inner part, which is characterized by stable climatic conditions (RH 100%, 15°C). Old and fresh guano are present in a lateral chamber (Fig. 7), covering a thick red clay deposit (rich in quartz and muscovite grains), originating from erosion of "*terra rossa*" at the surface, which then was brought in during an early phreatic phase. We sampled a crust between guano and clay (Gua 1b). The dolomitic walls are highly weathered and covered by a 5 mm-thick white paste (Gua 2).

Saint-Marcel Cave (Bidon, Ardèche, France)

Saint-Marcel Cave opens on the left bank of the scenic ~200 m-deep *Ardèche* Canyon that cuts through a Cretaceous limestone plateau covered by Mediterranean scrub ("garrigue"). The cave is 57 km long, including 18 km of underwater passages, has a total relief of 238 m (-101/+137), and consists mainly of large horizontal passages disposed in levels (Brunet et al., 2008; Fig. 8A-B). The cave has drained

the plateau and sinkholes along the *Ardèche* Gorge since Miocene times (Mocochain et al., 2006, 2011). Temperature in the cave is about 14°C, RH is generally close to saturation, and CO_2 varies seasonally from 0.1 to 3-4% in some places. The cave was used since Middle Paleolithic; today part of the cave is opened for tourism. A colony of about 1,000 individuals of *Rhinolophus euryale* was present in the 1950s. In the *Galerie des Chauves-souris* ("Bats Passage"), guano on the surface yielded a ^{14}C age of 1916 BC (Dodelin, pers. comm.). The guano accumulations (maximum thickness of 50 cm) extend along this passage, covering a surface of ~15 m^2. It occurs as black sticky material, poorly layered, resting on older clay deposits. We sampled pale yellow crystals (SM 2b) on the guano surface (Fig. 8C).

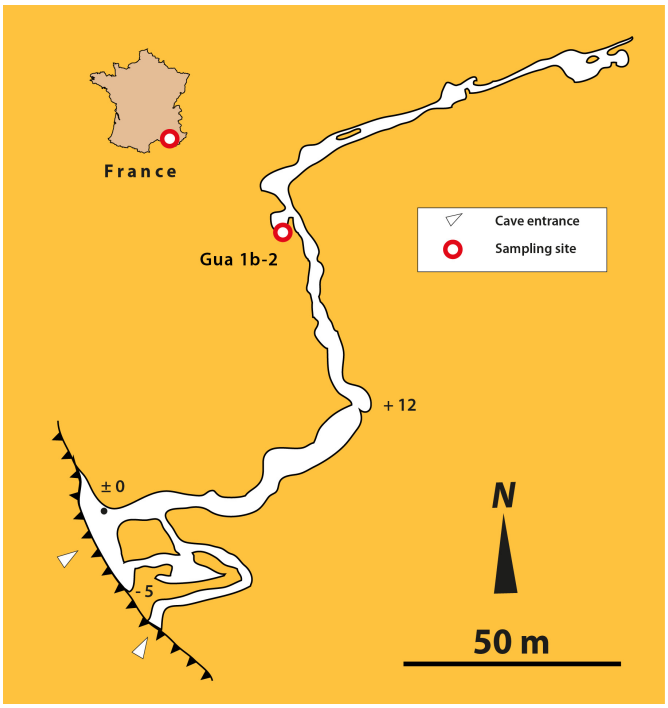

Fig. 7. Plan view of the Guano Cave, located in Provence, France (Survey after Créac'h 1967).

Grosse Marguerite Cave (Aiguèze, Gard, France)

Grosse Marguerite Cave is located about 4 km upstream of Saint-Marcel Cave at an altitude of ~200 m asl, on the right bank of the Lower *Ardèche* Gorge. It opens on a ledge below the top of the cliff, about 115 m above the *Ardèche* River. The cave corresponds to an ancient passage of an underground flow, now truncated by the cliff, and is clogged by sediments in its inner part. It is developed along ~200 m of rising passages, which split inward in two branches; passage size is about 10 m wide and 10 to 20 m high, with deep cupolas and chimneys where bat colonies gather (Fig. 9A). On the sampling day (15/09/2016), cave air was 15.1°C, with 780 ppm CO_2, and 95% RH. The studied site is located in the main cave branch, at the foot of the last slope 20 m from the cave end. The guano deposit is about 6 m wide, and lateral extension shows it might be as thick as 3 m. It is covered by dust sediments brought in by the repeated passage of visitors. Below this reworked sediment, the sticky guano is intact and the stratigraphy is reliable.

This guano accumulation was cored up to 60 cm depth and six ^{14}C dates were obtained (Fig. 9B). It is composed of 3 main units, which boundaries are located at 13 and 21 cm depth. The upper and lower units are made of dark sticky guano, with 3 to 5 mm-thick lighter brown beds in the lower unit. The central unit is made of a pure white soft crystalline powder (sample GM 2).

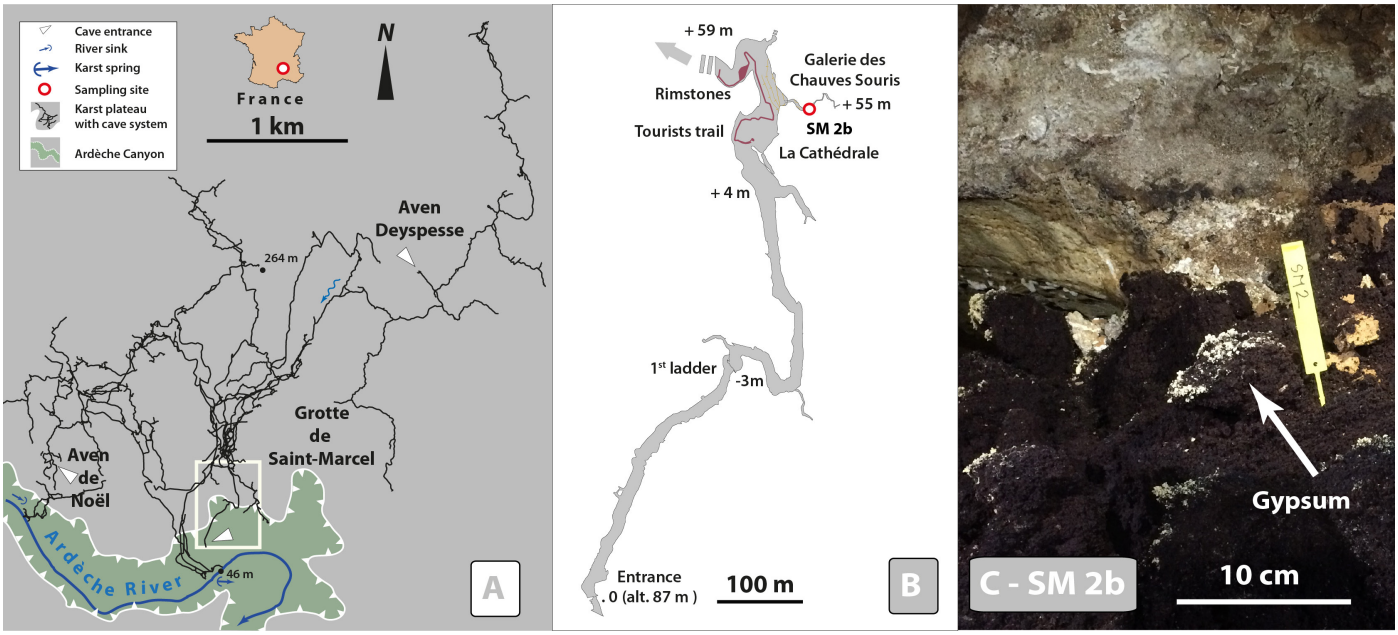

Fig. 8. A-B) Location of the Bats Passage and of SM 2b sampling site in Saint-Marcel Cave (survey after M. Faverjon, SCSM); C) SM 2 sampling site in Saint-Marcel Cave. The guano accumulation is covered by spots of pale-yellow crystals (sample SM 2b) (Photo by A. Chroňáková).

Mescla Cave (Malaussène, France)

Mescla Cave opens in a gorge in the Southern Alps at 184 m asl, 30 km upstream of the mouth of *Var* River in Nice. The cave contains 3.5 km of passage developed along strike, in the limb of an anticline showing strong dip (45°), in Portlandian (upper Jurassic) cherty limestone. The cave displays a looping profile typical of phreatic and epiphreatic flow (Fig. 10, Audra et al., 2002). Upper passages are dry,

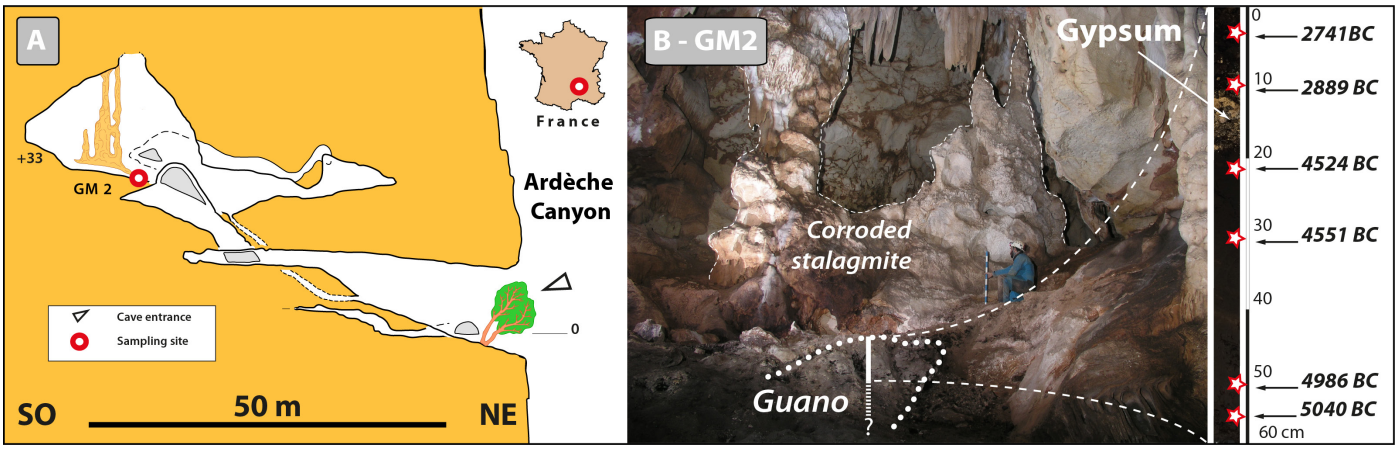

Fig. 9. A) Projected vertical profile of Grosse Marguerite Cave, which opens in the cliff of the *Ardèche* Canyon, France (after J.-Y. Bigot), with indication of sampling site; B) The GM 2 guano core accumulated between 5040 and 2741 BC, however its base was not reached. The guano is covered by dry clay and fire ash reworked along the pathway. A calcite stalagmite was strongly corroded by condensation waters forming above the guano (Photo by J.-Y. Bigot).

whereas the lower level corresponds to the active part of the river outflow. The upstream sump has been explored down to -267 m below the entrance, ranking it among the deepest explored phreatic caves in the world. The deep component of the water is thermal (23°C), with sulfated-chloride water (Reynaud, 2000). Calcite speleothems are present in the first sump, down to -12 m, demonstrating a recent rise of the water table due to sediment aggradation of the nearby *Var* River. Currently bats and guano deposits are not frequent in the cave. However, the divers identified accumulations of bat bones in the second sump, at about 5 m depth, further confirming the recent rise of the water table. In the first sump, between 3 and 7 m depth, we collected white clay (Mescla 1) preserved in fissures protected from high velocity flow, and a fragment of black crust covering most of the walls (Mescla 2).

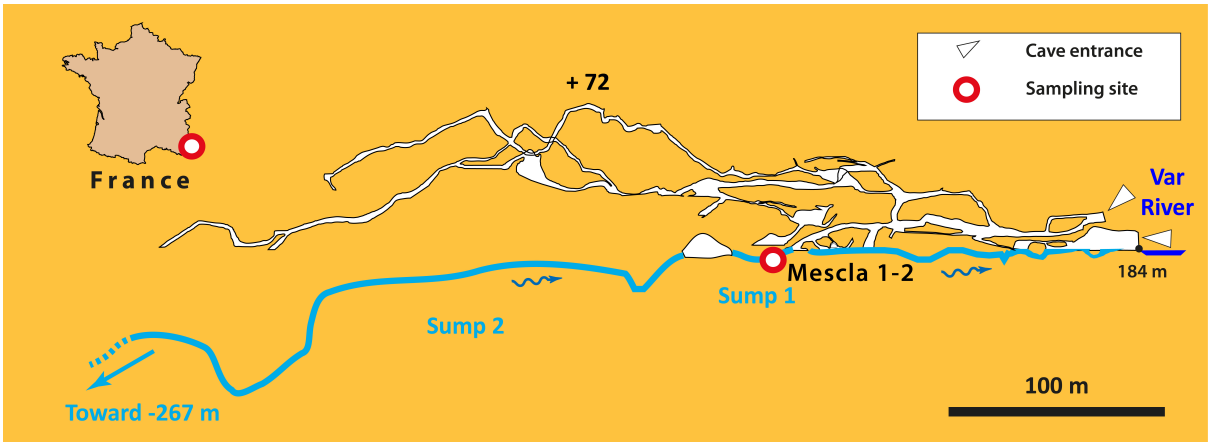

Fig. 10. Projected vertical profile of Mescla Cave showing the sampling sites (Survey after Audra et al., 2002).

Aramiska Peštera (Dragožel, Macedonia)

Aramiska Peštera opens at 660 m asl. It is a ponor cave located in the upstream parts of *Kamenica* Valley, part of the *Crna Reka* drainage basin, in the southern part of Macedonia (Fig. 11). It is developed in Upper Cretaceous limestone from sinking allogenic waters coming from the Pliocene-Early Pleistocene pyroclastic cover (Temovski, 2016). Back-flooding clay sediments are present throughout most of the cave, especially in the upper (older) parts. In the Room of Bones, remnants of human bones and skulls are covered with flowstone. Here we sampled pyroclastic-derived clay and sand material (AR1, AR2).

Karši Podot Cave (Vrpsko, Macedonia)

Karši Podot is a 200 m-long horizontal hypogene cave located in *Crna Reka* Valley. It is formed mainly in Precambrian dolomitic marble, and partly in Pleistocene alluvial and travertine deposits (Fig. 12A). Cave passages in the dolomitic marble formed by ghost-rock weathering with thermal waters leaving dolomitic sand residue (Temovski, 2013). The explorable passages were later opened due to backflooding from *Crna Reka*, removing the sediment, and redepositing it along with non-carbonate silt and clay coming from the allogenic waters or from the terrace deposits in which the northern parts of the cave are developed. A sediment profile in the Main Room has hydrothermally weathered dolomitic sand with fluvial clay and silt that was covered by a thick (30 cm to 1 m) guano deposit (Fig. 12B). We sampled a brown layer (KP06) from this profile (Fig. 12C).

Lekovita Voda Cave (Pravednik, Macedonia)

Lekovita Voda Cave is a 90-m long old passage, remnant of a larger system, developed in Upper Cretaceous (Turonian) limestone, and located high in the *Doljani* Valley, a tributary to *Crna Reka*. The cave mostly consists of a single horizontal gallery

Fig. 11. Extended profile of Aramiska Peštera with the sampling location (Temovski, 2016).

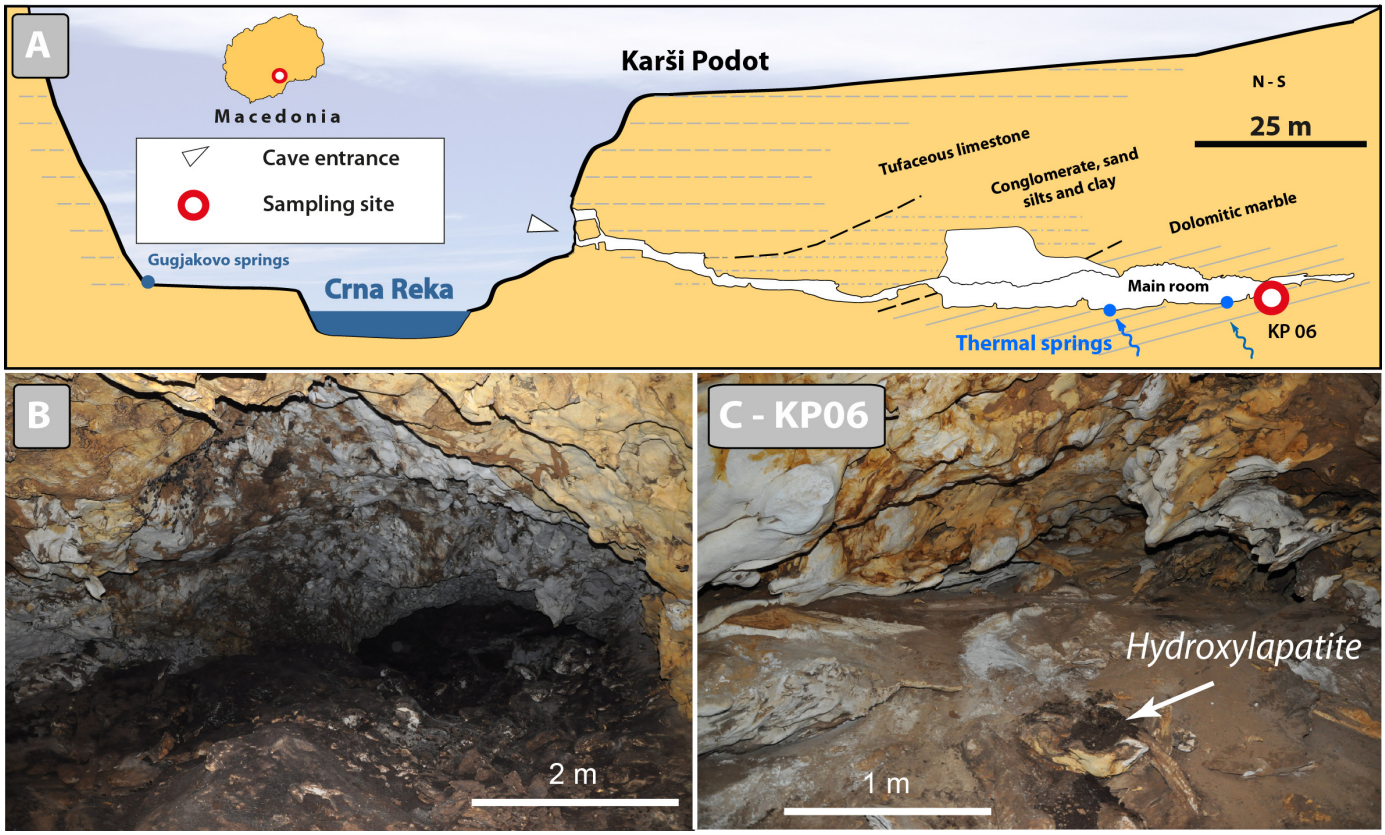

Fig. 12. A) Extended profile of Karši Podot Cave with sampling location (Temovski, 2016); B-C) Main Room in Karši Podot Cave, with detrital and weathered sand covered with thick guano deposits, where sample KP06 was collected (Photo by M. Temovski).

with a paragenetic ceiling morphology (Fig. 13A). It is mostly filled with gravel, sand, and clay sediments, which are partly exhumed and covered with thick flowstone deposits (Fig. 13B). It is presumed that the cave developed in Late Pliocene - Early Pleistocene, in relationship with the local geomorphic events (Temovski, 2016). The cave passage ends with a large sediment fill topped by a thick flowstone deposit, nearby which in a small niche we sampled a detrital yellow clay (LEK1).

The Monte Inici cave system - Grotta dell'Eremita and Abisso dei Cocci (Castellammare del Golfo, Trapani, NW Sicily, Italy)

Mount Inici is an isolated massif reaching 1064 m asl, close to the NW Sicilian coast. Two caves belong to the *Monte Inici* system: *Grotta dell'Eremita* and *Abisso dei Cocci*, both opening at about 500 m asl on the southern scarp of the mountain (Fig. 14). These are the two deepest caves in Sicily, with depths of 306 and 361 m (+61/-300), and developments of 2.9 and 2.1 km, respectively (Messana, 1994). They occur in Lower Jurassic limestones and dolomitic limestones (Inici Fm.), and Upper-Middle Jurassic reddish-gray limestones (Buccheri Fm.). The caves are typical 3D mazes with large, gently dipping galleries, and chambers connected by vertical shafts. They are of hypogene origin (Vattano et al., 2013, 2017), related to the nearby thermo-mineral spring with temperatures of up to 50°C (Grassa et al., 2006). Due to the heating of the rock above the thermal aquifer, the caves are warm (17.4 close to the entrances, up to 21.1°C in the lower parts) and dry (70-90% RH); CO_2 may reach 0.4% in the lowest confined areas.

Both caves are rich in phosphate minerals derived from large fossil bat guano deposits and occur especially in the deeper large rooms. Samples were taken in various parts, in small exploration trenches

Fig. 13. A) Profile of Lekovita Voda Cave with sample LEK 1 location (Temovski, 2016); B) View of the sediment choke at the southern end of Lekovita Voda Cave, with clay filled floor covered by thin black soot coating due to frequent visitors (Photo by M. Temovski).

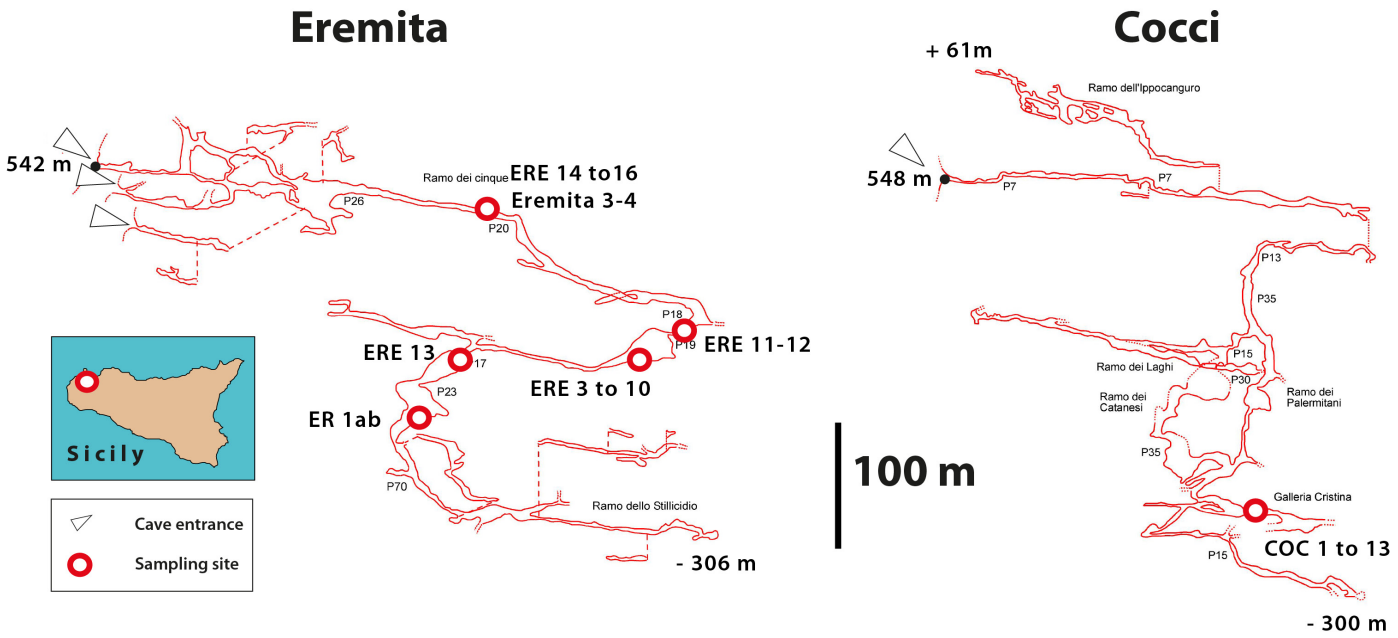

Fig. 14. Vertical profile of *Grotta dell'Eremita* and *Abisso dei Cocci* (after GS CAI Palermo and CSE Catania), with indication of sampling sites and their location within Sicily (inset map).

dug in old bat guano deposits until the underlying limestone was reached. Some broken stalactites found on the floor were also taken.

In *Eremita* Cave we collected 17 samples (Fig. 14-15): a grey-white laminated stalactite (ER1ab), soft laminated guano layers of various colors (white, yellowish, greenish) (ERE 3 and ERE 6 to 15), and a beige earthy part of a black crust (ERE 4-5) at the contact between rock and guano. In *Ramo dei Cinque* Passage, below a cone of old guano, we sampled a light beige soft powdery material in a white layer (ERE15), a white and pinkish earthy material from a yellowish layer (ERE16 and Eremita3), and a bright yellow layer (Eremita4).

In *Abisso dei Cocci* many samples were taken below the Cristina Passage (Fig. 14 and 16): white prismatic translucent crystals (COC1) found underneath boulders, a yellowish to white powder (COC4), a brownish crust covering the many boulders along this passage (COC5), a lemon-yellow colored vitreous layer (COC7), a part of a white layered stalactite showing no reaction with HCl (COC9), and a dark crust (COC10). In a shallow trench dug into the floor sediments a sequence of layers has also been sampled: a lower white layer in contact with the unaltered limestone below (COC11a), a layer with greenish spots inside a white mass (COC11b1) and with pinkish crystals (COC11b2). White microcrystalline powder was recovered in the center of the gallery (COC13).

Acqua Fitusa Cave (San Giovanni Gemini, Agrigento, Sicily, Italy)

Acqua Fitusa is an inactive water-table sulfuric acid cave (De Waele et al., 2016; Vattano et al., 2017). It is located in Central Sicily (Fig. 17A) along the north-eastern fault scarp of a N-S oriented westward-vergent anticline forming the *Mt. La Montagnola*. The cave formed in the Upper Cretaceous rudist breccia member of the Crisanti Formation, composed of conglomerates and reworked calcarenites. Chloride-sulfate alkaline-earth waters with temperature of 25.2°C (Grassa et al., 2006) still emerge 300 m to the north and at a lower altitude with respect to the cave. The cave consists of three stories of subhorizontal conduits, arranged in a maze pattern following sets of joints, forming large rooms on their intersections; its total length is 700 m and has a vertical range of 25 m (Fig. 17A). Due to the sulfuric acid speleogenesis (SAS), replacement gypsum crusts are present in fissures and pockets, and totally coat narrow blind passages. The cave environment is relatively dry, with a temperature of 12.8°C and RH of 76.5% (Dec. 2011). It hosts a community of *Rhinolophus euryale*, *R. ferrumequinum*, *R. hipposideros*, *Myotis myotis*, *M. capaccinii*, and *M. schreibersii* (Fulco et al., 2015). Samples were taken in the central part of the entrance chamber, where big blocks of collapsed limestone are covered with guano deposits and a dark brown crust has developed (FIT3) (Fig. 17B).

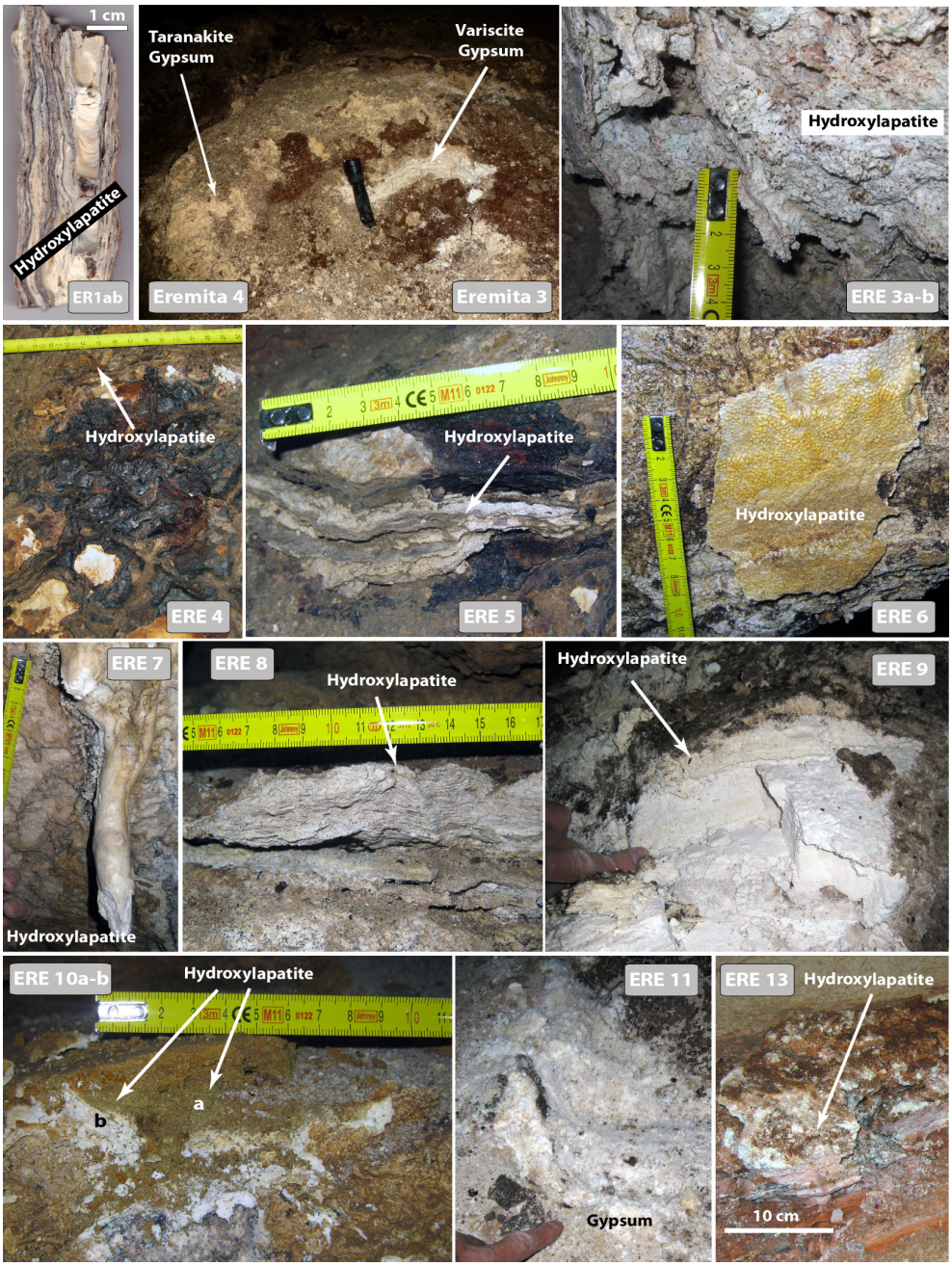

Fig. 15. Phosphates and sulfates sampled in Eremita Cave (see text for further details) (Photos by J. De Waele and Ph. Audra).

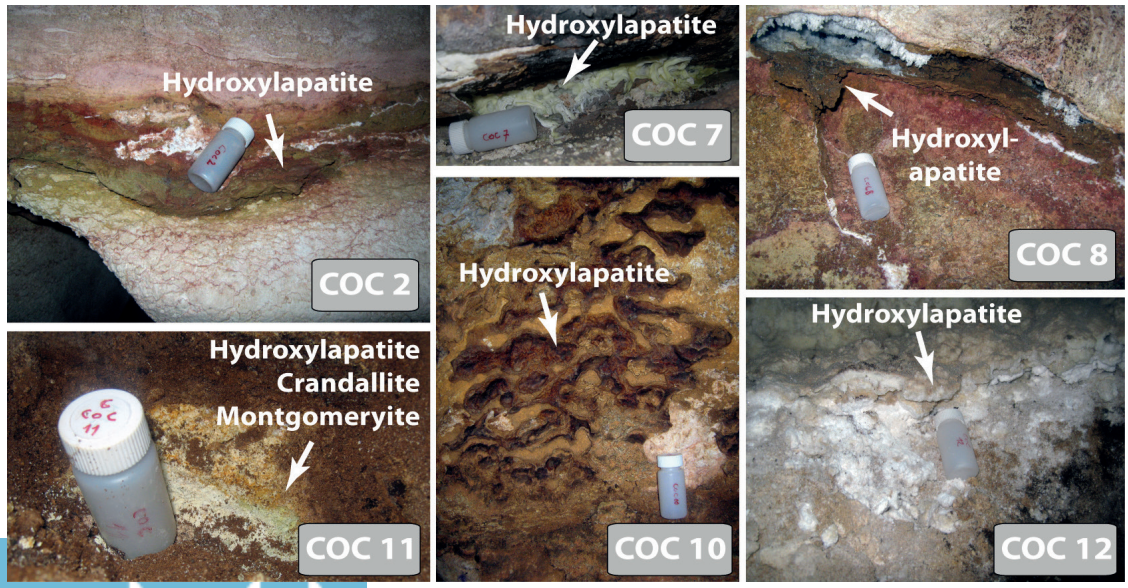

Fig. 16. Phosphates sampled in Cocci Abyss (Photo by J. De Waele).

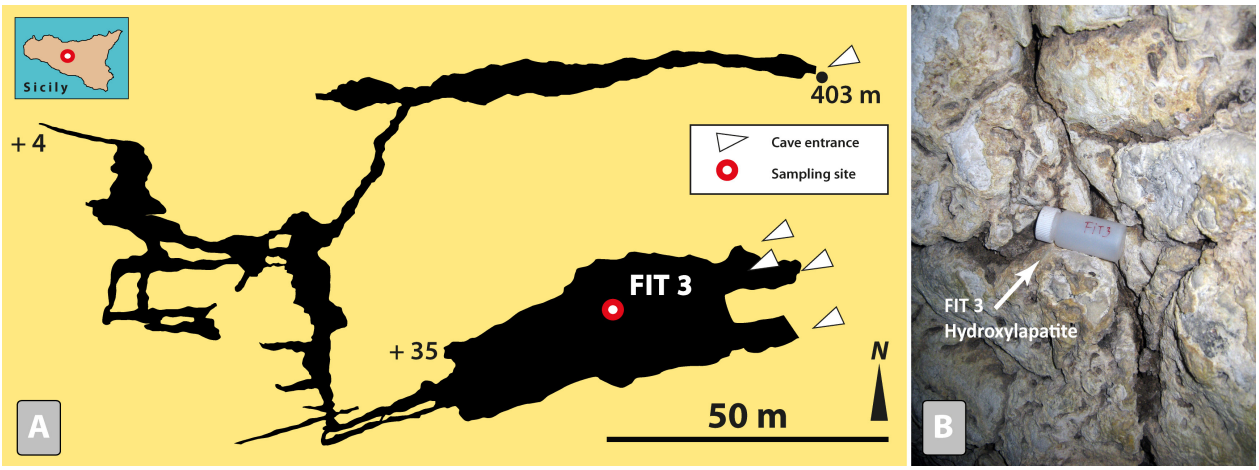

Fig. 17. A) Plan view of Fitusa Cave, with indication of the sampling site (Survey ANS Le Taddarite, Vattano, 2012). In inset, location of the cave in Sicily; B) Dark crust sampled in Fitusa Cave (Photo by J. De Waele).

Palombara Cave (Melilli, Syracuse, Sicily, Italy)

Palombara Cave opens at 150 m asl at the foot of the *Monti Climiti* on a plateau that inclines toward Syracuse Bay. The plateau is made of Miocene (Burdigalian-Serravalian) calcarenites, namely the Monti Climiti Formation (Lentini & Carbone, 2014). It is part of the Hyblean Plateau, which belongs to the African Plate. Volcanoes were active in this area during the Plio-Pleistocene until 1.4 Ma. The area was continuously uplifted during the Pleistocene as evidenced by several marine terraces and paleocliffs. Palombara Cave is about 800 m long, with a depth of ~80 m (Ruggieri, 2000). It consists of large subhorizontal passages cut by narrow mazes and shafts (Fig. 18A). The entrance is a collapse shaft that opens on the plateau. The cave displays phreatic morphologies, feeders, bubble trails, pointing toward a hypogene origin in relationship with deep CO_2 degassing, possibly brought about by the Hyblean magmatic bodies, and with the uplifting stages recorded by the Pleistocene marine terraces (Vattano et al., 2017). The cave contains fine-clay sediments, originating from clastic material brought in from the surface. Two samples display reverse paleomagnetic orientations, showing that the cave itself should be older than 780 ka, which would be consistent with the lowest mean uplift rates of 0.2 mm/a proposed by some authors (Dutton et al., 2009, and references therein). After its opening to the surface, the cave was accessible to Neolithic tribes and to bats. The latter have left extensive guano deposits, among which the pile in the Guano Chamber reaches ~8-10 m in height. Five species are currently present (*Myotis myotis*, *Miniopterus schreibersii, Rhinolophus ferrumequinum, R. euryale,* and *R. mehelyi*). The cave is protected by a Regional Law (Di Maggio et al., 2012). Two sites were sampled for phosphate mineralogy. After the main climb and before the Guano Chamber, an old guano deposit (P5) is covered by a colorful crust (Fig. 18B). A little further into the cave, an old guano deposit naturally cut by erosion is covered on a vertical face by a pale violet crust (PA23) (Fig. 18C).

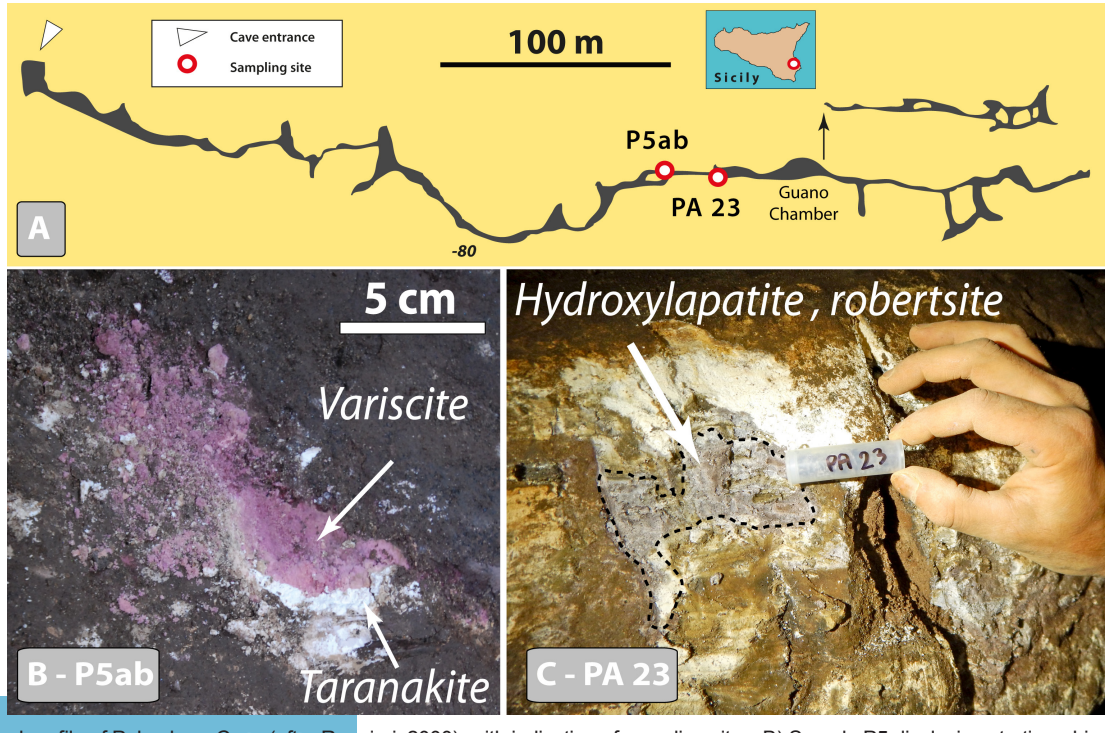

Fig. 18. A) Vertical profile of Palombara Cave (after Ruggieri, 2000), with indication of sampling sites; B) Sample P5 displaying stratigraphic succession of old guano covered by white and purple layers (Photo by M. Vattano); C) Sample PA23; A pale violet crust covers an old guano profile (Photo by D. Cailhol).

Monello Cave (Syracuse, Sicily, Italy)

Monello Cave opens at 100 m asl in the same area as Palombara Cave, at the foot of the Monti Climiti paleocliff. Also, this cave is preserved as nature reserve (Di Maggio et al., 2012). It consists of ~540 m of galleries developed along faults to a depth of 40 m and well decorated large chambers (Fig. 19A). To the south, a series of shafts lead to the lower point of the cave. As Palombara, numerous feeders, bubble trails, and ceiling channels point toward a hypogenic origin. Some clastic material was introduced by sinkholes and deposited as decantation clay in the deep parts. They bear normal paleomagnetic orientations, thus younger than 780 ka. Archeological material from Upper Neolithic has been found. Great accumulations of guano are present especially in the first large chamber; however, due to the closure of the cave, only few individuals of *Rhinolophus ferrumequinum* are now present. The lower gallery hosts pieces of collapsed calcarenite rocks, some being covered by a thin layer of brown decantation clay (Fig. 19B). Its surface is hardened by a thin (<1 mm) brown crust (MO 4) (Fig. 19C-D).

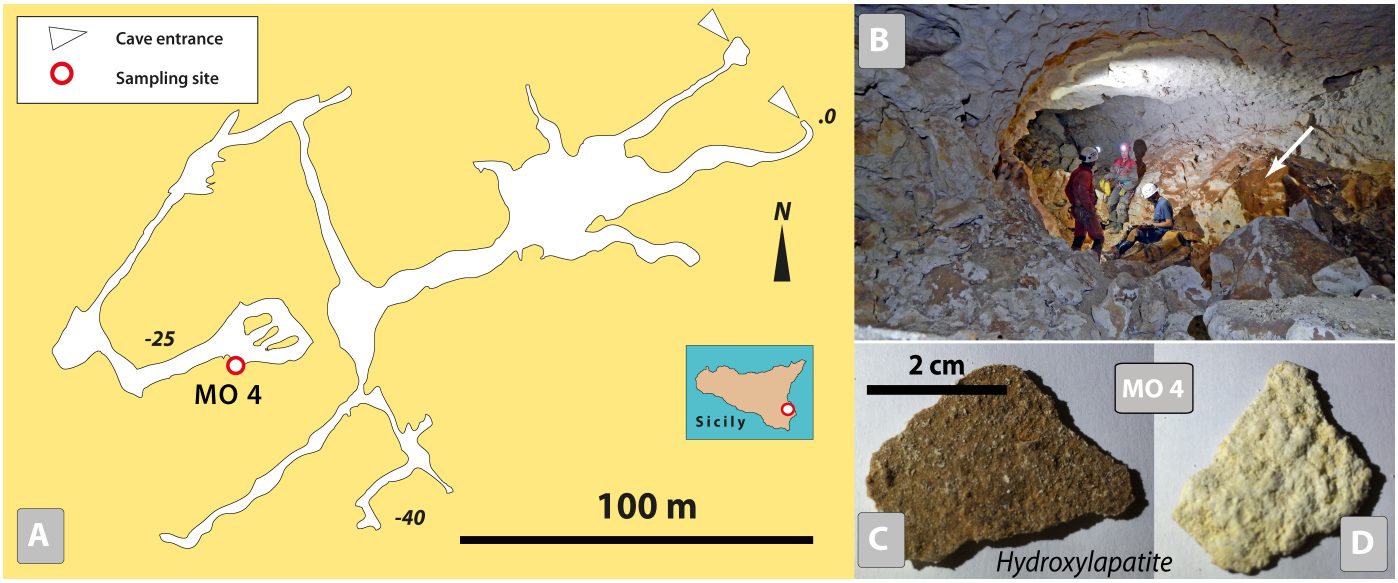

Fig. 19. A) Plan view of Monello Cave (after Ruggieri, 2000), with indication of sampling site; B) Floor of the lower gallery in Monello cave covered by collapsed calcarenite blocks, which in turn are covered by a thin crust of brown decantation clay and phosphate (Photo by D. Cailhol); C) close-up view of the upper part of the crust in B; D. lower side of the crust, at the contact with the calcarenite (Photos by Ph. Audra).

Grotta Scrivilleri (Priolo Gargallo, Syracuse, Sicily)

Grotta Scrivilleri, opening at 157 m asl, is an over 2 km-long maze of hypogene origin with most of the passages guided by prominent fractures (Fig. 20A). The cave is developed in the Miocene calcarenites of the Syracuse area, such as the Palombara and Monello caves. Since the cave was just recently opened by digging, no bats are present inside. At the bottom of the *Prima Frattura* Chamber, about 300 m from the entrance, a mixed deposit shows alternation of laminated clay deposited by flooding waters and white soft sandy residue originating from wall weathering by condensation (Fig. 20B). A thin dark-brown layer of presumed old guano (SC4) is present below the upper sandy layer, showing that some connection to the surface through which bats could have entered the cave existed sometime in the past.

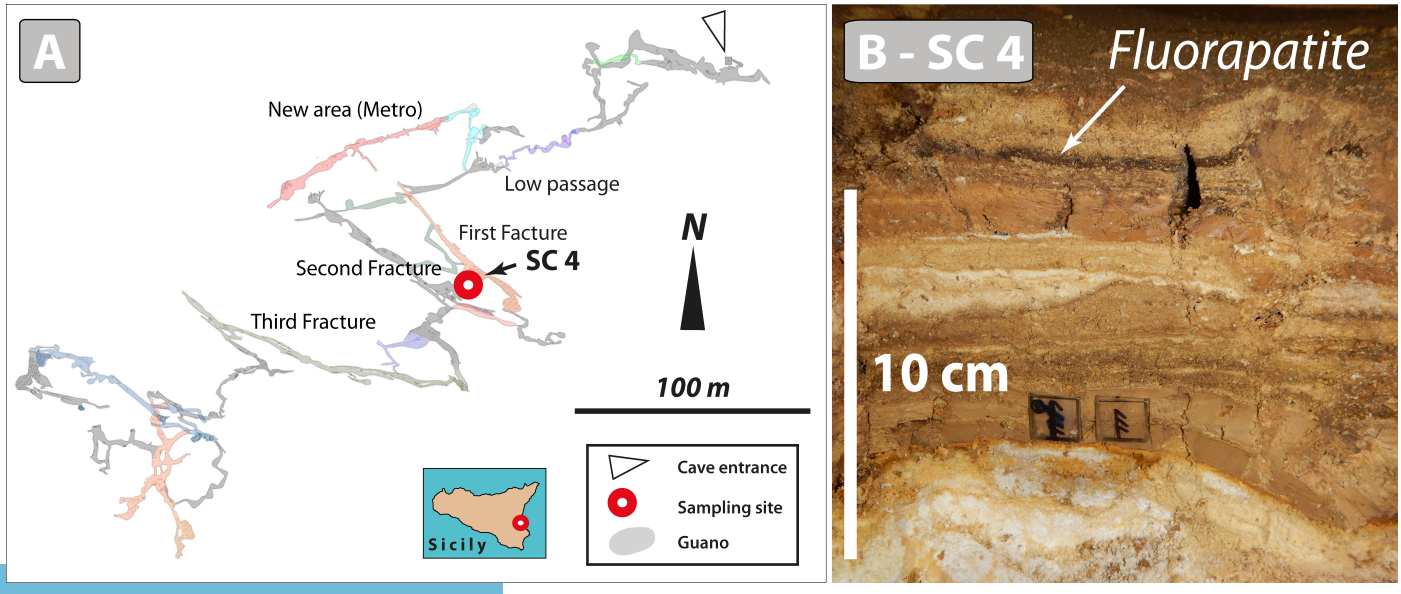

Fig. 20. A) Grotta Scrivilleri plan view, with sampling location (from Centro Speleologico Etneo, Gruppo Speleologico Siracusano, Speleo Club Ibleo); B) Sediment profile from where SC4 sample (a thin dark brown phosphate layer) was collected (Photo by D. Cailhol).

Personaggi Cave (Montevago, Agrigento, Sicily, Italy)

The *Grotta dei Personaggi* is known since the early 1900s and is famous for the archeological findings that cover a period from the Neolithic to historical times. The cave opens at 350 m asl along a fault scarp in the NW sector of Mt. *Magaggiaro* and is developed in well-bedded white platform limestones (Inici Formation, Lower Jurassic) and in nodular or massive reddish to brown pelagic limestones (Buccheri Fm., Upper-Lower Jurassic) of the *Saccense* Domain (Di Stefano et al., 2013). Thermal springs, characterized by chloride-sulfate alkaline-earth waters with an average temperature of 39.2°C (Grassa et al., 2006) are located about 3 km NW of the cave, which has a total length of ~1.7 km and a relief of 47 m (+15 m/-32 m). It consists of close-to-horizontal passages that follow bedding and fault planes forming a maze pattern with deep feeders along fractures pointing toward a hypogene origin (Fig. 21; Vattano et al., 2017). The cave morphologies are mainly linked to condensation-corrosion processes by convective airflow, such as upwardly developing cupolas, stacked spheres, weathered walls and boxworks. Alluvial deposits are absent. The cave hosts a large bat colony of *Rhinolophus euryale* responsible for an extensive amount of guano. A previous study of mineral chemistry shows the presence of phosphates, iron, manganese, and silica spherules, which are interpreted as being concentrated through microbial communities processing the impurities from host rock and clay (Vattano et al., 2015).

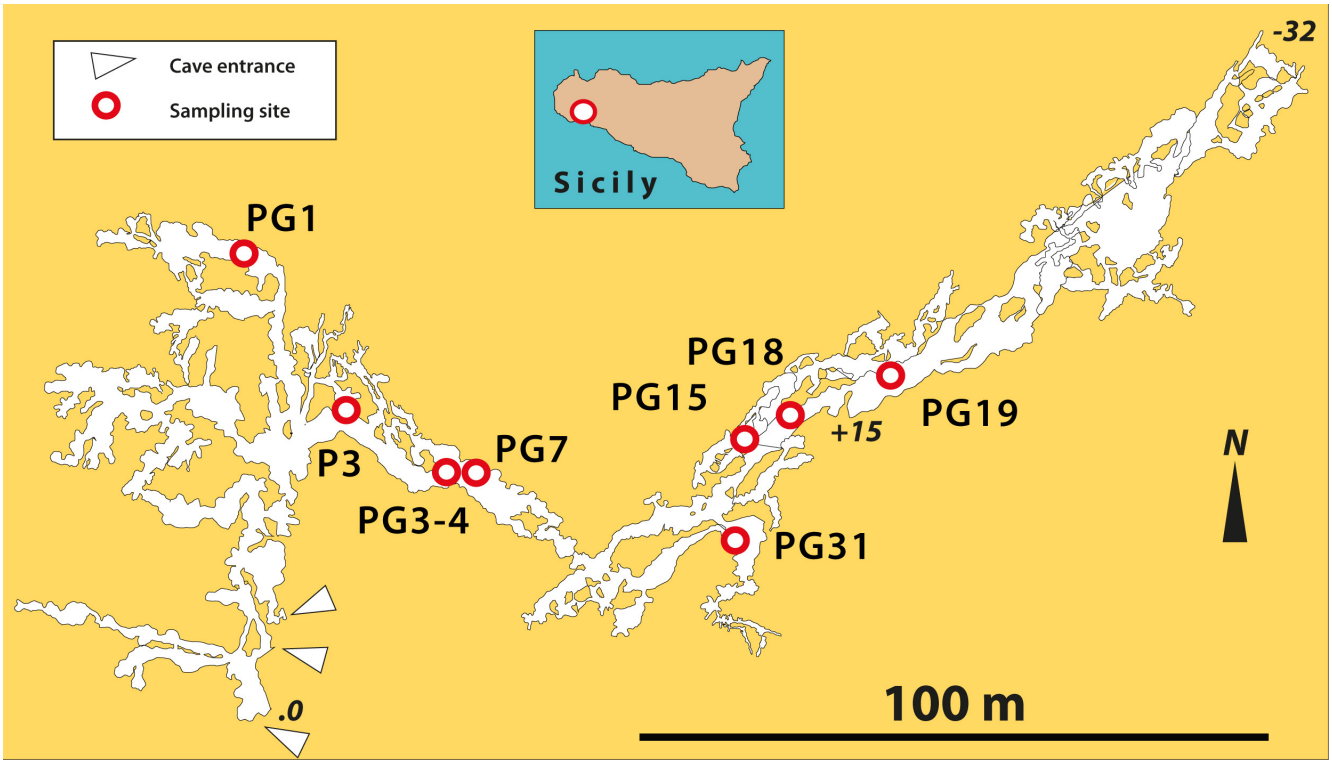

Fig. 21. Plan view of Personaggi Cave (Survey by ANS Le Taddarite, Vattano, 2014), with sample location.

Several soft samples were collected (Fig. 22): the lower black part of a crust in a cupola (PG1), the white part (PG3) and the blackish layer (PG4) of a deposit on a block, a blackish paste between white and reddish parts on the contact between guano and wall (PG7), a whitish paste at the bottom of gallery (PG15), a white-black-yellow crust attached to guano (PG18), a white-black-yellow crust in guano pot (PG19), a black crust on wall (PG31), and a multicolor green-white crust (P3).

Salnitro Cave (Sambuca di Sicilia, Agrigento, Sicily, Italy)

Salnitro Cave develops in Eocene carbonate breccia resting on the limestones of the Inici Formation. The Mt. *Arancio*, where the cave opens at 252 m asl, is an anticline limb cut by the antecedent canyon of *Tardara*. Salnitro Cave has two entrances and is composed of three, 20 m large and high chambers connected by short passages. Its total development is ~260 m and it has a depth of 18 m (Fig. 23A). The original shape of the cave voids is hidden by many rock falls, while the floor is covered with debris and large piles of guano (Fig. 23B). The roof is sculptured by cupolas probably related to condensation-corrosion processes above the guano heaps. The cave has been known for a long time, and in the past the guano deposits were mined as fertilizers. Salnitro Cave is home to *Myotis myotis*, *M. capaccinii*, *Miniopteris schreibersii* and only occasionally to *Rhinolophus euryale* and *Pipistrellus kuhlii*. Several samples of dark brown crusts were collected from boulders and cave walls in several areas of the main room (SAL1-4, Fig. 23E). Close to a dripping location (Fig. 23C), a powdery white crust (SN3, Fig. 23D) covered the dark guano deposits at the edge of wet guano, where evaporation occurred.

Carburangeli Cave (Carini, Palermo, Sicily)

Carburangeli Cave is located close to the city of Palermo. It is a 400-m long cave (Fig. 24), mainly horizontal, opening at 22 m asl on an elevated marine terrace attributed to MIS 5, at the foot of a paleocliff.

Fig. 22. Phosphates sampled in Personaggi Cave (Photos by M. Vattano).

The entrance part is developed in Pleistocene calcarenites and conglomerates, whereas the inner part extends in Triassic and Lower Jurassic limestones and dolomitic limestones (Madonia et al., 2003). The cave was probably a flank margin cave, transformed into resurgence at a later stage. Carburangeli Cave is famous for its archeological findings of Paleolithic and Neolithic age and is also of paleontological interest (Sicilian dwarf elephant). The cave is protected as natural reserve (Di Maggio et al., 2012), and it hosted an important colony of *Myotis myotis*. Three samples of phosphates were collected in the room where the bats are concentrated (CA1 to 3).

Pertosa-Auletta Cave (Pertosa, Salerno, Italy)

Pertosa-Auletta is a show cave. It opens on the flanks of the *Tanaro* Valley, along the eastern slopes of the *Alburni* Mts., and develops in well-bedded Jurassic micritic limestones (Santo, 1988). The cave is a resurgence with an important underground river in one of the galleries, and some fossil branches (Fig. 25A). The development is little over 3 km. It has two entrances (263 and 268 m asl, respectively), a positive altitude difference of 45 m, and temperatures ranging between 12.2 and 13.9°C. In several areas of the fossil branches old guano deposits are present (Fig. 25B). These were exploited in the 1940s, but parts of these sediments can still be seen along the show cave trail. Dark brown crusts are visible along the lower part of the walls and filling ceiling cupolas (samples P1 to 3). Along the underground river bank, a thick guano deposit is cut and shows an alternation of brown and more yellowish layers (P4, Fig. 25C).

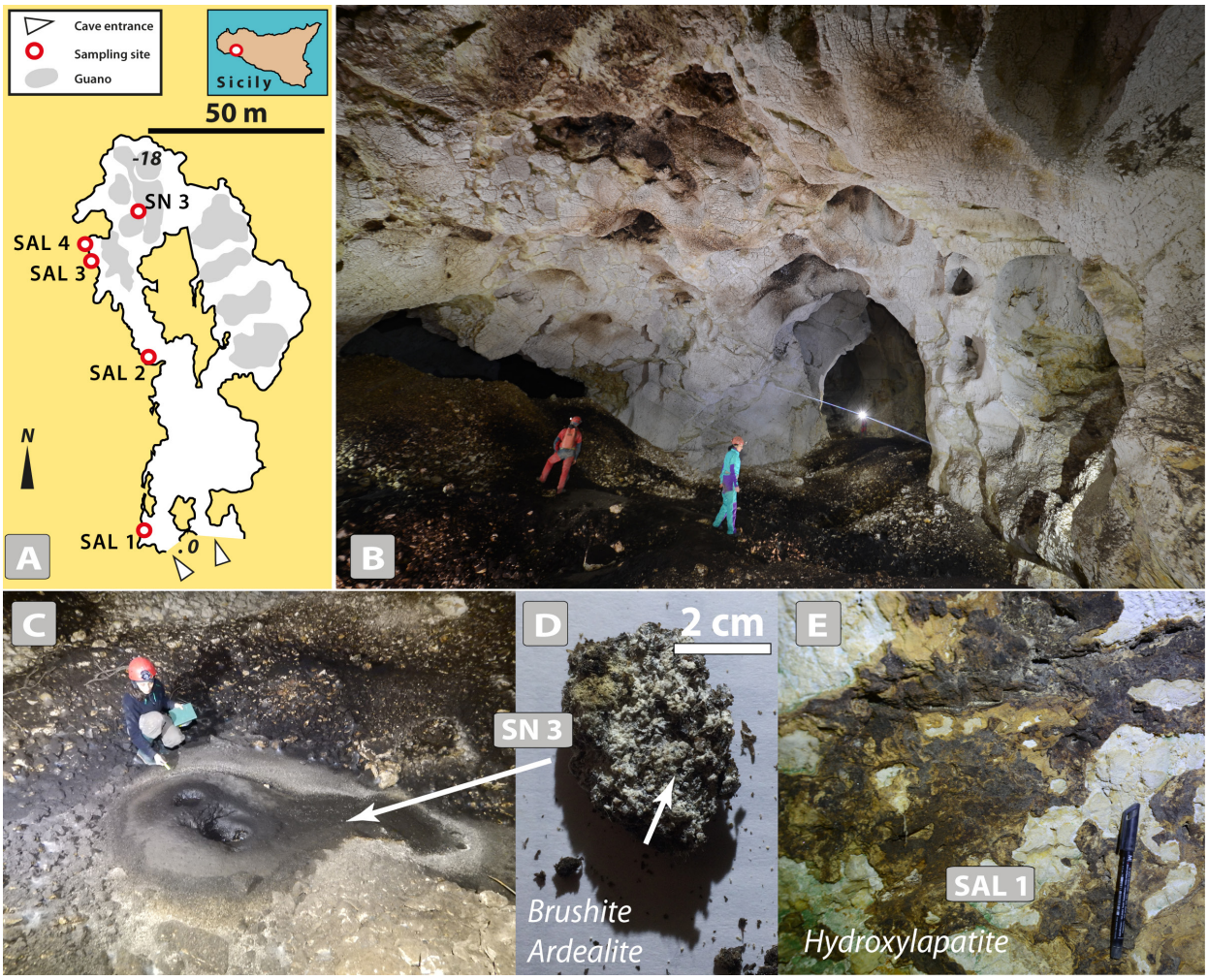

Fig. 23. A) Plan view of Salnitro Cave with sample locations (Survey ANS Le Taddarite, Vattano, 2010, 2015); B) Last chamber where extensive guano deposits cover the blocky floor (Photo by M. Vattano); C) The guano cone is wet in the center because of dripping, whereas its edge, D, is dry, allowing the crystallization of a ring of soft crystals; E) dark brown crust on the wall (Photos by M. Vattano and Ph. Audra).

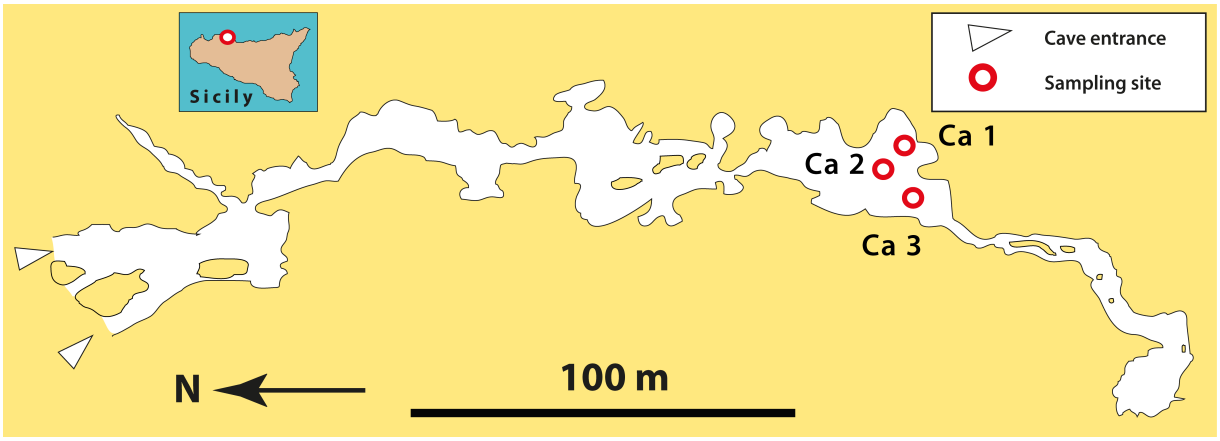

Fig. 24. Plan of Carburangeli Cave (Survey by A. Conigliaro, R. Di Pietro & D. Gueci, 1996-1997), with sampling locations.

Toirano cave system (Toirano, Savona, Italy)

The Toirano cave system is located in the *Varatella* Valley and develops in dolostones and dolomitic limestones of the *San Pietro ai Monti* Formation (Triassic). From the lower (186 m asl) to the upper level (247 m asl), the caves are organized as follows: *Básura*, *Santa Lucia Inferiore*, *Santuario*, and *Colombo*. Morphological indices suggest this cave system originated from rising, possibly hypogene flow, as a small thermal sulfidic spring surfaces in the village of Toirano. Cosmogenic-nuclide (Al-Be) burial dating of the fluvial gravels found in the upper *Colombo* tier yielded an age of 2 Ma, showing that the valley was a Messinian canyon eventually filled with thick Pliocene gravels, which were later eroded. Phosphates have been found and sampled only in the highest level of *Colombo*, which is a horizontal 310 m-long cave (Fig. 26A). Here, important bat guano deposits and associated intense condensation-corrosion features show that bats have used this cave for a long time. The cave is of archeological interest, as are most of the caves in the area, and guano deposits have been trenched by scientific excavations. We sampled a hard-yellow crust covering an intact old guano heap (C1, C3) (Fig. 26B).

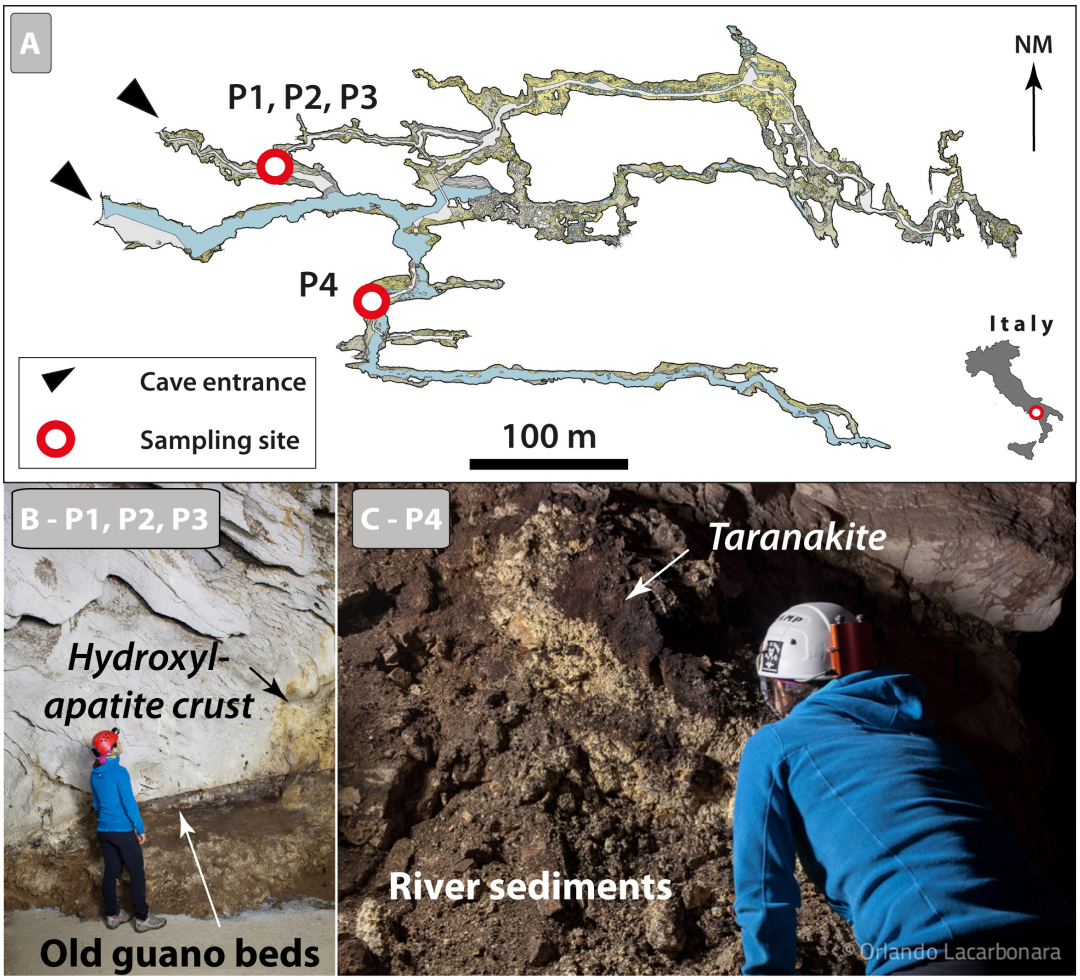

Fig. 25. A) Pertosa–Auletta Cave survey and sampling sites (survey F. Larocca, CRS "Enzo dei Medici"); B) sampling area of P1, P2, P3, with the old guano deposits on the lower part of the cave walls (dark areas); C) sample P4 is located on river sediments (Photos by O. Lacarbonara).

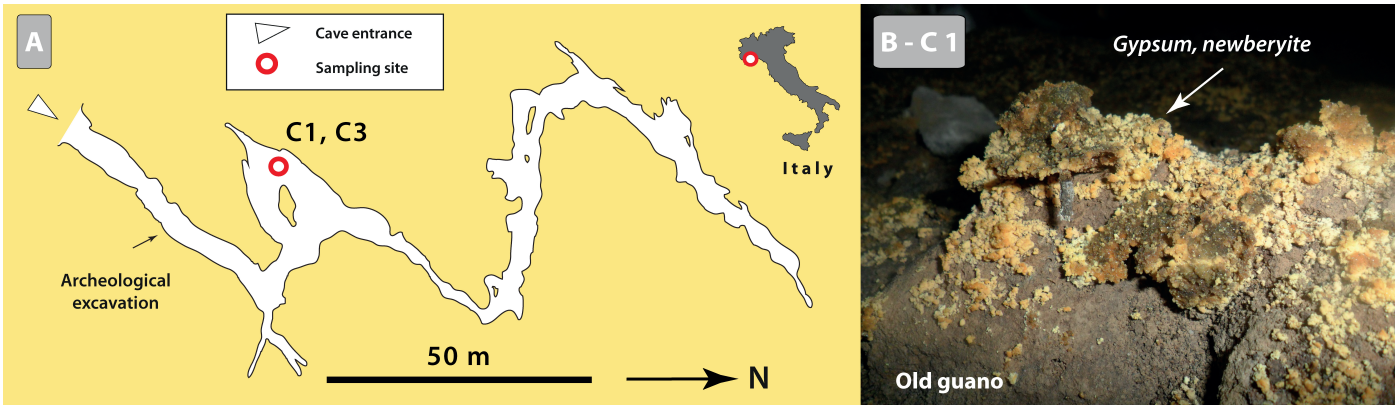

Fig. 26. A) Location of sampling sites in the highest tiers of *Colombo* Cave (after GS Cycnus, Toirano); B) Close-up view of sample C1 (Photo by J. De Waele).

Corona 'e sa Craba Cave (Carbonia, SW Sardinia)

Corona 'e sa Craba is a 250-long cave entirely carved in a quartzite vein at the contact with Cambrian dolostones (Sauro et al., 2014). The small entrance to the cave has been excavated by local mineral collectors and opens at an altitude of 260 m asl (Fig. 27A). In the *Corona 'e sa Craba* area there are several mines for Pb, Zn, and Ba ores, which were active until the early 1980s. The cave consists of a series of chambers and lacks the typical carbonate speleothems. After the first room, the cave continues with a wide and high gallery that hosts a large guano deposit generated by an important bat colony inhabiting the cave during spring-early summer. The rock walls are covered with powdery material and crusts of colors ranging from reddish to violet, brown, greyish, white, pale pink, blue, and black. These secondary minerals are mainly composed of oxides-hydroxides, sulfates, and phosphates. The sulfates are derived from the acid corrosion by sulfuric acid in a late stage of cave development (Sauro et al., 2014). Phosphates, on the other hand, derive from the interaction of the host rock and its minerals with fresh or old guano. Besides the common hydroxylapatite and taranakite, the rare minerals robertsite, spheniscidite (Fig. 27B), vashegyite, strengite, and possibly leucophosphite and berlinite were reported by Sauro et al. (2014).

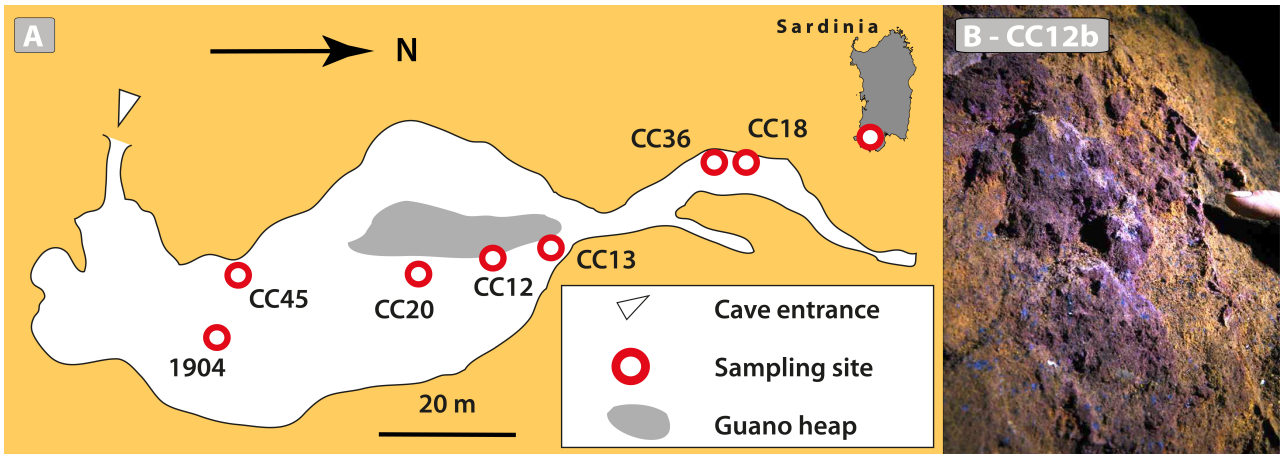

Fig. 27. A) Plan of the *Corona 'e Sa Craba* Cave (survey after GRSEAM caving Club, Carbonia); B) Purple-violet crusts (CC12b) with small blue fragments (Photo by L. Sanna)

RESULTS: GUANO-DERIVED CAVE MINERALS

The mineralogical results for the sampling sites on the figures of the previous section are reported in Supplementary Table. In the below reported Table 1 these results are summarized, reporting a total of 17 phosphates found in the investigated caves; these are shortly described below. Together with these phosphates, an almost ubiquitous secondary mineral produced by guano decomposition is gypsum, a sulfate. These minerals were identified by XRD analysis, with the following exceptions: Raman spectroscopy for Isturitz Cave (all samples), Raganeous Cave (RBB), and Palombara Cave (PA23); in Salnitro they were confirmed using EDAX.

Table 1. List of the 18 minerals (17 phosphates and 1 sulfate) found in the investigated caves. Chemical formulae are according to the IMA-CNMNC list of mineral names (http://nrmima.nrm.se//imalist.htm). For more details on the sampled that delivered these minerals in the different caves see Supplementary Table.

Mineral name	Chemical formula	Cave
Ardealite	$Ca_2(HPO_4)(SO_4)\cdot 4H_2O$	DB, RC, SN, TC
Berlinite	$AlPO_4$	CC
Brushite	$Ca(HPO_4)\cdot 2H_2O$	DB, RC, SN, TC
Crandallite	$CaAl_3(PO_4)(PO_3OH)(OH)_6$	GC, MI, CA
Fluorapatite	$Ca_5(PO_4)_3F$	DB, MC, AP, KP, LV, SC, *PE*, *PR*
Hydroxylapatite	$Ca_5(PO_4)_3(OH)$	DB, IO, RC, GC, *MC*, MI, AF, PA, MO, PE, SN, CA, PR, CC
Leucophosphite	$KFe^{3+}{}_2(PO_4)_2(OH)\cdot 2H_2O$	CC
Montgomeryite	$Ca_4MgAl_4(PO_4)_6(OH)_4\cdot 12H_2O$	MI
Newberyite	$Mg(HPO_4)\cdot 3H_2O$	TC
Robertsite	$Ca_2Mn^{3+}{}_3(PO_4)_3O_2\cdot 3H_2O$	PA, CC
Spheniscidite	$(NH_4,K)(Fe^{3+},Al)_2(PO_4)_2(OH)\cdot 2H_2O$	DB, JC, CC
Strengite	$Fe^{3+}(PO_4)\cdot 2H_2O$	JC, CC
Taranakite	$(K,NH_4)Al_3(PO_4)_3(OH)\cdot 9H_2O$	DB, MI, PA, PR, CC
Variscite	$AlPO_4\cdot 2H_2O$	MI, PA
Vashegyite	$Al_{11}(PO_4)_9(OH)_6\cdot 38H_2O$	CC
Vivianite	$Fe^{2+}{}_3(PO_4)_2\cdot 8H_2O$	GC
Whitlockite	$Ca_9Mg(PO_4)_6(HPO_4)$	GC
Gypsum	$Ca_2SO_4\cdot 2H_2O$	DB, IO, RC, SM, GM, MI, SN, TC

DB - Baradla-Domica, JC - Julio, IO - Isturitz-Oxocelhaya, RC - Raganeous, GC - Guano, SM - Saint Marcel, GM - Grosse Marguerite, MC - Mescla, AP - Aramiska, KP - Karsi Podot, LV - Lekovita Voda, MI - Monte Inici, AF - Acqua Fitusa, PA - Palombara, MO - Monello, SC - Scrivilleri, PE - Personaggi, SN - Salnitro, CA - Carburangeli, PR - Pertosa-Auletta, TC - Toirano, CC - Corona 'e sa Craba. Italics indicate an uncertain presence of the mineral.

Phosphate minerals

Ardealite displays as white to yellowish, soft powder (Hill & Forti, 1997). In Domica Cave, it is associated with gypsum, brushite, hydroxylapatite, and taranakite (Fig. 2A), as also identified by Kereskényi (2014) in this cave system. In Salnitro Cave it occurs together with brushite and gypsum (Fig. 23D), whereas at Toirano (Colombo Cave) it has been found with newberyite, brushite, and gypsum. In Raganeous Cave, all brown and white alternating layers are made of hydroxylapatite, brushite, and ardealite, but gypsum is also present (Fig. 6B). Further micro-Raman spectroscopy confirmed ardealite to be the major phase (Fig. 28). Since gypsum and brushite are isostructural, ardealite originating from an additional sulfate-ion exchange is frequently associated with these two minerals (Onac, 2012). This sulfate-calcium phosphate corresponds to the early stage of guano breakdown from the reaction of sulfuric and phosphoric acids with limestone (Hill & Forti, 1997; Puşcaş et al., 2014). It

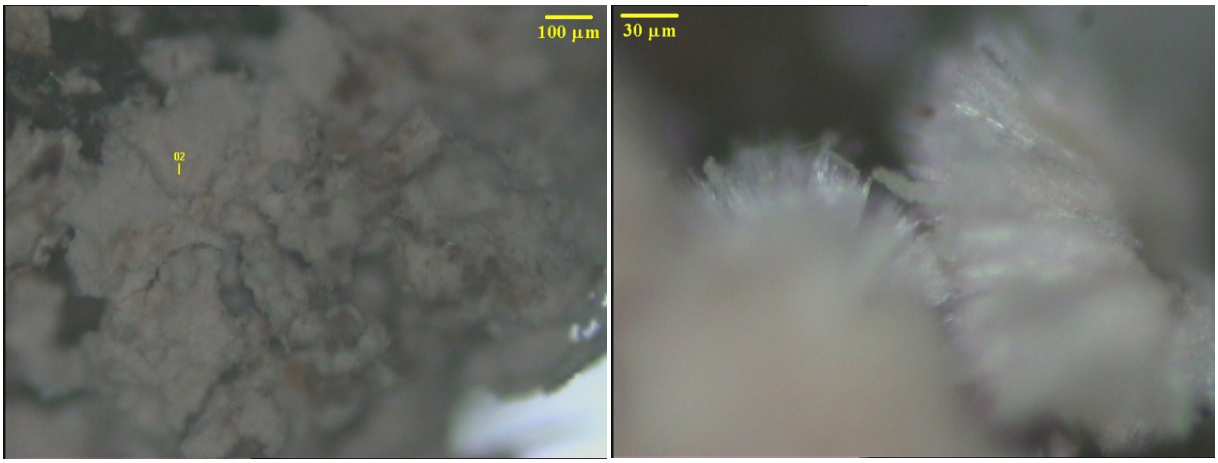

Fig. 28. Micro-photography of ardealite from Raganeous Cave (sample RBB).

is stable in slightly dry conditions and in an acidic environment, at pH of 5.7 to 6.6 (Puşcaş et al., 2014), or even less than 5.5, providing sulfur is available (Marincea et al., 2004a). Ardealite may form during successive stages involving hydroxylapatite ⇒ brushite ⇒ ardealite ⇒ gypsum, this last mineral depositing on the surface (Onac & Vereş, 2003; Marincea et al., 2004a; Onac et al., 2005a; Pogson et al., 2011).

The presence of **Berlinite** is suspected in Corona ‘e Sa Craba Cave based on XRD results. Berlinite is a very rare anhydrous phosphate that requires rather high temperatures to form (over 550°C; Muraoka & Kihara, 1997; Onac & White, 2003; Onac & Effenberger, 2007). In this cave, its presence is very likely, but further investigations are needed to understand its genesis.

Brushite occurs as ivory-yellow, soft, powdery nodules (Hill & Forti, 1997). In Salnitro Cave it occurs together with ardealite and gypsum (Fig. 23D); in Colombo Cave (Toirano) with newberyite, ardealite, and gypsum (Fig. 26B); in Raganeous Cave, with hydroxylapatite, ardealite, and some gypsum (Fig. 6B); in Baradla Cave with fluorapatite, taranakite, and gypsum. In Domica Cave, it is associated with ardealite and hydroxylapatite (Fig. 2A, 2C), where brushite occurs at the base of the guano pile, together with dominant gypsum and apatite. However, it mainly occurs as crusts at some distance below guano leachates, associated with calcite rims deposited later because of Ca oversaturation (Kettner, 1948). Brushite is often associated with gypsum, as a crust below gypsum in guano pots. Brushite, generally associated with ardealite and gypsum, is mainly present on the surface of guano piles and at the base close to the limestone contact, or as crust below guano leachates (Kettner, 1948). Brushite is a common cave mineral, stable in acidic (pH < 6) and damp conditions (Hill & Forti, 1997), with nucleation limits comprised between pH 5.5 and 8 (Onac et al., 2005b). Brushite and hydroxylapatite alternatively precipitate from the same solution, with a nucleation boundary at pH 6.2–6.8, with brushite being the stable species in more acidic conditions (Puşcaş et al., 2014). It forms after reaction of phosphoric acid with limestone rock, where ammonium phosphate derives from guano breakdown, according to the following reaction (after Frost & Palmer, 2011):

$$2NH_3 + H_3PO_4 \rightarrow (NH_4)_2(PO_3OH)$$

$$(NH_4)_2(PO_3OH) + Ca^{2+} + 2H_2O \rightarrow Ca(PO_3OH)\cdot 2H_2O + 2NH_4^+$$

Crandallite was identified only in three caves. In Cocci, it is located between old guano and weathered limestone, associated with montgomeryite and hydroxylapatite (Fig. 16, Fig. 29A). It occurs as light greenish spherules in a white-yellowish-greenish material. In Guano Cave, it is located between guano and clay, and is also associated with hydroxylapatite. It was also found in Carburangeli Cave. Crandallite forms after neutralization of phosphoric acid solutions at the contact with limestone that provides Ca, whereas Al comes from clay (Hill & Forti, 1997).

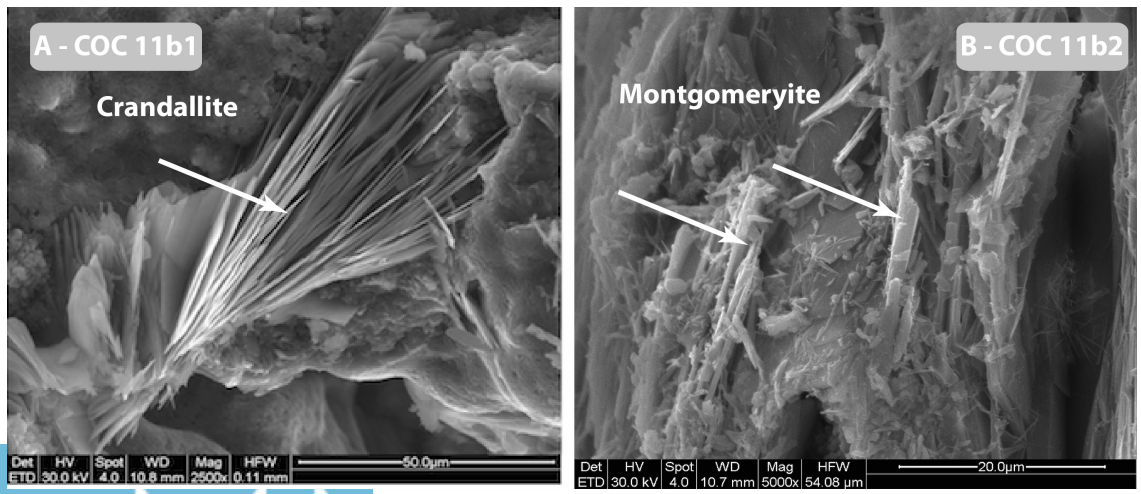

Fig. 29. SEM pictures of A) Crandallite and B) Montgomeryite from Cocci Cave (Photo by E. Galli).

Fluorapatite is found in Baradla Cave (Fig. 2C) in a yellow layer associated with brushite and quartz, in a crust now underwater in Mescla Cave (France), and in the caves of Macedonia region (Aramiska Peštera, Karši Podot (Fig. 12), and Lekovita Voda). A carbonate-rich fluorapatite is found in Scrivilleri (Fig. 20B) and Cocci caves, Italy, as a dark brown layer associated with detrital material (quartz, calcite, goethite, kaolinite).

Fluorapatite derives from hydroxylapatite after the replacement of the hydroxyl ion by fluorine, which may be provided by the host rock (Hill & Forti, 1997), but in our caves, it likely comes from paleontological remains (bones or teeth).

Hydroxylapatite exhibits various colors (brown, white, yellow, cream, etc.) and textures (crust, moonmilk paste, etc.). It is associated with brushite and ardealite in Domica Cave, with calcite in the "urine crust" covering ceiling cupolas of Baradla Cave and with gypsum in Cocci Cave (Fig. 16), as a stalactite in Eremita Cave (Fig. 15), and as crust associated to minor robertsite in Palombara Cave (Fig. 18C, Fig. 30). Hydroxylapatite is the most common phosphate mineral due to the neutralization of the acidic solution at the contact with limestone. It is stable at pH 6.2 - 6.6 (Hill & Forti, 1997) and indicates a low Mg environment since this element inhibits the precipitation of hydroxylapatite (Chang et al., 2010).

Hydroxylapatite is often difficult to distinguish through XRD analysis from fluorapatite. In Isturitz Cave, hydroxylapatite was identified on all four samples using Raman spectroscopy. The sample from Great Pillar Cave provided spectra with the characteristic bands of calcite (at 1,085, 711, 285, and 154 cm^{-1}) and of hydroxylapatite at 960 cm^{-1}, slightly distorted and wider than normal, indicating the presence of other phosphates (Fig. 31). EDXRF shows an increase of phosphorus concentration from the calcite host rock (3 mg/g) toward the phosphatized zones (40 to 120 mg/g). The highest concentration was found in the white weathered ring covering the inner part of the guano pot located in *Lithophone* site (Prieto et al., 2015).

Leucophosphite was identified only from Corona 'e sa Craba Cave. The mineral derives from interaction of bat guano solutions with iron-rich materials, such as

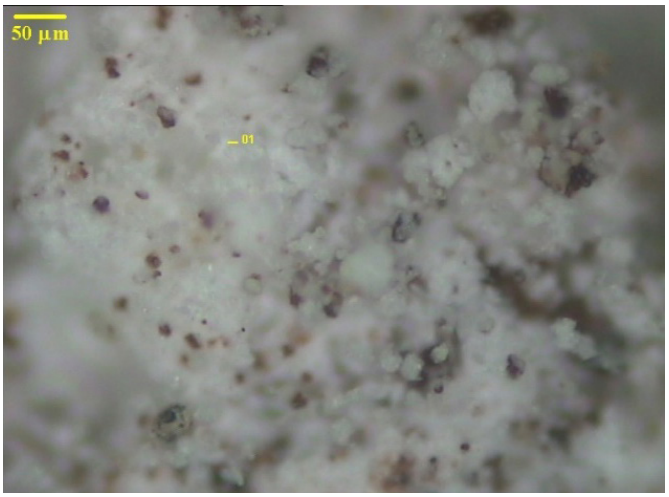

Fig. 30. Micro-photography of hydroxylapatite in Palombara Cave (PA23).

volcanic clays. It occurs together with its close relative spheniscidite, from which it is difficult to differentiate. The presence of leucophosphite was confirmed by SEM-EDS analysis showing the presence of potassium (Fig. 32).

Montgomeryite is present only in Cocci Cave, between old guano and weathered limestone, associated with crandallite and hydroxylapatite (Figs. 16, 29B). It appears as light pinkish aggregates in a white-yellowish-greenish material derived from reaction between guano and the host rock. Similar to crandallite, montgomeryite forms after neutralization of acidic solution at the contact with limestone, which supplies Ca and Mg, whereas Al comes from clay. Due to Ca and Mg leaching, it is metastable and converts into crandallite and eventually to variscite (Hill & Forti, 1997).

Newberyite has been discovered in Grotta del Colombo, part of the Toirano cave complex (Liguria). It was found together with gypsum as a hard-yellowish crust on old guano heaps in a large entrance hall in open communication with the outside atmosphere (Fig. 26B). This mineral is more typical of caves of a warm and dry climate (Hill & Forti, 1997). However, in Toirano, the genesis of this mineral likely comes from the interaction of phosphates with Mg provided by the disaggregation of dolomitic host rock or by seepage from this rock, whereas air exchanges with the atmosphere provide seasonal dry conditions.

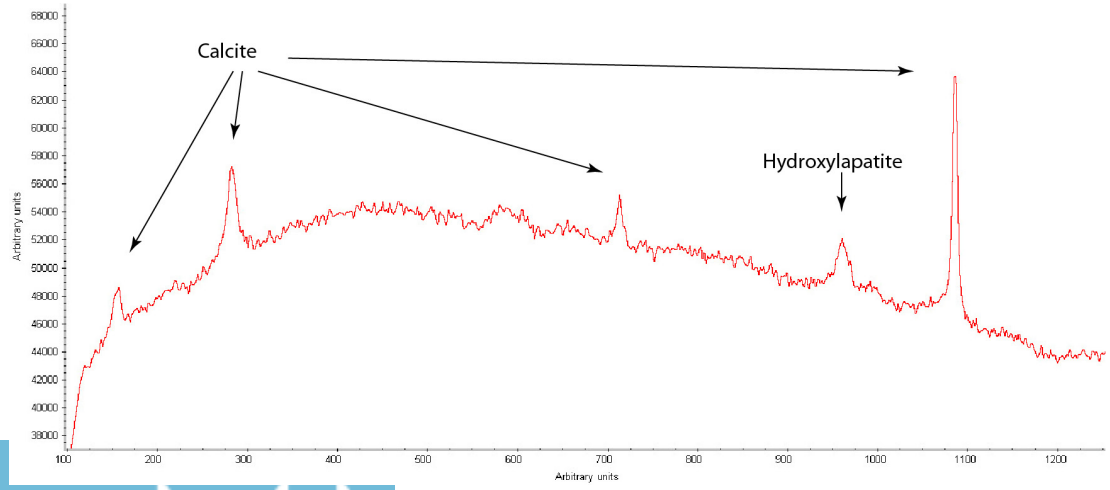

Fig. 31. Raman spectra from Isturitz Cave, France (Prieto et al., 2015).

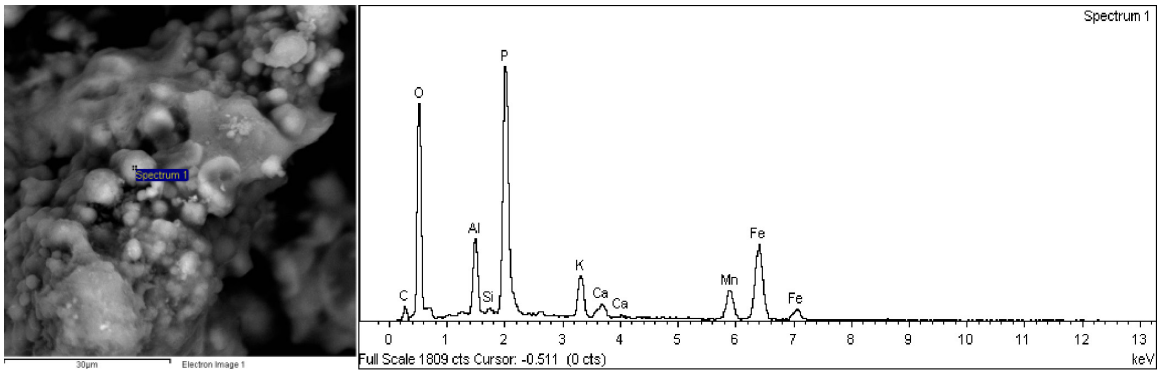

Fig. 32. SEM-EDS spectra of spheniscidite in Corona 'e sa Craba cave. Potassium (K) indicates the presence of a minor leucophosphite phase (Baldoni et al., 2013).

Robertsite is a calcium-manganese phosphate deriving from the reaction with host rock that provides the metallic ions. Robertsite is generally associated to the weathering of pegmatitic deposits. Its occurrence in caves is very rare, only reported in Puerto Princesa Underground River, Philippines (De Vivo et al., 2013), and in Corona 'e sa Craba Cave, Italy (Sauro et al., 2014). In Palombara Cave, robertsite is a minor compound associated with hydroxylapatite (Fig. 18C). Mn is likely related to rising fluids, since Palombara is a hypogene thermal cave. The presence of **Pararobertsite** was suspected from XRD. Further micro-Raman spectroscopy showed that manganese is indeed present in oxides (jacobsite or todorokite), but the Mn phosphate pararobertsite could not be confirmed because of the difficulty to distinguish its spectra from robertsite and hydroxylapatite.

Spheniscidite is found in Baradla Cave, in a white laminated layer near the bottom of a guano accumulation, close to the contact with limestone and clay substratum (Fig. 2C). It is associated with taranakite, quartz, and illite. In Corona 'e sa Craba Cave, small crystals of spheniscidite (10 µm) are forming purple-violet crusts that cover the walls close to fresh guano deposits (Fig. 27B). In Julio Cave, it crops out along with strengite as thick grey deposits derived from the weathering of fluvial silts. The chemical formula of spheniscidite is very close to that of leucophosphite (the latter containing Al and NH_4). The breakdown of bat urea first produces gaseous ammonia (NH_3), which in turn produces in the presence of water, the very soluble ammonium ion (NH_4^+). Spheniscidite forms from the reaction of ammonium-rich fresh guano leachates with clay sediments containing Fe, namely illite-group minerals. These three occurrences of spheniscidite are new additions to the first mention reported from a Sardinian cave (Sauro et al., 2014). This mineral is relatively soluble; therefore, it only occurs under conditions allowing its preservation as crusts in a dry environment (Corona 'e sa Craba Cave) or in places where drainage is low (Baradla, Julio).

Strengite has been found in Corona 'e Sa Craba and Julio caves. It derives from the interaction between acidic guano leachates and detrital material (clay, fluvial silts) or host rock providing Fe. A partial substitution of Fe by Al produces Al-rich strengite, a rare occurrence, which is not recognized by the IMA as a bona fide mineral (Onac et al., 2005a).

Taranakite appears as a soft flour-like white powder, and as nodules in clay (Hill & Forti, 1997). It occurs with calcium phosphates (brushite and ardealite), with gypsum in Domica (Fig. 2A, C) and Eremita caves (Fig. 15), with spheniscidite in Baradla Cave, and is always associated with clay material: illite in Baradla Cave; kaolinite in Palombara Cave (Fig. 18B); river sediments in Pertosa-Auletta cave system (Fig. 25C); kaolinite and montmorillonite in Eremita Cave. Taranakite forms in damp (Hill & Forti, 1997) and slightly acidic conditions at pH 5.7 – 6.1 (Onac, 1996; Puşcaş et al., 2014) from the reaction of guano-related phosphate solutions with clay substratum containing illite or kaolinite that provide K^+ and Al^{3+}.

In Palombara Cave (Sicily), **Variscite** occurs as an intense purple layer sandwiched below old guano and above white taranakite; this last mineral rests on clay substratum that contains quartz and kaolinite (Fig. 18B). In Eremita Cave, variscite is associated with gypsum and occurs as a white layer above a yellow accumulation of taranakite and gypsum, with the latter one resting on clay substratum that contains montmorillonite and kaolinite (Fig. 15). Variscite forms from guano-related phosphate leachates reacting with clays such as kaolinite that provide Al^{3+}, and where K^+ and Fe^{2+} are not available.

Vashegyite is present in Corona 'e Sa Craba Cave. It is a rare cave mineral resulting from the interaction of bat guano solutions with clays providing Al, in slightly acidic and permanent wet conditions (Forti et al., 2000; Onac et al., 2006b).

Vivianite is suspected to be present in Guano Cave. It is a rare cave mineral, mentioned first in Niah Great Cave, Malaysia (Bridge & Robinson, 1983), then in Megali Grava Cave, Greece (Theodorou et al., 2004) and Grotta Castellana, Italy (Hill & Forti, 1997). There, vivianite derives from the reaction of guano with "*terra rossa*" in a strong reducing environment, due to presence of coal and organic matter. We speculate similar conditions in Guano Cave.

Whitlockite is a rare mineral first described in a cave at Sebdou, Algeria (Bannister & Bennett, 1947) and in El Capote Cave, Mexico (Peréz Martínez & Wiggen, 1953). It constitutes various speleothems as isolated aggregates or earthy material (CAMIDA, 2018). We found whitlockite only in Guano Cave, on the weathered layer of a dolomitic wall. It is associated with hydroxylapatite and possibly vivianite (see above), together with muscovite, quartz, and birnessite (Mn

oxide of Ca-Na). The three last minerals are partly or entirely allogenic. Whitlockite derives from interaction of bat guano solutions with carbonate walls providing Ca and Mg. Alternatively, it could form from the dissolution of apatite and subsequent precipitation in the presence of low Ca concentration solutions (Peréz Martínez & Wiggen, 1953; Bridge & Robinson, 1983; Onac et al., 2009).

Sulfates

Gypsum is a common sulfate cave mineral, often related to bat guano deposits, the oxidation of pyrite from bedrock or sediments, or to sulfuric acid speleogenesis (De Waele et al., 2016). In the case of bat guano deposits, it occurs as crystalline crusts due to evaporation on the surface, or as interbedded lenses, pure or associated with other minerals. It forms from sulfuric acid solutions originating from the decaying guano that reacts with drippings providing carbonates in solution. As crystalline crust, it is present in yellow crystalline masses on old guano in Saint-Marcel Cave (Fig. 8C) and Raganeous Cave (Fig. 6C), in Colombo Cave associated with newberyite (Fig. 26B), in a black crust on a wall in Salnitro Cave associated to hydroxylapatite, in Eremita Cave as soft microcrystalline deposits on the surface of guano (Fig. 15), in Cocci Cave as crusts or transparent crystals. The thick white crust covering limestone blocks nearby old guano in *Rhinolophes* Chamber (Isturitz Cave; Fig. 5B), provided characteristic Raman spectra of gypsum. EDXRF shows that phosphorus concentration is here limited to 14 mg/g, whereas it reaches 40-100 mg/g in the uppermost dark phosphate crust directly exposed to bat drops (Prieto et al., 2015).

The second type of gypsum occurrence is that of layers of various thickness and purity. In Raganeous, Baradla, and Domica caves, as white paste, alone (Ba 4d), or associated with ardealite and brushite (Pr. B, RBB) (Fig. 2A). In Eremita (Eremita 3, 4, and ERE 14; Fig. 15) and Grosse Marguerite (Fig. 9B), pure gypsum constitutes a layer of soft yellow or compact white material, respectively.

Radiocarbon dating of guano piles

Thirty-two radiocarbon dates were performed on six guano piles, with 4 of them carried out along a vertical profile (Table. 2). Raganeous Cave shows a continuous deposit of about 1000 years. The oldest age at AD 1004, corresponds to the depth 1.72 m. The sample taken at 0.48 m deposited at AD 1843. The oldest cone was probably entirely mined for fertilizer around AD 1349 (according to the age of the wood torch found at a depth of 1.5 m), whereas the present cone has formed since. In Domica Cave, Prales guano pile is still actively accumulating, as compared to pictures taken about 65 years ago (Kettner, 1948). The two cores reaching the bottom date back to AD 1351 and AD 1102 respectively. Palmový Háj has a similar age at 1 m depth (AD 990; Krištůfek et al., 2008), whereas most of the accumulation between 60 cm and the subsurface is bracketed between AD 1654 and AD 1831. In Saint-Marcel, the date (1916 BC) corresponds to the surface of the guano accumulation, whereas in Baradla (281 BC) it corresponds to the bottom. For Grosse Marguerite, radiocarbon dates yielded calibrated ages comprised between 5040 BC and 2741 BC. The central white unit, made of pure gypsum, is framed between 4524 BC and 2889 BC.

Table 2. Radiocarbon dating of guano, including previous studies in Saint-Marcel (Dodelin, unpubl.) and Domica G1-5 samples (Krištůfek, 2008).

Cave	Site	Lab.	Lab. no.	Sample no.	Dist. from surface (cm)	Conventional radiocarbon age (AMS)	Median Probability Cal year AD/BC	cal AD/BC age ranges		Probability distribution
Raganeous	Guano hill (base of shaft)	Poznań Radiocarbon Laboratory	Poz-72000	RAG-C3-S4	48,5	85 ± 30 BP	1843	1809	1926	0.734
			Poz-59140	RAG-C3-S3	76,5	200 ± 30 BP	1771	1730	1809	0.567
			Poz-71999	RAG-C3-S3	79.5	175 ± 30 BP	1770	1725	1815	0.556
			Poz-59141	RAG-C3-S2	72,5	140 ± 30 BP	1807	1798	1891	0.383
			Poz-71998	RAG-C3-S2	99,5	180 ± 30 BP	1770	1726	1814	0.569
			Poz-71997	RAG-C3-S2	129,5	290 ± 30 BP	1566	1493	1601	0.675
			Poz-59142	RAG-C3-S1	125,5	260 ± 25 BP	1647	1630	1668	0.679
			Poz-72060	RAG-C3-S1	149,5	305 ± 30 BP	1562	1488	1603	0.745
			Poz-62932	Wood torch	158.5	620 ± 30 BP	1349	1292	1399	1.000
			Poz-59143	RAG-C3-S1	169,5	1015 ± 25 BP	1013	978	1042	0.981
			Poz-72061	RAG-C3-S1	171,5	1030 ± 30 BP	1004	962	1041	0.965
Saint-Marcel	Bat gallery	Centre de datation radiocarbone (CDRC), Lyon	Ly-16803	SM1	Surface	3565 ± 30 BP	1916 BC	1982 BC	1872 BC	0.834

Baradla	Libanon-Hegy	ARTEMIS (LMC14, Saclay)	SAC_45654	BA4 3-4	≈ 50	2205 ± 40 BP	281 BC	379 BC	177 BC	1.000
Domica	Palmový Háj. Guano hill	Poznań RL	Poz-18867	G1	0-3	109.51 ± 0.35 pMC	Modern (Post to 1957 AD)	> 1957 AD		
			Poz-18868	G2	0-3	120 ± 30 BP	1831	1801	1939	0.659
			Poz-18869	G4	0-3	135 ± 30 BP	1813	1799	1892	0.414
			Poz-18870	G3	60-65	250 ± 30 BP	1654	1626	1679	0.596
			Poz-18871	G5	100-105	1055 ± 30 BP	990	945	1024	0.883
	Palmový Háj. Guano hill	ARTEMIS	SAC_45652	PH 56-57	18	185 ± 30 BP	AD 1770	1726	1813	0,578
			SAC_45653	PH 20-21	54	155 ± 30 BP	AD 1776	1718	1784	0,359
		Poznań RL	Poz#2-79326	PH 1-2	73	250 ± 27 BP	AD 1654	1631	1675	0,658
	Prales Chamber. Guano hill	ARTEMIS	SAC_45651	PR1 4-6	35	915 ± 30 BP	AD 1102	1030	1188	1.000
		Poznań RL	Poz-79327	PR2 4-6	59	625 ± 26 BP	AD 1351	1337	1398	0,606
Grosse Marguerite	Guano hill (top of gallery)	ARTEMIS	SAC_46850	GM2 3-4	3,5	4145 ± 30 BP	2741 BC	2825 BC	2625 BC	0.805
			SAC_46851	GM2 10-11	10,5	4260 ± 40 BP	2889 BC	2937 BC	2854 BC	0.754
			SAC_45658	GM2 22-23	22,5	5690 ± 40 BP	4524 BC	4619 BC	4450 BC	0.956
			SAC_45657	GM2 32-33	32,5	5710 ± 45 BP	4551 BC	4625 BC	4458 BC	0.860
			SAC_45656	GM2 52-53	52,5	6110 ± 40 BP	4986 BC	5068 BC	4892 BC	0.936
			SAC_45655	GM2 58-59	58,5	6075 ± 35 BP	5040 BC	5208 BC	4942 BC	1.000
		ARTEMIS	SAC_46849	GM 1 3-4	3,5	4130 ± 30 BP	2725 BC	2780 BC	2617 BC	0.664
			SAC_45660	GM1 13-14	13,5	4230 ± 60 BP	2795 BC	2932 BC	2620 BC	0.989
			SAC_45659	GM1 31-32	31,5	5750 ± 40 BP	4601 BC	4701 BC	4500 BC	1.000

Acidity of the decaying guano

We measured two profiles along guano accumulations in Domica Cave in *Prales* (PR2) and *Palmový Háj* (PH) (Fig. 33). In *Prales* the guano is still actively accumulating; its basal layer was dated at about AD 1351. The pH profile shows a continuous decrease, from 4.3 to 3.7, with a slight increase at the very bottom. *Palmový Háj*, on the contrary, is not active anymore, showing an oscillation of pH in a narrow range between 3.9 and 3.5. No trend associated to depth-age is visible.

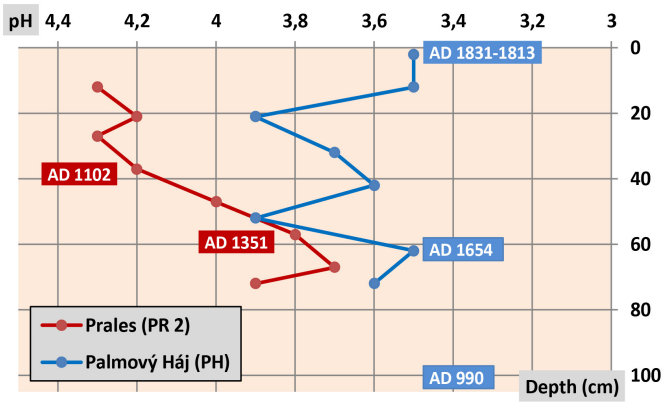

Fig. 33. pH decreases along the PR2 and PH cores in the guano hill of *Prales* Chamber and *Palmový Háj*, Domica Cave, with indication of calibrated ^{14}C ages.

DISCUSSION

Guano-related mineral genesis

The presence of seventeen different phosphate minerals and gypsum in the twenty-two investigated cave systems is related to the presence of different physico-chemical conditions and the availability of different elements in the host rock (Fig. 34). Guano can slowly transform by itself, but its leachates also react with the bedrock and minerals hosted therein (e.g., sulfides such as pyrite), clays, and airborne material. The processes leading to the formation and precipitation of these minerals are: acid digestion, microbially-driven organic decay, self-combustion (since guano decay is an exothermic reaction), and evaporation.

In limestone caves and in acidic, wet and fresh guano deposits, the typical mineral association is composed of brushite, ardealite, and gypsum. These are rather soluble minerals which often do not persist over long periods of times (as guano decomposes), and as such they are found only in rather fresh deposits. Such conditions exist in Salnitro and Toirano caves, and in Saint-Marcel and Raganeous caves. In this last cave, the low maturation of guano is interpreted to be the result of permanent airflow between the entrances that maintain dry conditions, which slows down mineralization. Often, hydroxylapatite also forms under similar conditions, with fluorapatite occurring where guano is in contact with skeleton remains, such as in the three Macedonian caves. These two minerals, which are typical for more neutral condition, due to the buffering effect of the limestone, are the most abundant phosphates found

in guano pots, or as crusts on the limestone walls and roofs. In some caves, these are the only phosphates (e.g., Isturitz, Acqua Fitusa, Monello, Scrivilleri, Personaggi). Their lower solubility makes them the most stable mineral phases during the initial guano digestion. In warmer and drier cave conditions, when bedrock is dolomitic, such as Toirano, newberyite has been found. The presence of gypsum on top of guano deposits is related to the evaporation of water, and these gypsum layers can become rather thick if the evaporative conditions prevail over long-time periods. This is the case for the Grosse Marguerite Cave (where the 15 cm-thick gypsum layer is about 5,000 years old), and in Eremita Cave in Sicily.

If the guano deposits and its leachates are in contact with clays (as interlayers in the limestone or as residual sedimentary deposits (both allochthonous and autochthonous), taranakite, variscite, and the rare montgomeryite and crandallite (e.g., Cocci Cave in Sicily) can typically form (Fig. 35). This often occurs in slightly more acidic conditions, because of the lower buffering effect of the carbonate rock. Both taranakite and variscite are among the most stable phosphates in the cave environment, and once formed they are often preserved over long periods of time, even in rather wet conditions (e.g., Pertosa Cave, Palombara and Eremita caves). Instead, the presence of sulfides, mainly pyrite, in the bedrock will trigger the formation of (Al-rich) strengite and leucophosphite. In a fresh guano environment, spheniscidite can also form in the presence of pyrite or other sulfides such as galena (e.g., Corona 'e sa Craba, Baradla, and Julio caves). Corona 'e Sa Craba is a uniquely rich mineralogical environment, as the cave develops in a quartz vein in close contact with dolomitic and sulfide-rich limestones, thus causing the formation of phosphates such as robertsite, spheniscidite, leucophosphite, vashegyite, strengite, and possibly the rare berlinite. Robertsite has also been found in Palombara Cave, and if combined with some geomorphological indicators, this mineral might point to a hypogene origin of this cave.

A mature occurrence of mineralized guano normally leads to the formation of apatite-group minerals, occurring in well-crystallized forms, even layered stalagmites and stalactites in Eremita Cave, Cocci Abyss, Sicily (D'Angeli et al., 2018).

Survival of the very soluble gypsum

As most sulfates, gypsum is rather soluble and therefore, in very wet cave environments it can be dissolved. However, gypsum can be present where it

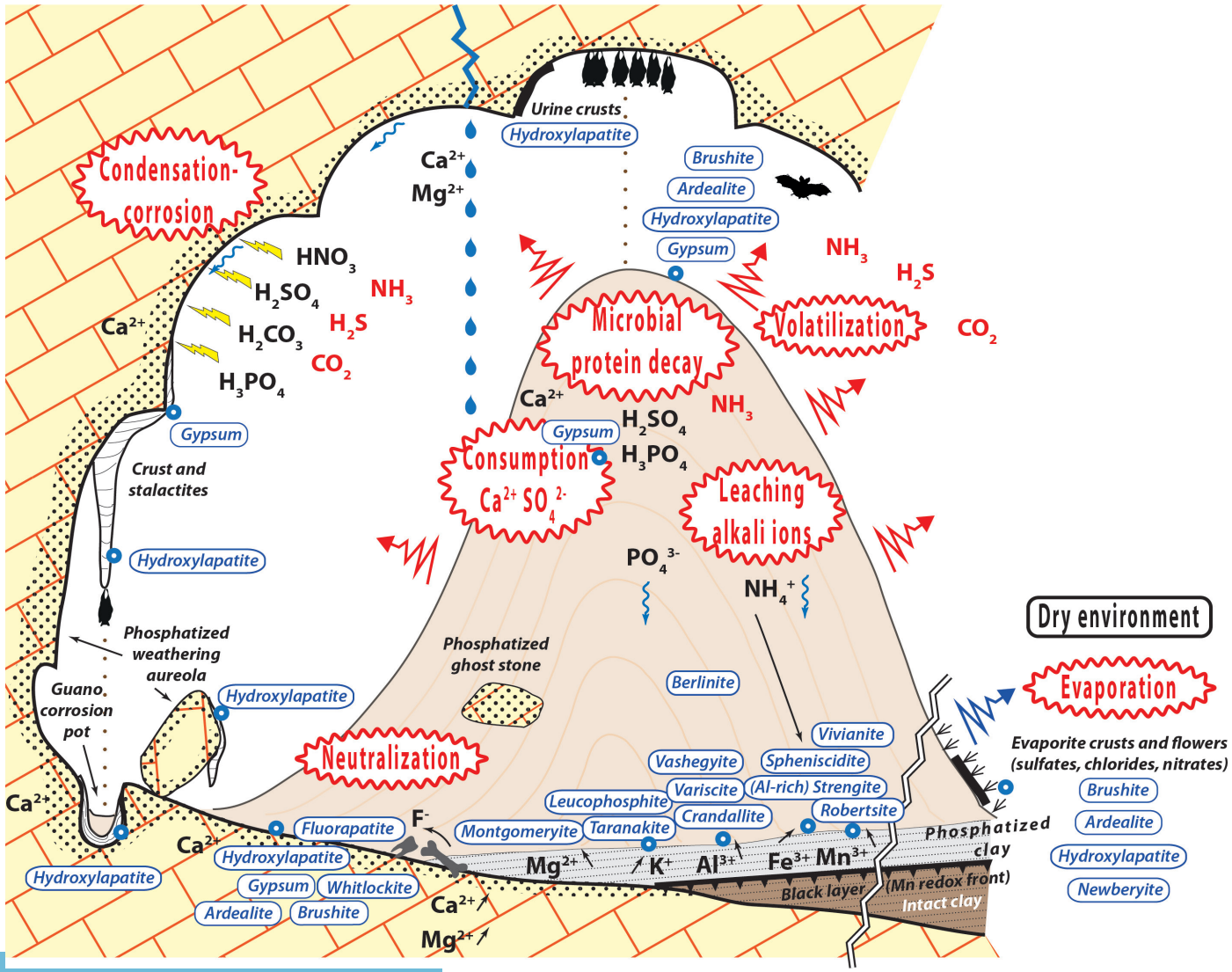

Fig. 34. Idealized diagram showing the occurrence of the eighteen guano-derived minerals in the studied cave environments and the processes involved in their formation.

forms from fresh guano decaying, in the upper part of guano piles which are drier. A typical occurrence is on the surface of a guano heap, especially at a distance from the dripping point location, where evaporation dries up the guano material, attracts the dissolved sulfates by capillary flow, and allows the crystallization and the conservation of sulfates at the interface between wet and dry areas. Providing no leaching occurs, gypsum can even be present at the wet base of guano deposits such as in Domica-Baradla. Gypsum can also persist in areas protected from dripping and leaching (Vanara, 2015).

Age and research potential of guano deposits

Some caves host long records covering the last millennium, such as in *Raganeous*, and possibly the two accumulations in Domica (*Palmový Háj* and *Prales*). Older records are available in *Grosse Marguerite* (2741 to 5040 BC), and possibly also for *Saint-Marcel*, older than 1916 BC, and *Baradla*, younger than 281 BC. These deposits kept their original stratigraphy and were only affected by strong compaction due to their own weight. High-resolution dating would help to show their continuity or their gaps resulting from temporary abandonment of the shelter by bats, generally in relationship with climatic and/or environmental changes. However, the regular laminated guano accumulation in *Raganeous* was demonstrated to be continuous over the last millennium (Bentaleb et al., in prep.). Since guano deposits can be used as paleo-environmental proxy, their potential for reconstruction based on the layered records, stable isotopes, pollen, and possibility of dating is very important (Onac et al., 2015; Cleary et al., 2017).

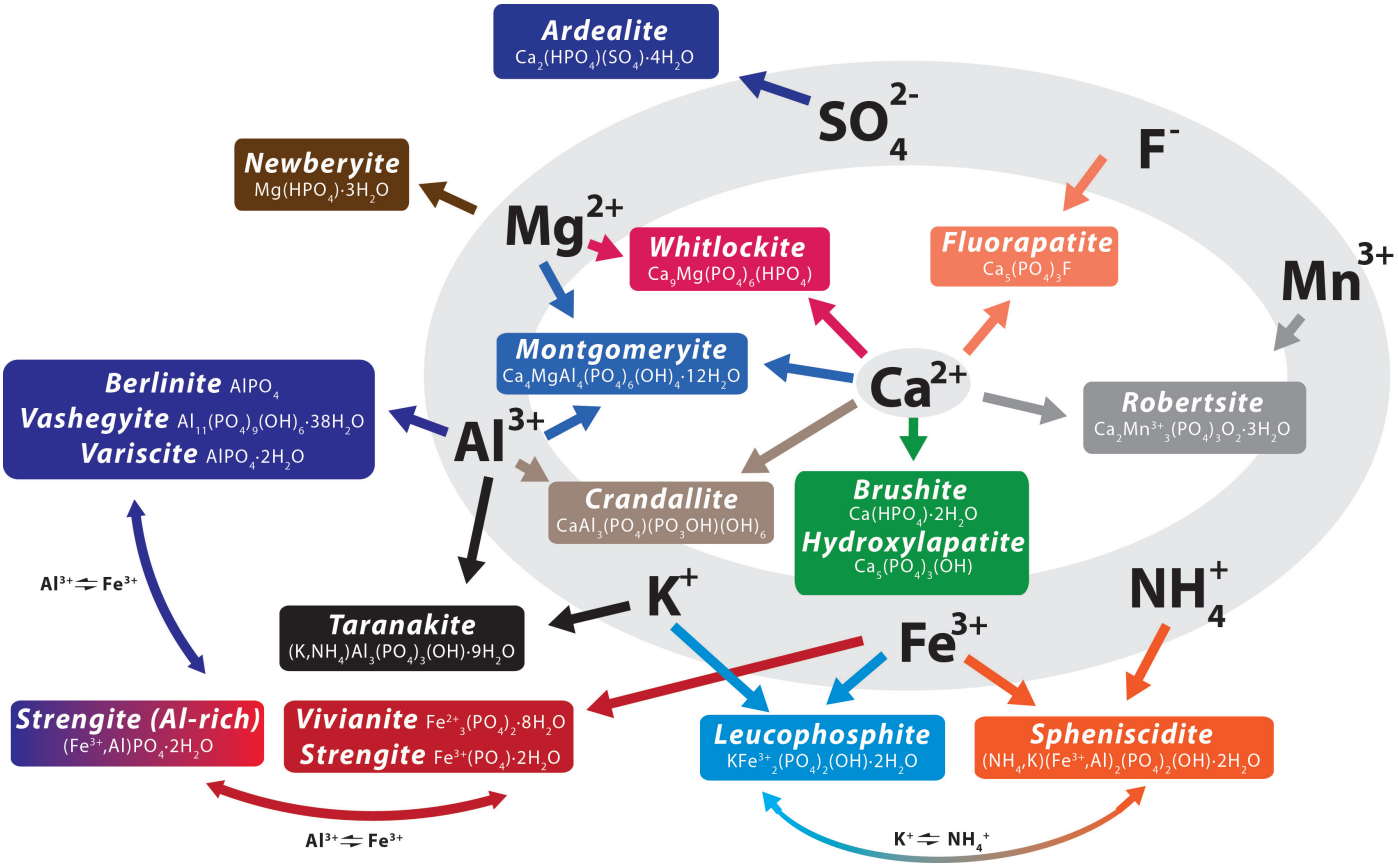

Fig. 35. Composition and inter-relationships of the 17 phosphate minerals according to the contribution of secondary components (Ca-Mg from host rock; Sulfate from organic decay or from pyrites; NH_4 from organic decay; F from bones or teeth; Al-K-Fe-Mn from detrital clay).

Strong acidity of the decaying guano and environmental conditions for mineral genesis

Although fresh guano is slightly alkaline (Audra et al., 2016), its organic decay progressively delivers acids (nitric, sulfuric, phosphoric, and carbonic) that contribute to the increase of acidity with pH as low as 2-4 (Martini, 1993, 2000; Hill & Forti, 1997, 2001). This acidic environment contributes to the genesis of minerals, mainly phosphates but also some sulfates and sometimes nitrates, through the interaction with organic matter (e.g., NH_4^+), with solutes from dripping (e.g., Ca, Mg), with the carbonate host rock (calcite or dolomite), and with detrital material providing Al, Fe, K, Mg, Mn, etc. In Domica Cave, we observed that the pH in the active guano pile decreases almost continuously with depth, where the 600-years old mineralized guano shows pH of 3.7. The slight increase to 3.9 at the bottom could be interpreted as the beginning of acid solutions neutralization at the proximity with the limestone pavement. On the contrary, in the inactive and already partly mineralized guano pile, the pH is very acidic all along the profile (3.5 to 3.9), with fluctuations that do not depend on depth. Such evolution of the acidity throughout the guano deposit profile leads to various environmental conditions that constrain the stability of minerals (Fig. 36). The stable end-members of phosphatization are the minerals of the apatite group formed in alkaline environment buffered by the carbonate substratum, and strengite and variscite in acidic conditions. Gypsum has a quite large stability field.

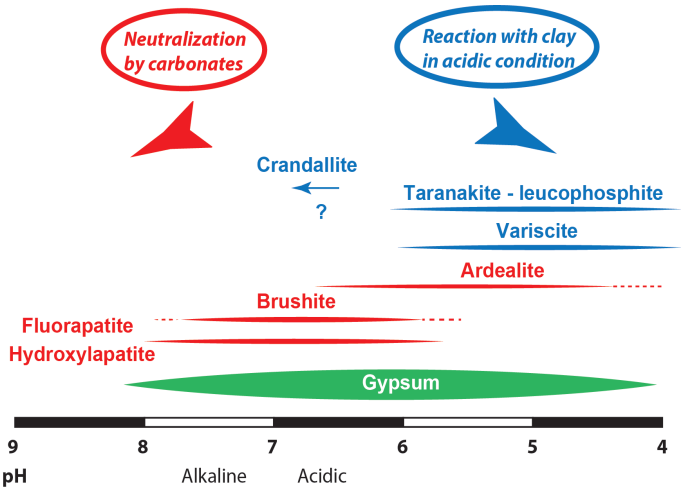

Fig. 36. Synthesis of approximate stability field of studied phosphate minerals and gypsum (after Onac & Vereş, 2003; Shahack-Gross et al., 2003; Onac et al., 2005b; Giurgiu & Tămaş, 2013).

CONCLUSIONS

We investigated guano-related minerals in 22 European caves located in the Slovak Republic, Hungary, France, Macedonia, and Italy. Using XRD, micro-Raman spectroscopy, and SEM, we identified 17 phosphate minerals (not considering Al-rich Strengite that is not recognized by IMA), some of them being very rare in caves, and one sulfate (gypsum). Combining pH and micro-climatic measurements with ^{14}C radiometric dates, we characterized some environmental parameters that control mineral genesis and the relationships between some minerals and their environment.

- On fresh decaying guano, the typical precursor mineral association is composed of brushite, ardealite, and gypsum. Such minerals are soluble and do not persist long in older guano accumulations.
- The apatite minerals (hydroxylapatite, fluorapatite) precipitate onto carbonates – limestone or calcite speleothems – by buffering of acid phosphate leachates. They generally occur as light or brown crusts on the walls and floors that can cover extensive areas. Their low solubility triggers high stability, hence the dominant abundance of this mineral association.
- The contact of acidic guano leachates with cave sediments, mainly clay and fluvial deposits and sometimes sulfides such as pyrite, allows the hydrolysis of the detrital minerals and the combination of their cations (Al, K, Fe, and Mn) with the phosphatic leachates. Taranakite, strengite, and variscite are the end-members of the mineral suites, hence the most stable and frequent minerals. However, the large amount of combinations and environmental characteristics allows the formation of rare phosphates, most of them being known only from a limited number of caves on Earth (montgomeryite, crandallite, (Al-rich) strengite, leucophosphite, vashegyite, vivianite, whitlockite, berlinite). Spheniscidite was found for the first time in caves in three of the studied sites, and robertsite is known only in three caves in the world, two of them presented in this study.
- Caves are generally wet, hence the abundance of hydrated phosphates. Less frequently, strong dehydration may produce rare minerals: guano self-combustion is suspected to be at the origin of a possible occurrence of berlinite (requiring temperatures above 570°C). Gypsum may persist in especially dry environment and even at the bottom of guano accumulation with poor drainage (damp conditions).
- Acidity of a decaying guano heap is well known. We measured pH as low as 3.5, which can persist even in old guano deposits. The distribution of acidity controls the mineral assemblage and the stability of end-member phosphates, in acid environment or alkaline at the contact with the limestone bedrock.
- We found guano more than 6000 years old, with an accumulation covering more than 2300 years in Grosse Marguerite Cave, France. Although the continuity of this deposit is still questioned, in Raganeous Cave it appears to be as old as 1000 years.
- Most of the previous studies on phosphate minerals, including this one, have been carried out by visually-oriented sampling strategy. Future investigations, which would also benefit from the fast development of portable analytical tools, should progressively turn to more continuous analyses. First, this will allow new mineral discoveries, and second it would lead to a better understanding of the environmental parameters that control mineral genesis. Finally, the use of different biological (pollen) and chemical (stable isotope) proxies available in guano offer a great potential for paleoenvironmental and paleoclimatic reconstruction.
- Some caves, characterized by specific environmental conditions, host rock composition, sediments, sulfides, or micro-climatic conditions, may represent outstanding sites for mineral studies, and particularly for phosphates and secondary sulfates related to bat guano deposits. Corona 'e sa Craba (Sardinia) and Domica-Baradla (Slovakia-Hungary), are two such examples of unique caves for their phosphate mineralogy.

ACKNOWLEDGEMENTS

We are deeply grateful to B.P. Onac and C.A. Hill for their thoughtful review that helped improving the paper. Part of this work was initiated by a French-Czech bilateral program PHC Barrande n° 33988RL (PA, IB, AC, VK). It also benefited of the International Cooperation Project - Cori 2012, Dipartimento di Scienze della Terra e del Mare (DiSTeM), Università degli Studi di Palermo (PA) and of the Program "The decorated caves of the Gaztelu Hill (Saint-Martin-d'Arberoue, Pyrénées-Atlantiques). Study of Paleolithic art: Isturitz, Oxocelhaya-Hariztoya and Erberua" funded by the Archeology Regional Service Nouvelle-Aquitaine, direction D. Garate. J. Benes, University of

South Bohemia, provided funding for the radiocarbon dating of Domica guano. We are grateful to many people who participated to this work: D. Borschneck (CEREGE) and V. Heresanu (CINaM), who performed the XRD analysis; D. Garate, M. Olivares, and K. Castro (Departamento de Química Analítica, Facultad de Ciencia y Tecnología, Universidad del Pais Vasco, UPV/EHU) for the EDXRF and Raman in-situ analysis in Isturitz-Oxocelhaya caves; B.P. Onac for his help during the analysis of the Corona 'e sa Craba mineral samples and for useful discussions. For permission to cave access and help during sampling: R. Chiesa, the Archaeological Superintendency of Liguria and Toirano Municipality for access granted to the Toirano caves; Francescantonio d'Orilia, Fondazione MiDa and the cave guides for help during sampling at Pertsosa-Auletta cave; F. Branca and E. Amore (Riserva naturale integrale Grotta Palombara); S. Costanzo (Riserva naturale integrale Grotta Monello); R. Di Pietro (Riserva Naturale Integrale Grotta di Carburangeli); J. Darricau (Grotte d'Isturitz, Association Gaztelu); Aggtelek National Park (Baradla Cave); V. Papáč (Slovak Caves Administration, Domica Cave), O. Peyronnel (Ardèche Gorges National Reserve). For their help in the field: P. and Z. Zentay, A. Hajnal, J. Petrásek, P. Tordjman, cavers from ANS Le Taddarite of Palermo, A. Cariola., L. Catsoyannis, G. Coquin and M.-L. Madelaine, who shared with us the discovery of the Raganeous Cave. M.-C. Lankester, for information about the bat community in Raganeous Cave. C. Dodelin, who provided the ^{14}C dating result of Saint-Marcel guano and guided us in this cave and M. Faverjon for the survey. J. Medina (Univ. Valladolid), for the in-depth XRD analysis on Palombara and Raganeous samples. P. Camps (Géosciences Montpellier), for the paleomagnetic measuring of Palombara Cave samples. I.B. thanks C. Moreau and J.-P. Dumoulin of ARTEMIS AMS facility (LMC14, Saclay, France) who performed radiocarbon dates referenced as "SAC" and T. Goslar of the Poznań Laboratory for Radiometric Dating reference as "Poznan LR". We are gratefull to MISTRAL-BIODIVMEX CNRS program for participating to the funding of Poznan radiocarbon datings.

REFERENCES

Audra P., Folléas C., Gimenez B., Hof B., Hotz B. & Sounier J.P., 2002 – *Spéléologie dans les Préalpes de Grasse*. Édisud, Aix-en-Provence, 180 p.

Audra P., Barriquand L. Bigot J.-Y., Cailhol D., Caillaud H., Vanara N. & Nobécourt J.-C., 2016 – *L'impact méconnu des chauves-souris et du guano dans l'évolution morphologique des cavernes*. Karstologia, **68**: 1-20.

Baldoni E., De Waele J., Galli E., Messina M., Onac B.P., Sanna L., Sauro F. & Villani M., 2013 – *Mineralogy and speleogenesis of the Corona 'e sa Craba quartzite cave (Carbonia, Southwestern Sardinia)*. In: De Waele J., Forti P. & Naseddu A. (Eds.), *Memorie dell'Istituto Italiano di Speleologia S.* **II**, **XXVIII** (Proceedings of the 2nd International Symposium on mine caves, Iglesias, 2012), 197-210.

Bannister F. & Bennett H., 1947 – *Whitlockite from Sebdou, Oran, Algeria*. Mineralogical Magazine and Journal of the Mineralogical Society, **28**: 29-30. https://doi.org/10.1180/minmag.1947.028.196.06

Bella P. & Lalkovič M., 2001 – *Jaskyňa Domica. Správa slovenských jaskýň, Liptovský Mikuláš*. Cave Domica, Slovak Cave Administration, Liptovský Mikuláš [in Slovak]. http://www.ssj.sk/en/jaskyna/7-domica-cave

Bella P., Bosák P., Braucher R., Pruner P., Hercman H., Minár J., Veselský M., Holec J. & Léanni L., 2019 – *Multi-level Domica–Baradla cave system (Slovakia, Hungary): Middle Pliocene–Pleistocene evolution and implications for the denudation chronology of the Western Carpathians*. Geomorphology, **327**: 62-79. https://doi.org/10.1016/j.geomorph.2018.10.002

Bridge P.J., 1977 – *Archerite $(K,NH_4)H_2PO_4$ - a new mineral from Madura , Western Australia*. Mineralogical Magazine, **41**: 33-35. https://doi.org/10.1180/minmag.1977.041.317.05

Bridge P.J. & Robinson B.W., 1983 – *Niahite - a new mineral from Malaysia*. Mineralogical Magazine, **47**: 79-80. https://doi.org/10.1180/minmag.1983.047.342.14

Brunet P., Dupré B. & Faverjon M. (Eds.), 2008 – *La grotte de Saint-Marcel-d'Ardèche*. Comité Départemental de Spéléologie de l'Ardèche, 242 p.

CAMIDA, 2018 – Cave Mineral Database. http://caveminerals.rc.usf.edu

Chang S.J., Blake R.E., Stout L.M. & Kim S.J., 2010 – *Oxygen isotope, micro-textural and molecular evidence for the role of microorganisms in formation of hydroxylapatite in limestone caves, South Korea*. Chemical Geology, **276**: 209-224. https://doi.org/10.1016/j.chemgeo.2010.06.007

Cleary D.M., Wynn J.G., Ionita M., Forray F.L. & Onac B.P., 2017 – *Evidence of long-term NAO influence on East-Central Europe winter precipitation from a guano-derived $\delta^{15}N$ record*. Scientific Reports, **7**: 14095. https://doi.org/10.1038/s41598-017-14488-5

Créac'h Y., 1967 – *Inventaire spéléologique des Alpes-Maritimes*. Fédération Française de Spéléologie & Bureau de recherches géologiques et minières, Orléans, tome II, 350 p.

D'Angeli I.M., Carbone C., Nagostinis M., Parise M., Vattano M., Madonia G. & De Waele J., 2018 – *New insights on secondary minerals from Italian sulfuric acid caves*. International Journal of Speleology, **47 (3)**: 271-291. https://doi.org/10.5038/1827-806X.47.3.2175

De Vivo A., Piccini L, Forti P. & Badino G., 2013 – *Some scientific features of Puerto Princesa Underground River (Palawan, Philippines)*. In: Filippi M. & Bosak P. (Eds.), *Proceedings of the 16th International Congress of Speleology*, Brno, **3**: 35-41. http://www.speleogenesis.info/directory/karstbase/pdf/seka_pdf13563.pdf

De Waele J., Audra P., Madonia G., Vattano M., Plan L., D'Angeli I.M., Bigot J.-Y. & Nobécourt J.C., 2016 – *Sulfuric acid speleogenesis (SAS) close to the water table: Examples from southern France, Austria, and Sicily*. Geomorphology, **253**: 452-467. https://doi.org/10.1016/j.geomorph.2015.10.019

Di Maggio C., Madonia G., Parise M. & Vattano M., 2012 – *Karst of Sicily and its conservation*. Journal of Cave and Karst Studies, **74 (2)**: 157-172. https://doi.org/10.4311/2011JCKS0209

Di Stefano P., Renda P., Zarcone G., Nigro F. & Cacciatore M., 2013 – *Carta geologica d'Italia alla scala 1: 50.000 e note illustrative del Foglio 619, Santa Margherita di Belice*. Roma: ISPRA, Servizio Geologico d'Italia. http://www.isprambiente.gov.it/Media/carg/note_illustrative/619_S_Margherita_di_Belice.pdf

Dutton A., Scicchitano G., Monaco C., Desmarchelier J.M., Antonioli F., Lambeck K., Esat T.M., Fifield L.K., McCulloch M.T. & Mortimer G., 2009 – *Uplift rates defined by U-series and ^{14}C ages of serpulid-encrusted speleothems from submerged caves near Siracusa, Sicily (Italy).* Quaternary Geochronology, **4**: 2-10. https://doi.org/10.1016/j.quageo.2008.06.003

Forti P., 2001 – *Biogenic speleothems*: an overview. International Journal of Speleology, **30**: 39-56. https://doi.org/10.5038/1827-806X.30.1.4

Forti P., Galli E. & Rossi A., 2000 – *Minerali geneticamente correlati al guano in una grotta naturale dell'Albania. Primo contributo.* Le Grotte d'Italia, **V (1)**: 45-59.

Frost R. & Palmer S.J., 2011 – *Thermal stability of the 'cave' mineral brushite $CaHPO_4{\cdot}2H_2O$ – Mechanism of formation and decomposition.* Thermochimica Acta, **521 (1-2)**: 14-17. https://doi.org/10.1016/j.tca.2011.03.035

Frost R.L., Palmer S.J. & Pogson R.E., 2011 – *Raman spectroscopy of newberyite $Mg(PO_3OH){\cdot}3H_2O$: A cave mineral.* Spectrochimica Acta Part A: Molecular and Biomolecular Spectroscopy, **79 (5)**: 1149-1153. https://doi.org/10.1016/j.saa.2011.04.035

Frost R.L., Palmer S.J. & Pogson R.E., 2012 – *Thermal stability of crandallite $CaAl_3(PO_4)_2(OH)_5{\cdot}(H_2O)$ a 'Cave' mineral from the Jenolan Caves.* Journal of Thermal Analysis and Calorimetry, **107 (3)**: 905-909. https://doi.org/10.1007/s10973-011-1578-6

Fulco A., Vattano M., Valenti P., Madonia G. & Lo Valvo M., 2015 – *The bat fauna of four cavities in south-west Sicily: microclimatic analysis and phenology of communities.* III Convegno Italiano sui Chirotteri, Trento, Abstracts, 30. Gruppo Italiano Ricerca Chirotteri, Roma. http://www.pipistrelli.net/drupal/system/files/GIRC2015_complete.pdf

Gaál F. & Vlček L., 2011 – *Tektonická stavba jaskyne DOMICA (Slovenský kras) Tectonic structure of cave Domica (Slovak Karst).* Aragonit, **16 (1-2)**: 3-11 [in Slovak with English abstract]. http://www.ssj.sk/sk/user_files/Aragonit16_komplet.pdf

Gallay M., Kaňuk J., Hochmuth Z., Meneely J.D., Hofierka J. & Sedlák V., 2015 – *Large-scale and high-resolution 3-D cave mapping by terrestrial laser scanning: a case study of the Domica Cave, Slovakia.* International Journal of Speleology, **44 (3)**: 277-291. https://doi.org/10.5038/1827-806X.44.3.6

Garate D., Labarge A., Rivero O., Normand C. & Darricau J., 2013 – *The cave of Isturitz (West Pyrenees, France): one century of research in Paleolithic parietal art.* Arts, **2 (4)**: 253-272. https://doi.org/10.3390/arts2040253

Giurgiu A. & Tămaş T., 2013 – *Mineralogical data on bat guano deposits from three Romanian caves.* Studia UBB Geologia, **58 (2)**: 13-18. https://doi.org/10.5038/1937-8602.58.2.2

Goldberg P. & Nathan Y., 1975 – *The phosphate mineralogy of et-Tabun cave, Mount Carmel, Israel.* Mineralogical Magazine, **40**: 253-258. https://doi.org/10.1180/minmag.1975.040.311.06

Grassa F., Capasso G., Favara R. & Inguaggiato S., 2006 – *Chemical and isotopic composition of waters and dissolved gases in some thermal springs of Sicily and adjacent volcanic islands, Italy.* Pure and Applied Geophysics, **163**: 781-807. https://doi.org/10.1007/s00024-006-0043-0

Hill C.A., 1999 – *Mineralogy of Kartchner Caverns, Arizona.* Journal of Cave and Karst Studies, **61 (2)**: 73-78. https://caves.org/pub/journal/PDF/V61/v61n2-Hill-Mineralogy.pdf

Hill C.A. & Forti P., 1997 – *Cave minerals of the world* (2nd Ed.). National Speleological Society, Huntsville, Alabama, 464 p.

Karkanas P., Rigaud J.P., Simek J.F., Albert R.M. & Weiner S., 2002 – *Ash bones and guano: a study of the minerals and phytoliths in the sediments of Grotte XVI, Dordogne, France.* Journal of Archaeological Science, **29 (7):** 721-732. https://doi.org/10.1006/jasc.2001.0742

Kaye C.A., 1959 – *Geology of Isla Mona, Puerto Rico, and notes on the age of Mona Passage.* U.S. Geological Survey Professional Paper, **317-C**: 141-178. https://doi.org/10.3133/pp317C

Kereskényi E., 2014 – *A Baradla—Domica-barlangrendszer ásványtani vizsgálata különös tekintettel a foszfátokra; valamint a guanóból származtatható foszfátok terhelése a barlangi környezetre* (*The Baradla cave mineralogical examination of the particular phosphates, as well as phosphates derived from guano of the cave environment*). Master Sc. Dipl. Thesis, University Miskolc, 85 p.

Kettner R., 1948 – *O netopyrím guanu a guanovych korosích v jeskynie Domici* (*The Baradla cave mineralogical examination of the particular phosphates, as well as phosphates derived from guano of the cave environment*). Sbornik Státního geologického ústavu, Praha, XV, p. 41-64.

Kováč Ľ., Elhottová D., Mock A., Nováková A., Krištůfek V., Chroňáková A., Lukešová A., Mulec J., Košel V., Papáč V., Luptáčik P., Uhrin M., Višňovská Z., Hudec I., Gaál Ľ. & Bella P., 2014 – *The cave biota of Slovakia.* State Nature Conservancy SR, Slovak Cave Administration, Liptovský Mikuláš, 192 p. https://www.researchgate.net/publication/269106565_The_cave_biota_of_Slovakia

Krištůfek V., Elhottová D., Kováč L., Chroňáková A., Žák K. & Světlík I., 2008 – *Stáří kopy netopýřího guána v jeskyni Domica (NP Slovenský Kras) a elektronová mikroskopie exkrementů netopýrů (The age of bat guano heap in Domica Cave (Slovak Karst NP) and electron microscopy of bat excrements.* Slovenský Kras - Acta Carsologica Slovaca, **46**: 165-172. https://issuu.com/dankez/docs/slovenskykras_1-2008

Lentini F. & Carbone S., 2014 – *Geologia della Sicilia.* Memoria descrittive della Carta Geologica d'Italia, **95**: 1-413 + map. ISPRA.

Madonia G., Frisia S., Borsato A. Macaluso T., Mangini A., Paladini M., Piccini L., Miorandi R., Spötl C., Sauro U., Agnesi V., Di Pietro R., Palmeri A. & Vattano M., 2003 – *La Grotta di Carburangeli ricostruzione climatica dell'Olocene per la piana costiera della Sicilia nord-occidentale.* Studi Trentini di Scienze Naturali, Acta Geologica, **80**: 153-167. http://www2.muse.it/pubblicazioni/6/actaG80/Vol_ACTA_80_2003_153-167.pdf

Marincea Ş. & Dumitraş D.G., 2005 – *First reported sedimentary occurrence of berlinite ($AlPO_4$) in phosphate-bearing sediments from Cioclovina Cave, Romania.* American Mineralogist, **90 (7)**: 1203-1208. https://doi.org/10.2138/am.2005.418

Marincea Ş., Dumitraş D. & Gibert R., 2002 – *Tinsleyite in the "dry" Cioclovina Cave (Sureanu Mountains, Romania).* European Journal of Mineralogy, **14 (1)**: 157-164. https://doi.org/10.1127/0935-1221/2002/0014-0157

Marincea Ş., Dumitraş D-G., Diaconu G. & Essaid B., 2004a – *Hydroxylapatite, brushite and ardealite in the bat guano deposit from Peştera Mare de la Mereşti, Perşani Mountains, Romania.* Neues Jahrbuch fur Mineralogie-Monatshefte, **10**: 464-488. https://doi.org/10.1127/0028-3649/2004/2004-0464

Martini J.E.J., 1993 – *A concise review of the cave mineralogy of Southern Africa*. Proceedings of the 11th International Congress of Speleology, Beijing, China, p. 72-75.

Martini J.E.J., 1996 – *Contribution to the mineralogy of the Caves of the Gcwihaba Hills, North-Western Botswana*. Bulletin of the South African Speleological Association, **36**: 14-18.

Martini J.E.J., 2000 – *La grotte et le karst de Cango, Afrique du Sud*. Karstologia, **36**: 43-54. https://doi.org/10.3406/karst.2000.1751

Messana E., 1994 – *Il sistema carsico del gruppo montuoso di M. Inici (Castellammare del Golfo, TP)*. Bollettino Accademia Gioenia Scienze Natutali, **27 (348)**: 547-562.

Mocochain L., Bigot J.-Y., Clauzon G., Faverjon M. & Brunet P., 2006 – *La grotte de Saint-Marcel (Ardèche): un référentiel pour l'évolution des endokarsts méditerranéens depuis 6 Ma*. Karstologia, **48**: 33-50. https://doi.org/10.3406/karst.2006.2587

Mocochain L., Audra P. & Bigot J.-Y., 2011 – *Base level rise and per ascensum model of speleogenesis (PAMS). Interpretation of deep phreatic karsts, vauclusian springs and chimney-shafts*. Bulletin de la Société Géologique de France, **182 (2)**: 87-93. https://doi.org/10.2113/gssgfbull.182.2.87

Muraoka Y. & Kihara, 1997 – *The temperature dependence of the crystal structure of berlinite, a quartz-type form of $AlPO_4$*. Physics and Chemistry of Minerals, **24 (4)**: 243-253. https://doi.org/doi.org/10.1007/s002690050036

Nemoz M., 2008 – *Conservation de trois Chiroptères cavernicoles dans le Sud de la France*. Final report LIFE 04NAT/FR/000080, SFEPM, Castanet-Tolosan, 120 p. http://www.sfepm.org/LifeChiropteres/images2/Resultats%20life/rapport_final_08.pdf

Onac B.P., 1996 – *Mineralogy of speleothems from caves in the Padurea Craiului Mountains (Romania), and their palaeoclimatic significance*. Cave and Karst Science, **23 (3)**: 109-120.

Onac B.P., 2012 – *Minerals*. In: Culver D.C. & White W.B. (Eds.), *Encyclopedia of caves* (2nd Ed.). Elsevier, New York, p. 499-508. https://doi.org/10.1016/B978-0-12-383832-2.00072-4

Onac B.P., 2019 – *Cave discovered by mining activities and mined caves*. In: Ponta G.M.L. & Onac B.P. (Eds.), *Cave and karst systems of Romania*. Springer International, Cham, p. 475-483. https://doi.org/10.1007/978-3-319-90747-5_54

Onac B.P. & Forti P., 2011a – *State of the art and challenges in cave minerals studies*. Studia UBB Geologia, **56 (1)**: 33-42. https://doi.org/10.5038/1937-8602.56.1.4

Onac B.P. & Forti P., 2011b – *Minerogenetic mechanisms occurring in the cave environment: an overview*. International Journal of Speleology, **40 (2)**: 79-98. https://doi.org/10.5038/1827-806X.40.2.1

Onac B.P. & Effenberger H.S., 2007 – *Re-examination of berlinite ($AlPO_4$) from the Cioclovina Cave, Romania*. American Mineralogist, **92 (11-12)**: 1998-2001. https://doi.org/10.2138/am.2007.2581

Onac B.P. & Vereş D.S., 2003 – *Sequence of secondary phosphates deposition in a karst environment: evidence from Măgurici Cave (Romania)*. European Journal of Mineralogy, **15**: 741-745. https://doi.org/10.1127/0935-1221/2003/0015-0741

Onac B.P. & White W.B., 2003 – *First reported sedimentary occurrence of berlinite ($AlPO_4$) in phosphate-bearing sediments from Cioclovina Cave, Romania*. American Mineralogist, **88 (8-9)**: 1395-1397. https://doi.org/10.2138/am.2005.418

Onac B.P., Kearns J., Breban R. & Cîntă Pânzaru S., 2004 – *Variscite ($AlPO_4{\cdot}2H_2O$) from Cioclovina Cave (Sureanu Mountains, Romania): a tale of a missing phosphate*. Studia UBB Geologia, **49 (1)**: 3-14. https://doi.org/10.5038/1937-8602.49.1.1

Onac B.P., Ettinger K., Kearns J. & Balasz I.I., 2005a – *A modern, guano-related occurrence of foggite, $CaAl(PO_4)(OH)_2{\cdot}H_2O$ and churchite-(Y), $YPO_4{\cdot}2H_2O$ in Cioclovina Cave, Romania*. Mineralogy and Petrology, **85 (3-4)**: 291-302. https://doi.org/10.1007/s00710-005-0106-4

Onac B.P., Fornós J.J., Ginés A. & Ginés J., 2005b – *Mineralogical reconnaissance of caves from Mallorca Island*. Endins, **27**: 131-140. http://www.raco.cat/index.php/Endins/article/view/122521/169644

Onac B.P., Effenberger H., Ettinger K. & Cinta Panzaru S., 2006a – *Hydroxylellestadite from Cioclovina Cave (Romania): Microanalytical, structural, and vibrational spectroscopy data*. American Mineralogist, **91 (11-12)**: 1927-1931. https://doi.org/10.2138/am.2006.2143

Onac B.P., Zaharia L., Kearns J. & Vereş D., 2006b – *Vashegyite from Gaura cu Muscă Cave (Locvei Mountains, Romania): a new and rare phosphate occurrence*. International Journal of Speleology, **35 (2)**: 67-73. https://doi.org/10.5038/1827-806X.35.2.2

Onac B.P., Sumrall J., Mylroie J.E. & Kearns J., 2009 – *Cave minerals of San Salvador Island, Bahamas*. The University of South Florida Karst Studies Series, **1**, 70 p. http://plantphys.info/bahamas/copyright/onac.pdf

Onac B.P., Forray F.L., Wynn J.G. & Giurgiu A.M., 2014 – *Guano-derived $\delta^{13}C$-based paleo-hydroclimate record from Gaura cu Musca Cave, SW Romania*. Environmental Earth Sciences, **71 (9)**: 4061-4069. https://doi.org/10.1007/s12665-013-2789-x

Onac B.P., Hutchison S.M., Geanta A., Forray F.L., Wynn J.G., Giurgiu A.C. & Coroiu I., 2015 – *A 2500-year Late Holocene multi-proxy record of vegetation and hydrologic changes from a cave guano-clay sequence in SW Romania*. Quaternary Research, **83**: 437-448. https://doi.org/10.1016/j.yqres.2015.01.007

Ország G., Vid Ö., Szilágyi F., Végh Z. & Gyuricza G., 1989 – *Baradla-barlang. 1:10000*. Magyar Karszt és Barlangkutató Társulat és a KPVDSZ Vörös Meteor Természetbarát Egyesület, Budapest.

Peréz Martínez J.J. & Wiggen R.W., 1953 – *Los depositos de fosforitas de Salsimas Hidalgo y Ayancual, Estado de Nuevo León*. México Instituto Nacional para la Investigacion de Recursos Minerales Boletin, **32**: 1-33.

Pogson R.E., Osborne R.A.L., Colchester D.M. & Cendón D.I., 2011 – *Sulfate and phosphate speleothems at Jenolan Caves, New South Wales, Australia*. Acta Carsologica, **40 (2)**: 239-254. https://doi.org/10.3986/ac.v40i2.9

Prieto N., Carrero J.A., Olivares M. & Madariaga Mota J.M., 2015 – *Forme sobre medidas in situ mediante espectroscopía RAMAN y EDXRF en la cueva de Isturitz*. In: Garate D., Darricau J., Labarge A., Normand C. & Rivero O. (Eds.), *Les grottes ornées de la colline de Gaztelu (Saint-Martin-d'Arberoue, Pyrénées-Atlantiques)*. Étude de l'art pariétal Paléolithique: Isturitz, Oxocelhaya-Hariztoya et Erberua, Service régional de l'archéologie d'Aquitaine, p. 287-294.

Puşcaş C.M., Kristaly F., Stremțan C.C., Onac B.P. & Effenberger H.S., 2014 – *Stability of cave phosphates: case study from Liliecilor Cave (Trascău Mountains, Romania)*. Neues Jahrbuch fur Mineralogie-Abhandlungen (J. Min. Geochem.), **19 (1-2)**: 157-168. https://doi.org/10.1127/0077-7757/2014/0254

Reynaud A., 2000 – *Fonctionnement d'un aquifère karstique décollé sur une semelle de Trias évaporitique, exemple du massif du mont Vial (Arc de Castellane, Alpes-Maritimes).* Thesis, Université de Franche-Comté, Besançon, 246 p.

Reimer P.J., Bard E., Bayliss A., Beck J.W., Blackwell P.G., Ramsey C.B., Buck C.E., Cheng H., Edwards R.L., Friedrich M., Grootes P.M., Guilderson T.P., Haflidason H., Hajdas I., Hatté C., Heaton T.J., Hogg A.G., Hughen K.A., Kaiser K.F., Kromer B., Manning S.W., Niu M., Reimer R.W., Richards D.A., Scott E.M., Southon J.R., Turney C.S.M. & van der Plicht J., 2013 – *IntCal13 and MARINE13 radiocarbon age calibration curves 0-50000 years cal BP.* Radiocarbon, **55 (4)**: 1869-1887. https://doi.org/10.2458/azu_js_rc.55.16947

Ruggieri R. (Ed.), 2000 – *Il carsismo negli Iblei e nell'area sud mediterranea.* Atti del 1° Seminario, Ragusa 1999. Speleologia Iblea, Centro Ibleo di Ricerche Speleo-Idrologiche, Ragusa, **8**: 1-242.

Santo A., 1988 – *Alcune osservazioni sul carsismo ipogeo dei M. Alburni.* L'Appennino Meridionale, Annuario CAI sez. Napoli, p. 71-88.

Sauro F., De Waele J., Onac B.P., Galli E., Dublyansky Y., Baldoni E. & Sanna L., 2014 – *Hypogenic speleogenesis in quartzite: the case of Corona 'e Sa Craba Cave (SW Sardinia, Italy).* Geomorphology, **211**: 77-88. https://doi.org/10.1016/j.geomorph.2013.12.031

Schadler J., 1932 – *Ardealit, ein neues Mineral* $CaHPO_4CaSO_4 + 4H_2O$. Central-blatt Minealogie Abt. A., 40-41.

Shahack-Gross R., Berna F., Karkanas P. & Weiner S., 2004 – *Bat guano and preservation of archaeological remains in cave sites.* Journal of Archaeological Science, **31**: 1259-1272. https://doi.org/10.1016/j.jas.2004.02.004

Stuiver M. & Reimer P.J., 1993 – *Extended* ^{14}C *data base and revised CALIB 3.0* ^{14}C *age calibration program.* Radiocarbon, **35 (1)**: 215-230. https://doi.org/10.1017/S0033822200013904

Temovski M., 2013 – *Phantom speleogenesis in a thermal environment.* 21st International Karstological School "Hypogene speleogenesis", 10-14.06.2013, Postojna, Slovenia.

Temovski M., 2016 – *Evolution of karst in the lower part of Crna Reka river basin.* Springer Theses. Springer International Publishing, Cham, 265 p. https://www.springer.com/us/book/9783319245454

Theodorou G., Barlas K. & Stathopoulou E., 2004 – *On the presence of the mineral vivianite in the sediments of the "Megali Grava" cave in Loutses (Corfu, Greece).* Annales géologiques des pays helléniques, **XL (A)**: 133-142.

Vanara N., 2015 – *Karstologie de la colline de Gatzelu.* In: Garate D., Darricau J., Labarge A., Normand C. & Rivero O. (Eds.), *Les grottes ornées de la colline de Gaztelu (Saint Martin d'Arberoue, Pyrénées-Atlantiques). Étude de l'art pariétal paléolithique.* Isturitz, Oxocelhaya-Hariztoya et Erberua, Service régional de l'archéologie d'Aquitaine, p. 263-305.

Vattano M., Scopelliti G., Fulco A., Presti R., Sausa L., Valenti P., Di Maggio C., Lo Valvo M. & Madonia G., 2015 – *La Grotta dei Personaggi di Montevago (AG), una nuova segnalazione di cavità ipogenica in Sicilia.* In: De Nitto L., Maurano F. & Parise M. (Eds.), *Atti del XXII Congresso Nazionale di Speleologia*, Pertosa-Auletta (SA), 30/05-02/06/2015. Memorie dell'Istituto Italiano di Speleologia, **II (29)**: 295-300. http://hdl.handle.net/10447/132894

Vattano M., Madonia G., Audra P., D'Angeli I.M., Galli E., Bigot J.-Y., Nobécourt J.-C. & De Waele J., 2017 – *Update on the hypogenic caves of Sicily.* In: Klimchouk A., Palmer A.N., Audra P., De Waele J., Auler A. (Eds.), *Hypogene karst regions and caves of the world.* Springer, New York, p. 199-209. https://doi.org/10.1007/978-3-319-53348-3_12

Yoshimura K., Urata K., Someya T. & Akiyoshi-Do Cave Research Group, 1989 – *The role of bat guano in the formation of some mineral deposits in limestone caves.* Journal of the Speleological Society of Japan, **14**: 40-50.

International Journal of Speleology	48 (1)	107-109	Tampa, FL (USA)	January 2019

Available online at scholarcommons.usf.edu/ijs

International Journal of Speleology

Official Journal of Union Internationale de Spéléologie

Comment on "*Assessing preservation priorities of caves and karst areas using the frequency of endemic cave-dwelling species*" by Nitzu et al. (2018), Int. J. Speleol., 47 (1): 43-52

Oana T. Moldovan and Traian Brad*

"Emil Racoviță" Institute of Speleology, Romanian Academy, Clinicilor 5, Cluj-Napoca, Romania

Keywords: cave fauna, endemism, database, protection, red list

Received 6 December 2018; Revised 13 February 2019; Accepted 13 February 2019

Citation: Moldovan O.T. and Brad T., 2019. Comment on "*Assessing preservation priorities of caves and karst areas using the frequency of endemic cave-dwelling species*" by Nitzu et al. (2018), Int. J. Speleol., 47 (1): 43-52. International Journal of Speleology, 48 (1), 107-109. Tampa, FL (USA) ISSN 0392-6672 https://doi.org/10.5038/1827-806X.48.1.2241

In a recent paper published by Nitzu et al. (2018), the authors propose an algorithm to identify "hotspots of vulnerable karst areas" that uses frequency of endemic "cave-dwelling species". The authors viewpoint is that the occurrence of endemic troglobionts and stygobionts, or cave-dwelling species as given in the title, in 3-4 caves up to a maximum of 37 caves, can be used to rank caves in terms of their vulnerability. The proposed ranking is based on a published list of endemic species that can be found in Romanian caves (Nitzu et al., 2016). We discuss here the type of errors that encumber the correct and equitable protection of cave species and their habitat, which can derive from the use of quantitative criteria based on incomplete or incorrect datasets on cave fauna (troglobionts and stygobionts).

Type I error: assuming that the quantitative ranking of caves is based on a complete and correct inventory of cave species. The incomplete number of species is prone to inevitable errors (species present but not found or not published, incomplete databases etc.), which would place the caves with important species or communities at low ranks. In the list of Nitzu et al. (2016), notorious examples of missing data are apparent. For example, in Peştera (Cave) Vântului only six species are mentioned, while this cave is one of the richest in Romania with respect to cave fauna, containing twelve troglobionts and stygobionts, some of them strictly endemic to this cave. As a result, Peştera Vântului is not considered as one of the vulnerable caves. Peştera Lazului, one of the richest in cave fauna with eight troglobitic and two stygobitic species, is also under-ranked.

Out of more than 12,000 caves known in Romania, 830 are considered in Nitzu et al. (2016, 2018), with many others that might be biospeleologically overlooked. In order to be certain that a species is present in one or more caves, repeated sampling is needed. Moldovan et al. (2012) have shown the large heterogeneity of stygobiontic fauna in caves, where some species were collected only once during several months in a single drip/pool inside a cave.

Type II error: assuming that the list of ranked caves is based on strictly regional endemic species. The list published by Nitzu et al. in 2016 has many examples of troglophilic species that are not even endemic at national level. For example, *Trachelipus trilobatus* is a troglophile isopod also mentioned from Poland and *Orthonychiurus ancae* is a troglophile also present in Slovenia (de Jong et al., 2014). There are also troglophilic species with wide distribution in Romania. For example, *Hyloniscus flammuloides* is distributed in two different mountain massifs of the Southern Carpathians with possible more extensive distribution (Tabacaru & Giurginca, 2013).

Niphargus "ablaskiri variabilis" (correct *N. variabilis*) is not endemic to only some particular caves, but present in the Bihor, Vâlcan and Şureanu Mountains (Apuseni Mountains and Southern Carpathians, respectively). *N. bihorensis* is also present in several other caves in the Apuseni Mountains, and not only in Meziad Cave (Dobreanu & Manolache, 1957). "*N. stygocharis stygocharis*" (correct *N. stygocharis*) is present in Peştera de la Vadu Crişului, but also in the hyporheic environment of the Crişul Repede River and in several drinking water wells along this river.

We argue that endemic species should be only considered when isolated populations are present in specific areas characterized by particular geological and geographical features. When a species is present

*traian.brad@iser.ro

in a larger territory such as that of a ~250.000-km^2 country, with such a heterogeneous landscape, then the species can no longer be considered a regional endemism.

Type III error: assuming that troglobionts and troglophiles are equal in setting protection priorities. Considering that caves can be ranked by using troglophilic species means prioritizing the protection of cave fauna by way of adding species that also use surface habitats. We picked randomly from the list (Nitzu et al., 2016) two examples of caves from Southern Carpathians: Peştera Piatra Scrisă, with two troglophile species and sharing the same ranking with Peştera Vacilor din Cheile Orzeştilor, which houses one troglobiont and one troglophile. Similarly, Peştera Piatra Scrisă has a higher ranking than Peştera de la Gălăşeni, which has two troglobionts and one stygobiont, with one species being endemic to this cave, or higher than Peştera din Pietrele Negru, with one stygobiont and two troglobionts, one endemic to a few caves within a small area.

Troglophilic species might be mentioned in dozen of caves, but there is no study on their presence and abundance in surface and subsurface habitats. Troglophilic species can be found at the entrance of any small cave or even sheltered under the rocks at the surface and their distribution is higher than estimated.

Type IV error: assuming that frequency is a true estimator of endemicity. Sampling in a few caves in one area is also subject to erroneous frequency estimation of a species distribution. For example, the ranking of a species found in 30 caves in an area of 10 km^2 is the same as the ranking of a species found in the same number of caves (30) in an area of 100 km^2, where the other possible 300 caves with fauna were not inspected. Ideally, sampling should be carried out in all caves in a relatively small area. On the contrary, it becomes more difficult to estimate the presence/absence of species in larger areas, where the number of caves can be higher and nearly impossible to be entirely sampled.

Type V error: ignoring species that should be on a red list of Romanian cave species. Some species are known to be very rare in caves, even when repeated sampling attempts are made, while other species form big populations in caves. Even if caves are not the unique habitat for the cave animals, they are part of their ecosystem and one cannot ignore the importance of caves as habitat. The cave species may be distributed in extremely limited areas in one cave. For example, Peştera Jgheabul lui Zalion is low ranked, although it contains a unique representative of the genus "*Romanosoma*" (correct *Hylebainosoma*) that is not present in other regions of Romania. In the same region, Peştera de la Izvorul Tăuşoarelor, absent in the list of Nitzu et al. (2016), is the habitat of an endemic troglobiontic Diplura (*Litocampa humilis comani*), also representative of a rare fauna group in Romanian caves (Sendra et al., 2012).

Type VI error: ignoring the potential threats to cave fauna. By ranking caves that are highly vulnerable to anthropic impacts at low levels based on quantitative data is as dangerous as declaring the caves free to any usage. Although Nitzu et al. (2018) promised to add other criteria to cave ranking, we consider that one cannot start prioritizing caves for protection based solely on the number of species and their frequency and ignoring the actual threats. Many strategies of caves protection also include the possible or existent threats (e.g., Souza-Silva et al., 2015; Souza-Silva & Ferreira, 2016, and references in Nitzu et al., 2018). In Appendix 1 (Nitzu et al., 2018), 66 caves in Apuseni Mountains and 103 caves in Southern Carpathians have a small endemicity index, leaving less than 19 caves in Apuseni Mountains and 14 caves in Southern Carpathians for protection. According to the same reasoning, none of the caves in Banat Mountains (one of the most important hot-spots for cave endemics in Romania) are in the red zone and require protection. The same stands for caves in Eastern Carpathians, which contain less endemic species and therefore do not deserve much protection. Each of these mountain ranges has cave genera and species that are endemic to one or a few caves in a small area.

Today, one of the most important threats to caves in Romania is the so-called 'specialized speleological tourism' (literally translated from Romanian). This type of tourism involves the visiting of wild caves by groups of ordinary tourists that are provided with speleological equipment and a guide. The phenomenon is rapidly growing in Romania and affords access to hundreds of people in a single day, even in highly protected caves with little or no control and without knowing that they may destroy some of the most important and unique habitats for rare cave species. This threat was ignored by Nitzu et al. (2018). In Vântului Cave, which is often visited during weekends by hundreds of people, eleven species out of a total of twelve were described only in the lower level of the cave. This is exactly the place where the access for speleological tourism was granted, assuming incorrectly that the cave fauna can be found also in the upper levels, which is not the case.

Type VII error: ignoring the legislation in force that protects cave habitats or cave species. The idea of prioritizing caves based on species number can lead to unnecessary protection for caves that are not under threat, and to insufficient protection for caves that have not been studied enough and where rare species may live. First, it is hard to understand the need to prioritize cave conservation in Romania, since all caves (except for the show-caves) are protected by the European and Romanian legislations in force (Habitat Directive, (1992) Council Directive 92/43/EEC of 21 May 1992 on the conservation of natural habitats and of wild fauna and flora; Law 49/2011).

Conclusions such as "...caves where high EI (endemicity index) were recorded should be prioritized at national level in terms of conservation concern, while those with low EI should be included in regional conservation agendas" (Nitzu et al., 2018) should be considered with care. There are no such 'regional

conservation agendas' in Romania. A classification of caves based on such an index cannot be made, and caves cannot be prioritized for protection accordingly. A "low endemicity-index cave" can house at least one endemic species and so the habitat of this species should be unquestionably protected. A cave cannot be judged as being less important than others because of a lower "endemicity index", and so a prioritization of caves and karst areas in the context of their preservation, protection and sustainable management should not be made.

In the absence of a red list of cave species, which must be based on solid facts, cave fauna is protected through their habitats by Romanian and European legislation. The unit for protection and conservation of cave fauna must be the uniqueness, endangerment and irreplaceability of the species and their potential habitats. The number of species can be used in some cases of new threats to caves or cave habitats, like the opening of caves for uncontrolled tourism, but in no case for prioritizing caves for protection when legally all caves are protected. As a conclusion we consider that both poorly documented fauna lists and impact studies can represent major threats to the integrity of caves and their fauna.

ACKNOWLEDGEMENTS

We are grateful to Peter Trontelj and Alberto Sendra for the useful suggestions. We thank Silviu Constantin for critical observations and constructive discussions during the preparation of this work. This work was supported by a grant of Minister of Research and Innovation, CNCS - UEFISCDI, project number PN-III-P4-ID-PCCF-2016-0016, within PNCDI II.

REFERENCES

Dobreanu E. & Manolache C., 1957 – *Noi contributii la studiul amphipodelor hipogee din Republica Populara Romina*. Academia Republicii Populare Romine. Buletin Stiintific. Sectia de biologie si stiinte agricole (Seria Zoologie), **9**: 307-333.

de Jong Y., Verbeek M., Michelsen V., de Place Bjørn P., Los W., Steeman F., Bailly N., Basire C., Chylarecki P., Stloukal E., Hagedorn G., Wetzel F.T., Glöckler F., Kroupa A., Korb G., Hoffmann A., Häuser C., Kohlbecker A., Müller A., Güntsch A., Stoev P. & Penev L., 2014 – *Fauna Europaea - all European animal species on the web*. Biodiversity Data Journal, **2**: e4034. https://doi.org/10.3897/BDJ.2.e4034

Moldovan O.T., Meleg I.N. & Perşoiu A., 2012 – *Habitat fragmentation and its effects on groundwater populations*. Ecohydrology, **5**: 445-452. https://doi.org/10.1002/eco.237

Nitzu E., Giurginca A., Nae A., Popa I., Baba S., Meleg I.N. & Vlaicu M., 2016 – *The catalogue of caves with endemic cavernicolous arthropod fauna of Romania*. Travaux de l'Institut de Spéologie "Emile Racovitza", **55**: 3-62. http://speotravaux.iser.ro/16/art01.pdf

Nitzu E., Vlaicu M., Giurginca A., Meleg I.N., Popa I., Nae A. & Baba S., 2018 – *Assessing preservation priorities of caves and karst areas using the frequency of endemic cave-dwelling species*. International Journal of Speleology, **47 (1)**: 43-52. https://doi.org/10.5038/1827-806X.47.1.2147

Sendra A., Nitzu E., & Sanjuan A., 2012 – *Half a century after Ionescu's work on Romanian Diplura – a faunal contribution based on material collected from karst areas*. Travaux de l'Institut de Spéologie "Emile Racovitza", **51**: 37-66. http://speotravaux.iser.ro/12/art02.pdf

Souza-Silva M., Martins R.P. & Ferreira R.L., 2015 – *Cave conservation priority index to adopt a rapid protection strategy: A case study in Brazilian Atlantic rain forest*. Environmental Management, **55**: 279-295. https://doi.org/10.1007/s00267-014-0414-8

Souza Silva M. & Ferreira R.L., 2016 – *The first two hotspots of subterranean biodiversity in South America*. Subterranean Biology, **19**: 1-21. https://doi.org/10.3897/subtbiol.19.8207

Tabacaru I. & Giurginca A., 2013 – *Cavernicolous Oniscidea of Romania*. Travaux de l'Institut de Spéologie "Emile Racovitza", **52**: 3-26. http://speotravaux.iser.ro/13/art01.pdf

International Journal of Speleology	48 (1)	111-113	Tampa, FL (USA)	January 2019

Available online at scholarcommons.usf.edu/ijs

International Journal of Speleology

Official Journal of Union Internationale de Spéléologie

A reply to the comment on "*Assessing preservation priorities of caves and karst areas using the frequency of endemic cave-dwelling species*" by Nitzu et al. (2018), Int. J. Speleol., 47 (1): 43-52

Eugen Nitzu, Ioana N. Meleg*, and Andrei Giurginca

"Emil Racoviță" Institute of Speleology, Romanian Academy, Calea 13 Septembrie, 050711, Bucharest, Romania

Keywords: cave fauna, karst, preservation, Romania

Received 30 December 2018; Revised 12 February 2019; Accepted 13 February 2019

Citation: Nitzu E., Meleg I.N. and Giurginca A., 2019. A reply to the comment on "*Assessing preservation priorities of caves and karst areas using the frequency of endemic cave-dwelling species*" by Nitzu et al. (2018), Int. J. Speleol., 47 (1): 43-52. International Journal of Speleology, 48 (1), 111-113. Tampa, FL (USA) ISSN 0392-6672 https://doi.org/10.5038/1827-806X.48.1.2245

We appreciate the attention of our two colleagues, Oana Teodora Moldovan (OTM) and Traian Brad (TB), to our article "Assessing preservation priorities of caves and karst areas using the frequency of endemic cave-dwelling species" (hereafter referred to as IJS-2018). Due to space limitation, we will address in short their comment (hereafter IJS-Comment) on IJS-2018 Article.

The IJS-Comment reflects a misunderstanding and erroneous interpretation of the data and basic aim of IJS-2018: to propose a tool based on the principle of using endemic species to assess the patrimonial value of caves and consequently their conservation and management needs in terms of their biological peculiarities. IJS-2018 didn't propose: 1) to discuss the correctness of systematics, once species are listed in recognized international systematic databases; 2) to address issues related to "external threats"; and 3) to ignore the current regulations, but to provide scientific support needed for regulatory framework implementation and improvement. Moreover, the IJS-2018 authors: 1) didn't claim that inventories or databases are complete; and 2) based their proposed index on several groups of Arthropoda. It is self-explanatory that instruments for data collection and management are perfectible and constantly updated. Therefore the proposed index and its concept may be extended beyond Arthropoda based on identified *in situ* needs.

To start with, some of the comments in IJS-Comment refer to another paper of ours (Nitzu et al., 2016), and not to IJS-2018. Since Nitzu et al. (2016) dataset was used in IJS-2018, we will reply to all comments on both papers.

In the introductory part of their comment, OTM and TB raised the problem of type of errors in IJS-2018 that "encumber the correct and equitable protection of cave species". Starting with the introductory part of IJS-Comment, OTM and TB misstated: "The authors' viewpoint is that the occurrence of cave dwelling species … in 3-4 caves up to a maximum 37 caves can be used to rank the caves…" In reality, we mentioned (p. 44) that we have taken into consideration all endemic arthropod species known up to present to inhabit the caves from the studied area, starting from one cave (*unique species*) to the maximum counted number of caves (see Table 1 and all discussion from 46 caves in our paper).

We turn now to a discussion of the so-called "type errors" in IJS-Comment.

1) Answer to the "type 1 error".

The affirmation of OTM and TB is incorrect. In our paper, in the supplemental "Annex 1", Peştera Vântului (Cave) is ranked on the 46-th position of the total of 380 (E.I. = 1.62), taking an important place in the classes of conservation concern, as we have mentioned in our article (p. 48, paragraph 1).

Regarding the number of endemic cave–dwelling species from Vântului Cave, we referred to the Arthropod fauna, the best studied for over 100 years in the area (see introductory part in Nitzu et al., 2016). And yes, from the total number of **endemic cave dwelling Arthropoda** recorded in the Vântului Cave, only six fulfilled the selection criteria.

We agree that "repeated sampling is needed in order to be certain that a species is present in one or more caves", but we have worked with all reliable data available up to present of biospeleological studies on **Arthropoda** (see Nitzu et al., 2016).

*ioana.meleg@gmail.com

OTM and TB observed that "out of more than 12,000 caves known in Romania, 830 are considered in Nitzu et al. (2016), with many others that might be biospeleologically overlooked". There is a relatively high possibility that some endemic-cave dwelling arthropods exist in new other caves, others could be described in the future, but we worked with all known data available on this subject, as such the number of assessed caves (in the studied area) with endemic cave-dwelling arthropods (see p. 44, "Dataset" from Nitzu et al., 2016).

As for the remark of OTM and TB on the rich cave fauna of Lazului Cave, the authors seem to forgot that we refer only to the endemic cave dwellers, not to all the species inventoried in this cave. If OTM and TB know other species of endemic cave-dwelling Arthropoda species, other than those mentioned by us in the catalogue (Nitzu et al., 2016), we ask them to ground their affirmation.

2) Answer to "type II error".

OTM and TB claimed that "We argue that endemic species should be only considered when isolated populations are present in specific areas characterized by particular geological features".

We were unable to see where they "argued" such a theory. Instead, in our article IJS-2018, at methodology (p. 44) we defined the term *endemic* reported to the specific geographic area, and based on the bibliography used for the accepted definition of *endemism*.

We do not understand what are the arguments of OTM and TB regarding the presence of endemisms in a heterogeneous landscape, but as it could be observed in IJS- 2018, 131 taxa were found only in one cave, and only five species have been found in 23 to 37 caves (Table 1, p. 46), most of them in the same mountain massif (Nitzu et al., 2016) and Fig. 2 IJS-2018.

Taxa related misstatements: the authors are making assumptions without presenting any proof for their affirmations.

1. The affirmation that *Trachelipus trilobatus* was found in Poland and *Orthonychiurus ancae* is present in Slovenia.

All the papers concerning the genus *Trachelipus* agree on the status of Romanian endemite for *Trachelipus trilobatus*: Schmidt (1997), Schmalfuss (2003), Tabacaru & Giurginca (2013), and Tomescu et al. (2015). So, it would be better if the authors of the IJS-Comment will cite here the paper on this matter, otherwise the affirmation is null. On the other hand, if their affirmation is based on the maps from Fauna Europaea, then it has no value since Fauna Europaea contains numerous errors concerning the Oniscidea and as such is not reliable. To mention just one glaring error: their inclusion of five species of *Mesoniscus* (see Jong et al., 2014) when there are only two, a fact argued exhaustively in 1963 by Gruner and Tabacaru and included by Schmalfuss in 2003 in his world catalogue of Oniscidea. The same observation for *Orthonychiurus ancae* (see Gruia, 2003).

2. The affirmation "There are also troglophilic species with wide distribution in Romania. For example, *Hyloniscus flammuloides* …", this does not come from Tabacaru & Giurginca (2013). The paper does not claim that *Hyloniscus flammuloides* might have a possible more extensive distribution. There is nothing in the mentioned paper even slightly suggesting or supporting this affirmation. And in any case, *Hyloniscus flammuloides* is not "an example of a troglophilic species with wide distribution in Romania". The species *Hyloniscus flammuloides* is recorded in only two locations (see Giurginca et al., 2015, pages 38 and 121). Is this "a possible more extensive distribution" or just an affirmation without support?

3. Amphipoda

The name of the species presented in IJS-2018 and Nitzu et al. (2016) are listed in Fauna Europaea, https://fauna-eu.org/cdm_dataportal. All the other comments related to amphipods have no reference in the IJS-2018, nor Nitzu et al. (2016): we never reported *Niphargus ablaskiri variabilis*, *Niphargus bihorensis* as species recorded in a single cave (see the detailed list in Nitzu et al., 2016). As for the presence of *Niphargus stygocharis stygocaris*, our aim was to list its presence in cave habitats, since Nitzu et al. (2016) and IJS-2018 deal with cave habitats. However, the presence of *N. s. stygocharis* in other groundwater habitats within the same hydrographic basin is no doubt obvious, as for other groundwater species. Consequently, that is one of the reasons, among others, for proposing a 10 km^2 area for mapping the karst area vulnerability.

3) Answer to "type III error".

OTM and TB seem to forgot that we referred to the **endemic troglophilic** species (eutroglophilic species are dependent in a certain phase of their onthogenesis by the subterranean habitat), and yes, these **endemic** troglophilic species are also important in the protection of karst areas. For more discussions on this subject please see p. 48 in IJS-2018. If OTM and TB argue that "trogophilic species might be mentioned in dozen of caves", while further suggesting that "is ***no*** study on their presence", then, based on what they sustain their affirmation?

4) Answer to "type IV error"

In IJS-2018 we have not "ranked species" as OTM and TB affirmed, but caves, and this was made on the accumulated reliable data up to present. The periodically sampling and adjustment could be possible in time. In the chapter "Conclusions" (p. 50) we have mentioned that "the proposed *EI* was generated as a solution for prioritization of small and isolated habitats at medium scale, different by the suitable solutions available… for large scale areas". Moreover, Rabelo et al. (2018) have tested our *EI* in a large karst area of Brazil, and their conclusion was that "The *EI* (Nitzu et al., 2018) has shown to be a great index for the conservation of endemic cave dwellers but requires an accurate database of the distribution of the troglobiotic species to be satisfactorily applied".

5) Answer to "Type V error".

There is no published "red list of Arthropoda" for Romania, so we do not see the sense of this comment here.

Regarding a unique representative of the genus "*Romanosoma*" (correct *Hylebainosoma*)", indeed, Tajovský et al. (2014) argued that the genus *Romanosoma* is not valid and included *Romanosoma* in *Hylebainosoma*. In IJS-2018 we have followed here the opinion of Mauriès (2015), which not only validates *Romanosoma* but also regards it as distinct from *Hylebainosoma*. That *Romanosoma* is a valid genus is also the opinion of Kime & Enghoff (see de Jong et al., 2014).

"In the same region, Peştera de la Izvorul Tăuşoarelor, absent in the list of Nitzu et al. (2016), is the habitat of *Litocampa humilis comani*" (Sendra et al., 2012)." Yes, that was an omission in Nitzu et al. (2016).

6) Answer to "type VI error".

Assessing the potential threats was not the purpose of the IJS-2018, but to prioritize the caves for protection from bispelolological point of view (see more at p. 50). Another erroneous affirmation of OTM and TB is that we stipulated in our article that only caves from the red zone (those with highest EI) should be protected and the others not. On the contrary, at p. 48, we emphasized that the caves with *EI* from 1.94 to 1, despite their lower diversity in terms of endemic taxa compared to those from the first cluster, should be regarded and protected. Please see also our comment from point (1).

7) Answer to "type VII error".

Here we address only specific points related to cave protection regulation in Romania and not the personal interpretations that most of the time, have no reference in IJS-2018. To start with, article 8 of the Emergency Government Ordinance 57/2007 (Ordonanța de Urgență a Guvernului 57/2007, hereafter OUG 57/2007), the law for natural protected areas in Romania, establishes the designation and the regime of the natural protected areas (IUCN categories, Natura 2000). Moreover, for caves designated as natural protected areas, the article 43 of the OUG 57/2007 classifies the caves in four classes of protection based on their patrimonial value assessed through specific scientific studies. According to the law 5/2000 and Government Decision (Hotărârea) 2151/2004, out of 12,000 caves, only 132 caves are designated natural protected areas (i.e., nature reserve/monument) and are classified based on their patrimonial value. In this context, the *EI* proposed in IJS-2018 is a valuable tool that may be used for assessing the biological patrimonial value of caves, in support of cave designation as natural protected areas and their classification.

ACKNOWLEDGMENTS

This work was financially supported by the "Emil Racoviță" Institute of Speleology (Romanian Academy) within the Project 1 of the Program I framework.

REFERENCES

Giurginca A., Munteanu C.M., Vlaicu M. & Tabacaru I.G., 2015 – *Cavernicolous Oniscidea of Romania*. "Semne" Publishing House, Bucharest, Romania, 166 p., ISBN: 606-15-0673-2.

Gruia M., 2003 – *Collembola from Romanian caves*. Travaux du Museum d'Histoire Naturelle „Grigore Antipa", **35**: 139-158.

Gruner H.E. & Tabacaru I., 1963 – *Revision der Familie Mesoniscidae Verhoeff, 1908 (Isopoda, Oniscoidea)*. Crustaceana, **6**: 15-34. https://doi.org/10.1163/156854063X00318

Hotărârea nr. 2151/2004 privind instituirea regimului de arie naturală protejată pentru noi zone.

Jong de Y., Verbeek M., Michelsen V., Bjørn P.P , Los W., Steeman F., Bailly N., Basire C., Chylarecki P., Stloukal E., HagedornG., Tobias Wetzel F., Glöckler F., Kroupa A., Korb G., Hoffmann A., Häuser C., Kohlbecker A., Müller A., Güntsch A., Stoev P. & Penev L, 2014 – *Fauna Europaea - all European animal species on the web*. Biodiversity Data Journal, **2**: e4034. https://doi.org/10.3897/BDJ.2.e4034

Legea nr. 5/2000 privind aprobarea Planului de amenajare a teritoriului național – Secțiunea a III-a - zone protejate.

Mauriès J.P., 2015 – *Platydesmidan and polyzoniidan millipedes collected in the Northwest of Iberian Peninsula by British expeditions in 1993 and 2004 (Diplopoda: Platydesmida, Polyzoniida)*. Russian Entomological Journal, **24 (4)**: 325-341.

Nitzu E., Giurginca A., Nae A., Popa I., Baba S., Meleg I.N. & Vlaicu M., 2016 – *The catalogue of caves with endemic cavernicolous arthropod fauna of Romania*. Travaux de l'Institut de Spéologie "Emile Racovitza", **55**: 3-62. http://www.speotravaux.iser.ro/16/art01.pdf

Ordonața de Urgență a Guvernului nr. 57 / 2007 privind regimul ariilor naturale protejate, conservarea habitatelor naturale, a florei şi faunei sălbatice, aprobată cu modificări şi completari prin Legea nr. 49/2011, cu modificările şi completarile ulterioare.

Rabelo L.M., Souzo-Silva M. & Ferreira R.L., 2018 – *Priority caves for biodiversity conservation in a key karst area of Brazil: comparing the applicability of cave conservation indices*. Biodiversity Conservation, **27 (9)**: 2097-2129. https://doi.org/10.1007/s10531-018-1554-6

Schmidt C., 1997 – *Revision of the European species of the genus Trachelipus Budde-Lund, 1908 (Crustacea: Isopoda: Oniscidea)*. Zoological Journal of Linnean Society, **121**: 129-244. https://doi.org/10.1111/j.1096-3642.1997.tb00337.x

Schmalfuss H., 2003 – *World catalog of terrestrial isopods (Isopoda: Oniscidea)*. Stuttgarter Beitrage zur Naturkunde, Serie A **654**: 341 p.

Tabacaru I. & Giurginca A., 2013 – *Cavernicolous Oniscidea of Romania*. Travaux de l`Instut de Spéologie "Émile Racovitza", **52**: 3-26. http://www.speotravaux.iser.ro/13/art01.pdf

Tajovský K., Mock A. & Papáč, V.,2014 – *The genus Hylebainosoma Verhoeff, 1899 (Diplopoda, Chordeumatida, Haaseidae): Redescription of Hylebainosoma tatranum, description of a new troglobiont species and notes to the Hylebainosoma–Romanosoma species group*. Zootaxa, **3764 (5)**: 501-523. https://doi.org/10.11646/zootaxa.3764.5.1

Tomescu N., Teodor L.A., Ferenți S. & Covaciu-Marcov S.D., 2015 – *Trachelipus species (Crustacea, Isopoda, Oniscidea) in Romanian fauna: morphology, ecology, and geographic distribution*. North-Western Journal of Zoology, **11** (Supplement 1): S1-S106. http://biozoojournals.ro/nwjz/content/v11s1/nwjz_e150301_Tomescu.pdf